NASA Conference Publication 3187, Vol. II

Space Technology Interdependency Group

Sixth Annual Workshop on Space Operations Applications and Research (SOAR '92)

Volume II

Proceedings of a workshop held in
Houston, Texas
August 4–6, 1992

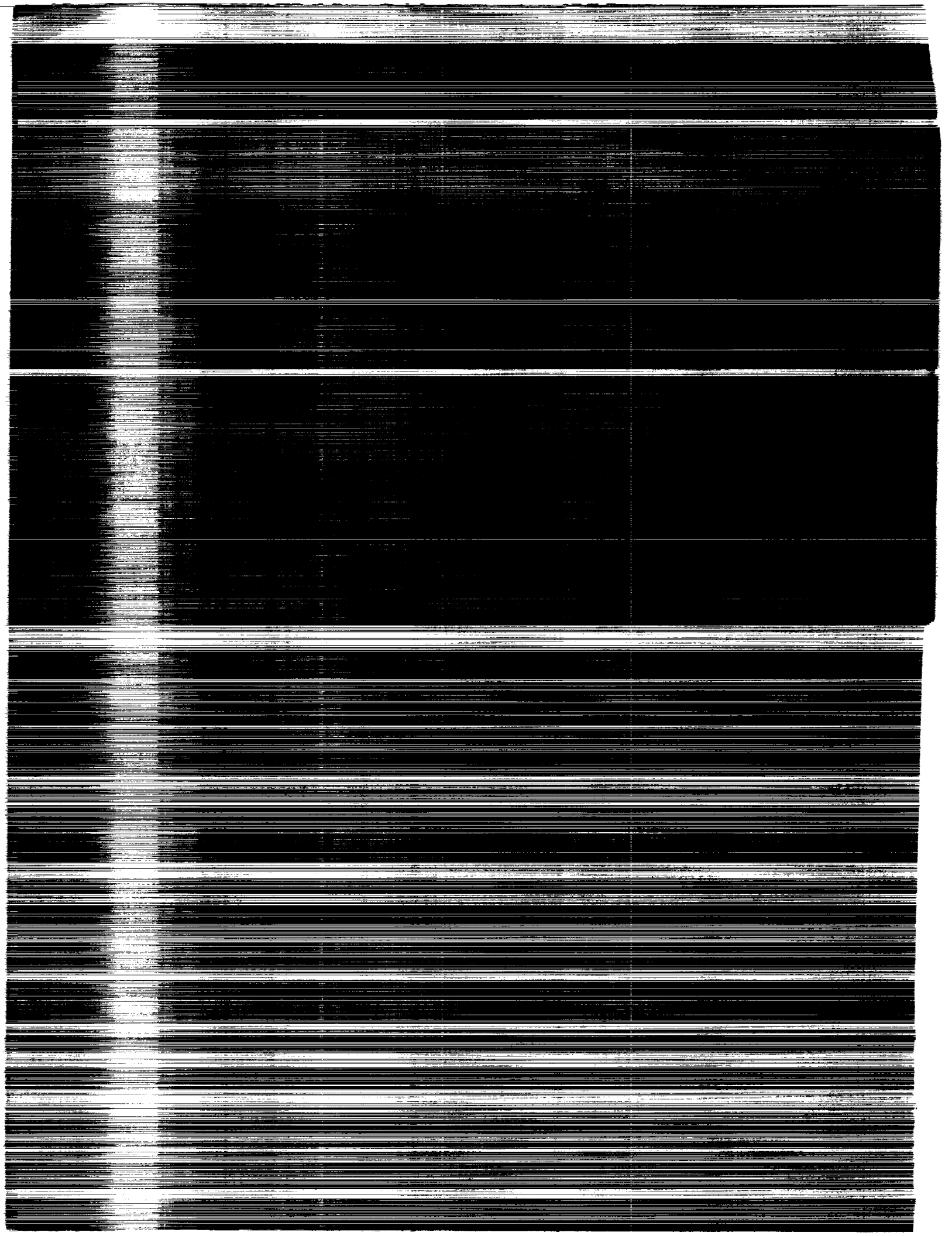

NASA Conference Publication 3187, Vol. II

Sixth Annual Workshop on Space Operations Applications and Research (SOAR '92)

Kumar Krishen, Editor
NASA Lyndon B. Johnson Space Center
Houston, Texas

Proceedings of a workshop sponsored by the National Aeronautics and Space Administration Washington, D.C., the U.S. Air Force, Washington, D.C., and cosponsored by the University of Houston-Clear Lake, Houston, Texas, and held in Houston, Texas August 4-6, 1992

National Aeronautics and Space Administration

Science and Technical Information Branch

CONTENTS

SECTION II: AUTOMATION AND INTELLIGENT SYSTEMS

Session A1: ADVANCED KNOWLEDGE-BASED SYSTEMS TECHNOLOGY
Session Chair: Dr. Abe Waksman

Session A2: PLANNING AND SCHEDULING I
Session Chair: Lt. Jennifer Skidmore

Session A3: PLANNING AND SCHEDULING II
Session Chair: Andrew Mayer

Session A4: MONITORING AND CONTROL
Session Chair: Dr. Robert Lea

SECTION III

HUMAN FACTORS

Session H1: HUMAN PERFORMANCE MEASUREMENT I— PSYCHOPHYSICAL RESEARCH

Session Chair: Dr. Mary Connors

HUMAN FACTORS TRACK INTRODUCTION

Col. Donald Spoon and Dr. Mary M. Connors

Abstract unavailable at time of publication.

N94-11528

Quantitative EEG Patterns of Differential In-flight Workload

M.B. Sterman, C.A. Mann, and D.A. Kaiser
V.A. Medical Center, Sepulveda, and School of Medicine, UCLA

ABSTRACT

Four test pilots were instrumented for in-flight EEG recordings using a custom portable recording system. Each flew six, two minute tracking tasks in the Calspan NT-33 experimental trainer at Edwards AFB. With the canopy blacked out, pilots used a HUD display to chase a simulated aircraft through a random flight course. Three configurations of flight controls altered the flight characteristics to achieve low, moderate, and high workload, as determined by normative Cooper-Harper ratings. The test protocol was administered by a command pilot in the back seat. Corresponding EEG and tracking data were compared off-line.

Tracking performance was measured as deviation from the target aircraft and combined with control difficulty to achieve an estimate of "cognitive workload". Trended patterns of parietal EEG activity at 8-12 Hz were sorted according to this classification. In all cases high workload produced a significantly greater suppression of 8-12 Hz activity than low workload. Further, a clear differentiation of EEG trend patterns was obtained in 80% of the cases. High workload produced a sustained suppression of 8-12 Hz activity, while moderate workload resulted in an initial suppression followed by a gradual increment. Low workload was associated with a modulated pattern, lacking any periods of marked or sustained suppression.

These findings suggest that the quantitative analysis of appropriate EEG measures may provide an objective and reliable in-flight index of cognitive effort that could facilitate workload assessment.

INTRODUCTION

The referential electroencephalographic (EEG) signal, obtained from one active EEG electrode referrenced to an indifferent site, such as the earlobe, reflects the summated electrical activity from pools of neurons around the active site. This summation depends upon the collective behavior of individual cortical neurons which, in turn, reflects the presence or absence of input to these neurons (Anderson and Anderssen, 1968). In the non-engaged, eyes closed state metabolic and circuit influences at a major cortical input source, the thalamus, cause some of its elements to discharge synchronously, and to send gated volleys to related areas of cortex (Steriade and Llinas, 1988). These gated excitatory volleys from thalamus give rise to rhythmic cortical field potentials that produce a dominant 8-12 Hz pattern in the corresponding EEG.

When the eyes are opened this pattern is attenuated, or "blocked" (Berger, 1930). This is presumed to result from the

fact that many cells become active and cease their gated discharge. However, not all cells are activated, and a sufficient number remain in the gated state so as to produce residual activity in the dominant frequency band of the EEG. With further cognitive challenge additional cells are activated but primarily in brain sites related to that challenge. Thus, differentially localized further attenuation of 8-12 Hz activity has been documented (Sterman et al, 1992). Localized decreases in this activity were found to be related specifically to signal processing and were not a simple consequence of increased movement.

The discovery of this meaningful relationships between the EEG and cognitive effort was facilitated by the application of quantitative frequency analysis methods. The use of the Fast Fourier Transform to achieve quantitative spectral estimates of frequency density simultaneously at many cortical recording sites has provided a sensitive and efficient EEG tool for this application. The combination of a potentially reliable EEG metric for cognitive effort, and the capacity for an efficient quantitative assessment of this metric, suggested to us that an objective, physiological measurement of "cognitive workload" could now be achieved. We report here on a preliminary assessment of this measurement within the context of an in-flight air-to-air tracking task in the Calspan NT-33 experimental training aircraft. This study sought to advance the search for an objective, biological index of workload.

METHODS

Four 90 minute designated test flights were carried out in the Calspan NT-33 aircraft at the Test Pilot School, Edwards Air Force Base, California. This specially configured two-seat trainer aircraft provides for systematic modification of both aircraft handling characteristics and HUD avionics displays. Four volunteer test pilots were specially instrumented for EEG recording during these flights.

A portable EEG recording system for in-flight applications has been under development in our laboratory for the past five years. This system consists of a fire-resistant cloth helmet liner containing 12 pre-positioned EEG recording sites marked by velcro-sealed ports. Gold-plated recording electrodes are hard-wired to adjacent custom-designed, miniature pre-amplifier units. Inputs from linked earlobe references are connected to the output of these preamplifier units to provide for referential (monopolar) EEG recordings. The custom preamplifier units, developed in collaboration with the Teledyne Corporation, provide very high input impedance (10 megaohms), a high-pass filter, and an instrumentation amplifier. These units remove all DC variations of the input signal and significantly attenuate low frequency artifact. They also provide amplification at the signal source and a high common-mode rejection ratio.

The preamplifier outputs are led through a light-weight coaxial cable to a second stage filter/amplification unit. This

unit uses a six layer printed circuit board to accomplish analog signal conditioning, including filtering and second stage amplification. It is carried, together with a DC battery power supply unit, time-code generator, audio communications patch, and microrecorder in the pockets of a modified standard flight vest. The second-stage amplifier provides isolation and variable gain for matching output level to recorder input level requirements. Downstream from the isolation amplifier are two switch-capacitor filter banks (3rd order high-pass and 5th order low-pass) which narrow the EEG bandwidth to a range of 4-16 Hz, and provide anti-aliasing and noise rejection for the recorded signal. An audio patch connection between the aircraft intercom system and one channel of the microrecorder provides a continuous record of vocal transactions during the flight. The microrecorder provides for up to three hours of continuous recording of EEG and audio communications data.

Six sequential tracking tests were performed by each pilot. A blue helmet visor together with an orange canopy cover created blackout conditions restricting control to the HUD instrumentation. Each test required continuous tracking performance over a period of 1.5 to 2 minutes. These were marked on the data tapes by verbal protocol and by a special audio tone coded for the start and finish of each test. A continuous video record of the HUD display was recorded throughout the flight.

Unpredicted, random movements of the HUD target aircraft were matched by the pilot flying the T-33 aircraft into corresponding orientations. Accuracy was measured as sampled deviation from target throughout the test. Three configurations of flight controls altered the flight characteristics of the aircraft to achieve low, moderate, and high workload, as determined by previously registered normative Cooper-Harper ratings. The test protocol was administered by a command Calspan pilot in the back seat.

Space and technical considerations for this test limited EEG recording to four channels, including F3, T4, P3, and P4, placed according to the International 10/20 System. These sites were selected on the basis of previous findings. EEG recording was continuous during each test flight. Additionally, two minute reference periods of eyes closed and eyes open were obtained prior to and during each flight. Data were subsequently downloaded to laboratory computers off-line, and subjected to digital transform and Fast Fourier Analysis. Log transformed spectral magnitude values in the 8-12 Hz frequency band were generated for sequential two-second epochs and tabulated for the baseline conditions and for each tracking test segment. EEG data were plotted graphically for each tracking test for magnitude, trend, and pattern analysis. Statistical comparisons used the Analysis of Variance Test.

RESULTS

As in previous studies, EEG spectral values in the 8-12 Hz frequency band were found to be highest during the eyes closed

condition and to decrease significantly with eyes open. A further attenuated and/or differential modulation was seen during the tracking tests. Tracking test EEG data from some recording sites was fragmented due to a preamplifier design problem that has since been corrected.

The tracking tesks were scored for three categories of "cognitive workload", according to a scale which combined both flight characteristics and actual performance. Thus, both good handling and good performance was rated as low cognitive workload, while bad handling and bad performance was rated as high on this scale. Intermediate performance in an aircraft with medium handling was rated as moderate cognitive workload. However, poor performance in a medium handling aircraft was rated as high, instead. All other combinations were scored as moderate cognitive workload. This classification scale is shown together with performance ranking, aircraft handling characteristics, and Cooper-Harper scores for each pilot and all tracking tesks in Table 1. Tracking tests were ordered according to performance rank in this table.

Table 1. Comparisons of pilot performance, aircraft handling, Cooper-Harper, and Cognitive Workload Scale in four subjects participating in the NT-33 Tracking Study.

	Performance Rank	Handling Character	Cooper-Harper	Cognitive Workload Scale
Subject 1				
Test 6	1	Good	4	Low
Test 1	2	Med	4	Mod
Test 2	2	Bad	6	High
Test 4	2	Bad	6	High
Test 3	5	Good	4	Mod
Test 5	6	Med	6	High
Subject 2				
Test 6	1	Good	3	Low
Test 4	2	Bad	8	Mod
Test 3	3	Good	2	Low
Test 5	4	Med	6	Mod
Test 1	5	Bad	6	High
Test 2	5	Med	7	High
Subject 3				
Test 5	1	Good	3	Low
Test 2	2	Bad	6	Mod
Test 3	3	Med	3	Mod
Test 6	4	Good	5	Mod
Test 1	5	Med	8	High
Test 4	6	Bad	5	High
Subject 4				
Test 4	1	Good	2	Low
Test 1	1	Good	2	Low
Test 5	3	Med	5	Mod
Test 3	4	Med	5	Mod
Test 2	5	Bad	8	High
Test 6	6	Bad	8	High

Available EEG data segments for each tracking test were

sorted into these three categories and evaluated for magnitude and trend characteristics in the 8-12 Hz frequency band. Data for frontal and parietal sites were combined for the evaluation of overall spectral magnitudes for the three categories of cognitive workload. Analysis of Variance followed by Planned Comparison t-tests showed that magnitude was significantly decreased with high cognitive workload (Fig. 1). Average magnitude, however, did not differentiate low from moderate cognitive workload.

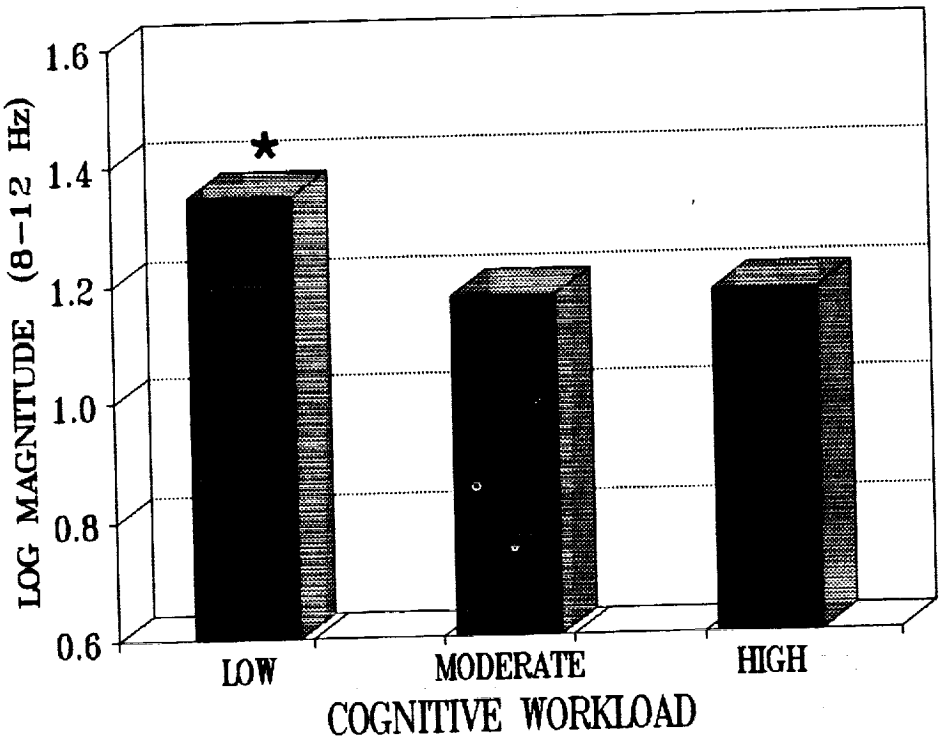

Figure 1. Comparison of mean EEG spectral magnitude values at frontal and parietal sites in the 8-12 Hz frequency band during in-flight tracking tests in four pilots across three categories of "cognitive workload". Activity in the 8-12 Hz band was significantly suppressed during high cognitive workload (* = $p<0.10$).

Trend analysis of parietal EEG data (P4), on the other hand, differentiated 80% of all tracking tests according to this scale. High workload was associated with a pattern of sustained, low 8-12 Hz activity, ofter characterized by transient epochs of further suppression. Moderate workload showed a pattern of initially low 8-12 Hz activity followed by a gradual increment with occasional sharp decrements across the test period. Finally low workload resulted in a pattern of higher 8-12 Hz activity with distinctive modulation across the test period. A representative example of these patterns is shown in Figure 2.

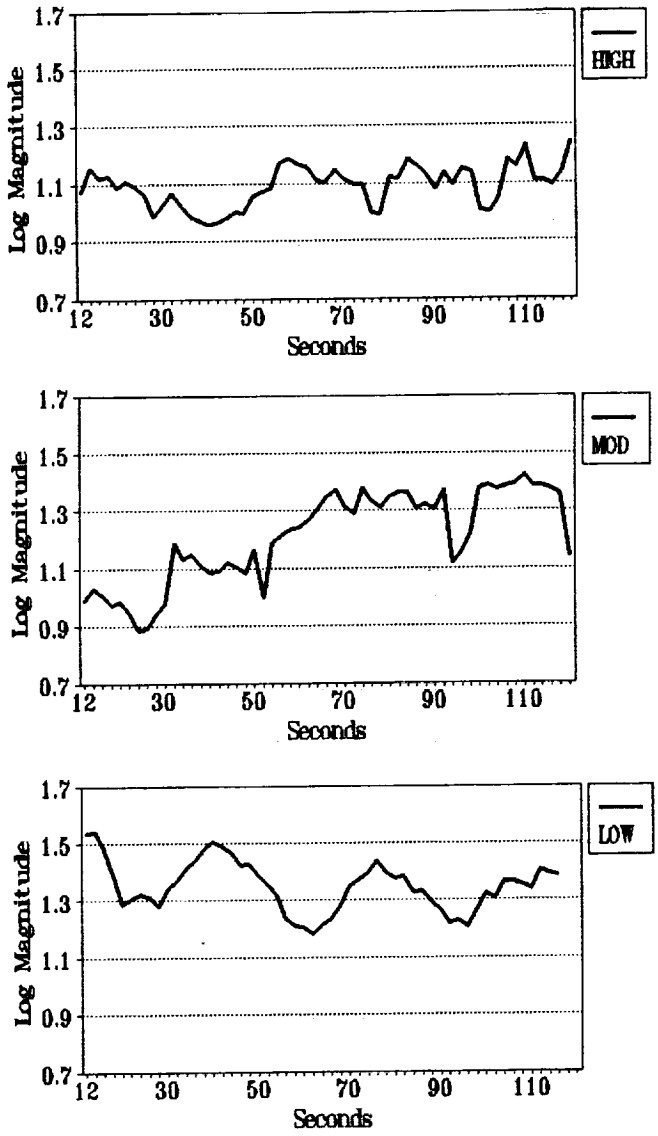

Figure 2. Representative EEG spectral magnitude trends for 8-12 Hz activity at three cognitive workload levels for tracking tasks in the NT-33 aircraft. Data were smoothed by 20 second moving average and are all from right mid-parieatal recording site (P4) in the same pilot. Note magnitude and pattern differences.

DISCUSSION

Collectively, these findings agree with concepts derived from earlier laboratory and in-flight studies (Sterman, et, al, 1988, 1992), and suggest that selected EEG measures may successfully distinguish cognitive workload, at least when a combination of system configuration and performance outcome are the basis for validation. EEG spectral magnitude trends associated with this scale also provided for a meaningful resolution of events during each test. These patterns appeared

to reflect attentional modulation related to target movements and to changes in the pace of target activity. Thus, for low workload situations, increases in parietal 8-12 Hz activity accompanied successful target acquisition and/or reductions in the pace of target movements. With moderate workload, tracking was difficult initially but adaptation to handling characteristics eventually developed, leading to a graded increment in 8-12 Hz activity. Occasional, abrupt reversals were most likely due to transient increases in effort. In the case of high workload such an adjustment was minimal, since the pilot was rarely "caught up", and 8-12 Hz activity remained suppressed. Even at this level of effort additional load was accompanied by further, transient attenuations.

It is important to point out that very few EEG sites were available for analysis in this test. Laboratory simulator studies have shown that dynamic medial-lateral shifts in spectral magnitude occur in certain areas with escalating task saturation (Sterman, et al, 1992), aspects of the EEG which could not be examined with the restricted data acquired here. Despite this limitation, we were able to demonstrate that EEG data could be successfully acquired during demanding tactical flight. Most importantly, however, a combination of magnitude level, trend characteristics, and trend modulation provided a consistent EEG discrimination of workload as defined here. Computer algorithms for pattern analysis are currently being developed to extract this information from the EEG directly in order to provide an integrated metric. Clearly, the limited data obtained here have justified the effort, and will help to guide future studies.

Finally, our approach to the definition of workload may be controversial. Using a concept of cognitive workload, based on both system and human performance, we were able to demonstrate consistent physiological correlates which could lend a needed objective aspect to the somewhat diffuse concept of workload. The sample of subjective ratings reviewed here underscores the shortcomings of existing definitions.

REFERENCES

Andersen, P. and Andersson, S.A. Physiological Basis of the Alpha Rhythm. 1968, Appleton-Century-Crofts, New York.

Berger, H. On the electroencephalogram of man. Journal fur Psychologie und Neurologie, 1930, 40:160-179.

Steriade, M. and Llinas, R.R. The functional states of the thalamus and the associated neuronal interplay. Physiological Reviews, 1988, 68(3):649-742.

Sterman, M.B., Kaiser, D., Mann, C., and Francis, J. Topographic EEG correlates of the Basic Attributes Test for air force candidate selection. In: Proceedings of the Human Factors

Society, 36th Annual Meeting, 1992, Human Factors Society, Santa Monica, California.

Sterman, M.B., Schummer, G.J., Dushenko, T.W., and Smith, J.C. Electroencephalographic correlates of pilot performance: simulation and in-flight studies. In: Electric and Magnetic Activity of the Central Nervous System: Research and Clinical Applications in Aerospace Medicine. AGARD Conference Proceedings No. 432, 1988, North Atlantic Treaty Organization, pp (31)1-16.

Supported by the Veterans Administration, Northrop Corporation, Test Pilot School, Edwards Air Force Base, and the National Aeronautics and Space Administration.

N94-11529

PSYCHOPHYSIOLOGICAL MEASURES OF COGNITIVE WORKLOAD IN LABORATORY AND FLIGHT

Glenn F. Wilson, PhD
Albert Badeau, Major

Armstrong Laboratory
Human Engineering Division
Performance Assessment Branch
Wright-Patterson AFB, OH 45433-6573

ABSTRACT

Psychophysiological data have been recorded during different levels of cognitive workload in laboratory and flight settings. Cardiac, eye blink and brain data have shown meaningful changes as a function of the levels of mental workload. Increased cognitive workload is generally associated with increased heart rates, decreased blink rates and eye closures and decreased evoked potential amplitudes. However, comparisons of laboratory and flight data show that direct transference of laboratory findings to the flight environment is not possible in many cases. While the laboratory data are valuable, a data base from flight is required so that "real world" data can be properly interpreted.

INTRODUCTION

Psychophysiological measures can provide continuous estimates of operator workload in a non-invasive manner. They are relatively easy to obtain and are useful in many situations. In order to fully understand these measures and their relationship to human performance, laboratory experiments are conducted that provide a great deal of control over the subject's environment so that extraneous variables can be eliminated or controlled. This permits us to develop databases and to develop and test theories so that we can understand the basic phenomena. This gives us a framework within which we can collect physiological data in flight and properly interpret it, assuming that there is a direct relationship between laboratory and flight data. This may not be the case, since they are quite different environments. For the past several years we have performed laboratory experiments exploring the realm of cognitive workload so that we would be able to properly use physiological data in the flight environment. By understanding the basic relationships between cognitive workload and physiological responses, we are better equipped to deal with flight data. As reported below, we have had mixed success applying what we have learned in the laboratory to flight. This report will deal with three of the physiological variables that we have extensively investigated in the laboratory and applied to flight. They are cardiac activity, eye blinks and brain activity.

CARDIAC ACTIVITY

Heart rate has a long history of use in psychophysiological research and has been the most widely used physiological measure in flight studies. Since the heart's main function is to provide nutrients and hormones to body tissues and remove metabolic by-products, its activity is controlled by the physical demands of the body. However, cognitive activity, performed by the cerebral cortex, also places demands upon the cardiac system and causes changes in its activity as well. With regard to the cognitive effects, the typical finding is that heart rate increases with increasing cognitive workload. This includes comparing no-task to performing a cognitive task (Molen, Somsen &

Orlebeke, 1985), assessing the effects of increasing task difficulty in single task (McCanne & Hathaway, 1979) and multiple task situations (See Wilson & Eggemeier for a review, 1991).

In our laboratory we have studied the effects of graded changes in cognitive activity produced by changing task difficulty in a standardized task battery. We were unable to reliably find the expected increases in heart rate with increased task loads (McCloskey, 1987; Wilson et al., 1986; Yolton, et, al., 1987). After careful comparison with the literature, it became obvious that there were two important methodological differences between our studies and those in the literature. Both of these have very direct bearing upon the issue of making use of physiological measures in "real world" situations such as flying. The first was that we practiced our subjects to a performance criterion before we collected the physiological data. The second was that our subjects were all accustomed to the laboratory since they served as subjects in many experiments in different laboratories. The studies in the literature typically did not practice their subjects or gave them minimal familiarization with the tasks to be performed and their subjects were naive to the laboratory and laboratory practices. In effect, these subjects were learning the tasks and becoming accustomed to the laboratory as the data were being collected. We performed a study using naive subjects and measured their heart rates while they performed 30 blocks of trials of a mathematics task having two levels of difficulty that was new to them. We found significant increases in heart rate to the difficult level of the task only during the first four blocks of trials and not in the remaining blocks (See Figure 1). Further, there was a significant decrease in heart rate from beginning to end of the three-hour session. These data demonstrate that learning and adaptation to the data collection environment are extremely powerful. This is a crucial variable when collecting data from subjects such as pilots and air crew who are highly over practiced in their jobs and extremely familiar with their work environment. We must beware of interpolating from the standard laboratory data to "real world" environments: the laboratory data may not be at all appropriate to extrapolate to the "real world".

The range of the data and the dynamics of the cardiac system also are different in laboratory and flight environments. We found four to ten percent increases in heart rate for F4 pilots and weapon systems officers (WSOs) when performing a laboratory tracking task compared to a resting baseline. During flight, the pilots' heart rates increased up to 45% and the WSOs up to 35% when engaged in air-to-ground training missions (Wilson & Fullenkamp, 1991). This large discrepancy in percent change suggests that the cardiac system dynamics may well be quite different in these two situations and follow different functions.

The variation of the heart rhythm has been reported to be influenced by cognitive activity (Mulder & Mulder, 1980). Mental activity decreases the variation of the cardiac rhythm, making it more constant from beat to beat. These results are derived from laboratory studies and we tested the utility of heart rate variability (HRV) in flight by examining the HRV in several segments of the F4 study mentioned above (Wilson, 1991). These data included the laboratory tracking task segments and several flight segments including take-off, cruise, bombing range and landing (See Figure 2). We found that the HRV, calculated three ways, provided only either-or information. That is, situations requiring higher levels of mental workload were all associated with the same level of HRV reduction including the laboratory tracking task. The HRV measure was not sensitive to different levels of workload, it was at either one level or the other for all segments, laboratory and flight. Simple heart rate, on the other hand, demonstrated a great deal of sensitivity to

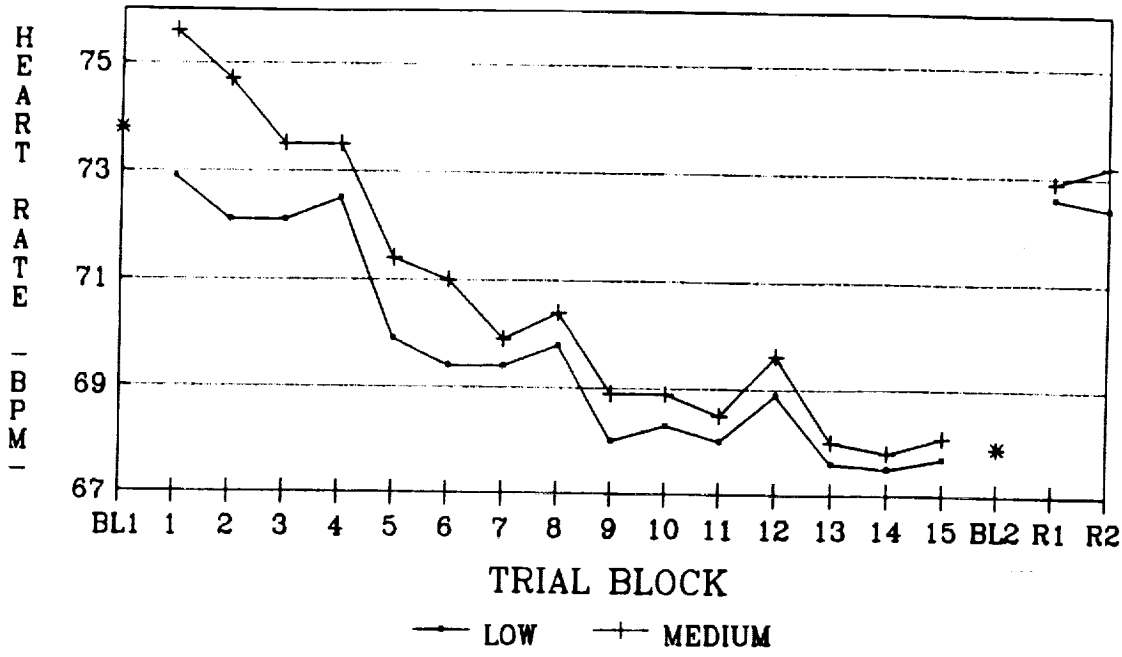

Figure 1. Mean heart rate for eight subjects while performing 15 three-minute blocks of a mathematics task at two levels of difficulty. Pre- and post-task baselines were included.

the several levels of cognitive demand, with the flight segments associated with higher heart rate levels than the laboratory tracking task (See Figure 3). From these data, HRV is not a sensitive measure of mental workload during flight.

EYE BLINK ACTIVITY

The eyes have been called the windows into the soul - this may or may not be true, but the eyes do regulate and process visual input. Blink activity interrupts the flow of visual information so visually demanding situations should decrease blinking and shorten the duration of the blinks (Stern, Walrath & Goldstein, 1984). Preliminary data from a recent sleep loss study in our laboratory showed that blink rate was lowest of the twelve tasks during the tracking task and that blink rate actually increased after the one night of sleep loss.

Blink rates were measured in the F4 study mentioned above and were found to be very low during the laboratory tracking task. In fact, one subject blinked only one time during the two-minute task. However, when compared to the flight data, the laboratory blinks were seen as actually being inhibited. The lowest blink rates during the flight were recorded during the bombing range segments and the rate was approximately three times higher than that found when performing the laboratory tracking task. The laboratory task produced abnormally low blink rates when compared to a very highly visually demanding "real world" task.

In a study with A7 pilots in which they flew three times, once as lead of a four ship formation, once in a wing position and once in a simulator, the shortest blink closures were when they flew in the wing position (Wilson, Skelly, Purvis, Fullenkamp & Davis, 1987). This was no doubt due to the higher visual demands associated with maintaining ship position relative to the lead while the lead position does not demand as much concern about relative position.

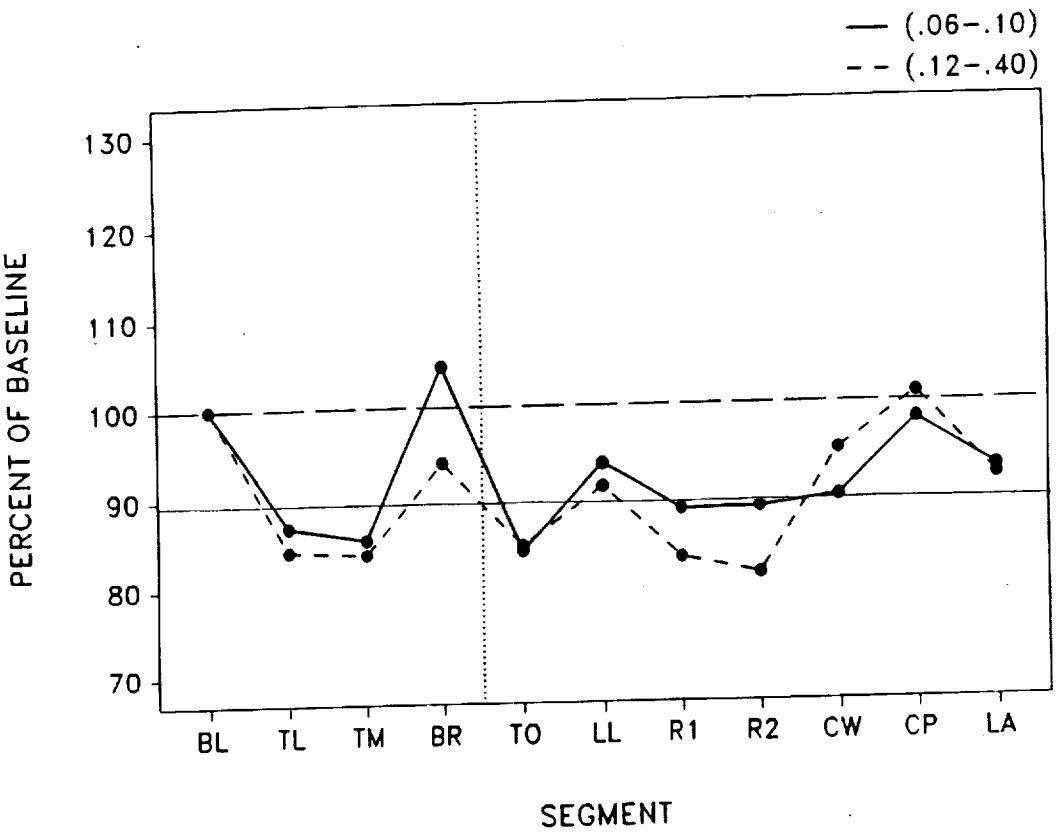

Figure 2. Heart rate variability for the 0.06 to 0.10 Hz and the 0.12 to 0.40 Hz bands from 10 F4 pilots during 11 segments. The solid horizontal line separates the statistically significant values. Note that there are only two groups, which include both flight and ground segments. The segments are listed on the X-axis and are: BL - baseline, TL - low difficulty tracking task, TM - medium difficulty tracking task, BR - preflight briefing, TO - take-off, LL - low level flight, R1 and R2 - bombing range segments, CW - Cruise - WSO flying, CP - cruise - pilot flying, LA - landing.

Further, in a recent study with students at the Air Force Test Pilot School, we found that blink pattern was determined by the nature of the task. The students participated in familiarization flights with radar and infrared detectors. Their job was to detect the radar reflector and identify the individual components of the reflector. Blinks were suppressed during the search and identification phases and occurred after identification or when adjusting equipment. This demonstrates that blink activity can be controlled by the visual demands of the job and long periods of blink inhibition can naturally occur if the operator is engaged in a single task that is visually demanding, such as operating a radar set.

A final example is that of a C-130 transport pilot performing a low altitude parachute extraction (LAPES). During the maneuver, the aircraft is flown very close to the ground and five to fifteen tons of equipment are pulled out of the back of the aircraft with parachutes. This, of course, causes the flight characteristics of the aircraft to change dramatically and very rapidly. This is a potentially dangerous maneuver and is associated with high cognitive workload. Our data, seen in Figure 4, showed that the LAPES was preceded by a slow, regular pattern of blinking with moderate closure durations and the actual LAPES segment itself produced inhibition of blinking for approximately 10 seconds and increased heart rate. Following the LAPES the eye blinks became more normal in pattern and duration.

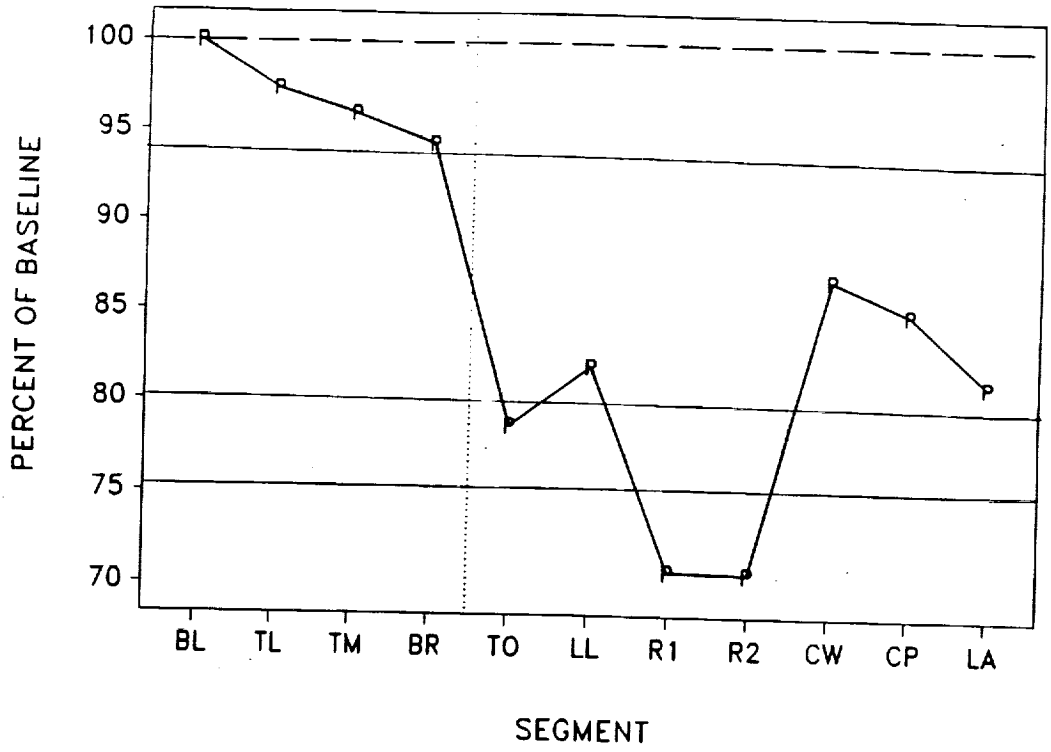

Figure 3. Mean interbeat intervals for 10 F4 pilots. The solid horizontal lines separate segments that are statistically different from one another. Note that there are four groups. The X-axis labels are the same as Figure 2.

These data show that eye blinks are a very good measure of visual demand, with high demand being associated with fewer, faster blinks which reduces the probability of missing important information.

We have used heart rate and eye blinks together to classify flight segments. We took advantage of the unique response patterns of individual crew members to permit classification of the segment of flight. Discriminant analysis was used on the data from each subject to determine the best linear combination of variables to classify the flight segments. We were able to correctly classify the eight selected segments 93% of the time for the F4 pilots and 89 % of the time for the WSOs (Wilson & Fisher, 1991a).

ELECTROENCEPHALOGRAM - EVOKED POTENTIALS

We have used brain evoked potentials to study the changes in brain activity associated with increasing task demands. Evoked potentials are the small changes in the electrical activity of the brain that are associated with processing of information contained in discrete stimuli. We have used standard and topographical methods to follow the time course of the evoked potentials and their topographical distribution over the scalp. The latter involves the recording from 20 electrodes placed over the scalp and using the resulting data to determine the pattern of electrical activity changes over the head as the subject processes information. We have found, in several studies, that the amplitude of the late evoked potential components decreases with increasing task difficulty. We have used several cognitive tasks, including spatial (Wilson, Swain & Davis, 1988), mathematical, linguistic and stimulus degradation tasks (Wilson, Palmer, Oliver and Swain, 1991).

We have also used spectral analysis of the ongoing brain activity to classify the cognitive tasks that the subjects were performing. Discriminant analysis was used to derive linear combinations of the spectral components from 20 electrodes to classify the seven tasks. The data were divided into a training

and test sets and we were able to correctly classify the seven tasks 80% of the time for our eight subjects. This demonstrates that brain activity can be used to determine the nature of the task that subjects are performing (Wilson & Fisher, 1991b). Since it is simple to implement the classifier, it would be possible to perform the classification in real time while the subjects are performing tasks or even flying. This could be a very useful application of brain activity to the determination of operator state in real time.

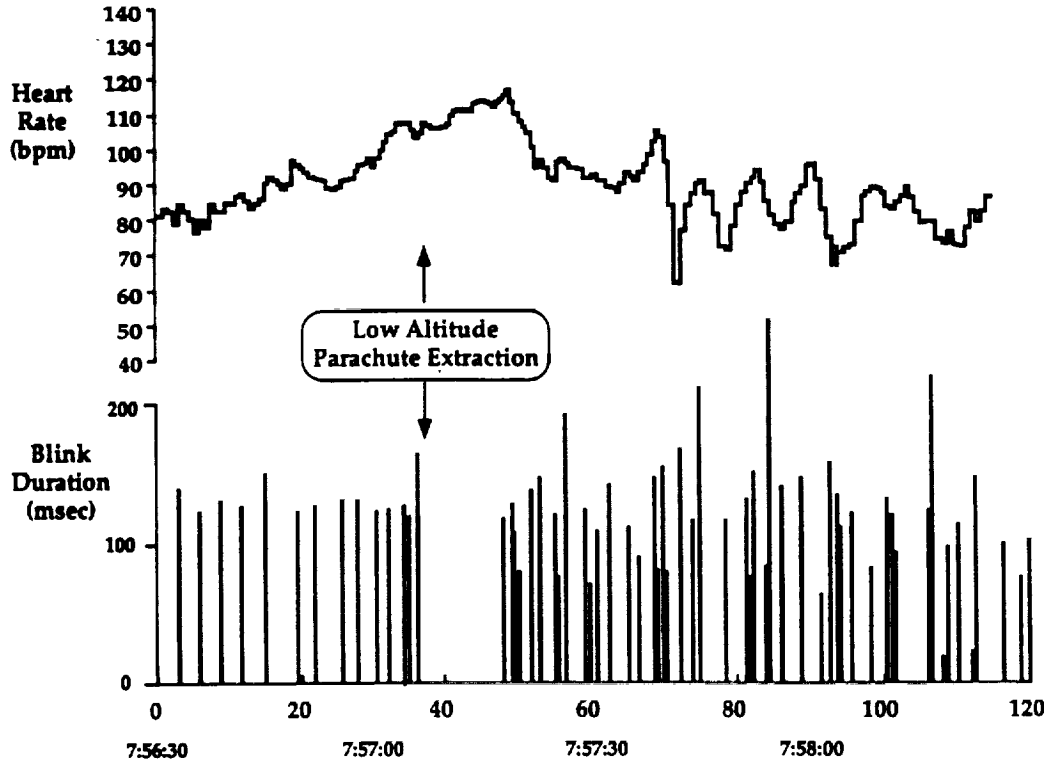

Figure 4. Interbeat intervals, top, and eye blinks, bottom, from a C-130 transport pilot during a low altitude parachute extraction (LAPES). Note that heart acceleration reaches it's maximum following the LAPES. The eye blinks exhibit a regular pattern with even blink durations prior to the LAPES, an inhibition for approximately 10 seconds during the LAPES, followed by a more normal blink pattern following the LAPES.

We have extended the use of evoked potential techniques to the flight environment for the first time (Wilson & Fullenkamp, 1991). Evoked potentials were recorded from pilots while they performed an auditory discrimination task on the ground and while flying. Evoked potentials were recorded during two cruise flight segments (Figure 5). During one segment the pilot was actually flying the aircraft and during the other the WSO was flying the aircraft. The main objective was to demonstrate that evoked potentials could be recorded during flight and the secondary objective was to see if the evoked potentials would provide information concerning the mental workload of the pilots. The first objective was met as was the second. Evoked potentials were recorded and it was found that one component of the evoked activity, the P2, was significantly reduced while the pilot was actually flying the aircraft compared to the ground segment and the other flight segment when the WSO was actually flying and the pilot was primarily a passenger. This opens up the flight environment to the use of evoked potentials as a measure of cognitive activity during the different aspects of flight.

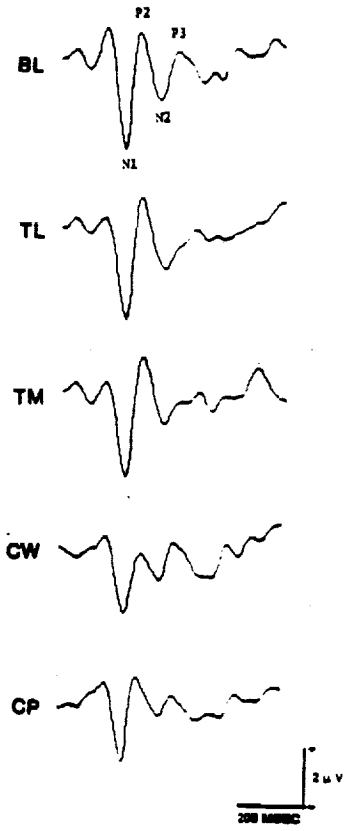

Figure 5. Averaged evoked potentials from auditory stimuli from seven F4 pilots during five segments. The four measured components are labeled, two positive and two negative. The conditions were BL - baseline, tone only, TL - low tracking difficulty, TM - medium tracking difficulty, CW- Cruise, pilot flying, CP - Cruise, WSO flying.

SUMMARY

Laboratory data is required to develop methods and theories of cognitive workload and to develop a database. However, these measures and methods must be validated in "real world" situations, such as flight, so that their applicability to these situations can be tested since all of them will not be useful in the "real world." The examples cited above of blink rate and heart rate demonstrate that laboratory data may not be at all applicable to the "real world." The difference in operator experience and the dynamic range of the physiology means that flight databases must be developed in order to provide a milieu in which flight data can be interpreted. The collection of physiological data during flight is not the problem, the concern now is having a large enough database to provide for proper interpretation.

REFERENCES

McCanne, T. R. & Hathaway, K. M., Autonomic and somatic responses associated with performance of the Embedded Figures Test, Psychophysiology, 1979, 16, 8-14.

McCloskey, K., Evaluating a spatial processing task using EEG and heart rate measurements, Proceedings of the Human Factors Society, 1987, 74-77.

Molen, M. W., Somsen, R. J. M. and Orlebeke, J. F. The rhythm of the heart beat in information processing. In Ackles, P. K., Jennings, J. Richard and Coles M. G. H. (Eds.), Advances in Psychophysiology, 1985, 1- 88.

Mulder, G., and Mulder, L. J. M., Coping with mental workload, in Levine, S. and Ursin, H. (Eds.), Coping and Health, 1980, New York: Plenum Press, pp.233-58.

Stern, J. A., Walrath, L. C. and Goldstein, R. The endogenous eyeblink, Psychophysiology, 1984, 21, 22-33.

Wilson, G. F. The use of heart rate and heart rate variability to measure workload in F4 pilots and WSOs during training flights and a tracking task. Aviation Space and Environmental Medicine, 1991, 62, 450.

Wilson, G., McCloskey, K. and Davis, I. Linguistic processing: Physiological, performance and subjective correlates. Proceedings of the Human Factors Society, 1986, 72-75.

Wilson, G. F., Purvis, B., Skelly, J., Fullenkamp, P. and Davis, I. Physiological data used to measure pilot workload in actual flight and simulator conditions, Proceedings of the Human Factors Society, 1987, 779-783.

Wilson, G. F., Swain, R. A. and Davis, I. Human event-related potentials during spatial processing: A topographical distribution. Society for Neuroscience Abstracts, 1988, 1014.

Wilson, G. F. and Eggemeier, F. T. Psychophysiological assessment of workload in multi-task environments. In Damos, D. (Ed.), Multiple-task Performance, London, Taylor & Francis, 1991,329-360.

Wilson, G. F. and Fisher, F. The use of cardiac and eye blink measures to determine flight segments in F-4 crews, Aviation Space and Environmental Medicine, 1991a, 62, 959-962.

Wilson, G. F. and Fisher, F. Cognitive task classification using EEG spectra, Psychophysiology, 1991b, 28, S62.

Wilson, G. F. and Fullenkamp, P., A comparison of pilot and WSO workload during training missions using psychophysiological data. Stress and Error in Aviation, Volume II, 1991, 27-34.

Wilson, G. F., B. Palmer, C. Oliver and Swain, R. Topographical Analysis of Cognitive Task Difficulty. Brain Topography, 1991, 3, 45.

Yolton, R. L., Wilson, G. F., Davis, I. and McCloskey, K. Physiological correlates of behavioral performance on the mathematical processing subtest of the CTS battery. Proceedings of the Human Factors Society, 1987, 770-773.

TRANSFER OF TRAINING FOR AEROSPACE OPERATIONS: HOW TO MEASURE, VALIDATE, AND IMPROVE IT

Malcolm M. Cohen, Ph.D.
NASA-Ames Research Center
Moffett Field, CA 94035-1000

ABSTRACT

It has been a commonly accepted practice to train pilots and astronauts in expensive, extremely sophisticated, high fidelity simulators, with as much of the real-world feel and response as possible. High fidelity and high validity have often been assumed to be inextricably interwoven, although this assumption may not be warranted. The Project Mercury rate-damping task on the Naval Air Warfare Center's Human Centrifuge Dynamic Flight Simulator in Warminster (Johnsville), Pennsylvania, the shuttle landing task on the NASA-Ames Research Center's Vertical Motion Simulator at Moffett Field, California, and the almost complete acceptance by the airline industry of full-up Boeing 767 flight simulators for transition training of airplane captains, are only a few examples of this approach. For obvious reasons, the classical models of transfer of training have never been adequately evaluated in aerospace operations, and there have been few, if any, scientifically valid replacements for the classical models. This paper reviews some of the earlier work involving transfer of training in aerospace operations, and discusses some of the methods by which appropriate criteria for assessing the validity of training may be established.

Introduction

Effective functioning of aerospace systems critically depends on how well the operator can be trained to perform his relatively complex tasks under the unique environmental conditions encountered in space operations. Human factors considerations in the design of aerospace systems, while acknowledged to be extremely important, have frequently taken a back seat to the adaptability and the great capacity of the operators to learn how to control complex systems. For example, the space shuttle is operated, and must function effectively, during launch, orbital flight, re-entry, and landing. Although the control characteristics of the vehicle change dramatically under these different segments of the flight profile, the operator must be trained to make the system function effectively under all conditions. Extensive, and expensive, training has traditionally been used to help the operator learn how to perform appropriately.

Training and Transfer of Training

Probably, the most important aspect of any training program that should be evaluated to determine its efficacy is the phenomenon known as "transfer." Transfer of training occurs whenever the performance on one task has an effect, either beneficial or detrimental, on the performance of another task that is performed subsequently. Positive transfer results when performance on the initial task leads to improved performance on a subsequent task; negative transfer results when performance on the first task has a detrimental effect on performance of the second task. (1,2)

To quantify the amount of transfer between two tasks, researchers generally obtain a score based on the initial performance of the second task for those individuals who had previously practiced the first task, and compare the score with the score of initial performance on the second task obtained from individuals who did not practice on the first task. A criterion for the amount of practice, or the degree of mastery, on the first task is usually specified in advance. Traditionally, the scores are based on the amount of practice needed to reach the criterion, e.g., speed of performance, accuracy of performance, a combination of speed and accuracy, or some other stable measure that can be used to characterize the performance on each task. (3)

Measuring Transfer of Training

Two classical means of specifying the amount of transfer involve the concepts of savings and transfer effectiveness. For example, consider a case where individuals require an average of ten hours of actual flight time to achieve adequate proficiency for them to fly their first solo. If one hour of practice in a ground-based simulator (i.e., first task) allows a

similar group of individuals to solo after only 8 hours of flight time (second task), we see that there is a savings of 2 hours of flight time.

Expressed quantitatively,

$$S = T_{(t2:t1=0)} - T_{(t2:t1)}$$

Where S is the savings, $T_{(t2:t1=0)}$ is the time required to master task 2 given no practice on task 1, and $T_{(t2:t1)}$ is the time required to master task 2 given previous practice on task 1. The effectiveness of transfer between training in the ground-based simulator versus the actual aircraft can be expressed as a ratio of the difference between flight time needed for the control group (flight practice only) and the training group (simulator and flight practice), relative to total simulator time.

Expressed quantitatively,

$$TE = [T_{(t2:t1=0)} - T_{(t2:t1)}] / T_{(t1)}$$

where TE is the training effectiveness ratio, $T_{(t2:t1=0)}$ is the time required to master task 2, given no practice on task 1, $T_{(t2:t1)}$ is the time required to master task 2, given practice on task 1, and $T_{(t1)}$ is the time actually spent on task 1.

In the example given, we have 10 hours of flight time needed for the control group [$T_{(t2:t1=0)}$] minus 8 hours of flight time needed for the group who had trained on the simulator [$T_{(t2:t1)}$], divided by 1 hour of time in the simulator $T_{(t1)}$. This yields a transfer effectiveness ratio of 2, which means that the one hour spent in the simulator provided training that was as effective as two hours in the actual aircraft. From a practical perspective, this makes good sense, because much time is often wasted in the aircraft before it is can be used for training. For example, to learn techniques for recovery from a stall, the student pilot must be at sufficient altitude over an appropriate practice area, and it takes time to get there in an aircraft.

Because gains in performance that are achieved from practice usually decrease over time (i.e., learning is a negatively accelerating function), the transfer effectiveness ratio also decreases with increasing time spent in practice. When the transfer effectiveness ratio declines to 1.0, there is no training advantage to be obtained from additional use of a simulator or training device, although there still may be other significant advantages.

If, for example, training in an aircraft costs three times as much as training in a simulator, there will still be a financial advantage in using the simulator until the training effectiveness ratio declines to 1/3.

Predicting Transfer of Training

As a general rule, the more similar two tasks are, the more likely it is that they will interact with one another. Further, the beneficial or detrimental nature of the resulting transfer between two tasks usually depends on the similarity of the displays (stimulus conditions) and on the similarity of the controls (required responses) in the two tasks. (4) Four cases may be distinguished: (5)

Case 1 - HiHi Where the displays and controls on both the initial and the subsequent tasks are so similar that they are practically indistinguishable from one another, transfer will usually be both large and positive; learning to perform the first task can provide the equivalent of an opportunity to practice on the second task. For example, learning to fly in a particular aircraft, and then attempting to fly another aircraft of the same type would have extremely high positive transfer. Another example would be to fly a high-fidelity simulator of the aircraft as the first task.

Case 2 - LoLo Where the displays and controls on the initial and subsequent task differ dramatically from each other, there is generally little transfer of training between them. For example, learning how to play a piano probably will not help someone to learn how to fly an airplane.

Case 3 - LoHi Where the displays are different, but the controls on the two tasks are similar, transfer of training is usually positive (but much less effective than in Case 1). This would generally be the case where one initially learns to fly in one type of aircraft, and subsequently attempts to fly a different type of aircraft.

Case 4 - HiLo This case is somewhat more complex than the other three cases cited. Where the displays are similar, but the controls are different, either weak positive transfer or negative transfer may occur. The weak positive transfer could result when the displays are highly similar, but the controls are so different that confusion between them would be very unlikely; an example would be that occasioned by a flashing red light when driving an automobile (apply the brakes), or a flashing red

light indicating the failure of a landing gear to have locked (recycle the lowering of the gear). The major advantage of training in this type of situation may lie in having the individual learn to pay careful attention to the appropriate stimulus display. In contrast, if the controls are not only different, but conflicting, negative transfer would be expected. This would be the case where two aircraft have similarly appearing control levers that are placed in the same location in the cockpit, but with different resulting functions (e.g., flaps and throttle levers in reversed positions in two different aircraft). Learning to fly the first aircraft could interfere with subsequent flying of the second aircraft (and it could lead to a major accident).

The Use of Simulators in Training

Simulators, and other training devices, have been widely used throughout the aviation industry, but their use in the space program had been different, at least until recently. Generally, commercial pilots and aircrew were given extensive opportunity to practice their skills in the operational system before they were officially required to perform in actual operations. Further, transfer of training could be determined in checkout flights, and the efficacy of specific training programs could be evaluated in depth. Recently, however, the use of high-fidelity simulators for training has received such wide acceptance by the aviation industry that, following an authorized training program on a high-fidelity simulator of some new commercial passenger aircraft, the very first flight of a pilot-in-command can often be a revenue flight. This relatively recent development in commercial aviation parallels the training of astronauts, which usually demands that the first flight after training be an operational mission, providing little or no opportunity for additional training. The aviation industry is now using a technique that was originally developed in the space program.

If we consider the conditions under which astronauts are generally expected to perform in space missions, we find that both the displays and controls for training specific operational tasks can often (but not always) be made to be highly similar. This type of condition corresponds to Case 1 - HiHi, discussed previously, and yields a high degree of transfer of training.

A particularly relevant application of this training paradigm was used in the early days of manned space flight, when the original astronauts of project Mercury experienced realistic acceleration profiles, and performed control tasks in a Mercury capsule that was mounted in the (Johnsville) Naval Air Development (now, Naval Air Warfare) Center's human centrifuge. (6,7) The centrifuge was used as a dynamic trainer for a re-entry rate damping task, largely because it added realistic acceleration cues to the instrument displays; it also was used to train the astronauts in sequence monitoring and emergency procedures during simulated launch and re-entry profiles. Following their high-fidelity simulation training, the astronauts mastered the necessary skills, and were considered to be well prepared to function in the actual operational environment.

Similarly, the shuttle landing simulations conducted at Ames Research Center over the past several years (8) have also taken advantage of this general approach to training. A realistic mock-up of the shuttle cockpit, mounted in the Vertical Motion Simulator (VMS), was used to train astronauts to land the shuttle under various conditions, including reduced visibility approaches, high cross-winds, and steering mechanism failures upon landing. Before any shuttle pilots ever performed an actual landing in the shuttle itself, they had already experienced several landing scenarios in the VMS. As a result of their performance on the VMS, they were regarded as well prepared to perform effectively in the actual shuttle landings.

Cost versus Validity of Simulators

The major cost of striving to attain a large degree of transfer of training in high-fidelity simulators is actual financial cost. Since we know that high display and control similarity leads to the best transfer of training, we sometimes go overboard in insisting that a training simulator must have high face validity or unnecessarily high fidelity in representing the actual vehicle. In addition, the financial payoffs for the simulator manufacturers lie in providing the most advanced state-of-the-art devices. The pull of the user community for more and more sophisticated simulators as training devices, coupled with the push of the manufacturer to provide all of the "bells and whistles" often combine to drive simulator costs ever higher. Although true validity of training and high fidelity of training devices are often related, they are definitely separable. This is an area where considerable research needs to be done, both to reduce costs, and to establish how much high

fidelity is actually needed to produce the best transfer of training.

Limitations of Ground-based Simulation

If one wishes to train an astronaut to function effectively in the space environment, it is not always possible to make both displays and controls (i.e., stimulus conditions and required responses) sufficiently similar here on Earth to expect a high degree of positive transfer. For example, attempting to don or doff a space suit on Earth versus in orbit probably involves both similar and different stimulus conditions that are coupled with similar and different motor responses. The issue of donning or doffing a space suit on Earth and in orbit leads to obvious questions regarding how one should go about training astronauts to perform effectively in different environments.

Skylab experiment M-151 provides an excellent case in point. The time required to don a space suit on Earth initially was between 900 and more than 1400 seconds. With practice, this time was reduced to between 800 and 850 seconds. The time required to don a space suit in orbit initially shows a dramatic increase when compared against the preflight times following practice on Earth, with an initial value for the first donning in orbit around 1000 to 1100 seconds. Subsequent attempts in orbit lead to significantly improved performance, and eventually, some of the astronauts even perform better in orbit than they ever did on Earth, with times as low as 669 and 740 seconds. (9)

Although this study was not directed towards evaluating transfer of training between the terrestrial and orbital environments, it is clear that the initial *apparent* disruption of performance in orbit could have been due to three of the four possible cases of transfer of training that we discussed previously. First, the task of donning a space suit in orbit could have been disrupted by attempts to don the suit on the ground; i.e., there was negative transfer between the two tasks such that the techniques acquired on Earth interfered with the techniques required to don the suit in orbit (Case 4, with negative transfer). A second possible explanation is that the two tasks were so very different from one another that donning the suit on the ground had no effect on donning the suit in orbit and, had the subjects never practiced on the ground, the same results would have been obtained in orbit; i.e., there was no transfer between the two tasks (Case 2). A third possible explanation is that there was positive transfer of training from ground-based results to orbital donning of the suit, and that the apparent disruption in orbit would have been significantly greater than that actually obtained if the terrestrial practice in donning the suit had not been undertaken (Case 3).

If control groups were used, and donning times were obtained in orbit for individuals who did not practice on the ground, it would have been possible to evaluate the alternatives discussed above. From a practical point of view, however, it is not likely that mission planners would have an astronaut don a space suit for EVA for the very first time in orbit without any opportunity to practice the task before he/she gets there. As a result, this issue may have to remain unresolved for some time. Nevertheless, because there was an apparent initial disruption of performance in orbit, it is clear that the task of donning the space suit on the ground is not the same as that of donning the suit in orbit (i.e., not Case 1).

To describe a complex task, such as donning a space suit on Earth, and then to compare it with the task of donning the same suit in microgravity, requires the specification of differences in both stimuli and responses (displays and controls) under both terrestrial and space conditions. Although the complexity of the task, and the lack of a theoretical model with which to characterize the relationships between stimuli and responses make the solution of this problem extremely difficult, the general approach remains feasible.

A similar approach that has been used frequently is to attempt to create a training environment that is similar to the operational environment in which the subjects are expected to perform. Under such conditions, a high degree of stimulus similarity can be expected, and if the training task itself is similar to the operational task, then a high degree of transfer might also be expected. Unfortunately, as the next example illustrates, this approach does not always work as well as might be desired.

The value of underwater training to simulate the effects of microgravity had been strongly supported for EVA space assembly tasks such as those initially proposed for Space Station Freedom; further, the Soviet cosmonauts who were to perform EVAs in missions on Mir were also given extensive underwater training. It was believed that this approach, coupled with work on air-bearing platforms, would be appropriate for training astronauts in the satellite

recovery tasks such as those that were required for STS-49. Apparently, the inertial and viscous damping characteristics of the underwater environment, and the limited degrees of freedom for movements on the air-bearing platforms, were sufficiently different from the conditions encountered in space that the training was not fully adequate to prepare the astronauts for their tasks in STS-49. For example, continuous reactive rotational movements of the astronauts are difficult to initiate under water, but they are relatively easy to stop; in space these movements are extremely easy to initiate, but they are very difficult to stop. Similarly, air-bearing platforms will not respond to forces that are applied orthogonally to their surfaces; no such "null-planes" are present in space. The delays and difficulties in retrieving the satellite appear to have been at least partially due to the inadequacy of the underwater training.

In fact, based on the available evidence, the actual value of the underwater training for STS-49 cannot be fully determined. As was previously noted in the context of Skylab experiment M-151, we have no means to establish how good the astronauts' performance would have been without the underwater training. Thus, although it is clear that underwater training on the satellite recovery task did not completely prepare the astronauts for performing the task in orbit, it could have been of value, or it could have actually provided negative transfer by having the astronauts master techniques that relied on viscous damping and other characteristics of the underwater environment that were not available in orbit. Nevertheless, the flexibility and the perseverance of the astronauts allowed for successful completion of their mission despite possible inadequacies in their training.

Space in Little Pieces: The Value of Training in Microgravity

For the training of astronauts, there is probably no better way than parabolic flight in the KC-135 or similar aircraft to familiarize them with the kinds of problems that they will encounter in space.

Although the duration of any single parabolic phase is too brief for the conduct of a complex task, such as donning a space suit, parabolic flight does provide a close approximation of the microgravity conditions encountered in space. Further, the appreciation of the value of parabolic flight as a technique for training astronauts to function appropriately in the microgravity environment of space is a relatively recent phenomenon. At Johnson Space Center, the KC-135 aircraft has been used to fly "zero-gravity" parabolas. The astronaut trainees have taken advantage of the 20 to 30 seconds of "weightlessness" that are produced in this aircraft to practice on critical tasks that they are expected to perform in orbit. It is now generally believed that, if practice is restricted to the hypogravity phases of parabolic flight, the astronauts will be able to master new techniques that would have been extremely difficult, if not impossible, to learn on the ground. (10)

Similarly, operational tasks to be performed in orbit, such as obtaining blood samples, conducting surgical procedures, operating control devices, attaching sensors, implementing various experimental protocols, or donning a space suit, are now practiced, part by part, during the brief periods of hypogravity achieved in parabolic flight. By performing small individual segments of the task in hypogravity, and combining segments across multiple parabolas, astronauts are believed to achieve a high degree of proficiency before they actually enter orbit. Thus, the cumulative effects of training across several hypo-gravity phases of a series of parabolas probably can be extremely useful, particularly if the training is done systematically.

Validating and Improving Transfer of Training: A Reasonable First Step

Unfortunately, as was the case with the centrifuge simulations of the Mercury launch and reentry profiles at Johnsville, the shuttle landing simulations on the VMS at Ames, and the underwater training in the WETF at JSC, there has been little scientific evaluation or documentation of the value of the training methods described above. Despite the adoption of these general techniques throughout the aerospace industry, the choice and use of simulations remains more art than science.

Recently, and particularly within NASA, it has become a popular dictum that it is impossible to manage something unless one is able to measure it. As far as transfer of training is concerned, we know how to measure it. Nevertheless, as a rule, we do not do so. Without measures of transfer of training, there are no ways to validate the training or to improve it. Thus, one of the most important tasks that currently lies before the training community is to provide measures of transfer of training that can be used for validating and improving the training.

An important, and reasonable, first step in substantiating the already common use of parabolic flight in training astronauts could be to revisit Skylab experiment M-151. That study was discussed here as a demonstration of the value of microgravity in training; it should be repeated, but with a new twist. In this case, we could have astronauts train in donning a space suit either on the ground or in the hypogravity phase of parabolic flight. If the previously reported disruption occurs following ground-based training, but not following parabolic flight training, the practical value of parabolic flight for training purposes will have finally been appropriately documented.

References

1. Holding, D.H. (1977) Transfer of Training. In: R.A. Schmidt and E.A. Fleishman (Eds.) Section IX: Psychomotor learning and performance. In: B. B. Wolman, (Ed.) International encyclopedia of neurology, psychiatry, psychoanalysis and psychology. New York: Van Nostrand.

2. Holding, D.H. (1981) Human Skills. New York: John Wiley & Sons.

3. Holding, D.H. (1987) Concepts of training. In: G. Salvendi (Ed.) Handbook of Human Factors. New York: John Wiley & Sons. pp. 939-962.

4. Osgood, C.E. (1949) The similarity paradox in human learning, a resolution. *Psychological Review.* 56:132-143.

5. Holding, D.H. (1965) Principles of Training. Oxford, England: Pergamon Press.

6. Voas, R.B. (1961) Project Mercury: Astronaut Training Pro-gram. In: B.E. Flaherty (Ed.) Physiological Aspects of Space Flight. New York: Columbia University Press. pp. 96-116.

7. Chambers, R.M. & Nelson, J.G. (1961) Pilot performance capabilities during centrifuge simulations of boost and reentry. *American Rocket Society Journal.* 31:1534-1541.

8. Nguyen, V.H., Nishimi, J.T., Payne, T.H., & Woosley, E.W. (1990) Space shuttle descent flight verification by simulation: A challenge in implementing flight control system robustness. AGARD Conference Proceedings CP-489: Space vehicle Flight Mechanics. Neuilly sur Seine, France: North Atlantic Treaty Organization. pp. 9-1 - 9-17.

9. Kubis, J.F., McLaughlin, E.J., Jackson, J.J., Rusnak, R., McBride, G.H., & Saxon, S.V. (1977) Task and work performance on Skylab missions 2, 3, and 4: Time and motion study - Experiment M151. In: R.S. Johnson & L.F. Dietlein (Eds.) Biomedical results from Skylab. Washington: National Aeronautics and Space Administration. pp. 136-154.

10. Cohen, M. M. Perception and action in altered gravity. *Annals New York Academy of Sciences,* 1992, 656:354-362.

Session H2: HUMAN PERFORMANCE MEASUREMENT II—COGNITION AND PROBLEM SOLVING RESEARCH

Session Chair: Tandi Bagian

N94-11531

Signal Detection Theory and Methods for Evaluating Human Performance in Decision Tasks.

Kevin O'Brien
(primary contact)
Lockheed Engineering & Sciences Co.
2400 NASA Road 1
C95
Houston, Tx. 77058-3711
(713) 333-7130

Evan M. Feldman
Rice University
Department of Psychology
P. O. Box 1891
Houston, Tx. 77251
(713) 527-8101 ext. 2216
emfeld@ricevm1.rice.edu

Signal Detection Theory (SDT) can be used to assess decision making performance in tasks that are not commonly thought of as perceptual. SDT takes into account both the sensitivity and biases in responding when explaining the detection of external events. In the standard SDT tasks, stimuli are selected in order to reveal the sensory capabilities of the observer. SDT can also be used to describe performance when decisions must be made as to the classification of easily and reliably sensed stimuli. Numbers are stimuli that are minimally affected by sensory processing and can belong to meaningful categories that overlap. Multiple studies have shown that the task of categorizing numbers from overlapping normal distributions produces performance predictable by SDT. These findings are particularly interesting in view of the similarity between the task of categorizing numbers and that of determining the status of a mechanical system based on numerical values that represent sensor readings. Examples of the use of SDT to evaluate performance in decision tasks are reviewed. The methods and assumptions of SDT are shown to be effective in the measurement, evaluation, and prediction of human performance in such tasks.

INTRODUCTION

The purpose of this paper is to discuss the relevance of Signal Detection Theory (SDT) to the evaluation of human decision making. SDT is typically thought of in terms of observers detecting faint, experimental stimuli in the hopes of revealing something about the sensory system of the observer. Such an experiment takes advantage of only a part of the information SDT can provide and assumes that SDT is only applicable to describing sensory functions. This paper will review the scope of SDT and report specific examples of application of SDT to more cognitive tasks.

The contribution of SDT is its attempt to explain detection performance by taking into account both the sensitivity and the response bias of the observer. An observer, say a fighter pilot, is aware of an object in the distance. As the distance between the pilot's craft and the perceived object decreases, the pilot's ability detect an object would be expected to increase. In addition, the pilot would be expected to more accurately identify the object as a hostile aircraft, simply a dark spot in clouds, or as some other uninteresting object. The pilot's decision that an object is a hostile aircraft is also a function of willingness to report a target and in doing so to risk sounding a false alarm. SDT offers explanations for the difficulty encountered in detecting or discriminating objects, and how a criterion for responding is established. SDT has contributed greatly to the revitalization of interest in the study of psychophysics, but the theory and methods are not limited to the study of sensory stimuli.

This research was performed under contract from the National Aeronautics and Space Administration, Johnson Space Center. The research was conducted in the Human-Computer Interaction Laboratory in the Flight Crew Systems Division at Johnson Space Center. Marianne Rudisill was the manager of the laboratory.

Psychophysics is the study of the relationship between physical events and the resulting mental events. Two basic questions are asked: does a physical event result in a mental event, and do incremental changes in physical events result in equal increments in mental events. For example, can the observer detect the onset of a single pixel on a dark computer screen? Can the observer tell the difference between the onset of one pixel and two pixels? These questions address the sensitivity of the visual system, the readiness of the observer to report an event, and the scale of perceptual change.

In psychophysics we often assume that the observer could appropriately assign a response to the event if only the event could be clearly sensed. On the other hand, some events that are clearly sensed are difficult to assign to a response. Classification of a bat as a mammal or a bird would be difficult on the basis of a limited set of information because so many of the obvious characteristics of the bat seem to match those we attribute to bird. While SDT has always been used to understand sensory tasks, SDT methods are becoming more widely used in addressing classification tasks. Swensson (1980) used SDT to describe the performance of radiologists in interpreting chest x-rays. Swets (1988) argued for the use of SDT methods in measuring the accuracy of diagnostic systems providing examples from the medical field, weather forecasting, and materials testing. Parasuraman and Wisdom (1985) suggest the use of SDT to evaluate the rules of expert systems and as a guide for designing systems in which automated expert systems assist human operators. Sorkin and colleagues (Sorkin & Woods, 1985, Sorkin & Robinson, 1984, Sorkin, Kantowitz, & Kantowitz 1986) have dealt with the issue of automated expert based alarms in system control environments. In each of these cases, SDT is applied to problems of categorizing easily detected information as being either meaningful or inconsequential. SDT can be used to describe the process by which one category is distinguished from another and how response biases affect responding. The body of this paper details the applicability of SDT to these problems and describes the use of SDT methods to examine the processing of multiple sources of information.

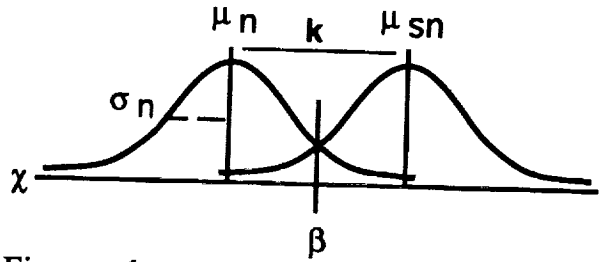

Figure 1. Hypothetical probability distributions for noise (n) and signal-noise (sn).

SDT: THEORY, METHODS, & METRICS

Theory

SDT attempts to account for differences in sensitivity and response bias starting from the assumption that uncertainty surrounds the processing of an event. Uncertainty is present because a variable level of background noise surrounds every interesting event, or in SDT terms, signal. Borrowing an example from Baird and Noma (1978), consider the circumstance that you are listening to the stereo and the phone rings. The sound from the stereo is background noise and the phone ring is the signal of interest. The more distinct the signal is from the noise, the more likely the signal, in this case the ringing phone, will be detected. Uncertainty arises from the fact that on some occasions what you have heard could as easily be attributed to the stereo alone as to the ringing phone with the stereo in the background.

Figure 1 helps us to think of the uncertainty of detecting a signal in a more detailed manner. The continuum χ is the evidence gathered by the observer from some event. The noise present at any given time is expected to be a random observation from a distribution of noise events having a mean μ_n and a variance σ_n. The presence of a signal along with the noise adds a constant, k, to the values in the noise distribution resulting in the signal-noise distribution with a mean μ_{sn} and variance equal to that of the noise distribution. As can be seen in the figure, intermediate levels of evidence are included under the distributions for both the noise and signal-noise distributions; and therefore, the

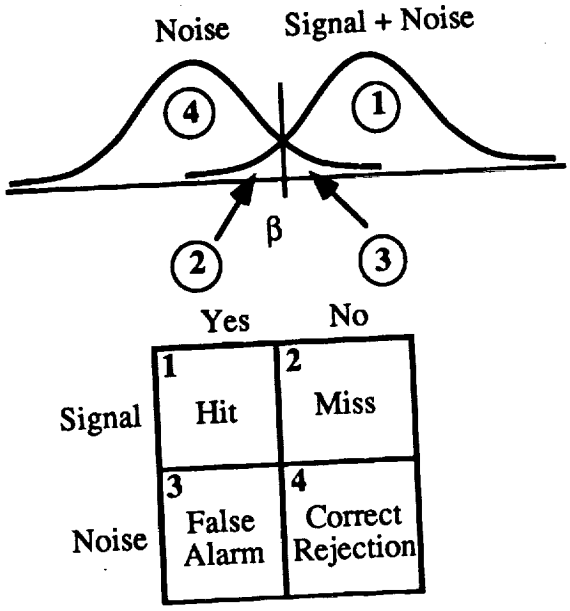

Figure 2. The response criterion, β, separates the noise and signal-noise distributions into four response categories: hit, miss, false alarm, and correct rejection.

assignment of evidence to one distribution or the other is uncertain. The more variable the noise or the smaller the change introduced by adding the signal, the more uncertain the assignment of intermediate levels of evidence to one distribution or the other.

Two additional factors affect the observer's response selection: the establishment of a response criterion and the likelihood of a signal occurring. When an observer establishes a fixed response criterion, β, responding "yes" to evidence above β and "no" to evidence equal or below, responses are relegated to one of four categories (see Figure 2). Responding "yes" will result in either a correct detection (**hit**) given that a signal was present or a **false alarm** given only noise. Responding "no" will result in either a **correct rejection** given noise or a missed (**miss**) signal given the presence of a signal. An optimal placement of β would minimize the likelihood of false alarms and misses while maximizing the number of hits and correct rejections. Alternative criteria are possible. In the example of the ringing phone above, if one were expecting a very important call (but not important enough to turn off the stereo!) one would be more willing to risk picking up the phone when it hadn't rung (false alarm) than miss a real call. This liberal strategy would move β to the left on the χ axis. A conservative strategy would move β to the right and result in the commission of few false alarms at the expense of missing some calls. Varying the costs and benefits of different responses alters the placement of β by an observer. The likelihood of a signal also alters the response selection of the observer. Up to this point we have been assuming that the chance of a signal was equal to that of noise alone. On the other hand, as the likelihood of a signal declines from 50% to 10%, we would expect to see a similar reduction in the number of yes or signal present responses.

In summary, SDT is based on the assumption that there is uncertainty regarding the classification of an event. That uncertainty is related to the variability of noise and the resulting overlap between the noise and signal-noise distributions. Ability to detect the signal in noise increases as the overlap of the distributions decrease. Responding is also affected by response bias in terms of willingness to respond yes and/or the expectation regarding signal frequency.

Methods

The methods proposed by SDT involve manipulation of the signal, the responses, and the expectation/reward for a particular type of responding. As implied in the above examples, the task generally involves a observer being directed to make an observation and report whether the interval of observation contained a signal or only noise. In this case, the presence of a signal is contrasted with the absence of a signal. SDT can also be used to describe the processing of multiple signals (see Macmillan & Creelman, chap. 10, 1991). The use of multiple signals allows investigation of the observer's ability to identify the signals (signal A versus signal B) and the ability to detect the combination of multiple signals against noise.

The responses required of the observer can also be varied. The two most common variations being the yes/no response used in the preceding examples and the multiple interval rating. The yes/no response

produces a single estimate of the response criterion used by the observer. The rating method requires the observer to provide a measure of the certainty of responding. For instance, the observer could be told to respond using the numbers one through six with one representing absolute certainty of a noise event and six representing absolute certainty of a signal event. The ratings can then be summed into five levels of criterion with rating 1 versus the other five being the most liberal criterion. The advantage of collecting rating responses lies in being able to determine sensitivity at varying levels of response bias. If the sensitivity varied across levels of response bias, it would indicate that σ_n is unequal to σ_{sn}. An assumption of equal variance might result in inappropriate comparisons among levels of sensitivity, a condition that can be avoided when rating responses are collected (see Macmillan & Creelman, 1991, pg.82-85). Responding can also be manipulated by altering the likelihood of a signal, or the reward/punishment for exceeding a level of one of the four response categories (hit, miss, false alarm, correct rejection).

Metrics

The primary metrics developed in conjunction with SDT quantify two kinds of information: the sensitivity of the observer and the observer's response bias. Sensitivity is measured as the distance between the means of the noise and signal-noise distributions taking into account the variance of the distributions and is measured as d´.

$$d' = \frac{\mu_{sn} - \mu_n}{\sigma_n}$$

Response bias, β, is measured by the ratio of noise to signal probabilities multiplied by the difference between correct rejections (cr) and false alarms (fa) divided by the difference between hits (h) and misses (m).

$$\beta = \frac{p(n)}{p(sn)} \times \frac{cr - fa}{h - m}$$

Returning to Figure 1, it should be clear that given equal likelihood of noise and signal-noise, the optimal β would divide the distributions into equal proportions of hits and correct rejections, thereby resulting in a β of 1. Changing the rewards for a particular response type, say punishing false alarms, necessarily shifts β one way or the other. The resulting change in the distribution of responses among the four possible outcomes provides a measure of β.

UNCERTAINTY

Uncertainty with regard to signal and noise lies at the heart of SDT. The uncertainty is attributed to variability in the production and processing of the noise and signals. In many psychophysical experiments, the signals are taken to be relatively stable. Variability is introduced by the processing channel through which the signal is encoded. For instance, a visual stimulus is expected to be relatively constant. On the other hand, the perception of the stimulus is made variable by random neural firings, the effects of spatial summation, and the retinal location on which the image is projected to name a few. Each of these effects serves to increase the overlap between the noise and signal-noise distributions.

The critical point for this presentation is that variability can be introduced in other ways as well. Consider the task of sorting a box of school photos into two classes: former classmates versus persons unknown to you. The photo is a fixed image and your perception is not degraded by the only getting a brief look at the photo or the angle at which the photo is displayed. You could describe the photo with a clarity that would allow some other person to select it from the box. The difficulty that you encounter in classifying the photo is not related to your processing the image. Instead, the difficulty is related to your ability to extract from memory the characteristics that would allow you to distinguish former classmates from people you have never seen before. The similarity in facial features and the difficulty with assigning features to names results in a noise distribution.

Noise and signal-noise distributions can be produced using numbers. Numbers are reliably and accurately identified by most adults, yet meaningful categories of numbers can have a great deal of overlap. For instance, the heights of men and women have different means, yet if you were given an intermediate height, say 5'6", there would be

uncertainty with regard to knowing whether the height was that of a woman or a man. In an effort to determine whether β is fixed or changes over time, Kubovy, Rapoport, & Tversky (1971) conducted an experiment using the height classification task. The observed d′ was consistent with the d′ expected given the means and variance of the numerical distributions used as stimuli. Measures of the criterion supported a deterministic, fixed β strategy for criterion setting as opposed to a probabilistic, variable β strategy. Numbers have also been used as stimuli in studies examining the convergence of various psychophysical methods on perceptual scaling (Weissmann, Hollingsworth, & Baird, 1975), and the independence of sequential presentations of stimuli with respect to responding (Ward, Livingston, & Li, 1988).

In system control environments, the task of deciding whether the numerical temperatures from a cooling mechanism are more representative of a normal operating condition than a malfunction is very similar to deciding whether a given height is more likely to represent that of a man or a woman. The certainty with which the operating status of a system can be determined from an observation on the system is in part a function of the distance between the means of the normal and malfunction distributions and the extent to which the distributions overlap. Therefore, the performance of an operator deciding that the system is okay or failing can be evaluated in terms of SDT.

APPLICATION

To illustrate the application of SDT to a human decision making problem, we will describe the method and analysis used in a study we conducted. In this research, we are interested in how people use information from a variety of sources, particularly when one source, the expert advisor, is expected to be a more accurate source of information. Previous studies have looked at the effects of varying the criterion information provided by an expert advisor. The basic method used by Sorkin, Kantowitz, & Kantowitz (1988) was to compare decisions made by observers using system data (digital gauges) with observers using the gauges in conjunction with expert advice. The expert advice is provided in either a 1 bit (nominal, malfunction) or a 2 bit (certain nominal, possible nominal, possible malfunction, certain malfunction) message indicating the criterion used for a given event. The study showed that the addition of expert advice improved decision accuracy and gave some indications of extra advantage for the 2 bit message over the 1 bit.

Sensitivity, or d′, of the system was established by the mean and standard deviation of the normal distributions from which the values for a nominal and malfunction event were taken. The sensitivity of the expert advisor was set at a level higher than that of the four gauges. This difference made it difficult to determine whether the improvement in performance was the result of combining the information from the gauges with the expert advice or simply the result of relying on the expert advice. We set out to determine what information the observers used by conducting a study in which the sensitivity of the expert advice varied from worse than that of the gauges to better than that of the gauges.

The generation of stimuli and the analysis of these studies are both dependent on SDT. The stimuli were generated in much the same way as described in the height example above. The two categories, system normal and system malfunction, were defined as having numerical means of 3 and 4, respectively. For the gauges, the standard deviation for each distribution was set at 1.54, yielding an expected d′ for each gauge of .649 and a combined d′ of 1.298 for the four gauges, as will be explained below. The standard deviation of the distribution on which the automated expert based its advice was varied, resulting in d′ levels of .191, .929, 1.667, and 2.774. In order to elicit measures of sensitivity across a variety of response criteria, responses were collected using a rating scale method with six response categories.

Manipulating the d′ of information from the expert advisor allowed us to examine the differential effect of the advice in the face of a constant level of information from the gauges. From a theoretical perspective, the

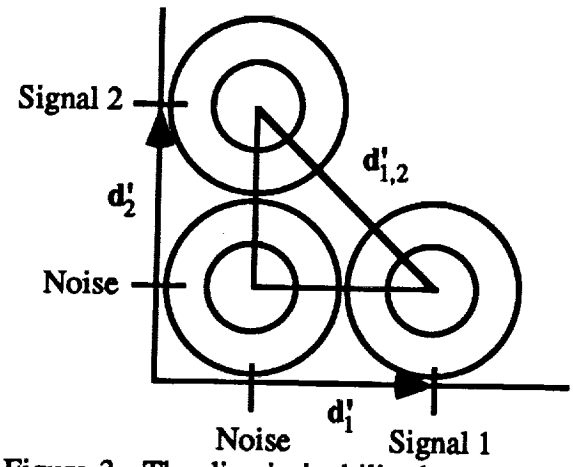

Figure 3. The discriminability between two stimuli, signal 1 and signal 2, is predicted by the distance between their means in d´ units.

use of information could be hypothesized as either the result of combining all the information or the result of selective filtering of the available information. SDT provides predictions regarding the combination of information (Tanner, 1956, Macmillan & Creelman, chap. 10, 1991, or for a comparison between the predictions of SDT and other theories see Massaro & Friedman, 1990). A common prediction discussed in the SDT literature takes advantage of d´ as a measure of distance. Take the case of two signals: sn_1 and sn_2 (see Figure 3). Independence is represented in the 90° angle of the intersection of the vectors. The two sources of information are assumed to share a common noise distribution ($n_{1,2}$). Using geometry, if sensitivity to sn_1 is described by d'_1 and sensitivity to sn_2 is described by d'_2, then the Pythagorean theorem allows us to predict the discriminability of sn_1 from sn_2 as

$$d'^2_{1,2}=d'^2_1+d'^2_2-2d'_1d'_2\cos(\theta).$$

When the signals are independent ($\theta=90°$, $\cos(90°)=0$) and d'_1 is equal to d'_2 then

$$d'_{1,2}=\sqrt{2}d'_1.$$

This line of thinking can be extended to predicting the detectability of the combined evidence, sn_1 and sn_2, against the noise distribution by changing our focus from calculating the distance between the means of sn_1 and sn_2 to calculating the distance between $sn_{1,2}$ and $n_{1,2}$. Changing the orientation of the legs of the triangle, it is obvious that the calculation remains the same. This prediction, referred to as the Euclidean metric, can be extended to m independent information sources having equal d´s by the formula $\sqrt{m}d'$. The Euclidean metric predicts that performance will exceed that expected from any of the component parts (see Figure 4, panel 1).

The simplest filtering prediction suggests that one source of information will be processed to the exclusion of other sources. Two sources are possible: the expert advice and the gauges. If only the expert advice is used, then one would expect a linear increase in performance corresponding to the increase in d´ of the expert advice (see Figure 4, panel 2). On the other hand, if the gauges were used, one would expect no change in performance as the d´ of the advice improved (see Figure 4, panel 3).

An alternative model based on filtering would suggest that through repeated exposure, the observer learns the relative sensitivity of available sources, and in some manner weights the contribution of the sources in accordance with the d´. The

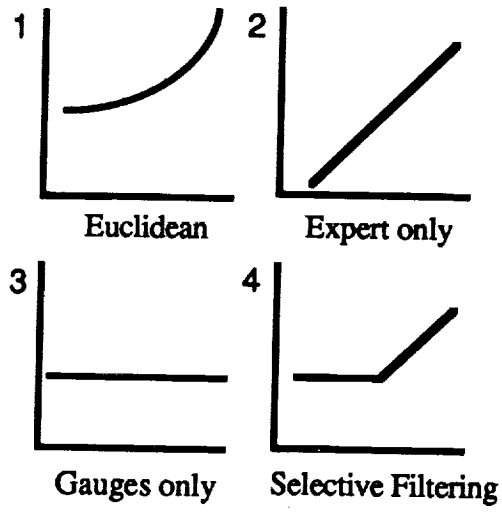

Figure 4. The effect of increasing expert system sensitivity on overall performance for four hypothesized outcomes based on combination of information (Euclidean) and filtering (expert only, gauges only, and simple selection).

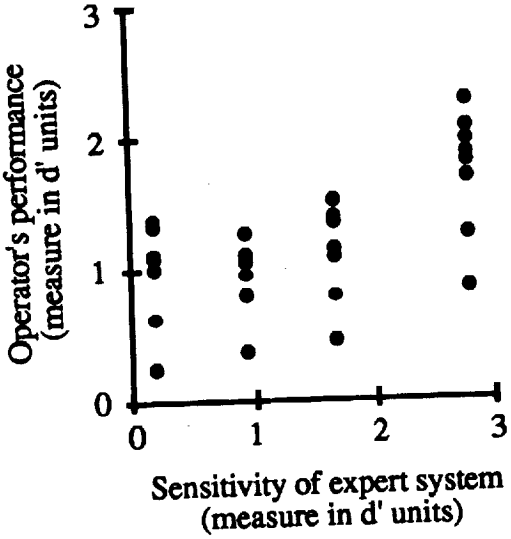

Figure 5. Observed performance showing the effect of expert system sensitivity on operator performance in the system control task.

simplest model based on this approach would predict that the observer would use only the source having the highest d´. The result would be a decision based on the information from the gauges when the advice is less sensitive than the gauges and on the advice when the advice was more sensitive than the gauges (see Figure 4, panel 4).

The experiment was conducted and the best fit for the data was a curve that increased at an increasing rate (see Figure 5). This result rules against accepting the filtering models that are based on only one source of information. Differentiating between the Euclidean metric model and filtering based on d´ is more difficult. Both would be predicted to be curvilinear and increasing at an increasing rate given the d´s provided in the task. The primary distinction between the two models relies on location of the curve. The Euclidean model predicts performance that exceeds that of either source. The filtering model predicts performance equal to the more sensitive of the sources. In practice, observed d´s frequently fall below predicted d´s. As such, selecting between models based on location of the curve has problems in addition to the variability of the data. Additional experiments manipulating the observer's knowledge of the sensitivity of each information source are being conducted to distinguish between the Euclidean and filtering models.

CONCLUSION

In conclusion, SDT provides an assessment of both the decision maker's sensitivity and response bias. Sensitivity can be a function of the variability of noise and signal processing inherent in sensory processes, or, as with numbers, a function of the uncertainty with which individual numbers are categorized. In numerous studies in which numbers have served as stimuli the theory and methods of SDT have been shown to be a valuable tool for explaining the decision making performance of observers. This is particularly valuable in view of the similarity between assigning numbers in a laboratory task and the task of using numbers to categorize the status of a mechanical system. Studies currently being conducted demonstrate the value of SDT in describing and predicting the influence of automated expert system advice on decision making. In one instance, SDT has been used to demonstrate that decision makers process both numerical system data and expert system advice in a task requiring assessment of system status.

REFERENCES

Baird, J. C., & Noma, E. (1978). Fundamentals of Scaling and Psychophysics. New York: J. Wiley & Sons.

Kubovy, M., Rapoport, A., & Tversky, A. (1971). Deterministic vs probabilistic strategies in detection. *Perception & Psychophysics, 9*, 427-429.

Macmillan, N. A., & Creelman, C. D. (1991). Detection Theory: A User's Guide. Cambridge: Cambridge University Press.

Massaro, D. & Friedman, D. (1990). Models of integration given multiple sources of information. *Psychological Review, 97*, 225-252.

Parasuraman, R. & Wisdom, G. (1985). The use of signal detection theory in research on human-computer interaction. *Proceedings of the Human Factors Society - 29th Annual Meeting*, 33-37.

Sorkin, R. D., Kantowitz, B. H., & Kantowitz, S. C. (1988). Likelihood alarm displays. *Human Factors, 30*, 445-459.

Sorkin, R. D., & Robinson, D. E. (1984). Alerted monitors: Human operators aided by automated detectors. (National Technical Information Service Report No. DOT/OST/p-34/85-021). Washington, DC: U.S. Department of Transportation.

Sorkin, R. D., & Woods, D. D. (1985). Systems with human monitors: A signal detection analysis. *Human-Computer Interaction, 1*, 49-75.

Swensson, R. (1980). A two-staged detection model applied to skilled visual search by radiologists. *Perception & Psychophysics, 27*, 11-16.

Swets, J. A. (1988). Measuring the accuracy of diagnostic systems. *Science, 240*, 1285-1293.

Tanner, W. P. Jr. (1956). Theory of recognition. *Journal of the American Acoustical Society of America, 28*, 882-888.

Ward, L. M., Livingston, J., & Li, J. (1988). On probabilistic categorization: The Markovian observer. *Perception & Psychophysics, 43*, 125-136.

Weissmann, S. M., Hollingsworth, S., & Baird, J. (1975). Psychophysical study of numbers: III. Methodological applications. *Psychological Research, 38*, 97-115.

N94-11532

CRITERIA FOR ASSESSING PROBLEM SOLVING AND DECISION MAKING IN COMPLEX ENVIRONMENTS

Judith Orasanu
NASA/Ames Research Center
Principal Investigator
Mail Stop - 262-4
Moffett Field, CA 94035

Training crews to cope with unanticipated problems in high-risk, high-stress environments requires models of effective problem solving and decision making. Existing decision theories use the criteria of logical consistency and mathematical optimality to evaluate decision quality. While these approaches are useful under some circumstances, assumptions underlying these models frequently are not met in dynamic time-pressured operational environments. Also, applying formal decision models is both labor and time intensive, a luxury often lacking in operational environments. Alternate approaches and criteria are needed. Given that operational problem solving and decision making are embedded in ongoing tasks, evaluation criteria must address the relation between those activities and satisfaction of broader task goals. Effectiveness and efficiency become relevant for judging reasoning performance in operational environments. New questions must be addressed: What is the relation between the quality of decisions and overall performance by crews engaged in critical high-risk tasks? Are different strategies most effective for different types of decisions? How can various decision types be characterized? A preliminary model of decision types found in air transport environments will be described along with a preliminary performance model based on an analysis of 30 flight crews. The performance analysis examined behaviors that distinguish more and less effective crews (based on performance errors). Implications for training and system design will be discussed.

N94-11533

MONITORING COGNITIVE FUNCTION AND NEED WITH THE AUTOMATED NEUROPSYCHOLOGICAL ASSESSMENT METRICS IN DECOMPRESSION SICKNESS (DCS) RESEARCH

Dr. Thomas E. Nesthus[1] and Dr. Sammuel G. Schiflett[2]
[1]KRUG Life Sciences, San Antonio Div.
P.O.Box 790644
San Antonio, TX 78279-0644
[2]Armstrong Laboratory
AL/CFTO
Brooks AFB, TX 78235

Hypobaric decompression sickness (DCS) research presents the medical monitor with the difficult task of assessing the onset and progression of DCS largely on the basis of subjective symptoms. Even with the introduction of precordial Doppler ultrasound techniques for the detection of venous gas emboli (VGE), correct prediction of DCS can be made only about 65% of the time according to data from the Armstrong Laboratory's (AL's) hypobaric DCS database. An AL research protocol concerned with exercise and its effects on denitrogenation efficiency includes implementation of a performance assessment test battery to evaluate cognitive functioning during a 4-h simulated 30,000 ft (9144 m) exposure. Information gained from such a test battery may assist the medical monitor in identifying early signs of DCS and subtle neurologic dysfunction related to cases of asymptomatic, but advanced, DCS. This presentation concerns the selection and integration of a test battery and the timely graphic display of subject test results for the principal investigator and medical monitor. A subset of the Automated Neuropsychological Assessment Metrics (ANAM) developed through the Office of Military Performance Assessment Technology (OMPAT) was selected. The ANAM software provides a library of simple tests designed for precise measurement of processing efficiency in a variety of cognitive domains. For our application and time constraints, two tests requiring high levels of cognitive processing and memory were chosen along with one test requiring fine psychomotor performance. Accuracy, speed, and processing throughput variables as well as RMS error were collected. An automated mood survey provided "state" information on six scales including anger, happiness, fear, depression, activity, and fatigue. An integrated and interactive LOTUS 1-2-3 macro was developed to import and display past and present task performance and mood-change information.

N94-11534

ANALYZING HUMAN ERRORS IN FLIGHT MISSION OPERATIONS

Kristin J. Bruno
Linda L. Welz

Jet Propulsion Laboratory,
California Institute of Technology
4800 Oak Grove Drive
M/S 125-233
Pasadena, California 91101
(818) 354-7891
email: kbruno@spa1.jpl.nasa.gov

G. Michael Barnes

Computer Science Department (COMS)
California State University
Northridge, California 91324
(818) 885-2299
email: renzo@ms.secs.csun.edu

Josef Sherif

Jet Propulsion Laboratory,
California Institute of Technology
4800 Oak Grove Drive
M/S 125-233
Pasadena, California 91101
(818) 354-8365

Abstract

A long-term program is in progress at JPL to reduce cost and risk of flight mission operations through a defect prevention/error management program. The main thrust of this program is to create an environment in which the performance of the total system, both the human operator and the computer system, is optimized. To this end, 1580 Incident Surprise Anomaly reports (ISAs) from 1977-1991 were analyzed from the Voyager and Magellan projects. A Pareto analysis revealed that 38% of the errors were classified as human errors. A preliminary cluster analysis based on the Magellan human errors (204 ISAs) is presented here. The resulting clusters described the underlying relationships among the ISAs. Initial models of human error in flight mission operations are presented. Next, the Voyager ISAs will be scored and included in the analysis. Eventually, these relationships will be used to derive a theoretically motivated and empirically validated model of human error in flight mission operations. Ultimately, this analysis will be used to make continuous process improvements to end-user applications and training requirements. This Total Quality Management approach will enable the management and prevention of errors in the future.

Introduction

A long-term program is in progress at JPL to reduce cost and risk of flight mission operations through a defect prevention/error management program. Flight mission operations require systems that place human operators in a demanding, high risk environment. This applies not only to the mission controllers in the "dark room", but also to the mission planners and flight teams developing sequences, to the Deep Space Network (DSN) operators configuring and monitoring the DSN, and to the engineering teams who must analyze spacecraft performance. This environment generally requires operators to make rapid, critical decisions and solve problems based on limited information, while following standard procedures closely. The mission operations environment is, therefore, inherently risky because each decision that a human operator makes is potentially mission critical, and in a high-demand environment, human errors occur frequently. Given the high risk in such an environment, these human errors can have grave financial (e.g., the Soviet loss of PHOBOS) or loss-of-life (in manned space flight) consequences.

To contain this risk at JPL, flight mission operations procedures include intensive human reviews. In addition, when an error does occur, rapid rework is required to ensure mission success. This strategy has worked well to reduce risk and has ensured the success of JPL missions. However, the large human labor investment in these reviews and rework has contributed substantially to the cost of flight mission operations. Prevention of such errors would reduce both cost and risk of flight projects. The motivation of this program is that risk can be contained more cost effectively by preventing human errors rather than reworking them. The goal of this program is the management, reduction and prevention of errors. The key facet of this program is to create an environment in which the performance of both the human operator and the computer system is optimized. Systems must be designed to enhance normal human performance (e.g., as described in Card, Moran, & Newell, 1983); training programs must be designed to alleviate likely errors; and functions that are human-error prone should be automated. Thus, to design and implement a successful defect/error prevention program requires a theoretically motivated model of human problem solving and decision making based on current theories of knowledge representation, the structure of memory, schemas, and mental models (e.g., Anderson & Bower, 1973; Norman, 1988). further, such a model must be data-validated to ensure its ultimate applicability to the flight mission operations environment. Principles of cognitive psychology, human-computer interaction, and Total Quality Management (TQM) are used to analyze past

errors and make changes to end-user applications and training requirements and task policies and procedures to prevent or manage these errors in the future.

Method and Results

The process developed for this program can be viewed as a continuos process improvement loop consisting of five steps:

1. Institute the Mission Operations and Command Assurance (MO&CA) function on JPL flight projects.
2. Analyze Incident Surprise Anomaly (ISA) data for causes of errors and patterns of causes.
3. Develop a prototype of a human process model of the underlying factors causing cognitive errors during flight operations based on the ISA data.
4. Develop a defect prevention/error management methodology based on the flight operations human process model.
5. Insert the methodology into Flight Mission Operations system development and training via system requirements and training prototypes and into policies and procedures via MO&CA.

Thus far in the program Step 1 has been successfully completed. MO&CA teams have been installed on flight projects to help reduce cost and risk. The main benefits of these teams are realized from collecting and analyzing error data in the form of ISA Reports. Based on these reports MO&CA teams make recommendations for subsequent changes to flight operations procedures, and work with the flight mission operations teams to incorporate the recommendations. The work of these teams is ongoing on several projects. The current work, reported in this paper, consists of extended analysis of error data (ISAs) to determine patterns of causes and develop a prototype human process model (Steps 2 and 3). Currently, error data with cause codes is available for three flight projects over a 14 year period.

The goal of Step 2 was to reduce the data to a meaningful subset of the most frequent causes of errors based on the TQM principle of investigating the most prevalent problems first in a defect prevention/error management program. ISA reports from two projects, Voyager and Magellan, were classified in one of 12 cause code categories. Each project used a slightly different taxonomy of detailed cause categories within the high-level cause. Thus, the detailed analysis entailed developing a composite cause category taxonomy of data for both projects making the detailed cause category analysis equivalent. The categories used were developed by MO&CA teams based on major functions in the flight mission operations environment. An early Pareto analysis was performed to determine the most frequent high-level causes of errors. The analysis showed that, of the 1580 ISA reports recorded, the three cause categories of Human (38%), Software (20%), and Documentation (10%) accounted for 68% of the errors (Figure 1).

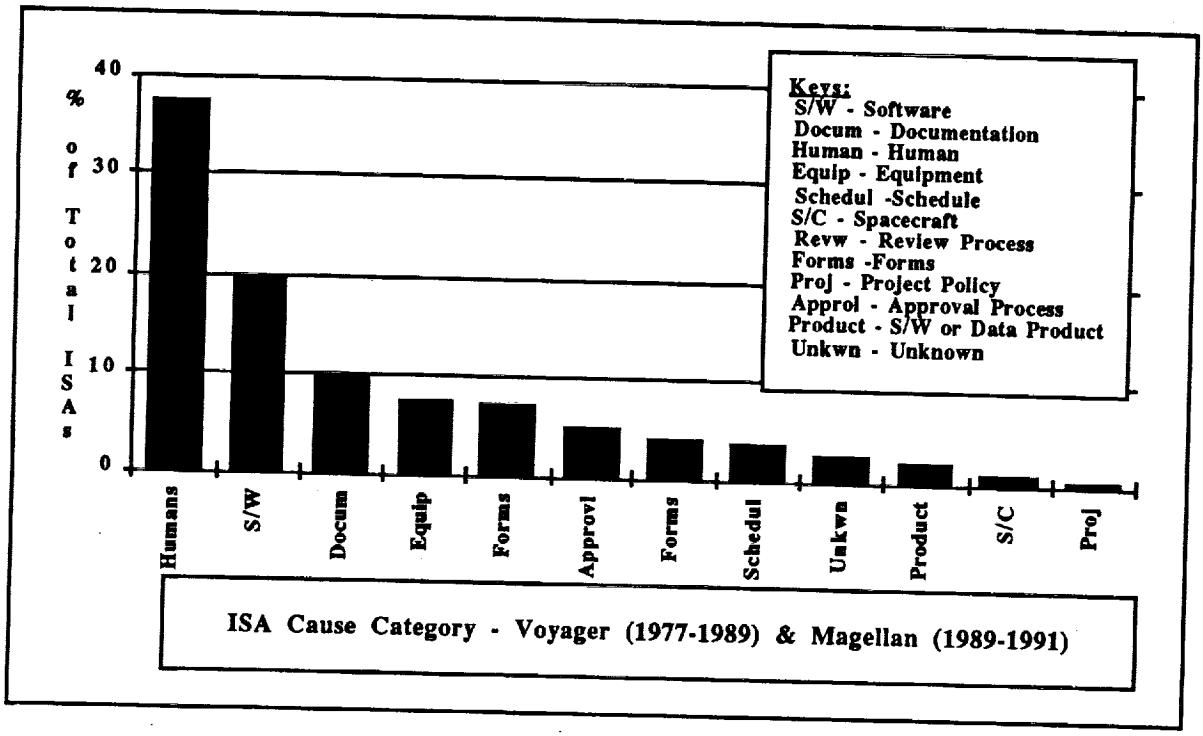

Figure 1
Voyager and Magellan ISAs - By Cause Code

Based on the high number of human errors, subsequent analysis of more specific cause codes was restricted to ISA reports for the Magellan project that were classified as Human Error. The taxonomy of cause codes was then used to score the 204 Magellan Human ISAs. Each ISA was read by a team of 2 investigators who assigned as many cause codes as was appropriate. In addition, each cause code was assigned a value of 0, 1, or 2. These values were assigned as follows: "2" was assigned if this cause alone caused the anomaly to occur and the ISA to be written; a "1" was assigned if this cause was an ancillary cause which contributed to the anomaly, but would not by itself have caused it; a "0" was assigned if this cause did not apply to the ISA. Thus, for the 204 Magellan Human Error ISAs examined, 269 cause codes were assigned.

Next, the Magellan human error data was subjected to a cluster analysis to identify clusters of cause code patterns. Interpretation of these clusters was expected to reveal the underlying factors causing cognitive errors. BMDP's cluster analysis, a multidimensional scaling technique, was used. The program groups the pair of cases (in this case ISAs), with the shortest Euclidean distance (the square root of the sum of squares of the difference between the values of the variables for two cases). In a step-wise manner, two cases or clusters are grouped such that initially each case is an individual cluster and at the end all cases are in one cluster. In the present analysis, 25 clusters were formed first at distance 0. Thus the internal distance among ISAs in each of those 25 clusters was 0; that is, the ISAs were scored identically. Figure 2 shows a Pareto chart of the size of the first 25 clusters. The 4 largest clusters contained 25, 21, 19, and 15 ISAs respectively, followed by a gap. The next cluster, of size 9, was the cluster of ISAs of unknown cause. Thus, only the 4 largest clusters were selected for interpretation. These 4 clusters consisted of ISAs with only one cause rated "2". They were Oversight (12%), Lack of Communication (10%), Edit Error in Product (9%), and Omission of Action (7%), respectively, and accounted for 39% of the 204 ISAs (Figure 3). At the next major level of clustering, distance 3.3, these 4 clusters joined, along with others, to account for 52% of the total ISAs. Finally, at the third major level of clustering, distance 6.6 , 95% of the ISAs joined. The final 5% of the ISAs did not join until distance 14.8 and these errors were rare, dissimilar cases.

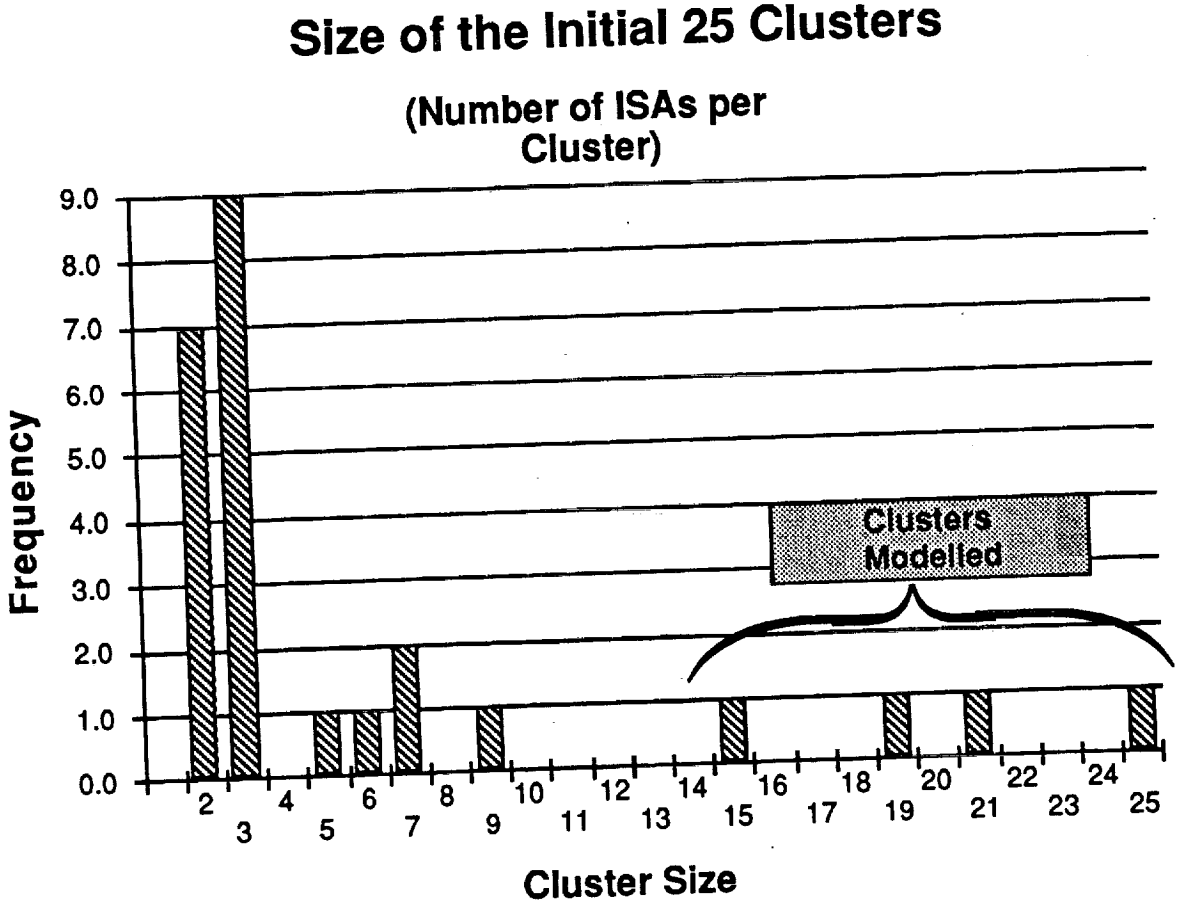

Figure 2
Magellan Human Error ISAs - By Cause Code

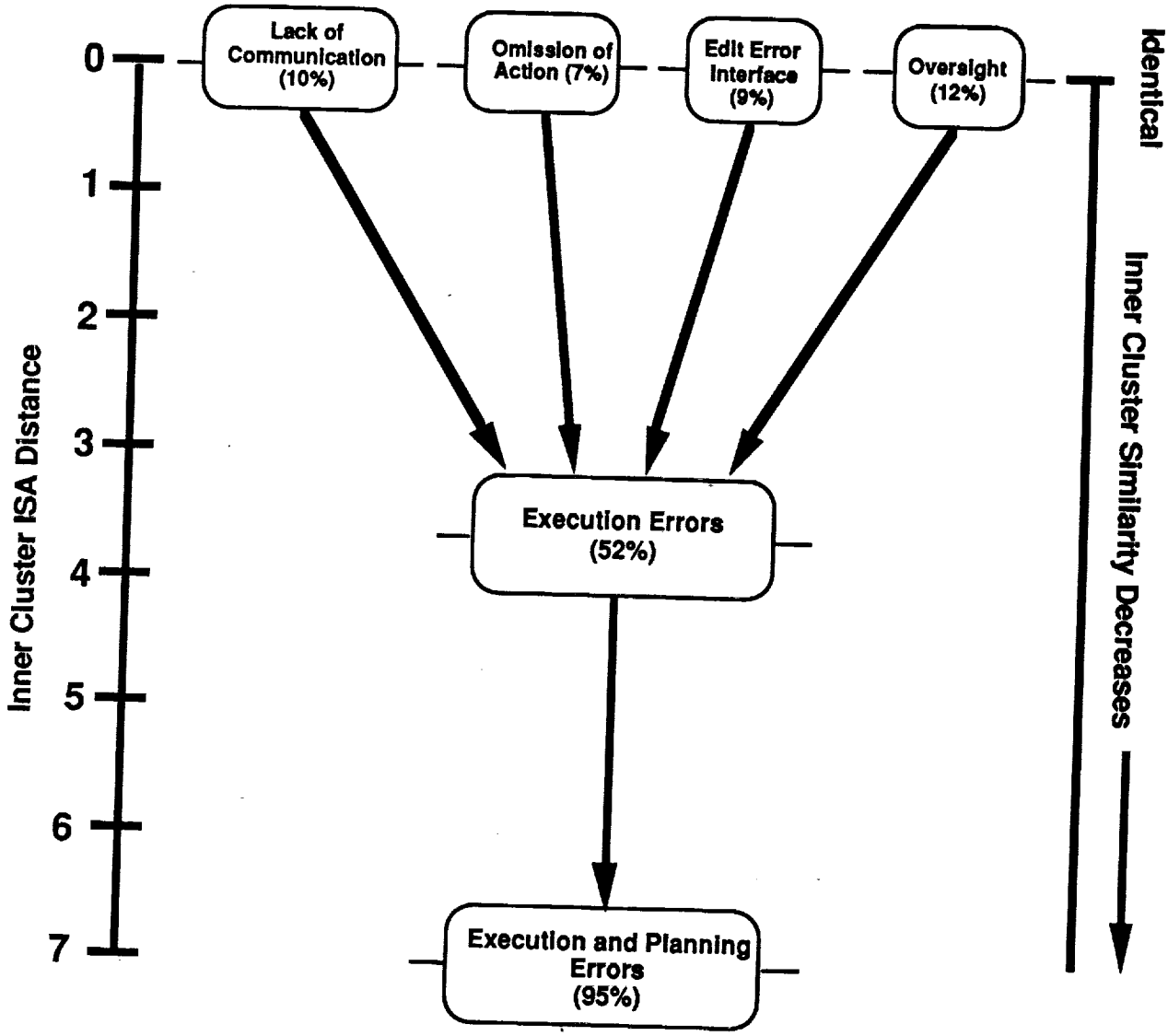

Figure 3
Magellan Human Error ISA Cluster Analysis

In order to model the underlying causes of the ISAs within the four initial clusters, each ISA within a cluster was reexamined for its specific characteristics. Characteristics common to all ISAs in the cluster were compared to known cognitive phenomena, particularly with human error theory. Several taxonomies of human error have been proposed (e.g., Norman, 1981, 1983; Reason, 1990). However, there is no general agreement on a single taxonomy. Thus, it has been suggested that a taxonomy must be tailored to a given environment (Senders & Moray, 1991). The taxonomy adopted here, in Appendix A, is tailored and simplified from Reason (1990). Figure 4 shows the cognitive mechanisms in the taxonomy. Tasks are divided into a planning and an execution component. The error types are Oversight (generally known as a slip), Omission of Action (generally known as a lapse), a mistake, and a violation. This general taxonomy was then used to model the common characteristics within each cluster. The four highest frequency clusters that joined at distance 3.3 exhibited at least two common cognitive elements, omission of action and oversight. In omission of action, a goal was acquired, but a subgoal was not executed for some reason, typically cognitive capture or a distraction. Cognitive capture generally refers to a psychological phenomenon in which a well-rehearsed action takes control of a less familiar action. This is particularly true when attention is drawn elsewhere. For example, one ISA (8508) documented a case in which DSN station operators did not notice for three days a special condition in the Sequence of Events (SOE) during Magellan support. The problem was caused by the fact that Magellan support had become routine and the SOE rarely changed. Thus, this routine support "captured" the processing of the changed SOE so that some new steps were omitted. This error

Error Type	Task Type	
	Planning	Execution
Oversight (slip)	OK	Followed plan, but performed a wrong action
Omission of Action (lapse)	OK	Followed plan, but skipped an action
Mistake	Faulty Plan	Followed faulty plan
Violation	OK	Intentionally deviated from plan

Figure 4
Human Error

resulted in a loss of data. The second common cognitive element in this cluster was oversight, in which the status of the task is not evident at any given point in time. Thus, an incorrect action (i.e., inappropriate at this point in the task) may be performed, or an incorrect object may be used. For example, another ISA (1973) documented an error in which a file was created using an old version of the required software. The problem was traced to the fact that, as new versions of the file generation software became available, they were simply installed on the appropriate machines. As time passed, multiple versions of the software were available. To the operator generating the file, it was not clear which was the correct version of the software. Thus, the task status was not evident, and a wrong object (the old software) was used. The lack of distinction between the current software and previous releases generated a description error. There were no salient attributes to facilitate the use of the correct software release. This error resulted in loss of time, since the problem had to be researched and the file regenerated, thus increasing operations costs. In addition, risk increased since an incorrect file was generated.

As these common cognitive elements were uncovered, it became clear that the single common element underlying this cluster was that all the ISAs were execution errors. Thus, this cluster, at distance 3.3, was labeled "Execution Errors"(Figure 3). Finally, at the third major level of clustering, at distance 6.6, planning errors joined the execution errors, thus suggesting a label of "Execution and Planning Errors."

Preliminary Conclusions

Although this defect prevention and error management program is in its infancy, some preliminary conclusions can be drawn from the initial analysis.

1. Flight mission operations human error data is amenable to interpretation via human error theory. JPL currently has a large volume of ISA data. While this data may be locally analyzed within a project during operations, particularly during a major anomaly, the analysis is typically ad hoc and localized to that one project. This preliminary work demonstrates that by modeling error data, underlying causes can be investigated in a systematic way, and classes of errors in this environment (such as execution errors) can be uncovered. In addition, this general information can then be shared across projects.

2. In JPL flight mission operations, a significant portion of human ISAs are errors in executing a task. The results of this study showed that 52% of the 204 Magellan human errors analyzed were execution errors. This provides a focus for possible solutions on execution problems. It is also speculated that execution errors will be found to be preventable or manageable.

3. System requirements, policies and procedures can be written to prevent known cognitive errors. As was previously mentioned, through this systematic analysis, classes of errors will be uncovered. In this way, solutions to manage errors that do occur, or solutions to prevent them from occurring can be generated. For example, to prevent errors like the one documented in ISA 8508, special conditions in a file can be highlighted to avoid capture in routine tasks. To avoid errors such as ISA 1973, proper configuration management policies and procedures should be written and enforced in operations. In this case, archiving old versions of the file-generation software off-line would eliminate operator confusion about which software to use in generating files and thus prevent this oversight or slip.

In summary, a method for analyzing human errors in flight mission operations has been presented. Although in a preliminary phase, it is clear that such a method in which error data is subjected to a cluster analysis, the resulting clusters are examined for common cognitive elements, and these elements are modeled using cognitive psychological theory, can lead to an understanding of the causes of errors and typical classes of errors. Using TQM principles, these findings can then be used at the beginning of a project's life cycle to improve system requirements, project policies and procedures, and operator training to manage errors that do occur, or prevent them from occurring at all. It is only through such a systematic analysis method that cost and risk can be reduced in flight mission operations. Finally, it is clear that this analysis has wide applicability to other errors. It is currently planned that this program will eventually expand to include analysis of other errors in Figure 1 such as software and documentation, and to other environments such as the DSN and system development.

Acknowledgement

The research described in this paper was carried out by the Jet Propulsion Laboratory, California Institute of Technology, under a contract with the National Aeronautics and Space Administration.

References

Anderson, J. R. & Bower, G. H., Human Associative Memory, V. H. Winston, Washington, D.C., 1973.

Card, S., Moran, T., & Newell, A., The psychology of human-computer interaction, Erlbaum Associates, Hillsdale, N.J., 1983.

Norman, D. A., "Categorization of action slips," Psychological Review, 88, 1981, 1-15.

Norman, D. A., "Design rules based on analyses of human error, " Communications of the ACM, 26 (4), 1983, 254-258.

Norman, D. A., The design of everyday things, Doubleday, New York, 1988.

Reason, J., Human error, Cambridge University Press, New York, 1990.

Senders, J. W. and Moray, N. P., Human Error, Lawrence Erlbaum Associates, Hillsdale, N.J., 1991.

APPENDIX A

Taxonomy of Human Error Cause Codes

HUMANS		
HUM		
HUM1	Inadequate Knowledge/ Inexperience	Error made due to inexperience or lack of knowledge if person is experienced.
-1	Procedures	
-2	Policies/guidelines/ requirements	
-3	S/C characteristics	
-4	Command procedures	
-5	Ground Operations	
-6	S/C Status	
-7	Constraints	
-8	Schedule change	
-9	Anticipated command effect	
-10	S/W Flight	
-11	S/W Ground	
HUM2	Violation of Rule/ Constraint/Procedure	Error made due to an intentional deviation from plan
-1	Procedures	
-2	Policies	
-3	Guidelines	
-4	Flight / Mission Rules	
-5	S/C Compatibility	
-6	Ground Operations - Compatibility	
-7	Operational Requirement	
HUM4	Error	Error made due to an unintentional deviation from plan
-1	Wrong Plan - Mistake	Plan is wrong, but was executed correctly
-2	Plan OK - Error Unknown	Plan is correct, error is unknown
-3	Plan OK - Omission of Action	Plan is correct, but an action was omitted during execution
-4	Plan OK - Oversight	Plan is correct, but an action during execution was wrong.
HUM5	Product Interface	Error made while producing a product
-1	Error in Copying	
-2	Error in calculation	
-3	Data entry error	Error in original data entry
-4	Edit Error	Error in editing an existing product
HUM6	Communication	
-1	Lack of communication	
-2	Miscommunication	

Session H3: HUMAN PERFORMANCE MEASUREMENT III—OPERATION SIMULATION

Session Chair: Capt. James Whiteley

N94-11535

Measures for Simulator Evaluation of a Helicopter Obstacle Avoidance System

Joe De Maio
Army Aeroflightdynamics Directorate
Crew Station Research and Development Branch

Thomas J. Sharkey
David Kennedy
Monterey Technologies Inc.

Micheal Hughes
Perry Meade
CAE Electronics

NASA/Ames Research Center
Moffett Field, CA 94035

Introduction

The U. S. Army Aeroflightdynamics Directorate (AFDD) has developed a high-fidelity, full-mission simulation facility for the demonstration and evaluation of advanced helicopter mission equipment. The Crew Station Research and Development Facility (CSRDF) provides the capability to conduct one- or two-crew full-mission simulations in a state-of-the-art helicopter simulator. The CSRDF provides a realistic, full field-of-regard visual environment with simulation of state-of-the-art weapons, sensors and flight control systems.

We are using the CSRDF to evaluate the ability of an obstacle avoidance system (OASYS) to support low altitude flight in cluttered terrain using night vision goggles (NVG). The OASYS uses a laser radar to locate obstacles to safe flight in the aircraft's flight path. A major concern is the detection of wires, which can be difficult to see with NVG, but other obstacles - such as trees, poles or the ground - are also a concern.

The OASYS symbology is presented to the pilot on a head-up display mounted on the NVG (NVG-HUD). The NVG-HUD presents head-stabilized symbology to the pilot while allowing him to view the image intensified, out-the-window scene through the HUD. Since interference with viewing through the display is a major concern, OASYS symbology must be designed to present usable obstacle clearance information with a minimum of clutter.

OASYS Display Evaluation

The evaluation of OASYS has been conducted in stages. The first stage was a laboratory test of the readability of a variety of display formats. This evaluation was conducted using static symbology. In the second stage, pilots provided subjective ratings of a number of display qualities after having flown a limited fidelity real-time

simulation. The third stage, now underway, consists of a high-fidelity simulator evaluation of selected OASYS displays in the CSRDF.

Preliminary Evaluations - The first two OASYS display evaluations provided preliminary screening to eliminate display formats that were too diffucult to read or were subjectively unacceptable to the study pilots. In the display readability experiment (1), straightforward measures of response time and accuracy were used. We used the results of this experiment to determine the set of candiate displays for evaluation in the limited fidelity simulation.

In the second experiment (2), involving simulated flight, we felt that the simulation fidelity was too low to permit use of objective data. Instead the pilots provided subjective seven-point ratings of the displays. The rating factors are shown in Table 1. The pilots also rank ordered the displays.

1. How interpretable was this symbology?
2. Rate the information content in this symbology.
3. Rate the clutter of this symbology.
4. Were you able to determine whether or not your turn rate exceeded the sensor's field of view?
5. Rate the amount of response time available with this symbology during turns.
6. Rate the amount of response time available with this symbology during straight flight.
7. To what extent were you able to determine the range of objects using this symbology?
8. To what extent were you able to distinguish between wires and blobs using this symbology?
9. How confident are you that this symbology will allow you to fly your aircraft without striking objects?
10. Overall, how would you rate this symbology?

Table 1. OASYS Display Rating Questions.

Only two of the rating questions showed significant inter-rater reliability. These were question 3 and question 8. Despite their consistency on question 8, the pilots did not feel that object type information (wires v non-wire blobs) was particularly important. They did feel that clutter was an important factor in display quality. Four of the highly rated display formats were selected for the full-scale simulator evaluation. A declutter option was also included for one display, based on the indicated undesirability of display clutter.

Full-scale Simulation - The purpose of the full-scale OASYS simulation test is to determine the ability of the system to support flight operation. This determination has several parts - does the OASYS reduce the incidence of wire and obstacle strikes, does the OASYS allow more precise or more aggressive flying, does the pilot's interaction with the display cause undesirable side effects. Issues here include increased workload, alteration of visual scanning and changes in flying technique.

We are measuring the effectiveness of the OASYS in preventing obstacle strikes simply by determining the rate of collisions with various types of obstacles. Obstacles other than wires fall into two categories, ground and objects projecting above the ground (e.g., poles, trees). Factors of interest regarding wire strikes are wire size and obliquity to the flight path.

Changes in visual scanning and pilot workload can occur because of display clutter, a problem identified in our preliminary studies. Problems of selective attention to symbology or outside scene imagery can also occur, and these may be exacerbated by registration mismatches caused by pilot head movement. We are addressing these issues both through subjective ratings and through analysis of pilot head movements, which are measured routinely for visual scene generation. Comparison of head movements with and without OASYS symbology will indicate whether presence of the OASYS display alters the way in which pilots scan the out-the-window scene.

An additional item of information that comes from the head position data is where the pilot looks for obstacles when not aided by OASYS. This information may be important for pointing the sensor during maneuvering, when the relevant information may not lay along the flight path vector. Such a situation is shown in Figure 1.

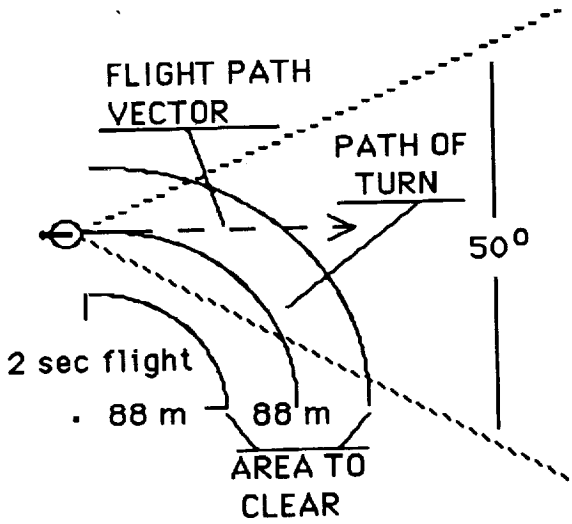

Figure 1. Location of Obstacle Information off Flight Path Vector. Desired clear path is 88 m wide, and desired look-ahead is 2 sec. OASYS field of regard is 50 deg.

The issue of changes in flying technique is challenging from the perspective of data collection and analysis. The simulation scenario involves free flight through a densely populated data base. Any object or terrain feature in the data base could potentially be an obstacle to flight. Thus the often used technique of triggering data collection or analysis based on mission time or location in the data base is not suitable. Instead it is necessary to identify maneuver initiation based on changes in the aircraft flight path and to determine the obstacle being avoided from the maneuver dynamics. Once the maneuver and obstacle have been identified, evaluation factors can be assessed for each obstacle avoidance maneuver individually.

The approach we are taking to maneuver identification is based on a procedure developed by De Maio et al (3). This procedure involves looking for threshold changes in the flight path to signal initiation of maneuvers. The salient points in a maneuver are shown in Figure 2. The threshold determination process works on rate of turn. Rate of turn is computed not in the horizontal plane, but instead it computes the turn rate in whatever plane the turn is executed. Thus a pull-up is a turn executed largely in the vertical, a level turn is execute largely in the horizontal and a climbing turn is intermediate between the two.

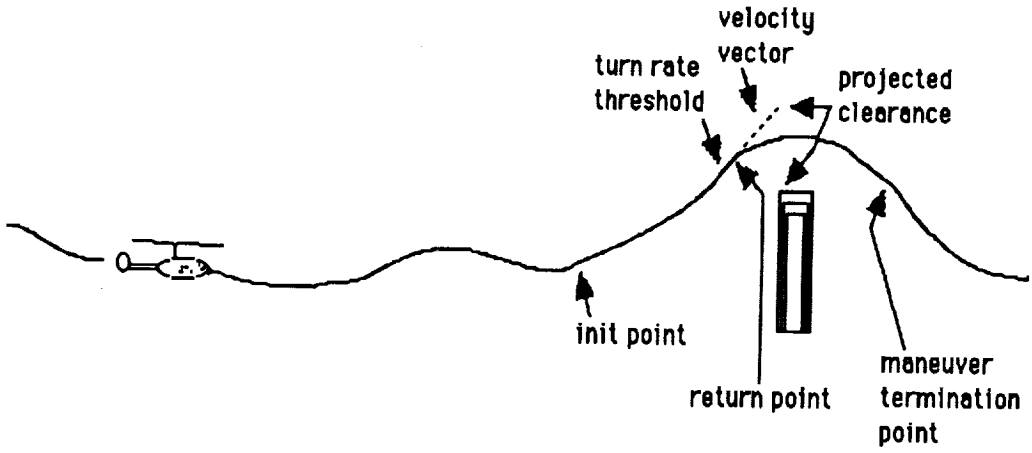

Figure 2. Obstacle Avoidance Maneuver Profile.

Once a suprathreshold turn rate is detected, the analysis works backward to identify the point at which the maneuver was intiated. This is the point where the direction of flight changes (e.g., down to up, left to right). From the initiation point we proceed down the original flight path to determine whether there was an object along it that would have constituted an obstacle to flight. If so a descriptive analysis of the avoidance maneuver is performed.

Conclusion

The CSRDF is being used for a comprehensive evaluation of the usability of OASYS to provide a pilot symbolic information necessary for obstacle avoidance. This evaluation included a preliminary evaluation of display readability using psychophysical methodology and measures. Based on this prescreening a set of candidate displays was developed for evaluation in a limited fidelity simulation. In this evaluation subjective pilot ratings were used to identify a set of four display for evaluation in full-scale simulation. The full-scale simulation provides realistic tasking under realistic conditions. In this simulation we are using conventional objective and subjective measures to evaluate OASYS performance. In addition we are developing innovative measurement procedures to respond to the specific requirements of the OASYS evaluation.

References

1. Sharkey, T.J. and Nemire, K. OASYS Information Requirements Experiment, Monterey Technologies Inc. Technical Report TR-890504-001, Nov, 1991.

2. Sharkey, T.J. OASYS Symbology Development Effort Part-task Simulation, Monterey Technologies Inc. Technical Report TR-910505-001, Jun, 1992.

3.De Maio, J., Bell, H.T. and Brunderman, J. *Pilot Oriented Performance Measurement*, Proceedings of the Fifth Annual Interservice/Industry Training Equipment Conference and Exhibition, Washington, D.C., Nov, 1983.

VIGILANCE PROBLEMS IN ORBITER PROCESSING

William W. Swart, Ph.D.
Robert R. Safford, Ph.D.
David B. Kennedy
Bert A. Yadi
University of Central Florida
Department of Industrial Engineering
and Management Systems
P.O. Box 25000
Orlando, FL 32806

Timothy S. Barth
NASA Kennedy Space Center
Operations Review and
Analysis Group
TP-VPD-2C
Kennedy Space Center, FL 32899

ABSTRACT

A pilot experiment was done to determine what factors influence potential performance errors related to vigilance in Orbiter processing activities. The selected activities include post flight inspection for burned gap filler material and pre roll out inspection for tile processing shim material. It was determined that the primary factors related to performance decrement were the color of the target and the difficulty of the target presentation.

INTRODUCTION

The high quality of work performed in most processing activities and the relatively low rate of occurrence of quality incidents paradoxically can be expected to lead to a particular type of human factors problem in tasks where human operators or inspectors are required to detect the occurrence of "low probability of occurrence" events. It is known that in tasks of this nature there is a "high probability" of failing to detect low probability of occurrence "events." The phenomena occurs in most all types of tasks where detection of low probability events is required and occurs despite the degree of training, skill, and alertness of the inspector or the apparent obviousness of the event to a person not involved in the inspection.

This problem has been demonstrated in numerous tasks such as air defense radar monitoring, microscopic inspection of tissue for cancer growth, and a variety of industrial type inspections for defects has been demonstrated. This problem is frequently called "the vigilance problem or phenomena" in the literature.

Examples of Orbiter processing tasks which could be expected to experience the problem because of the task structure and the relatively low probability of occurrence of events include:

- STR system post flight inspections
- TPS post flight and roll out inspections
- ECL radiator inspection prior to roll out
- STR system aft closeout inspection for removal of access equipment
- INS, COM, EPD electrical systems connection inspection

All of the above tasks involve visual inspection and the need to recognize the presence of a low probability of occurrence condition. Although the condition or event needed to be detected may seem "obvious" (e.g., unconnected electrical connectors, beam in aft, indentation in tile, etc.) research in the problem area suggests that error rates in the neighborhood of a 1 to 10 chance of failure to detect may occur when there is a probability of event occurrence of 1 in 100. Probability of inspection task failures would be expected to increase as the probability of occurrence decreases.

This paper presents the results of a study designed to demonstrate the potential for vigilance type problems in selected Orbiter processing activities and to determine the processing task characteristics influencing the magnitude of the vigilance decrement.

ORBITER PROCESSING TASKS

An experimental task simulating two Orbiter processing activities was designed for use in this study. The Orbiter processing tasks simulated in this study were:

- Post flight inspection of TPS (Thermal Protection System) tile gaps for charred gap filler material.
- Pre OPF (Orbiter Processing Facility) "roll out" inspection of TPS tile gaps for presence of processing shims.

The reasons for selecting these particular tasks included:

- The tasks are easily learned so that any vigilance decrement observed in the performance of the tasks should not be confounded with learning effects.
- The tasks do involve low probability of occurrence events. Given 25,000 or more tiles on the vehicle (depending on the particular vehicle being inspected) there are relatively few gaps in which shims are left after processing or in which burned gap filler is found.
- The tasks are the type of inspection task which the ample literature on vigilance suggests would be candidates for a vigilance effect.

THE EXPERIMENTAL TASK

The inspections described above are done by the technicians who work under the vehicle and look directly up at the tile gaps. The viewing distance in these inspection situations varies from about one foot to five feet. To simulate this situation, subjects in the experimental situation were required to look at successive iterations of the pattern shown in Figure 1.

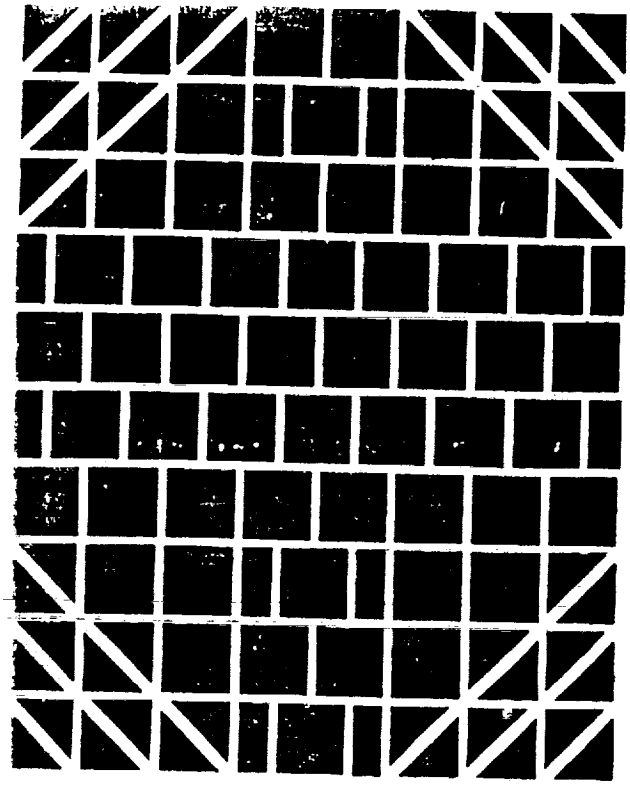

Figure 1: Simulated Tile Pattern Configuration

This pattern, which is similar to the tile patterns exhibited on the underside of the Orbiters, was projected on a white matte ceiling surface above the subjects in a manner that enabled the field of view of the subjects to be filled and enabled the simulated tile size to approximate an actual 6" by 6" "acreage" tile in terms of the visual angle subtended by the image.

Subjects participating in this task were required to view the image patterns and determine whether any of the gaps contained the presence of a "target" (i.e., whether the gaps were filled with a bright orange color or a dark brown color).

MAJOR EFFECTS

The major effects which were examined in the study were the color of the target material in the gaps between the tiles and the degree of visual difficulty. Figure 2 presents a schematic of the experimental design for these two effects.

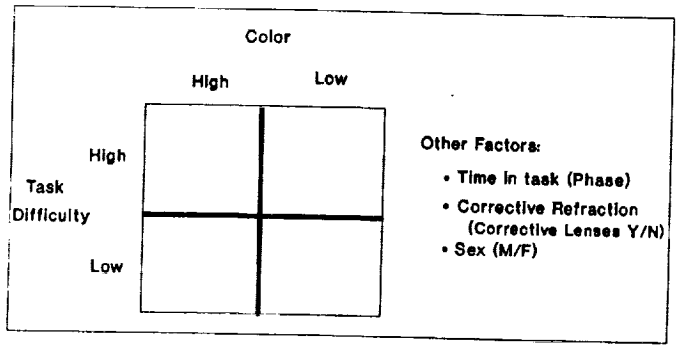

Figure 2: Schematic of Experimental Design

One of the target colors chosen was orange, a relatively high contrast color compared to the black (or grey) of the tiles, and the color of one of the widely used processing shims. The other color was a "low contrast" brown, the color of some of the darker plastic shim material.

Low difficulty targets were those that were relatively large (i.e., filled a wide gap for the length of a tile), and were located in the central area of the visual field. High

difficulty targets were smaller and were located in the peripheral areas of the visual field.

EXPERIMENTAL PROCEDURE

Forty subjects were tested. Each subject viewed 500 presentations of the "tile pattern" image. These images were presented for a viewing time of 5 seconds. Signal rate for both the orange and brown signals were 9%. Four of each color of the signals were classified as high difficulty, while the remaining five were classified as low difficulty signals.

RESULTS

The results of the statistical analysis of this experimental study are shown in Figure 3. As can be seen in the figure, both major effects of interest (i.e., color and task difficulty) were significant. In addition two significant interactions were noted.

Factor	Significance	Result
Main Effects:		
Color	«.005	Highly Significant
Task Difficulty	.025	Significant
Interactions:		
Refractive Correction X Color	.001	Highly Significant
Task Difficulty X Color	.018	Significant

Figure 3: Statistical Analysis of Experimental Study

The effect of color on target identification, the most significant effect, are shown in Figure 4. As can be seen, subjects correctly identified 93% of the orange targets . (Note: that still corresponds to a "miss rate" of 7%, a rate that could be expected to increase if the signal presentation rate of 9 per 100 were lowered). Brown, on the other hand, produced a "miss rate" OF 40%. Only 60% of the brown targets were correctly identified.

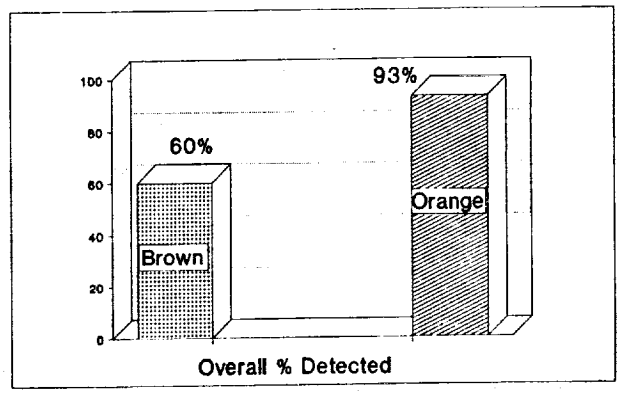

Figure 4: Effect of Color on Target Identification

CONCLUSION

This study demonstrates that a vigilance effect can be expected in Orbiter processing tasks and has delineated, for selected Orbiter processing activities, factors influencing the performance decrement. Knowledge of these effects can be readily used by process designers or in process improvement activities to help eliminate problems arising from vigilance tasks.

Results of this experiment will be used in the design of additional site studies to be conducted to further delineate the potential for vigilance problems and delineation of factors contributing to these effects in Orbiter processing activities.

N94-11537

MEASURING HUMAN PERFORMANCE ON NASA'S MICROGRAVITY AIRCRAFT

Randy B. Morris and Mihriban Whitmore
Lockheed Engineering and Sciences Co.
2400 NASA Rd. 1, C95
Houston, TX 77058

Abstract

Measuring human performance in a microgravity environment will aid in identifying the design requirements, human capabilities, safety, and productivity of future astronauts. The preliminary understanding of the microgravity effects on human performance can be achieved through evaluations conducted onboard NASA's KC-135 aircraft. These evaluations can be performed in relation to hardware performance, human - hardware interface, and hardware integration. Measuring human performance in the KC-135 simulated environment will contribute to the efforts of optimizing the human - machine interfaces for future and existing space vehicles. However, there are limitations, such as limited number of qualified subjects, unexpected hardware problems and miscellaneous plane movements which must be taken into consideration. Examples for these evaluations, the results, and their implications are discussed in the paper.

INTRODUCTION

In order to design environments and develop countermeasures as well as support systems that protect and enhance human capabilities, safety, health, and the productivity of future astronauts, we need a thorough understanding of the microgravity environment. By gaining this understanding, the probability of achieving greater mission successes is enhanced. One way of gaining this preliminary microgravity information is through the use of NASA's KC-135 aircraft, which simulates this environment. The KC-135 aircraft is ideally suited for short duration tasks. These tasks can evolve gross and fine motor activities and validating technology concepts. Some of the concerns with the various users are their anthropometric, physical, and physiological capabilities. A human factors goal is to provide designs/ interfaces for living and working in a microgravity environment and flight hardware in order to achieve optimal human performance, while providing safe human - machine interfaces. [1]

APPROACH

In order to achieve the best human - machine interface, human performance can be measured on the ground, KC-135, and the shuttle. These evaluations (KC-135) have been performed in relation to hardware performance, human - hardware interfaces, and hardware integration. One type of evaluation is to evaluate the hardware's

performance in microgravity conditions. These evaluations look at the equipments functionality and maintainability. Two examples of this type of evaluation are the video tape recorder (VTR) and Macintosh Powerbook 170 evaluations. This type of an evaluation is increasing in importance as the recent trend is to use commercially off the shelf products. While these products work quite well in the presence of gravity, in its absence, unforeseen problems can arise. Therefore, it is advantageous to test an off the shelf product for the microgravity environment and make modifications, if necessary, instead of designing a completely new product for microgravity use. Some examples of these problems include a trackball that had too much play in the ball (ball mechanism floated), and unexpected loss of camcorder battery power.

The VTR evaluation looked at the machine's servo circuits characteristics by way of the Horizontal Sync Jitter and Signal-to-Noise Ratio tests, as well as the man/ machine interface characteristics such as tape ejection and insertion, activating play, search (in both directions), fast forward and reverse (see Figure 1). All of the VTR's mechanical and operational tests were successful with no difficulties encountered. The only recommendation was to add a finger restraint to allow the operator to stabilize their hand for button activation.[2] While the Powerbook evaluation looked at the text/ graphics readability, display angle adjustability, select button activation pressure and location, keyboard location and the keys' pressure, restraint requirement, and size, shape, and location of the trackball. In general, the Powerbook computer worked well on the KC-135.[3]

Human hardware - interface involves the location, type, size, and ease of use of displays and controls.

Figure 1 - Subject Evaluating VTR

An example of this type of evaluation is the Cursor Control Device Evaluation (see Figure 2). The objective of this experiment was to aid in determining the best cursor control device design for use in microgravity. An optical mouse, trackball, mouse pen, and thumb ball are some of the cursor control devices that were tested. The experiment consisted of performing a text editing task which required pointing, dragging and clicking. Dragging time, pointing time and percentage of correct responses have been analyzed as

performance measures. Results of these evaluations showed mechanical deficiencies and performance differences among the devices. The ones which exhibited the best performance were selected for evaluations onboard the Shuttle.[4]

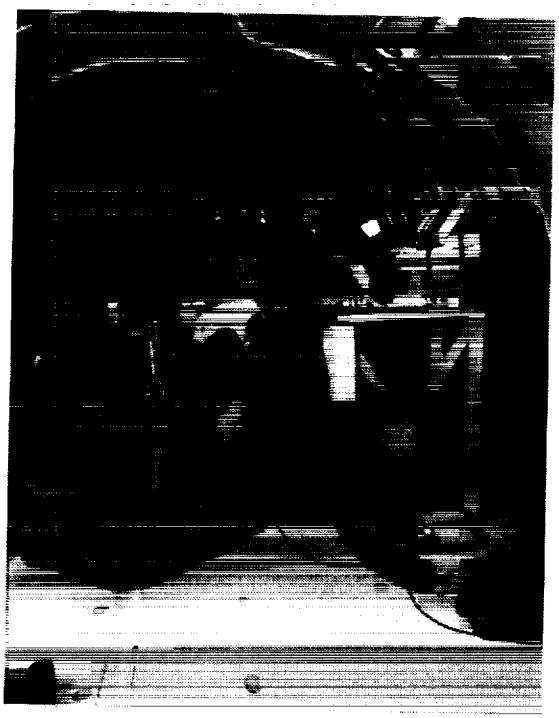

Figure 2 - Subject Evaluating Cursor Control Device

The third type of evaluation is the integration of the hardware into the overall system (e.g. is the proposed location for the equipment a feasible location). The workstation evaluations fall into this category (see Figure 3). The objective of this study was to evaluate the physical dimensions and layout of the workstation components. The workstation components consisted of the keyboard desk, translational hand controller, rotational hand controller, monitors, control panels and mobility aids while using different foot restraint systems. The entire evaluation was video taped for post flight computer simulation modeling. The results from the KC-135 flight showed that the workstation keyboard desk height and restraint systems concepts, as well as the location of the hand controllers would be critical for accommodating the required range of users (147.32 cm to 193.04 cm) in the microgravity neutral body position.[5,6]

The microgravity testing is an important part of hardware development as a tool to increase human performance because it allows the investigators to see the effects of weightlessness on the human - machine interface. It also gives you a chance to make some design refinements if any are necessary before it actually goes into space. This allows the investigators to save time and some potential problems.

Pre-flight Preparations

There are several preflight activities which must be completed no later than six weeks prior to the flight. One of these are the preparation of your hardware to ensure that it meets the qualifications for the KC-135. The equipment must be able to fit in the aircraft and be able to withstand the appropriate flight loads in the takeoff and landing configuration. Subject selection is another very key issue since there is a limited number of qualified subjects. The other two important issues are the selection of the performance measures that you want to measure and the design of your test protocol.

Figure 3 - Subject Evaluating Workstation

Baseline data was collected on the ground prior to the flight. This gives you performance measures in a normal ground (one g) environment to compare to the participants microgravity (zero g) performance measures. This baseline data collection also serves as a dry run to your actual experiment by familiarizing the participants with the hardware and what exactly they will be doing during this evaluation, as well as allowing you a chance to modify the test protocol if necessary.

Flight

NASA's KC-135 aircraft simulates a shirt sleeve space flight environment. It flies in a parabolic flight pattern that produces a microgravity period ranging between 20 and 27 seconds with an average of 23 seconds. The microgravity period is preceded by a two-g pull up and two-g pull out. The duration of these flights is approximately two hours with the total microgravity time being between fifteen and eighteen minutes.

During the KC-135 flights the human performance measures can either be objective or subjective. As a minimum, subjective data is collected during all of the evaluations. If the nature of the experiment allows, objective data is also collected. The subjective data is collected through questionnaires and audio comments that the

participants have made during the evaluations. While some examples of the objective measures are task completion time and percent error, frequency of use, anthropometric/ physiological measurements. These are collected through video recording or software.

Post Flight

After the flights, the participants are given a follow-up briefing and (if necessary) more data will be collected for analysis and comparison to the flight and baseline data that was collected previously.

RESULTS

The advantages of performing experiments onboard the KC-135 are that they are cost effective and, if applicable, design refinements can improve the interface and thereby improve human performance. A good example of this was during the cursor control device evaluations onboard the KC-135, where there was a mechanical deficiency with the trackball. This deficiency was that the ball floated due to too much "play" in the ball mechanism. Once it was modified, it worked as expected in the microgravity environment.

KC-135 evaluations allow us to see the effects of weightlessness on human performance while performing tasks and gives assistance in identifying the crew's needs and concerns. This was shown during the workstation evaluations, when the crew desired additional hand holds so that they would avoid accidently grabing onto any protruding controls.

However, there are some limitations to performing experiments onboard the KC-135. Some examples of these are that there are a limited number of qualified subjects, short set up times for the experiments, can encounter unexpected hardware problems and extraneous plane movements such as air turbulence. In addition, it is not suitable to test the effects of extended microgravity exposure.

CONCLUSIONS

Experiments conducted onboard the KC-135 enable us to achieve real time experience in a microgravity environment while creating challenges in selecting human performance measures and they can best serve the function as being a precursor for shuttle experiments.

Microgravity (KC-135) evaluations were very useful to determine the effects of "weightlessness" on human performance, to identify crew needs, and to refine overall designs. Measuring human performance in simulated microgravity environments, such as the KC-135, will contribute to the efforts of optimizing the human - machine interfaces for future and existing space vehicles. It will also ensure safe and productive work environments for the crewmembers.

REFERENCES

1. NASA Space Life Sciences 1991, Space Human Factors Discipline Science Plan 1991, Washington D.C., 1991

2. Morris, R.B., Wilmington, R.P. and Whitmore, M., Microgravity Evaluation of Video Tape

Recorder, JSC No.: 36046, LESC No.: 30197, Houston, TX: Johnson Space Center, 1992.

3. Morris, R.B. and Whitmore, M. (1992). Microgravity Evaluation of Macintosh Powerbook 170, JSC No.: 25815, LESC No.: 30222, Houston, TX: Johnson Space Center, 1992.

4. Detailed Test Objective Space Station Cursor Control Device Evaluation II and Advanced Applications, Final Report, Houston, TX: Johnson Space Center, 1991.

5. Whitmore, M., Wilmington, R.P. and Morris, R.B., Command and Control Workstation Anthropometric Evaluations for Space Station Freedom: Phase I, JSC No.: 36029, LESC No.: 30119, Houston, TX: Johnson Space Center, 1992.

6. Whitmore, M. and Morris, R.B., Command and Control Workstation Anthropometric Evaluations for Space Station Freedom: Phase II, Houston, TX: Johnson Space Center, 1992.

Noise Levels and their Effects on Shuttle Crewmembers' Performance: Operational Concerns*

Anton S. Koros (LESC), Susan C. Adam (NASA), and
Charles D. Wheelwright (LESC)

Lockheed Engineering and Sciences Company
2400 NASA Rd. #1 / MS-C95
Houston, TX 77058

NASA-Johnson Space Center
Mailstop-SP34
Houston, TX 77058

ABSTRACT

When excessive, noise can result in sleep interference, fatigue, interference with verbal communication and hearing damage. Shuttle crewmembers are exposed to noise throughout their mission. The contribution of noise to decrements in crew performance over these extended exposure durations was the focus of this study. On the STS-40/SLS-1 mission noise levels were evaluated through the use of a sound level meter and a crew questionnaire.

Crewmembers noted that sleep, concentration, and relaxation were negatively impacted by high noise levels. Speech Interference Levels (SILs) calculated from the sound level measurements suggested that crewmembers were required to raise their voice in order to be heard. No difficulty detecting caution and warning alarms was noted.

The higher than desirable noise levels in Spacelab were attributed to flight specific payloads for which acoustic waivers were granted. It is recommended that current noise levels be reduced in Spacelab and the Orbiter Middeck especially as longer missions are planned for the buildup of Space Station Freedom. Levels of NC 50 are recommended in areas where speech communication is required and NC 40 in sleep areas. These levels are in accordance with the NASA Man-Systems Integration Standards. Measurements proposed for subsequent orbiter missions are discussed.

INTRODUCTION

STS-40, with its payload of Spacelab Life Sciences-1 (SLS-1), was the fourth mission to fly the Spacelab module. However, it was the first mission completely dedicated to studying the physiological changes which occur in the human body when it is exposed to the microgravity of space. STS-40 was launched aboard Space Shuttle Columbia on the fifth of June, 1991. Along with a variety of medical studies Detailed Supplementary Objective (DSO) 904 Human Factors Assessment of Orbiter Missions was manifested. This DSO concentrated on the issues of tunnel translation; noise; vibration; task timelining; stowage, deployment and cable management. The results of the study on noise and the implications for future flights will be presented here.

Noise is defined as unwanted sound. The effects of noise on human performance have been well documented. Excessive levels of noise can result in a number of consequences, including permanent threshold shift (PTS), temporary threshold shift (TTS), interference with verbal communication and/or sleep, annoyance, irritability, and fatigue. In a survey of 33 Shuttle astronauts, Willshire and Leatherwood (1985) reported that more than half of the respondents found that noise disturbed their sleep. In addition, almost half experienced speech interference.

All manned space missions rely upon crewmember performance and so the consequences of excessive noise levels can hold severe implications for mission success. Therefore, noise limits have been imposed. These limits are usually expressed in A-weighted decibels (dB A). Leo Beranek (1988) explains that "the A-weighting of a sound level meter discriminates against sound pressure signals at frequencies below 1000 Hz and above 6000 Hz, and enhances levels between 1000 Hz and 6000 Hz." This scale is used because it approximates human perception.

The acoustic requirements for the Orbiter are presented in Section 3.4.6.1.3. of the Orbiter Vehicle End Item Specification (OVEI) (NASA, 1986), while for Spacelab the levels are contained in the Spacelab Payload Accommodations Handbook (SPAH) (NASA, 1985), Section 5.1.1.4.1. Currently the noise limits are 63 dB A on the Orbiter Flightdeck, 68 dB A on the Orbiter Middeck, and 59 dB A in Spacelab. Originally, the noise limits for both the

* Results previously presented at 123rd Meeting of the Aocustical Society of America 11-15 May 92, Salt Lake City, UT.

Orbiter and Spacelab were specified as NC 50 (56 dB A); however, due to implementation costs these limits were increased.

Before STS-40 flew, acoustic waivers were sought for several mission specific payloads including the Animal Enclosure Modules (AEM's), ergometer, and Orbiter Refrigerator/Freezer (OR/F). These waivers were granted with the understanding that the noise levels would be monitored to ensure hearing protection would be utilized if levels exceeded 76 dB A.

The objective of this portion of DSO 904 was to interpret crewmembers' subjective comments on the effects of noise during the STS-40 mission based on two objective measures—inflight sound level measurements and pre- and postflight audiometry results. It was anticipated that crewmembers would find the noise levels during sleep periods intrusive, and that when noisy payloads (such as the treadmill and vacuum cleaner) were operating noise levels would interfere with verbal communication. Subjective information was primarily sought to assess existing requirements. A secondary objective entailed determining if current noise levels impacted crew task performance.

Data presented in the Man-Systems Integration Standards (NASA, 1989, p 5-44) suggests that temporary threshold shift (TTS) can occur when noise levels exceed 75 decibels on the linear scale. Levels during STS-40/SLS-1 were expected to approach this level, and it was therefore suggested that the hearing threshold of individual crewmembers might be affected.

With the crews' consent, the flight surgeon provided audiometric data so that a statistical analysis could be performed to determine if crewmember's hearing thresholds were higher upon completion of the mission than ten days prior to lift off. It was also hypothesized that the frequencies tested with the audiometer would be affected to varying degrees, dependent upon the make-up of the acoustic environment.

Ward (1962) determined that recovery from noise exposure is generally complete within 24-48 hours. However, audiometric tests typically are not conducted on crewmembers until 3 days after landing—several hours after the anticipated recovery period has passed. Therefore, the Flight Surgeon's Office requested that arrangements be made for the audiograms to be taken as soon as possible after landing of STS-40.

Six measurements of the acoustic environment were made and stored on a one-third octave sound level meter. Since the measurements were intended to be estimates of the overall background noise level experienced by the crewmembers, and the environment was highly reverberant, the measures were taken in the center of each area (Middeck, Flightdeck and Spacelab) with the sound incidence correction factor set to 'diffuse'. Subjective evaluations of the acceptability of the sound levels were interpreted on the basis of objective measures.

METHOD

Subjects

The seven crewmembers assigned to the STS-40/SLS-1 mission participated in the evaluation. The crew consisted of four males and three females.

Apparatus

Questionnaire. The degree to which noise impacts an individual can be assessed by determining the degree to which the following occurred—annoyance, speech interference, or the need for implementation of hearing conservation techniques. Hearing conservation techniques include the use of earplugs, earmuffs and other protective devices. Post-flight questions were selected to assess each of these dimensions.

The postflight questionnaire consisted of 14 forced choice questions each with a five point rating scale. Questions fell into one of three categories—need for improvement, frequency of occurrence, or concurrence. Crew were also encouraged to provide comments on specific experiences. The comments collected via the postflight questionnaire were explored in greater detail in person with the crew during the postflight debrief.

Sound Level Meter. The sound level meter used was a Brüel & Kjær Type 2231 Sound Level Meter (Serial Number 1575194), B & K Octave Filter Set Type 1625 1/3-1/1 (Serial Number 1581549) and B&K Microphone Type 4155. The B & K Loudness Calculation Module BZ 7111 was loaded to enable the meter to measure and store ten one-third octave spectra. This sound level meter was selected because it required minimum preflight training and inflight time, was highly versatile, met the weight and volume restrictions, was similar to the Orbiter sound level meter that had already passed space qualification tests, and measured and stored one-third octave band data.

Audiometer. Both pre- and postflight audiometry measurements (consisting of air conduction screenings) were gathered by the Flight Surgeon's Office (Johnson Space Center) using Tracor audiometer Model RA400. The

Hearing Level for each crewmember at seven selected frequencies was received for both sets of measurements. Hearing Level refers to the difference in decibels between the threshold of the person being tested and the standardized audiometric zero (the average threshold of young individuals with no hearing impairment) at that frequency.

Procedures

Three months before launch a briefing was held with the STS-40 crewmembers to sensitize them to the issues to be investigated during the human factors evaluation. At five weeks to launch the questionnaire was submitted to the crew for content and procedure evaluation and two of the crew were trained to take the inflight sound level measures. The audiometric data was gathered by the Flight Surgeon's Office prior to and upon completion of the mission.

During the mission, DSO 904 personnel at Johnson Space Center monitored audio and video downlink to capture additional crew comments.

RESULTS

Questionnaire

Crewmember responses to the postflight questionnaire were received from the crew within three weeks of landing. In response to the questions of whether noise had interfered with their ability to concentrate, or to relax one individual in each case stated that interference had 'Never' occurred. Neither individual represented a Payload Specialist and therefore their duties did not restrict them to the Spacelab. Six of the seven crewmembers also found that noise interfered with their ability to relax. Three stated it had occurred frequently, and one found that noise always interfered with their ability to relax. One crewmember found that their ability to relax was never affected by noise.

Sound Level Meter

The evaluation called for ten one-third octave measurements to be made and stored by the crew; however, due to operational and time constraints only six were taken. Sound level measurments were made at the following locations and environmental conditions:

1) Center of the Middeck with the Orbiter Refrigerator/Freezer (OR/F) off and the Animal Enclosure Modules (AEM's) on;
2) Center of the Middeck with the OR/F and AEM's off;
3) In Middeck one foot from the AEM's while the AEM's and OR/F were operating;
4) Center of the Flightdeck during nominal operations;
5) Center of the Spacelab while one Spacelab Refrigerator /Freezer (R/F) compressor was operating; and,
6) In Spacelab, four feet from Spacleab R/F's while both compressors were running.

Figures 1 and 2 show the sound level measurement data graphed against the NC 50 curve. This U.S. Noise Criteria Standard has been included on the graphs to allow comparison with "acceptable" noise levels.

The DSO 904 measurements were taken during nominal operations; when levels would be expected to be at their minimum. This appears to be the case since the overall time weighted average noise level was 75.5 dB A on Flight Day 6 according to the dosimeter manifested by the JSC Orbiter Engineering Office.

This evaluation concentrated on the measurements made near the center of the acoustic spaces because they are believed to be the most representative of noise levels to which the crew was exposed. As one moves closer to the walls in a reverberant environment, such as in the Shuttle, sound level measurements double due to the pressure doubling effect at "hard" surfaces. Therefore, the measurement made one foot from the AEM's will not be included when describing the 'average' acoustic environment. This measurement (number 3) cannot be considered an accurate determination of whether the payload exceeds the applicable payload specification since the measurement includes the noise emitted by the source and the Orbiter ambient background noise level.

Audiometer

Audiograms were taken approximately an hour and a half after landing. Mean hearing level on the audiogram across crewmembers (and frequencies) prior to the mission was 8.52 decibels compared to 12.86 decibels afterwards. An analysis of variance comparing individual crewmembers pre- and postflight hearing levels on the audiometer suggests that hearing thresholds were statistically higher postflight than preflight, $F(1,6) = 5.27$, $p < .0242$.

An analysis of variance comparing the frequencies tested in the audiogram indicated that individual frequencies were effected differently, $F(1,6) = 6.69$, $p < .0001$. The Student-Newman-Keuls test confirmed that changes at the 6,000 and 8,000 hertz frequencies were significantly different from the changes that occurred at the 1,000 and 2,000 hertz frequencies.

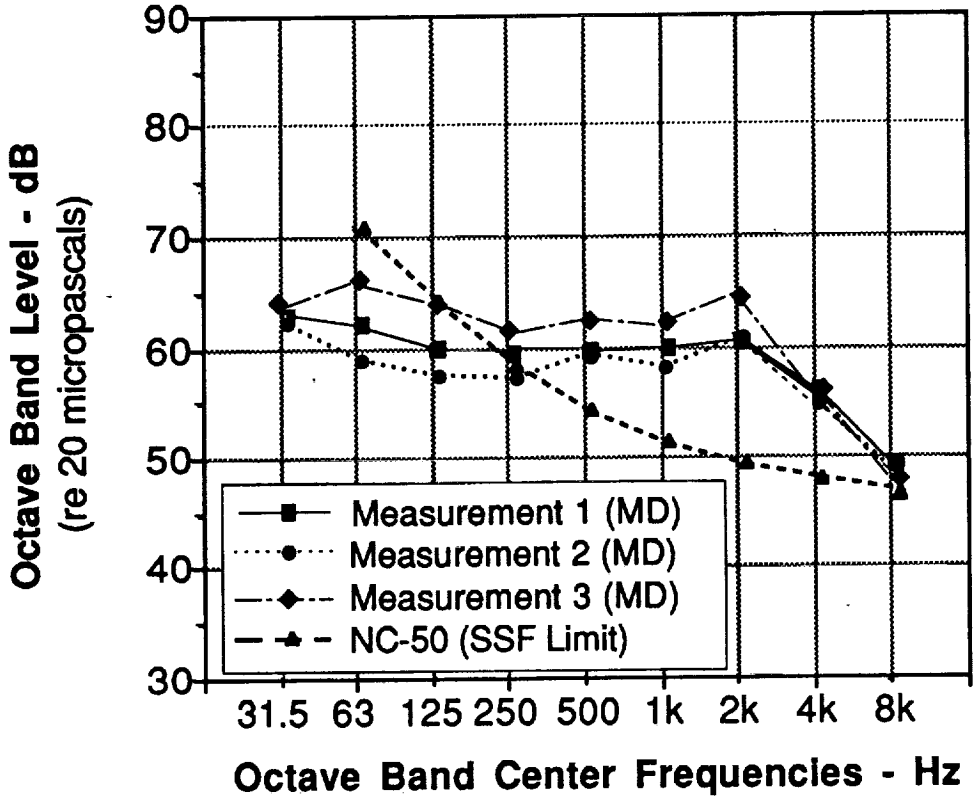

Figure 1. STS-40 Middeck noise measurements.

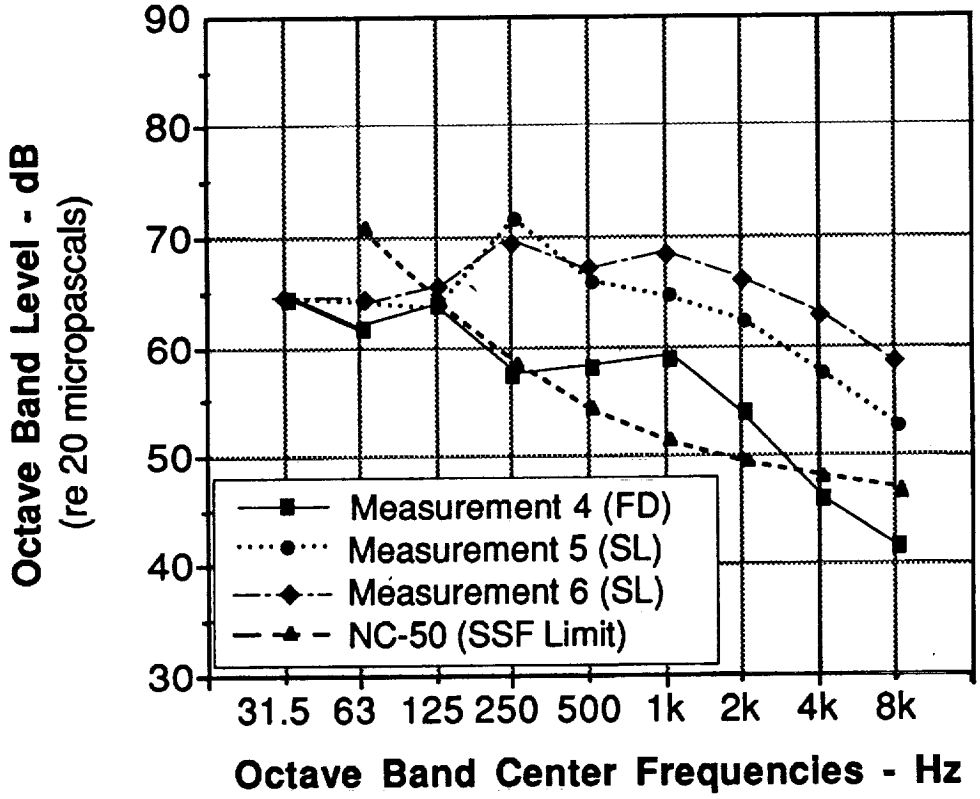

Figure 2. STS-40 Flightdeck and Spacelab noise measurements.

DISCUSSION

Overall noise levels

Although human reaction to noise is highly individualistic, a great deal of consistency was evident among rankings of the acceptability of noise levels by the STS-40 crew. Overall, reductions in noise levels were suggested for Spacelab and for specific pieces of equipment in the Middeck. No such recommendations were made in regard to the Flightdeck.

Crewmembers were asked to rate noise levels (based on their perception of the need for improvement) in each location. The areas perceived as louder by the crew did prove to be louder when measured with the sound level meter; see Figure 3 for comparison. Measurements made near the center of Spacelab were higher than those made near the center of the Middeck—the arithmetic averages being 70.1 and 63.85 dB A respectively. The Flightdeck was perceived as the quietest area and when measured it did receive the lowest value (61.8 dB A). These values reflect the average ambient noise level for each area during nominal operations based on the sound level measurements conducted during this investigation.

It is apparent from Figure 3 that for relatively small increases in noise level (as measured in A-weighted decibels) the perceived need for improvement increased dramatically. Especially noteworthy is the crew's discrimination between the Orbiter Middeck and Orbiter Flightdeck. Although there was only a two decibel difference in measured levels between the two areas, the crew stated that improvements (decreases) in the noise level of the Middeck were 'necessary'; while in the Flightdeck, improvements were rated as 'possible'. Noise is measured on the log scale and although a 3 decibel increase is equivalent to a doubling in intensity, Woodson (1981, p. 849) indicates that human listeners find a 3 decibel increase in noise levels barely perceptible. Therefore the difference in the crewmembers' perception of the two areas appears to be due to spectral differences in the makeup of the environments.

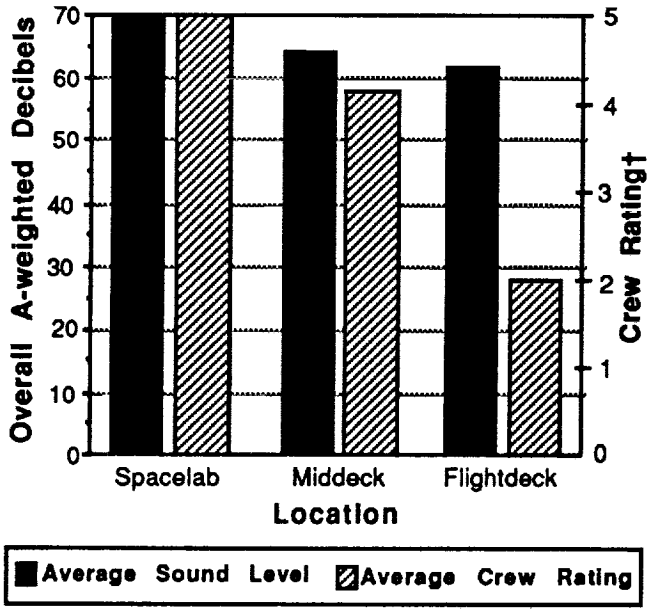

†5=Improvements Mandatory, 4=Improvements Necessary, 3=Improvements Desirable, 2=Improvements Possible, 1=Improvements NOT Needed

Figure 3. Average sound level and crew rating by location.

Comparison of the frequency spectra from the Middeck and Flightdeck measurements indicates that while levels are similar at most frequencies, at 2000 hertz the levels on the Middeck were higher than those on the Flightdeck. Since man is more sensitive to noise in the frequency range between 250 hertz and 2000 hertz the crew's rating of the Middeck as being more in need of improvements is consistent with data from the sound level meter measurements. Furthermore, the frequencies at which the Flightdeck was higher (31.5, 63 and 125 hertz) fell outside of this range. Spectra like those on the Middeck would also be more likely to result in annoyance and speech interference.

The entire STS-40 crew agreed that current noise levels would be unacceptable for longer duration missions. This supported the comments previously made that reductions in noise levels were mandatory for Spacelab during the current 9-day mission. The crewmembers suggested that the noise offending equipment should be "fixed". One individual felt that without these improvements crewmembers on longer duration missions may have to resort to periodically turning off offenders to reduce the noise.

Sleep Interference

Responses to the postflight questionnaire indicate that sleep interference was prevalent, even though ear plugs were used. Six crewmembers wore ear plugs at night and each recommended that noise levels be reduced during sleep periods—four of them believed the reductions to be mandatory.

Annoyance

When particularly loud noise sources such as the ergometer, treadmill and vacuum were operating, crewmembers found it harder to focus and they experienced difficulty relaxing.

Interference with the ability to concentrate was reported by six of the seven crewmembers. Three found that it had taken place frequently. One of the astronauts stated that noise was particularly bothersome in Spacelab when "coordination with other crewmembers was required."

Responses to the statement that "noise became increasingly bothersome" suggest that this dimension also varies greatly between individuals. Three of the crewmembers agreed that noise was more bothersome later in the mission, while one did not. The remaining three crewmembers were undecided. It appears that depending on the individual, continued noise can be, but is not necessarily, more bothersome.

This varied response across crewmembers is likely due to their individualistic response to noise. The threshold at which noise is considered to 'interfere' varies by individual—particularly with respect to the ability to sleep, concentrate and relax. This suggests that the amount of annoyance experienced by an individual cannot be predicted based upon the physical parameters of the noise environment alone.

Speech Interference

The crew noted that verbal communication was hampered by the noise levels. It was especially bothersome when the treadmill, ergometer, or vacuum cleaner were operating. As one crewmember said, it was necessary "to shout to nearby crewmembers during ergometer operations in the Spacelab, or speak at an uncomfortable level when at opposite ends of the Spacelab." Another comment addressed the consequences of such interference—noise "disrupted communications continuously requiring repeats and misunderstood instructions."

The extent to which speech interference takes place can be determined by evaluating the frequency range between 300 hertz and 6,000 hertz. The Speech Interference Level (SIL) was calculated for the DSO 904 measurements based on the American National Standards Institute (1977) standard. This standard defines the SIL as the average unweighted noise levels of the octave band center frequencies at 500, 1,000, 2,000, and 4,000 hertz. The SIL's for the two measurements taken in the center of the Middeck were averaged, as were the two Spacelab SIL's.

The DSO 904 measurements were made during nominal operations and therefore are considered to represent the best case scenario. Using a figure derived by Beranek (1988,p.559), the distances required between male and female speakers and listeners for satisfactory speech communication can be derived. For STS-40 this approach predicts that for astronauts speaking in a normal voice to communicate effectively they would have to be within approximately 0.6 meters (2 feet) of each other in the Flightdeck, 0.5 meters (1.6 feet) in the Middeck, and 0.2 meters (0.65 feet) in Spacelab. This may not present as significant a problem in the Middeck (or Flightdeck) since it is a relatively small area; however, Spacelab was 7 meters (22.97 feet) long and crewmembers were required to operate workstations separated by large distances and therefore non-aided communication in this environment would be extremely difficult.

In such an environment, individuals raise their voice to compensate—often without being aware of it. This increased vocal effort contributes to fatigue. Crew comments suggest that this did occur during STS-40. One crewmember stated regarding noise, "it was a major, if not the major contributor to fatigue."

Temporary Threshold Shift

Statistical analyses confirmed that the 4.34 dB increase in average postflight hearing threshold (across crewmembers and frequencies) over preflight was statistically significant. The greatest increases in hearing level occurred at 500 and 6,000 hertz, and were 7.86 and 6.78 dB respectively. Although the reliability of repeat audiograms is high, it should be noted that additional variance between the scores is likely to have occurred since testing conditions during both measurements could not be held constant due to operational constraints. Postflight audiometry data was gathered in California near the landing site—a different acoustic environment than during preflight measures.

Recommended Noise Levels

It is apparent that noise levels should be reduced. Allowable levels should be determined based upon the tasks that will be performed. In areas where speech communication is required, the NC 50 criterion is appropriate because above that level speech interference increases dramatically. Pearsons (1975, p. 7) predicted that in the Shuttle, an NC 50 curve would allow nearly 80% of key words to be understood correctly at a distance of five to eight feet. However, as levels increase to the NC 55 level, the percent of key words understood correctly drops to near 30%.

The NC 50 curve was originally adopted as the background noise criterion onboard the Shuttle during on-orbit conditions. The limit was subsequently increased to the existing standards due to the programmatic cost of compliance.

Beranek, Blazier, & Figwer (1971) suggest that background noise levels not exceed 47 dB A (equivalent to the NC 40) for sleeping, resting, and relaxing.

Current acoustic standards delineated for Space Station Freedom in the Man-Systems Integration Standards, Volume IV (NASA, 1989, p 5-44) specify the NC 50 curve for background noise levels in work areas where voice communication is required, and the NC 40 in sleep areas.

Data From Other Missions

Noise levels on Spacelab Life Sciences-1 (STS-40) were higher than for other missions on which acoustic data have been collected. Eilers (1987) states that during the STS-9 / Spacelab-1 mission, crewmembers found the general noise level of Spacelab to be low, and that on-orbit noise measurements supported this, with an overall noise level of 64 dB A being measured. In contrast, SLS-1 crewmembers found noise levels in Spacelab unacceptable, and background noise level measurements indicated the noise levels to be 70 dB A. The measurements made during the current DSO were taken during nominal operations when levels would be expected to be at their minimum. According to the dosimeter manifested by the JSC Orbiter Engineering Office the overall time weighted average noise level for Flight Day 6 was 75.5 dB A.

Preliminary results from measurements made during a subsequent flight of DSO-904 aboard the STS-50 / USML-1 mission indicate that noise levels were again much lower. In Spacelab during nominal operations (i.e. periods when only the life support and other essential systems are operating) average noise levels were about 62 decibels compared to the near 70 decibel levels measured during SLS-1. Crew comments also reflect a much improved noise environment.

CONCLUSIONS

The higher noise levels on SLS-1 appear to be directly attributable to mission specific equipment—a premise supported by the large number of acoustic waivers which were granted for the SLS-1 mission. While crew comments collected about the noise environment aboard SLS-1 are not representative of all Spacelab missions they provide valuable information about the impact of the acoustic environment on crew satisfaction and productivity.

Further evaluation of the Orbiter acoustic environment and its impact on crew operations is planned--the sound level meter has been manifested to fly again on both SpaceHab-01 and -02 missions due to launch during 1993.

ACKNOWLEDGEMENTS

This research was supported by the National Aeronautics and Space Administration under contract NAS9-17900.

REFERENCES

1. Beranek, Leo L., NOISE AND VIBRATION CONTROL, Washington, DC: Institute of Noise Control Engineering, 1988.

2. Beranek, L. L., Blazier, W. E., and Figwer, J. J., "Preferred noise criterion (PNC) curves and their application to rooms", JOURNAL OF THE ACOUSTICAL SOCIETY OF AMERICA, 50, 1971, p. 1227.

3. Eilers, D. "Audible noise control for pressurized modules PM4 and PM2", TECH REPORT COL-MBER-000-TN-0420-1, European Space Agency: MBB/ERNO, 1987.

4. NASA , MAN-SYSTEMS INTEGRATION STANDARDS, VOLUME IV (NASA-STD-3000), Houston, TX: National Aeronautics and Space Administration, 1991.

5. NASA , MAN-SYSTEMS INTEGRATION STANDARDS, VOLUME I (NASA-STD-3000), Houston, TX: National Aeronautics and Space Administration, 1989.

6. NASA , ORBITER VEHICLE END ITEM SPECIFICATION (OVEI) (MJ070-0001-1c), Houston, TX: National Aeronautics and Space Administration, 1986.

7. NASA, SPACELAB PAYLOAD ACCOMMODATIONS HANDBOOK (SLP 2104), Houston, TX: National Aeronautics and Space Administration, 1985.

8. Pearsons, Karl S., RECOMMENDATIONS FOR NOISE LEVELS IN THE SPACE SHUTTLE (Job Number 157160), Houston, TX: Bolt, Beranek, and Newman Inc, February, 1975.

9. Ward, W. D. , "Damage-risk criteria for line spectra", JOURNAL OF THE ACOUSTICAL SOCIETY OF AMERICA, 34, 1962, pp. 1610-1619.

10. Woodson, Wesley E., HUMAN FACTORS DESIGN HANDBOOK, New York: McGraw Hill, 1981.

11. Willshire, Kelli F. and Leatherwood, Jack D., SHUTTLE ASTRONAUT SURVEY, Langley, VA: National Aeronautics and Space Administration, 1985.

Session H4: HUMAN PERFORMANCE MEASUREMENT IV—FLIGHT EXPERIMENTS

Session Chair: Col. Donald Spoon

N94-11539

VISUAL EARTH OBSERVATION PERFORMANCE IN THE SPACE ENVIRONMENT

Human Performance Measurement IV - Flight Experiments

CPT John F. Huth, CAPT James D. Whiteley, CW3 John E. Hawker

ABSTRACT

A wide variety of secondary payloads have flown on the Space Transportation System (STS) since its first flight in the 1980s. These experiments have typically addressed specific issues unique to the zero-gravity environment, and use the experience and skills of the mission and payload specialist crew members to facilitate data collection and ensure successful completion. This paper presents the results of the Terra Scout experiment, which flew aboard STS-44 in November 1991. This unique Earth Observation experiment, specifically required a career imagery analyst as the payload specialist (operator) as part of the experimental design. The primary flight equipment was the Spaceborne Direct-View Optical System (SpaDVOS), a folded optical path telescope system designed to mount inside the shuttle on the overhead aft flight deck windows. Binoculars, and a small telescope, were used as backup optics. Using his imagery background, coupled with extensive target and equipment training, the payload specialist was tasked with documenting: 1) The utility of the equipment, 2) His ability to acquire and track ground targets, 3) The level of detail he could discern, 4) The atmospheric conditions, and 5) Other in-situ elements which contributed to or detracted from his ability to analyze targets. Special emphasis was placed on the utility of a manned platform for research and development of future spaceborne sensors. The results and lessons learned from Terra Scout will be addressed, including human performance and equipment design issues.

I. INTRODUCTION.

Since the very beginnings of the space program, various DOD organizations have shown an on-again, off-again interest in manned surveillance from a spaceborne platform. Unclassified literature indicates two of the earliest programs were the Dyna Soar and Manned Orbiting Laboratory (MOL) programs of the 1950s and 1960s, respectively [1]. Both of these programs were purportedly cancelled due to cost overruns and the political climate, before being tested. From the early 70s, when the Apollo program was winding down, until the beginning of the Shuttle program in the 80s, the DOD showed little interest in such programs. Whether this was due to opportunity or other reasons is unclear. Interest by the services surged in 1985 with the beginning of the Military-Man-In-Space (MMIS) program. The objective of the MMIS program is to capitalize on man's unique decision making abilities, and apply these skills to satisfy DOD objectives.

Various experiments were proposed by the military services at the beginning of the MMIS program. Included in the list of experiment proposals were three military earth observation experiments; one from each of the services. The three experiments -- Battleview, Moses, and Terra Scout were proposed by the Air Force, Navy, and Army, respectively. Terra Scout was unique in that the experiment required a payload specialist (PS) who was a military imagery analyst and would use specifically designed optics, rather than a career astronaut provided with off-the-shelf optics. The drawbacks to this approach were numerous, the optics had to be designed and tested, and using a PS meant a greater shuttle performance margin requirement as well as fighting numerous political battles. As one might predict, the other two earth observation experiments were flown prior to Terra Scout. Battleview, with Army input (known as Terra View), Moses, and another experiment called Space Debris were combined together as a Tri-Service experiment call M88-1. These experiments were conducted on STS-28 in August 1989. It was our opinion, after reviewing the results from this flight, that we were on the right track. The crew had reporting seeing ships, large swept wing aircraft, and the crew commander said with slightly better optics he would be able to see trucks on a highway. They also found that large aperture optics (a 6" Celestron) were useless because of the poor optical quality of the shuttle windows. This finding was later supported by optical tests of the space overhead windows by Armstrong Aeromedical Research Laboratory (AAMRL) and the Aerospace Corporation [2,3].

II. EXPERIMENTAL SETUP.

The primary optical equipment selected for the Terra Scout experiment was the Spaceborne-Direct View Optical System (SpaDVOS) (see Fig 1). The SpaDVOS was developed by AAMRL, with enough funding from the Air Force and Army to build two flight units. The SpaDVOS was originally designed for human factors experiments by AAMRL and was first flown on STS-38 in December 1990. Using the comments from the astronauts who used the SpaDVOS on-orbit, a number of hardware modifications were made to prepare for the Terra Scout experiment.

The original purpose of the Terra Scout experiment was to collect data which could be used to determine the ability of the PS to collect valuable information in real time. During the seven year development of the experiment, the objective evolved to include a variety of R&D issues such as: testing the flexibility of the man-in-the-loop, estimating how well the Soviet cosmonauts could see from their manned platforms, identifying potential utility/benefit of real-time observations to the DOD (e.g., crisis augmentation), the utility or advantages of live-color analysis, and the utility of the Shuttle as an R&D platform for future experimentation.

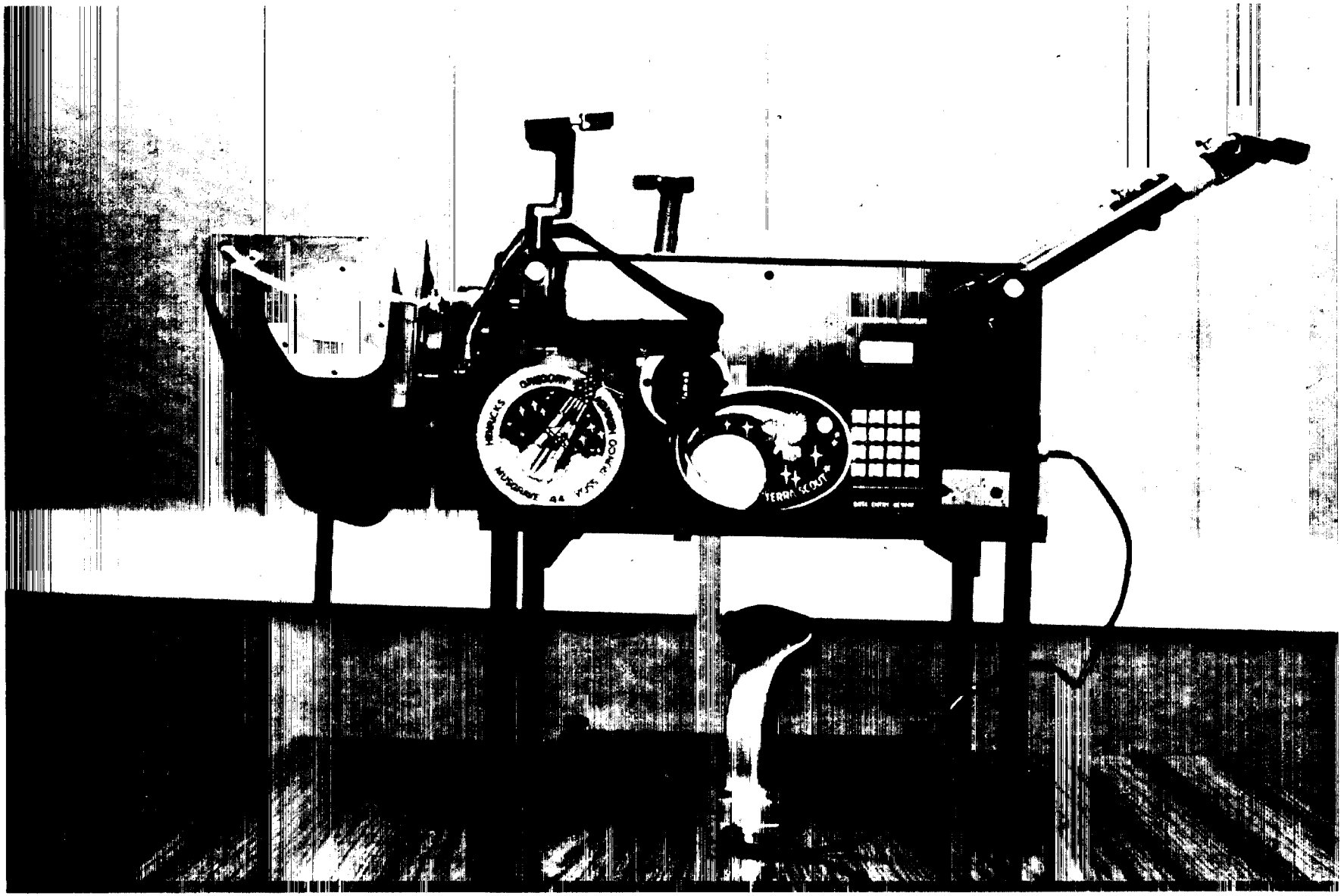

Figure 1

The general approach for data collection used by the PS was to mount the SpaDVOS optics in the overhead, aft flight deck windows using the window shade clamps. Next the SpaDVOS was connected to the 28VDC orbiter power and orbiter Video Tape Recorder (VTR) system then switched on. The PS then initialized the system by moving the tracking mirror forward/aft and side to side. Target data was entered for up to three targets. This data included the Mission Elapsed Time (MET) of closest approach to the target, the off-nadir angle or direction to the target, and the orbiter altitude and velocity at that MET. By entering this information on a keypad, an internal computer provided the operator pointing cues to the target from one minute prior to acquisition until visual loss of the site. These cues were displayed by two LED displays in the eyepiece providing cross-track and along-track data. When these LED displays were "zeroed-out" the operator was assured that his target was in the telescope's field of view. While target acquisition was strictly manual, once the target site had been acquired, tracking could be done manually, or in a semi-automated mode using a joystick to control the along-track velocity of the tracking mirror. While the target was being tracked, the operator could zoom in or out and change the aperture setting (f-stop) with two handles on the bottom side of the SpaDVOS (see Fig 2). Three eyepieces were provided so the operator could select the best magnification for the target site. These covered a magnification range from 4X to 67X. Each of these eyepieces, as well as other SpaDVOS functions, were tested during the characterization pass over the first ground site.

The way that the SpaDVOS unit was able to capture light and record on a video tape is as follows:

> The optical path of the SpaDVOS has a beamsplitter just before the light is reflected into the eyepiece. The beamsplitter routes half the light to the eyepiece and the other half to a Charge Coupled Device (CCD). The CCD image was recorded using the obiter VTR system. Since the CCD image is not magnified by the eyepiece, the visual and recorded images have different scales. The purpose of the recording was to visually confirm the operator was in the target areas, and record his verbal comments on the audio track. As alternate optics, the PS also had a pair of 14X70 Fujinon binoculars and a 15-60X Bausch & Lomb spotting telescope.

The PS was to analyze both pre-planned and ad hoc targets. Pre-planned targets were selected during mission planning, and the PS was familiar with these by studying target folders. These folders were taken aboard for reference and refresher prior to target acquisition, and to annotate comments about target status after a target pass. Pre-planned targets included a variety of military and geographical targets, as well as four large resolution grid targets (see Fig. 3). The pattern of disks on the

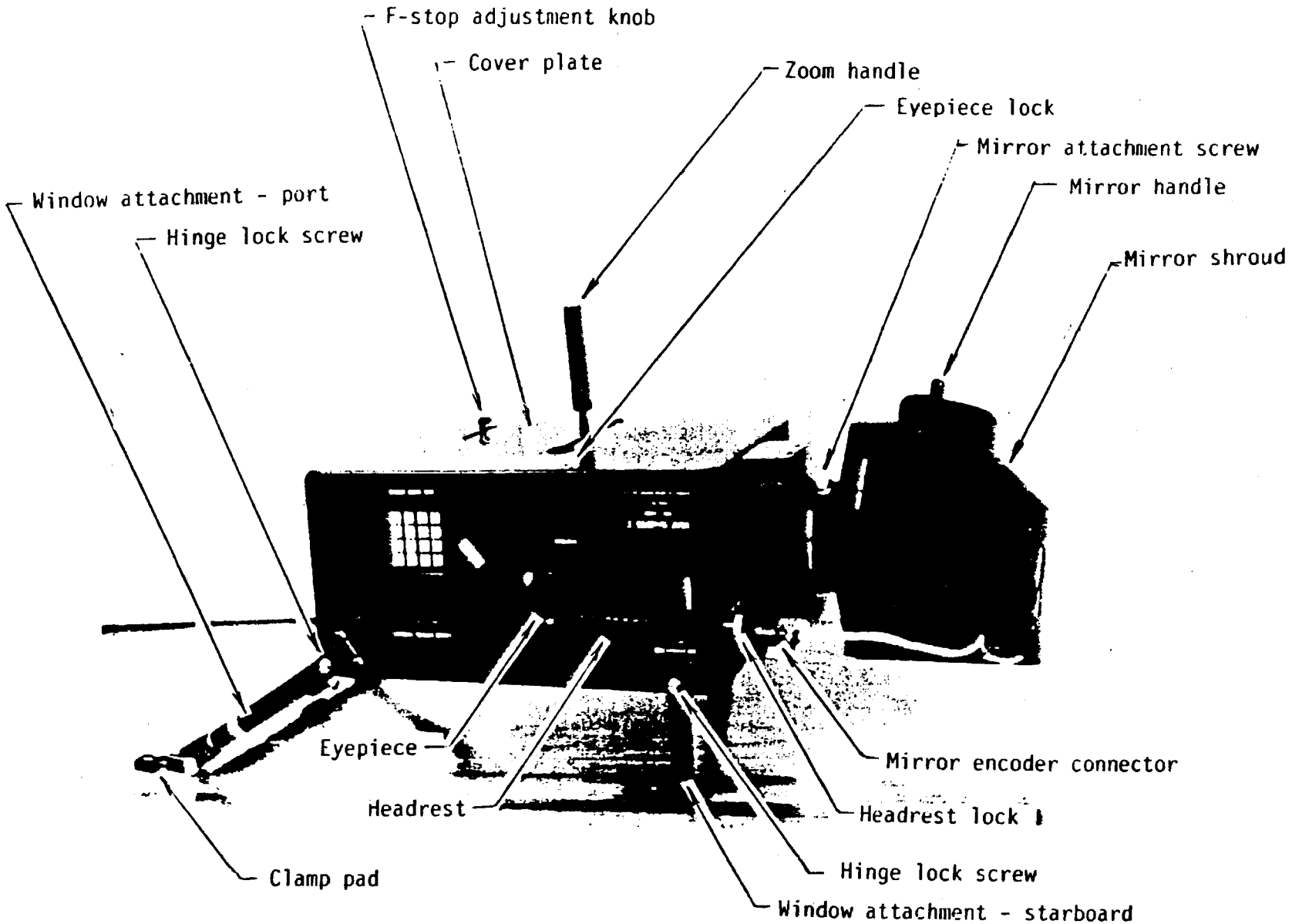

Figure 2 Fully Assembled Unit.

resolution grid, which are known as Blackwell disks, were changed after each shuttle overflight by teams on the ground. They also measured the illumination (contrast) and collected weather measurements at the four resolution sites. Ground truth for the other sites was provided by national technical means. Ad hoc targets were targets which were uplinked to the PS during the mission, and for which no target folders existed.

The PS trained for the experiment by extensive study of target folders, becoming familiar with the hardware, and by using the Flexible Image Generation System (FIGS) at AAMRL. The FIGS simulates what he would see looking at the earth with SpaDVOS at shuttle altitudes and velocities. Additionally, he had the opportunity to use the SpaDVOS during testing on a Lear Jet and several "Zero-G" (KC-135) flights.

Terra Scout was manifested for flight in June of 1990. The flight assigned was STS-44, which was scheduled for an early 1991 launch. While things started to pull together during the preparation for launch, there were several technical and operational concerns. Window tests on spare overhead windows made the case for smaller aperture optics, such as SpaDVOS, to be near optimal. The concern was what the usable magnification would be even with a near optimal aperture [2,3]. Several improvements were made to SpaDVOS as a result of STS-38. The eyepiece focus adjustment was redesigned and additional eyepieces were tested and added to better cover the magnification range. An along-track motor drive was added to the SpaDVOS unit, despite the short time before launch. This allowed smoother tracking than could be done manually. There were also indications from both the STS-38, as well as the "Zero-G" flight, that having the PS stable during target acquisition and tracking could be a problem; a means of restraining him with a harness and straps from the treadmill was devised.

A primary human factors concern was if the PS would experience space sickness and how this would effect his skills to conduct the experiment. Atmospheric effects were another key concern. Not only should you count on almost doubling the number of opportunities you need to account for weather, but the effects of recent volcanic activity, oil fires, and rain forest burning were evident in the sunsets. We were curious about the effect this would have on our data collection. A study done for us by the Army Research Institute in 1987 estimated we would need 20 good observation opportunities for statistical significance [4]. Under the experimental design we were to make comparisons between our spaceborne observer and a ground-based observer, who was provided with similar data to analyze. Taking 20 as our minimum sample size, and with 42 opportunities in our flight plan, we were near where we needed to be, using the rule of thumb for weather. However, the other factors were still complete unknowns.

JSC-24164

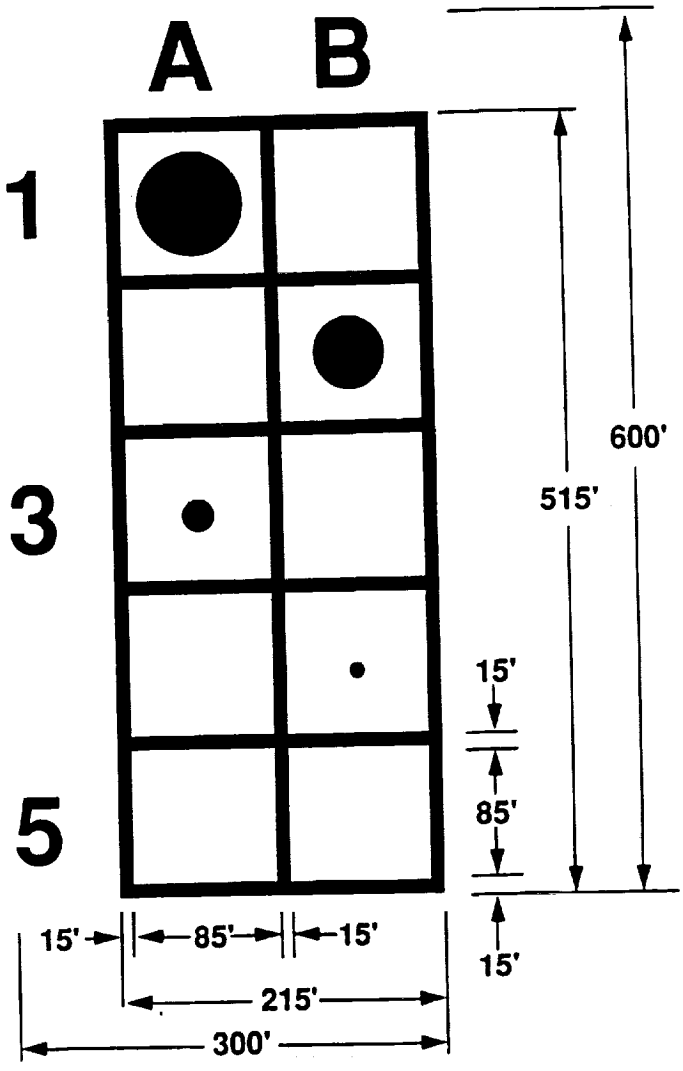

Figure 3

C-2

III. RESULTS AND DISCUSSION.

On 15 Nov 91 we conducted our L-5 (5 days prior to launch) checkout of the experiment hardware, the last check before it was moved to the Vertical Assembly Building (VAB) and then into the middeck lockers. STS-44 launched just after 6:30 p.m. on 24 Nov 91. The next day, on orbit 17, was the first scheduled observation opportunity. This was a characterization pass on a resolution target. The pass was successful and the resolution grid and largest circles were acquired. However, several minutes later, on another resolution target pass the cueing system malfunctioned. It was discovered that by cycling the power, the anomaly could be corrected. This problem never occurred prior to flight, and could not be duplicated nor the source discovered afterward.

The calibration passes, which were done during the early part of the mission, indicated that the best eyepiece to use was the 21mm at maximum zoom. This provided a magnification of approximately 30x.

Another anomaly, which occurred was the lack of smoothness in the tracking. This also had never occurred during ground or Zero-G testing. Although the initial thought was that launch vibrations may have damaged the hardware, a post-mission analysis of the hardware and discussions with the PS and commander made us suspicious that the hardware may have been damaged between L-5 and flight. This possibility was based on the two anomalies discussed, as well as damage to the eyepieces and the outside of the SpaDVOS. None of these conditions existed prior to launch, but were present on-orbit. Damage to eyepieces and on the outside of a piece of hardware, that are surrounded by foam packing, would not be expected by normal launch vibration, nor were they experienced with the hardware on STS-38 or with the M88-1 hardware on STS-28 or STS-44.

The hardware anomalies, however, did not significantly impact the mission objectives. Rather, the combination of window quality and atmosphere had the most adverse effects. The windows limited the effective magnification of the 9mm eyepiece, such that it was not usable in full zoom. However, atmospheric conditions were the greatest detractor from the experiment. STS-44 was described as one of the cloudiest missions in shuttle history. Additionally, the combination of environmental factors, which were responsible for recent spectacular sunsets, also degraded our observation capabilities. Satellite data analyzed by the Space Shuttle Earth Observation Office indicated that the atmosphere over our resolution sites were well below optimal. Also, the comments recorded by the PS indicated that the resolution sites were typically clearer than the other ground targets. Comments by the veteran astronauts on the flight supported the PS comments and the satellite data analyzed by NASA.

On day seven of the mission, a malfunction in the space shuttle's back-up IMU forced an early termination of the mission. Not only were there eleven more opportunities planned, but the PS and MS for the M88-1 experiment who had previously been competing for window space, managed to find a way of using both experiments in the window simultaneously. This would have provided more observation opportunities for both experiments, as well as other potential synergistic outcomes. In the final tally only eight of the observation opportunities provided enough data for adequate analysis.

Our concerns about the stability of the observer in the eyepiece turned out not to be an issue as the PS had no problem with stability. Also, concern over the space sickness effects on the PS satisfactorily resolved itself as the PS experienced no space sickness. One issue that did arise during the course of the experiment was the complication involved in communication with the PS. Trying to resolve anomalies to get experiment status would be much clearer if the PI were allowed direct communication with the PS/MS.

With the small sample size, statistical analysis was difficult, at best. Even without statistical significance, we believe that with the data collected, we have successfully met our objectives. The ability of the PS to dynamically acquire targets other than those which were provided to him in real time, detect target motion, work around or fix hardware anomalies, and use his decision making abilities to streamline the conduct of the experiment, demonstrated the flexibility and utility of the man-in-the-loop. These were all worthwhile data points which are hard to quantify.

The SpaDVOS was very capable of providing target acquisition and tracking capability. Under certain conditions, the PS reported seeing the disks down to 24ft., as well as identifying the 15 foot wide grid lines outlining the grids. Note that grid lines being long, linear features aids in their identification. His observations also indicated the strong correlation between resolution and the angle off nadir to the target. Most of the opportunities did not allow sufficient resolution for analysis primarily due to atmospheric and window conditions limiting effective magnification. Based on previous window tests, as well as the limited number of good observations we did make, it seems unlikely that good resolution through the windows would be consistently available to do any analysis further than identifying surface ships or large aircraft. These conditions combined with shuttle orbital parameters make tactical target detection serendipitous at best. This is not to say that further testing of other available optics should not be done, as the variables which effect in-cabin resolution and their relative effects are not sufficiently understood. Hardware with characteristics similar to

SpaDVOS would be useful for geological and weather applications, however, the device should have a single optical path. This would preclude poor video recording caused by optimizing the aperture for the observer, and leaving insufficient light for recording images.

While the resolution needed for detailed target analysis was not sufficient, the level of detail that was available from the SpaDVOS and the 14X70 binoculars did allow the PS to observe ships and large aircraft. Observations of this type activity does have direct impact on operations security. Just as the Soviet's have conducted extensive testing on color vision, there are strong indications that their manned orbiting vehicles have been used to conduct extensive military experiments. These experiments have most likely included the evaluation of man's ability to identify, track, and locate targets and R&D of advanced reconnaissance and surveillance systems [5]. Knowing they have windows in their space station and given their interest in exploiting their space capabilities, it is not unreasonable to assume that their windows are likely of optical quality. This would provide them with an "in-cabin" resolution capability much better than our current capability. This should be well considered for our future manned systems if we plan to test systems for military or environmental purposes.

The capability of viewing a scene in color seems to be a significant contributor to target acquisition, tracking, and analysis. This is based on comments from the PS, which support the comments of other cosmonauts and astronauts. The phenomena of color vision and color observation from orbit has been investigated extensively by the Soviet's [6] and warrants further analysis. It is the spectral content of a ground scene which we are planning to exploit in future experiments.

The major advantage in using the current shuttle program for military earth observation would be to test advanced sensors in the payload bay. For testing advanced sensors the shuttle provides:

- A controllable platform at many available altitudes and attitudes.

- Easily returnable payloads.

- Testing in the space environment.

The advantages of using a PS for specific experiments are significant when a particular skill is needed. A Principal Investigator (PI) should always use the most qualified person for the task. Therefore, he is better and more intensively trained on experiment specific tasks. He is more available for feedback,

providing his feedback to the experimenters in a common language, making it easier to relate his experiences. Additionally, our PS was completely integrated into the crew, becoming involved with other experiments as well as Terra Scout. This worked to the advantage of everyone. This was particularly true of the medical experiments, which will further our understanding of physiological effects of spaceflight on the human body.

It is our conclusion that the experiment was an overall success and related follow-on experimentation, research and development should be pursued.

REFERENCES

[1] Timothy D. Killebrew, "Military Man In Space: A History of Air Force Efforts to Fund a Manned Space Mission," Air Command and Staff College, Report #87-1425, May 1987.

[2] Harold S. Merkel, Harry L. Task, "Optical Test of the Space Shuttle Overhead Windows," AAMRL Report AAMRL-TR-90-024, May 1990.

[3] Karen P. Scott, "Space Shuttle Overhead Windows, Optical Tests," Aerospace Corporation Report #TR-0091(6508-21)-1, June 1991.

[4] George W. Lawton, "Suggested Terra Scout Experiment Plan," Army Research Institute Working Paper WPHUA 89-02, January 1989.

[5] Johnathan Litchman, "The Soviet Manned Space Program in Support of Ground Forces," How They Fight, DIA Document #ATC-WP-2600-034-90, January-March 1990, pp. 19-21.

[6] Vladimir V. Vasyutin, Artur A. Tishchenko, "Space Coloristics," Scientific American, July 1989, pp. 84-90.

TEST PILOT PERSPECTIVE ON HUMAN PERFORMANCE IN FLIGHT

Maj. Pete Demitri

Abstract unavailable at time of publication.

ROUND TABLE DISCUSSION OF PROGRESS, DIRECTIONS, AND NEEDED ACTIVITIES IN HUMAN PERFORMANCE AND ITS MEASUREMENT

Led by Dr. Mary Connors and Col. Donald Spoon

Abstract unavailable at time of publication.

SECTION III

LIFE SUPPORT

Session L1: BAROPHYSIOLOGY I

Session Chair: A. Pilmanis, M.D.

N94-11540

USE OF ULTRASOUND IN ALTITUDE DECOMPRESSION MODELING

Dr. Robert M. Olson[1] and Dr. Andrew A. Pilmanis[2]
[1]KRUG Life Sciences, San Antonio Div.
P.O.Box 790644
San Antonio, TX 78279-0644
[2]Armstrong Laboratory
AL/CFTO
Brooks AFB, TX 78235

A model that predicts the probability of developing decompression sickness (DCS) with various denitrogenation schedules is being developed by the Armstrong Laboratory, using human data from previous exposures.* It was noted that refinements are needed to improve the accuracy and scope of the model. A commercially developed ultrasonic echo imaging system is being used in this model development. Using this technique, bubbles images from a subject at altitude can be seen in the gall bladder, hepatic veins, vena cava, and chambers of the heart. As judged by their motion and appearance in the vena cava, venous bubbles near the heart range in size from 30 to 300 M. The larger bubbles skim along the top, whereas the smaller ones appear as faint images near the bottom of the vessel. Images from growing bubbles in a model altitude chamber indicate that they grow rapidly, going from 20 to 100 M in 3 sec near 30,000 ft altitude. Information such as this is valuable in verifying those aspects of the DCS model dealing with bubble size, their growth rate, and their site of origin.

*The voluntary, fully informed consent of subjects used in this research was obtained as required by AFR 169-3.

N94-11541

HYPOBARIC DECOMPRESSION PREBREATHE REQUIREMENTS AND BREATHING ENVIRONMENTS. James T. Webb*, Ph.D., KRUG Life Sciences, San Antonio Division, and Andrew A. Pilmanis, Ph.D., Armstrong Laboratory, Brooks AFB, TX. The voluntary, fully informed consent of the subjects used in this research was obtained as required by AFR 169-3.

To reduce incidence of decompression sickness (DCS), prebreathing 100% oxygen to denitrogenate is required prior to hypobaric decompressions from a sea level pressure breathing environment to pressures lower than 350 mm Hg (20,000 ft; 6.8 psia). The tissue ratio (TR) of such exposures equals or exceeds 1.7; TR being the tissue nitrogen pressure prior to decompression divided by the total pressure after decompression ([0.781*14.697]/6.758). Designing pressure suits capable of greater pressure differentials, lower TRs, and procedures which limit the potential for occurrence DCS would enhance operational efficiency. The current 10.2 psia stage decompression prior to extravehicular activity (EVA) from the Shuttle in the 100% oxygen, 4.3 psia suit, results in a TR of 1.65 and has proven to be relatively free of DCS. Our recent study of zero-prebreathe decompressions to 6.8 psia breathing 100% oxygen (TR = 1.66) also resulted in no DCS (N = 10). The level of severe, Spencer Grades 3 or 4, venous gas emboli (VGE) increased from 0% at 9.5 psia to 40% at 6.8 psia yielding a Probit curve of VGE risk for the 51 male subjects who participated in these recent studies. Earlier, analogous decompressions using a 50% oxygen, 50% nitrogen breathing mixture resulted in one case of DCS and significantly higher levels of severe VGE, e.g., at 7.8 psia, the mixed gas breathing environment resulted in a 56% incidence of severe VGE versus 10% with use of 100% oxygen. The report of this study recommended use of 100% oxygen during zero-prebreathe exposure to 6.8 psia if such a suit could be developed. For future, long-term missions, we suggest study of the effects of decompression over several days to a breathing environment of 150 mmHg O_2 and approximately 52 mmHg He as a means of eliminating DCS and VGE hazards during subsequent excursions. Once physiologically adapted to a 4 psia vehicle, base, or space station segment, crewmembers could use greatly simplified EVA suits with greater mobility and no prebreathe requirement.

ALTITUDE DECOMPRESSION MODEL DEVELOPMENT

T. Scoggins
Armstrong Laboratory
AL/CFTS
Brooks AFB, TX 78235-5000

Abstract unavailable at time of publication.

N94-11542

JOINT PAIN AND DOPPLER-DETECTABLE BUBBLES IN ALTITUDE (HYPOBARIC) DECOMPRESSION

Michael R. Powell
NASA/Johnson Space Center
Space Biomedical Research Institute,
Environmental Physiology/Biophysics Section
2101 Nasa Road 1
Houston, TX 77058

The observation that altitude decompression sickness (DCS) is associated with pain in the lower extremities is not new, although it is not a consistent finding. DCS in divers is generally in the upper body, an effect often attributed to non-loading of the body while immersed. In caisson workers, DCS is reported more in the lower extremities. Surprisingly, many researchers do not mention the location of DCS joint pain, apparently considering it to be random. This is not the case for the tissue ratios encountered in studying decompression associated with simulated EVA. In NASA/JSC tests, altitude DCS generally presented first in either the ankle, knee, or hip (83% = 73/88). There was a definite statistical relation between the maximum Spencer precordial Doppler Grade and the incidence of DCS in that extremity, although this is not meant to imply a causal relation between circulating gas bubbles and joint pain. The risk of DCS with Grade IV was considerably higher than that of Grades 0 to III. The DCS risk was independent of the "tissue ratio" (calculated for the 360-minute halftime tissue). There was a predominance of lower extremity DCS even when exercise was performed with the upper body. The reason for these locations we hypothesize to be attributed to the formation of tissue gas micronuclei from kinetic and tensile forces (stress-assisted nucleation) and are the result of individuals ambulating in a one-g environment. Additionally, since these showers of Doppler bubbles can persist for hours, it is difficult to imagine that they are emanating solely from tendons and ligaments, the supposed site of joint pain. This follows from Henry's law linking the volume of joint tissue (the solvent) and the solubility coefficient of inert gas; there is volumetrically insufficient connective tissue to produce the prolonged release of gas bubbles. If gas bubbles are spawned and released from connective tissue, their volume is increased by those from muscle tissue. Therefore, the nexus between Doppler-detectable gas bubbles and joint-pain decompression sickness is essentially a statistical, rather than a direct, one.

N94-11543

ARTERIAL GAS EMBOLI IN ALTITUDE-INDUCED DECOMPRESSION SICKNESS

Andrew A. Pilmanis[1] and Robert M. Olson[2]
[1]USAF Armstrong Laboratory
AL/CFTS
Brooks AFB, TX 78235-5000
[2]KRUG Life Sciences
P.O. Box 790644
San Antonio, TX 78279

Exposure to high altitudes can result in the evolved-gas condition referred to as decompression sickness (DCS). Ultrasonic monitoring techniques have clearly demonstrated the presence of venous gas emboli (VGE) during decompression. Although important to DCS research and our understanding of the physiological mechanisms of this condition, VGE *per se* have not been considered clinically hazardous, unless in extreme numbers. Arterial gas emboli (AGE), on the other hand, are generally viewed with great concern. AGE can enter the cerebral arterial circulation and arrest blood flow, resulting in potentially serious injury.

Left ventricular gas emboli were observed with echo imaging in five volunteer subjects during exposure to simulated altitude. These serendipitous findings occurred during altitude exposure under 3 separate research protocols involving 79 subject exposures. The voluntary, fully informed consent of the subjects used in this research was obtained as required by AFR 169-3. A Hewlett-Packard SONOS 1000 Echo Imaging System was used to monitor for precordial gas emboli. The improved resolution of the SONOS 1000 appears to account for these new findings. Four subjects had high incidence DCS and VGE during previous research flights. One subject only had one flight. The altitudes and AGE onset times for the five cases were: (1) 25,500 ft/2:23, (2) 29,000 ft/0:27, (3) 19,500 ft/3:49, (4) 29,500 ft/3:15, and (5) 29,500 ft/1:31. In all five cases, at the time of AGE onset, the VGE scores were high from all monitored locations. Four of the cases were symptomatic at the time of AGE onset (pain and skin mottling). No cerebral manifestations were observed. All subjects were immediately recompressed to ground level and successfully treated wither with 2 hours of post-breathing or with hyperbaric oxygen therapy.

In conclusion, previously undetected AGE were demonstrated—with and without DCS symptoms—during exposure to altitude. It appears that this gas transferred from the venous side to the arterial side via either intracardiac defects or the pulmonary circulation. The clinical and operational implications of this finding are yet to be determined.

Session L2: BAROPHYSIOLOGY II

Session Chair: M. Powell, M.D.

N94-11544

TRANSCRANIAL DOPPLER ULTRASOUND AND THE ETIOLOGY OF NEUROLOGIC DECOMPRESSION SICKNESS DURING ALTITUDE DECOMPRESSION

W. T. Norfleet, M. R. Powell, K. V. Kumar*, and J. Wallgora
Space Biomedical Research Institute and *KRUG Life Sciences
NASA/Johnson Space Center, Houston,Texas 77058

ABSTRACT The presence of gas bubbles in the arterial circulation can occur from iatrogenic mishaps, cardiopulmonary bypass devices, or following decompression, e.g., in deep-sea or SCUBA diving or in astronauts during extravehicular activities (EVA). We have examined the pathophysiology of neurological decompression sickness in human subjects who developed a large number of small gas bubbles in the right side of the heart as a result of hypobaric exposures. In one case, gas bubbles were detected in the middle cerebral artery (MCA) and the subject developed neurological symptoms; a "resting" patent foramen ovalae (PFO) was found upon saline contrast echocardiography. A PFO was also detected in another individual who developed Spencer Grade IV precordial Doppler ultrasound bubbles, but no evidence was seen of arterialization of bubbles upon insonation of either the MCA or common carotid artery. The reason for this difference in the behavior of intracardiac bubbles in these two individuals is not known. To date, we have not found evidence of right-to-left shunting of bubbles through pulmonary vasculature. The volume of gas bubbles present following decompression is examined and compared with the number arising from saline contrast injection. The estimates are comparable.

INTRODUCTION

A. DECOMPRESSION SICKNESS

1. Manifestations

Decompression sickness (DCS) can manifest itself in many forms dependent upon (i) the site of gas phase growth in the tissues or (ii) migration of bubbles by the blood stream. The forms generally include the following although this listing is not complete (missing, for example, is lymphatic obstruction):

(a) neurologic DCS from the formation of gas bubbles in the brain or spinal cord, or from gas embolization of the brain or cord,

(b) joint-pain DCS from the formation of a gas phase in the connective tissues (tendons, ligaments) of joints,

(c) "the chokes" from the accumulation of gas bubbles in the pulmonary vasculature,

(d) "skin bends" and pruritis from the formation of gas bubbles (purportedly) in the capillaries of the skin,

(e) the "staggers" from the formation of a gas phase in the cerebellum or VIIIth cranial nerve or the organs of balance,

(f) cardiovascular collapse from the appearance of a very large gas bubble load in the right heart leading to a great reduction in cardiac output,

(g) dysbaric osteonecrosis, presumably from the presence of a gas phase in bone.

2. NASA Interest in Cerebral Gas Bubbles

The present study was conducted to

investigate the development and pathophysiology of intravascular gas bubbles arising from decompressions to hypobaric conditions, a process that is a part of extravehicular activities. As a portion of this work, provisions were made for (i) the detection of decompression gas bubbles in the arterial circulation of human subjects, and (ii) screening for the presence of patent atrial septal defects (ASDs) by means of B-mode ultrasound and saline contrast echocardiography. Individuals with a patency were not excluded since:

(1) Current evidence is indecisive with regard to the relationship between an ASD and an increased incidence of neurologic DCS in SCUBA divers. Wilmshurst et al. (1990) found a prevalence of patent right-to-left shunts of 25% (26/105) in a subgroup never experiencing DCS versus a prevalence of 24% (8/34) in a group experiencing late neurologic DCS and 15% (3/20) for joint-pain DCS.

(2) No studies indicate that subjects with numerous decompression gas bubbles (e.g., Spencer Grade IV) develop central nervous system (CNS) DCS or peripheral nerve involvement with an incidence of approximately 25%. This might be expected since the prevalence of PFOs in a population determined post-mortem is ≈ 20 to 30%.

(3) The presence of a PFO is not medically disqualifying for astronauts, i.e., candidates are not currently eliminated from astronaut selection because of such a right-to-left shunt.

Clinically, the detection of a PFO involves echocardiographic imagery during intravenous injections of microbubbles in saline followed by a respiratory maneuver intended to provoke shunting of bubbles across the atrial septum. If bubbles are not detected in the left ventricle by means of a transthoracic imaging device, many practitioners elect to utilize a trans-esophageal imager, a noxious test for the patient. Other methods that have been suggested for detecting "arterialization" of gas bubbles include monitoring of the ascending aorta and the middle cerebral artery (MCA) utilizing a range-gated Doppler device.

In the present study during both saline contrast injections and hypobaric decompressions, the following were assessed:

(i) detection of gas bubbles in the pulmonary arteries, and/or

(ii) detection of gas bubbles in the MCA or the ascending aorta.

B. BACKGROUND HYPOTHESIS: CEREBRAL GAS BUBBLES

Inert gas bubbles possessing a radius of less than 50 microns have their genesis in tissue capillaries during decompression and then are released during muscle contraction into the central venous return. As a consequence of their small diameter, they may not be completely sequestered by the pulmonary vascular filter. Questions concerning these gas bubbles are:

(i) If present, could they represent a potential source of emboli and act as causative agents of subtle neurologic lesions in astronauts during EVA?

(ii) If present, can these inert gas microemboli be detected easily and non-invasively in the middle cerebral artery (MCA) of human subjects by utilizing transcranial Doppler ultrasonography?

C. PULMONARY GAS EMBOLISM AND ARTERIALIZATION

Embolization of the central nervous system by inert gas bubbles arising within or entering into the systemic arteries is at least a theoretical possibility whenever a large change of ambient pressure occurs and an inert gas is being breathed. These gas bubbles may result from:

(i) *de novo* genesis in the arteries (Brubakk et al., 1981),

(ii) release from supersaturated

tissues into the venous return with subsequent transpulmonary transport (Emerson et al., 1967; Powell, 1977),

(iii) rupture of small airways (Waite et al., 1967).

Numerous studies have investigated the question of pulmonary gas embolism over the years. However, these investigations have treated the situation where the gas bubbles existent in the vena cava have been large (approximately 0.1 to 1 mm in radius) (Durant et al., 1947; Spencer and Oyama, 1971; Powell and Johanson, 1978; Powell et al., 1982). Mechanisms for passage to the arterial system have been recognized for many years; they include normal and well-defined anatomical shunts such as pulmonary arteriovenous anastomoses, bronchial venous shunts, large pleural capillaries (Catchpole and Gersch, 1947; Haymaker and Johnson, 1955; Wittmer, 1962), and pathologies such as patent foramen ovalae.

Hills and Butler (1981) have stated that the surface tension of gas bubbles actually encountered in body tissues should be less than the theoretical value of 50 dynes/cm^2. This large value for surface tension yields a retarding pressure of 150 torr for a bubble of 5 micra. A reduction of surface tension to 2 dyne/cm^2 can be produced by dipalmitoyl lecithin (DPL), a normal lung surfactant. DPL can also induce a contact angle of up to 70°, thus reducing the retarding pressure to approximately 3 torr.

Powell and Spencer (1980) reported that when gas was introduced into the venous return of sheep *not by means of a catheter that would generate large gas bubbles* (> 0.1 mm radius) but rather by means of *small gas bubbles spawned in tissues following decompression* (with the creation of microbubbles), the results were opposite. In this latter case, "arterialization", or the passage of gas bubbles from the venous circulation into the systemic arterial circulation, was *not uncommon* even in the *absence of an elevation of the right ventricular systolic pressure (RVSP)*.

D. CENTRAL NERVOUS SYSTEM (CNS) DECOMPRESSION SICKNESS

In general, the involvement of the central nervous system (CNS) in decompression sickness has been considered to be uncommon. However, some studies have indicated a greater degree of involvement. A number of investigations (Kelly and Peters, 1975; Levin, 1975; Peters et al., 1977) demonstrated that neurological and psychological problems exist following CNS decompression sickness. The problems noted, in order of frequency, were: personality change, headache, recent memory impairment, disco-ordination, paresthesia and weakness, hearing loss, vertigo, urinary symptoms, and dysphasia. Impaired divers also demonstrated low scores on verbal and non-verbal portions of the Wechsler Adult Intelligence Scale; the manner in which the subjects were divided (test and control) makes these studies less than ideal, however.

Deep sea divers with decompression sickness have a high incidence of subtle, subjective complaints such as lethargy, confusion and mental cloudiness, and a general perception that all is not well; this may indicate cerebral involvement. Many of these symptoms have also been experienced by individuals who have undergone a safe decompression, and who have *not* experienced what classically would be called frank decompression sickness.

E. NEUROLOGIC SEQUELAE

The presence of detectable gas bubbles in the middle cerebral artery (MCA) is not *prima facie* evidence that neurologic damage is occurring. Possible untoward events could be mitigated by several factors:

(i) The presence of numerous over lapping collaterals would serve to protect brain tissue from anoxia if embolism is not extensive.

(ii) The gas bubbles are composed primarily of oxygen and would dissolve and be metabolically consumed by the tissues of the brain even if they were able to embolize the capillaries. Arterial gas emboli that appeared in the early portion of the decompression, when the brain is not yet denitrogenated, would be considered to be the most pathogenic from a neurologic perspective.

(iii) Numerous air bubbles have been detected by means of surgically implanted Doppler ultrasound probes placed around the carotid artery of sheep (Powell and Spencer, 1981); these subjects rarely demonstrated evidence of neurologic damage.

(iv) Spencer (1990) and Powell (unpublished observations) have noted both gaseous and formed element emboli in the MCA while monitoring with the transcranial Doppler (TCD) at surgery. Spencer reports that a post-operative analysis of 100 TCD monitorings demonstrated gaseous emboli in 44 patients and formed element emboli in 11 patients. Only one patient gave evidence of post-operative stroke; the bubble emboli were detected for 14 seconds in this individual. Two patients with extensive formed-element emboli sustained severe post-operative strokes.

(v) Last, we might consider historical evidence. Human subjects have utilized many decompression profiles in the past with no obvious evidence of CNS involvement. If gas bubbles are detected in the MCA, however, it would be prudent to consider the initiation of a program of psychometric testing as has been done with deep sea divers (Vaernes et al., 1989).

F. TRANSCRANIAL DOPPLER (TCD) ULTRASONOGRAPHY

Aaslid et al. (1982) discovered that the vessels of the brain could be interrogated non-invasively by means of Doppler ultrasound. Placement of a hand-held probe over the temporal region of the skull will position it over a relatively thin region of osseous tissue. With proper angulation, the ultrasound beam can be made to insonate the major blood vessels of the brain including the deep-lying circle of Willis.

The blood vessel which is the easiest to locate and most utilized for intracranial hemodynamic monitoring is the middle cerebral artery (MCA). Gas bubbles present in the MCA produce very intense reflections of the transmitted ultrasound signal superimposed upon the normal blood flow signal. Bubbles that may have escaped the pulmonary filter could be detected with ease as either discrete reflections (Aaslid and Lindegaard, 1986; Spencer 1990) or from the increase in the Doppler signal intensity (Ries et al., 1989).

G. DETECTION OF GAS BUBBLES IN THE CEREBRAL CIRCULATION

Gas bubbles of a radius equal to or greater than 50 microns are expected to give discrete reflections. Gas bubbles smaller than this could be expected to reveal their presence by a modification of the pattern of blood flow.

The amplitude of the reflected Doppler ultrasound beam is a function of the difference in acoustic impedance between the conducting medium (serum) and the individual scattering sites. This difference is modest for erythrocytes but is compensated by their large numbers. The difference between the acoustic impedance of gas bubbles and serum is very high; this will produce an increase in the returned signal intensity even when discrete, individual bubbles are not detectable.

METHODS

1. To monitor for the presence of a gas phase in the pulmonary artery and, in some experiments, the aorta or carotid arteries, use was made of a commercially-available 2 MHz pulsed (or continuous, depending on the subjects) Doppler ultrasound device (*Transpect*, MedaSonics, Fremont, CA). Standard precordial Doppler ultrasound techniques (Powell et al., 1982) were used similar to those employed at NASA/JSC in previous hypobaric trials (Conkin et al., 1987).

2. To monitor for the presence of cerebral gas microemboli, a 2 MHz pulsed Doppler ultrasound device was employed (*Transpect*, MedaSonics, Fremont, CA). The MCA was identified on the basis of: (i) anatomic position of the transducer, (ii) depth of the vessel as determined by range gating, and (iii) characteristics of the blood flow signal (Fujioka et al, 1989). "Control" transcranial Doppler signals were obtained from subjects prior to their entrance into the hypobaric chamber.

3. Flow signals in the MCA were expected to be free of gas bubbles when the subjects were resting. Upon flexure of a joint, showers of gas bubbles were detected in the pulmonary artery by means of a precordial Doppler bubble detector in some subjects. These same individuals were checked for the presence of bubbles in the MCA following joint flexure.

4. Gas bubbles in the MCA with a radius equal to or greater than approximately 50 micra were expected to give discrete acoustic reflections. (Spencer, 1990; Powell, unpublished observations). Spencer described these signals as:

> (a) transient, less than 0.1 second in duration depending on their position in the velocity/frequency fast Fourier transform (FFT) spectrum;
> (b) random in position in the cardiac cycle;
> (c) greater than 6 dB above the background Doppler flow signal; and
> (d) unidirectional.

Smaller gas bubbles could be expected to reveal their presence by an increase in the reflectance of the Doppler signal; this would be seen as brightening of the FFT display on the instrument's screen (Chimowitz et al., 1991).

5. In separate studies not involving decompression, saline contrast echocardiography was performed by rapidly drawing saline back and forth between two syringes in tandem following the addition of a small volume of air to fill the hub of one syringe. This solution was then injected in a bolus through a catheter placed into an antecubital vein. The subject was positioned supine with a slight tilt to the left, and he or she breathed normally. The echocardiograph screen was observed for the appearance of bubbles. If gas traveled into the left heart, a diagnosis of a "spontaneous" or "resting" ASD was applied. In the absence at this point of gas bubbles in the left ventricle, a provocation or augmentation maneuver was performed wherein the contrast agent was injected as the subject bore down (Valsalva's maneuver) and then exhaled. This method is standard clinical practice and has been successful in the detection of ASDs (Teague and Sharma, 1991; Lin et al., 1992; Chimowitz et al., 1991).

RESULTS

A. GAS BUBBLES IN THE MCA CIRCULATION

The majority of individuals with even numerous gas bubbles present in the right heart did not have ultrasonically detectable gas bubbles in the systemic arterial circulation.

The number of individuals with neurologic DCS (Type II), presumably from arterial gas bubbles, was approximately what would have been expected from the results of Powell and Spencer (1981) with Doppler-monitored sheep. In these animals, during 86 decompressions resulting in Spencer precordial Grade III or higher, bubbles were detected in the carotid artery in 7 percent with Grade IV precordial bubbles, and in 50 percent with Grade IV+ (it is not known if IV+ is realistically attained in humans under usual conditions). In the human subjects of the present study, 13 had Grade III bubbles or higher, and one (8%) had arterial bubbles.

Of the three people with resting PFOs who participated in the present study, two experienced Spencer Grade IV bubbles. One of these individuals demonstrated arterialization and developed neurological symptoms. The other subject did not give any evidence of right-to-left shunting either by insonation of the left ventricular outflow tract or with the TCD. The third subject did not display a high grade of bubbles according to Spencer's scheme, but the FFT display "brightened" during his experiment, possibly indicating the presence of a very large number of very small bubbles in the pulmonary artery. Transcranial Doppler monitoring was not performed in this individual. This person developed symptoms of decompression sickness that consisted of skin marbling and orthostatic instability, and the subject received hyperbaric therapy.

A summary of these results is presented in Table I.

B. NUMBER OF GAS BUBBLES IN THE RIGHT HEART

The maximum number of gas bubbles in the right heart during decompression is not known, although an estimate can be made.

1. Gas Loads Following Decompression

Powell and Spencer (1981) determined from steady-state infusions of gas through a capillary into sheep and by additional deep-diving experiments that the gas content of a Spencer precordial Doppler Grade IV is:

$$^{beat}V_{decomp} \approx 2.5 \times 10^{-2} \text{ [cc/kg/min]} \times 50 \text{ [kg]} / 80 \text{ [beats/min]}$$

$$^{beat}V_{decomp} \approx 1.6 \times 10^{-2} \text{ [cc/beat]}$$

2. Gas Loads Upon Contrast Injection

These gas volume estimates are derived from the work of Keller et al. (1987) and Sanders et al. (1991) where they estimate the radius of the air-filled microbubbles at 3 micra. We can thus calculate:

$$V = [4/3]\,\pi\, r^3$$

$$V_{microbubble} \approx 1 \times 10^{-10} \text{ [cc/bubble]}$$

These investigators estimate that for full opacification of the right ventricle upon B-mode visualization, 0.04 [cc injectate/kg] of fluid containing 4×10^8 [air-filled microspheres/cc injectate] are required. This would approximately correspond to the B-mode opacification (or be somewhat greater) seen upon visualization during decompression:

$$V_{microbub} \approx 1 \times 10^{-10} \text{ [cc air/bubb.]} \times 4 \times 10^8 \text{ [bubbles/cc inject.]} \times 5 \times 10^{-2} \text{ [cc inject./kg]} \times 80 \text{ [kg]}$$

$$V_{microbub} \approx 16 \times 10^{-2} \text{ [cc]}$$

This volume appears over approximately 16 heart beats. Thus

$$V_{microbub} \approx 16 \times 10^{-2} \text{ [cc]} / 16 \text{ [beats]}$$

$$^{beat}V_{microbub} \approx 1 \times 10^{-2} \text{ [cc/beat]}$$

Thus the injected microspheres (microbubbles) and the decompression bubbles (for a

Grade IV) are approximately equal in volume.

DISCUSSION

1. Earlier Studies

During air injection experiments (*per* catheter into the jugular vein of sheep) when large (r ≈ 100-300 micra) bubbles served as the pulmonary embolizing agent, gas bubbles were not detected by perivascular Doppler cuffs on the carotid artery when RVSP was less than 150 percent of pre-injection control (Powell et al., 1980). In studies to achieve these steady-state pressure elevations, air injections were conducted for 10 to 20 minutes. In cases where small microbubbles were infused (r = 10 to 90 μ), but for short injection periods (t $\leq$ 2 minutes), Doppler-detectable gas was again not found on the systemic arterial side (Butler and Hills, 1979). One could conjecture that a combination of small bubble radius in conjunction with elevation of pulmonary artery pressure act in concert to effect arterialization. Both conditions are necessary and neither alone is sufficient. The very smallest of bubbles (r < 5 micra) might be expected to dissolve during transpulmonary passage (Meltzer et al., 1980).

A singular contribution of Doppler ultrasonic bubble detectors to our field has been the demonstration that bubbles can appear copiously in the central venous return, but are seen only rarely in the arterial system. Studies of gas separation in two highly perfused organs, kidney and brain, have indicated that these tissues do not readily produce a gas phase following decompression -- even when rather aggressive efforts are undertaken to induce one (Powell and Spencer, 1980). Thus, a highly perfused tissue, such as the brain, seems to be resistant to gas phase formation in all but the severest cases of decompression. Neurologic decompression sickness in the brain could have an origin in arterial gas embolism.

The question of transpulmonic passage of the gas phase was first investigated in rats by Emerson, Hempleman and Lentle (1967); their work indicated that a gas phase could not readily pass the pulmonary barrier under normal physiological conditions. Similar studies by Powell (1971) with rats indicated that arterial bubbles could be found in those subjects which expired, although not all rats with arterial bubbles would necessarily die. Furthermore, the majority of these animal subjects showed no evidence of systemic arterial bubbles following decompressions on profiles known to result only in limb-bend decompression sickness.

It is logical to assume that since venous bubbles appear before arterial bubbles, the source of arterial bubbles is the pulmonary vasculature. It should be stressed here that, in situations where the vena cava is monitored, this vessel will contain a number of gas bubbles before any are noted in the arterial system. In some cases (e.g., viewing of a small field through a microscope), researchers have seen bubbles moving prodromically in an arterial branch when the conjugate venule was bubble-free. The arterial phase did arise from pulmonary arterialization, and an "arterial paradox" does not exist. Arterial gas tensions are thought to closely follow inspired pressures, not be supersaturated, and not produce bubbles. This lack of nucleation was found to be true in sheep decompressed at the rate of 10 fsw/sec (Powell and Spencer, 1982). When Doppler probes were placed around the femoral artery, no gas bubbles were detected even though the supersaturations (from the transit time of blood from lung to leg) were estimated to be 5 ATA at the surface.

In Doppler-monitored sheep, during 86 decompressions in which the animals displayed Spencer Grade III or higher, bubbles were detected in the carotid artery in 7 percent of the subjects displaying Grade IV precordial bubbles, and in 50 percent of those with Grade IV+ (Powell and Spencer, 1980). As Grade IV effects the greatest increase in RVSP, one sus-

pects venous bubbles were arterialized in part by forced passage through A-V shunts or the alveolar capillaries themselves. While Grade IV is not commonly encountered in human divers, it is not as rare an event as one might imagine, especially in hypobaric decompressions or in caisson workers. From the Spencer and Powell studies, it appears that the appearance of Doppler-detectable gas bubbles in the systemic arterial circulation is a rare, but not totally improbable, event; it even occurs in the absence of massive pulmonary vasculature overload (Powell and Spencer, 1980).

Arterialization occurred at definite pressures for Butler and Katz (1988) in dogs, and the mechanism would appear to be straightforward. A rise in RVSP would drive the gas phase through the pulmonary vasculature as seen in a rat study (cf. Powell and Spencer, 1980). However, when other measurements were made with rats as subjects, the results were inconclusive; numerous combinations of RVSP and time of appearance of arterial bubbles were seen. Similar results have also been found in pigs (Vik, et al., 1989).

Cardiac septal defects could be a source of arterial bubbles, although these emboli might be "silent" (produce no symptoms) in most cases. Wilmshurst et al. (1990) found no relationship between type II DCS and the presence of septal defects (3/34 = 24%); curiously, these defects occur in about one quarter of the general population (26/105 = 25%). Similarly, Brubakk and Grip (1981) reported finding asymptomatic arterial bubbles by Doppler devices in ascents from deep diving.

Moon et al. (1991) reported on 90 recreational divers who had suffered decompression sickness (59/90 had neurologic involvement). Echocardiography on these individuals demonstrated that a "resting PFO" (i.e., a Valsalva maneuver was not necessary to provoke the passage of detectable saline contrast bubbles into the left heart) was found in 37% of these stricken divers compared to 10.9% of the controls. The odds ratio was a 4.9-fold risk for neurologic decompression sickness when compared to the controls. They suggested that Valsalva-induced shunts were probably not a factor in the natural history of neurologic DCS. What could not be determined in the studies of Moon et al. is the precordial Doppler bubble grade which occurred during the dives resulting in DCS. The production of such bubbles is, of course, significant if arterialization of bubbles is to occur at all.

In altitude decompressions, the gas loads to the right heart could be expected to be considerably greater than those in diving and thus to pose a larger threat of neurologic DCS. A study reported by Clark and Hayes (1991) examined the prevalence of PFOs in those individuals having encountered Type II DCS during hypobaric training flights. They found 16% (4/24) had a patency demonstrated by saline contrast echocardiography following a Valsalva maneuver; there were no patencies with only spontaneous breathing. They found that controls demonstrated a 5% (9/176) incidence with spontaneous breathing and another 6% (10/176) with Valsalva provocation. They considered the difference not to be statistically significant. The prevalence of PFOs certainly would not explain the origin of the CNS problems in the remaining 84%. Surprisingly, the latencies for symptoms in this study averaged 16 hours with a range of 2 to 21 hours.

The question of the pathophysiology of arterial embolism has been of importance to clinicians with regard to the mechanism of "paradoxical stroke" and its suspected embolic origin. Teague and Sharma (1991) found an incidence of right-to-left shunting of 26% at rest and an additional 15% with Valsalva strain with 2-D echocardiography in stroke patients being evaluated for ASDs. With the addition of TCD, a 41% incidence of ASDs was detected. Lin et al. (1992) compared transthoracic versus transesophageal echocardiography and

reported that both methods possessed an approximately 90% success rate in discovering ASDs. Chimowitz et al. (1991) studied few individuals with TCD (N = 4) but one displayed evidence of numerous microbubbles by an increase in the amplitude of the Doppler audio FFT spectrum; classical single bubble echoes appeared 30 to 60 seconds later. However, ASDs can not be found in all paradoxical stroke patients.

We have not yet been able to identify why one individual who had positive echoes in the left atrium by saline contrast (in the recumbent position) did not also evince bubbles (when lying likewise in the recumbent position) when displaying Grade IV bubbles with lower extremity movements. This individual was checked in the left ventricular outflow tract and in the MCA. As with paradoxical stroke, the presence of right-to-left shunts does not explain the whole problem.

2. CNS Consequences

In general, the involvement of the central nervous system (CNS) in decompression sickness has been considered to be uncommon; less than 10% of individuals presenting with decompression sickness in the U. S. Navy were classified as having CNS, or Type II, decompression sickness. However, deep sea divers with decompression sickness have a high incidence of subtle, subjective complaints such as lethargy, confusion, mental cloudiness, and a general perception that all is not well; this may indicate cerebral involvement. Many of these symptoms have also been experienced by individuals who have undergone a safe decompression, and who have not experienced what classically would have been called frank decompression sickness.

Vaernes, Klove and Ellertsen (1989) noted mild-to-moderate (>10% impairment) neuropsychological changes in measures of tremor, spatial memory, vigilance, and automatic reactivity in divers having undergone saturation decompression. These subtle effects of decompression were found by Curley et al. (1989) in many cases to be refractory to recompression treatment. This has led to concern regarding the risk for long-term, decompression-induced lesions of the central nervous system in the diving population.

Using injection of $^{99}Tc^{m}$-hexamethylpropyleneamine oxime and single positron emission tomography, Adkinson et al. (1989) found perfusion deficits in the cerebral circulation of all human divers one month post an episode of CNS decompression sickness. This was true even when clinical involvement of the brain was absent and only signs of spinal cord lesions were evident. This indicated that Type II decompression sickness is a diffuse, multifocal disorder. Neuropsychological testing has been used to quantify some lesions (Becker, 1984; Kelly and Peters, 1975; Levin, 1975; Peters et al., 1977).

Studies by Gorman et al. (1986, 1987) have shown that gas bubbles in the cerebral arterial circulation could be expected to traverse these capillaries under certain conditions. Cerebral gas distribution is dependent upon the perfusion pressure, and this is an interaction of the arterial blood pressure, cerebrovascular resistance, and intracranial pressure. The relation is complex since the resistance is a function of the blood pressure because the system maintains a relatively constant flow over a range of blood pressures (cerebral autoregulation).

In cerebral gas infusion studies, discrete microbubbles were not seen after the gas entered the arteriolar circulation; rather, coalescence, or fusion, occurred and cylinders of gas formed. Entrapment occurred in vessels when the diameter was reduced to 50 to 200 micra. Transcapillary passage was dependent on systemic blood pressure and embolus length, L. If the embolus length in this vessel was greater than 5,000 micra, blockade was inevitable; if $L < 500$, blockage never occurred. Intermediate gas bolus lengths ($500 < L < 5000$ micra) were

found to pass within 3 minutes. These values accord with those of Masurel et al. (1989) who calculated that a bolus would become trapped when its length exceed 10 times its radius.

It is possible to make some estimates from these results. If the volume V of a cylindrical capillary of length L and radius r is given by

$$V = \pi r^2 L,$$

calculation shows the following:

$$V_{500\mu} = 7.7 \times 10^6 \ [\mu^3]$$
$$V_{5,000\mu} = 77 \times 10^6 \ [\mu^3].$$

With the lower boundary of detectable gas bubble radii as r = 50 micra, the volume V of such a bubble can be calculated from $V = (4/3)\pi r^3$ as 3×10^5 cubic microns. We could determine the number of such gas bubbles needed to fill the 5,000 micron-long capillary and estimate that approximately 260 are needed. Employing Spencer's (1990) observation that one subject who sustained a post-surgical stroke demonstrated gas emboli in the MCA for 14 seconds, this would arithmetically equate to 18 bubbles/second. This volume is easily detected and is more than was found in severe decompressions in animal (sheep) studies (Powell and Spencer, 1980).

In situations where a Doppler probe was placed over the sagittal sinus (surgically implanted in sheep) gas bubbles were heard just moments after their appearance in the carotid artery (Powell and Spencer, 1980). This would indicate that, **in many cases, gas bubbles easily pass through the capillary circulation of the brain** (as is true of other tissues as well) since a gas bubble is so highly deformable. The question of a "clinically silent" gas phase may rest with the ability of the systemic arterial blood pressure to force the cylindrical gas emboli through the brain capillaries. Systolic arterial pressure will be a function of, amongst others, the gas load in the right ventricle and its ability to influence cardiac output. (Unfortunately, formed emboli do not possess the same property of deformability.) The transcranial Doppler device (Aaslid, 1986; Aaslid and Lindgaard, 1986; Aaslid et al., 1982; Fujioka et al., 1989) is providing information on this question of the presence of arterial bubbles, and more data will be forthcoming in the near future.

Evidence of the "silent" nature of some arterial gas bubbles comes from observations of Spencer (1990) made with the transcranial Doppler flowmeter at surgery. During carotid endarterectomy, when the arterial wall was invaded, bubble signals could be found in 38% (35/91) of the patients. He notes, "It is clear that not all of the detected emboli signals produced symptoms. Even when many bubble signals occurred, stroke was rare. Also, since visual deficits were never noted postoperatively, even when bubble emboli obviously had passed through the ophthalmic artery, the retina must be relatively unaffected by them." However, these observations in anesthetized individuals must be applied cautiously to awake subjects because of the profound changes in cerebral metabolism and autoregulation that occur during anesthesia.

REFERENCES

Aaslid, R., [ed.], (1986). *Transcranial Doppler Sonography*. Springer-Verlag. New York.

Aaslid R. and K.-F. Lindegaard (1986). Cerebral Hemodynamics. In: Aaslid, R., [ed.], (1986). *Transcranial Doppler Sonography*. Springer-Verlag. New York.

Aaslid, R; T. M. Markwalder, and H. Nornes (1982). Noninvasive transcranial Doppler ultrasound recording of flow velocity in basal cerebral arteries. J. Neuroscience.,57, 769.

Adkisson, G. H.: M. Hodgson; F. Smith; Z. Torok; M. A. Macleod: J. J. W. Sykes; C. Strack, and R. R. Pearson (1989). Cerebral perfusion deficits in dysbaric illness. Lancet, 15 July, 119

Becker, B. (1984). Neuropsychologic sequelae of a deep-saturation dive: a three-year follow-up. In: Bachr-

ach A. J. and M. M. Matzen, eds., *Proceedings, VIII Symposium on Underwater Physiology.* Undersea Medical Society, Bethesda, MD.

Brubakk, A. O.; A. Grip; B. Holland; J. Onarheim and S. Tonjum (1981). Arterial gas bubbles following ascending excursions during He-O_2 saturation diving. Undersea Biomed. Res. 8 (suppl.) 10.

Butler, B. D. and B. A. Hills (1979). The lung as a filter for microbubbles. J. Appl. Physiol. Respirat. Environ. Exercise Physiol.,47 (3), 537.

Butler, B. D., and Katz, J. (1988). Vascular pressures and passage of gas emboli through the pulmonary circulation. Undersea Biomed. Res, 15, 203.

Catchpole, H. R. and I. Gersch (1947). Pathogenic factors and pathological consequences or decompression sickness. Physiol. Rev., 27, 360.

Chimowitz, M. I.; J. J. Nemec; T. H. Marwick; R. J. Lorig; A. J. Furlan; and E. E. Salcedo (1991). Transcranial Doppler ultrasound identifies patients with right-to-left cardiac of pulmonary shunts. Neurology, 41, 1902.

Clark, J. B.; and G. B. Hayes (1991). Patent foramen ovale and Type II altitude decompression sickness. Aviat. Space Environ. Med., 62 (Suppl.), A1.

Conkin, J.;B. F. Edwards; J. M. Waligora, and D. J. Horrigan, Jr. (1987). *Empirical Models for Use in Designing Decompression Procedures for Space Operations.* NASA Technical Memorandum 100456. NASA/JSC. Houston, TX 77058.

Curley, M. D.; H. J. C. Schwartz, and K. M. Zwingelberg (1989). Neuropsychological assessment of cerebral decompression sickness and gas emboli. Undersea Biomed. Res., 15 (3), 223.

Durant, T. M.; J. Long and M. J. Oppenheimer (1947). Pulmonary (venous) air embolism. Am. Heart J., 33, 269.

Emerson, L. V.; Hempleman, H. V.; and Lentel, R. G. (1967). The passage of gaseous emboli through the pulmonary circulation. Resp.. Physiol., 3, 219.

Fujioka, K.; K. Kuehn; N. Sola-Pierce, and M. P. Spencer (1989). Transcranial pulsed Doppler for evaluation of cerebral arterial hemodynamics. J. Vas. Technol., 13, 95.

Gorman, D. F. and D. M. Browning (1986). Cerebral vasoreactivity and arterial gas embolism. Undersea Biomed. Res., 13, (3), 317.

Gorman, D. F.; D. M. Browning and D. W. Parsons (1987). Redistribution of cerebral gas emboli: a comparison of treatment regimens. In: *Proceedings of the Ninth Symposium on Underwater Physiology*, Bethesda, MD, 1031.

Haymaker, W. and A. D. Johnson (1955). Pathology of decompression sickness: a comparison of the lesions in airmen with those in caisson workers and divers. Mil. Med., 117, 285.

Hills, B. A. and B. D. Butler (1981). Migration of lung surfactant to pulmonary air emboli. In: *VII Symposium on Underwater Physiology.* Bachrach, A. J. and Matzen, M. M. (eds.), Undersea Med. Soc., MD.

Keller, M. W.; S. B. Feinstein; and D. D. Watson (1987). Successful left ventricular opacification following peripheral venous injection of sonicated contrast agent: an experimental evaluation. Am. Heart J., 114, 570.

Kelly, P. J. and B. H. Peters (1975). The neurologic manifestations of decompression sickness. In: *International Symposium on Man In the Sea.* Undersea Med. Soc., Bethesda, MD., 227.

Lin, S. L.; C. T. Ting; T. L. Hsu; C. H. Chen; M. S. Chang; C. Y. Chen; and B. N. Chiang (1992). Transesophageal echocardiographic detection of atrial septal defect in adults. Amer. J. Cardiol., 69, 280.

Levin, H. S. (1975). Neuropsychological sequelae of diving accidents. In: *International Symposium on Man In the Sea.* Undersea Med. Soc., Bethesda, MD., 233.

Masurel, G., Gutierrez, N., and Colas, C. (1989). Considerations on the pulmonary removal of circulating bubbles. Undersea Biomed. Res. 16 (Suppl.), 90.

Meltzer, R. S.; E. G. Tickner and R. L. Popp (1980). Why do the lungs clear ultrasonic contrast? Ultrasound Biol. Med., 6, 235.

Moon, R. E.; J. A. Kisslo; E. W. Massey; T. A. Fawcett; and D. R. Theil (1991). Patent foramen ovale (PFO) and decompression illness. Undersea Biomed. Res., 18 (Suppl.), 15.

Peters, B. H.; H. S. Levin and P. J. Kelly (1977). Neurologic and psychologic manifestations of decompression illness in divers. Neurology, 27, 125.

Powell, M.R. (1971). *Mechanism and Detection of Decompression Sickness.* Union Carbide Technical Memorandum: UCRI-673, Tarrytown, N. Y.

Powell, M. R. (1977). The physiological significance of Doppler-detected bubbles in decompression sickness. In: *Early Diagnosis of Decompression Sickness.* Undersea Medical Society, Bethesda, Maryland.

Powell. M. R. and D. C. Johanson (1978). Ultrasonic monitoring of decompression sickness. In: *Proc. 6th Symp. Underwater Physiology*, (eds) Shilling, C. W. and Beckett, FASEB, Bethesda, Maryland.

Powell, M. R. and M. P. Spencer (1980). *The Pathophysiology of Decompression Sickness and the Effects of Doppler-Detectable Bubbles.* Final Technical Report: O.N.R. Contract #N00014-73-C-0094. I.A.P.M., Seattle, Wash., 98122.

Powell, M. R., and Spencer, M. P. (1982). *In situ* arterial bubble formation and "atraumatic air embolism." Undersea Biomed. Res., 9 (suppl.), 10

Powell, M. R.; M. P. Spencer and O. von Ramm (1982). Ultrasonic Surveillance of Decompression. In: *The*

Physiology and Medicine of Diving, Eds: P. Bennett and D. H. Elliott. Bailliere Tindall, London.

Ries, F.; R. Schulthiess; R. Kaal: and L. Solymosi (1989). Clinical applications and perspectives of TCD-signal enhancement with standardized air microbubbles. *3rd International Symposium on Intracranial Hemodynamics: Transcranial Doppler and Cerebral Blood Flow.* February 11 - 13, San Antonio, TX

Sanders, W. S., Jr.; J. Cheirif B; R. Desir; W. A. Zoghbi; B. D. Hoyt; P. E. Schultz; and M. A. Quiñones (1991). Contrast opacification of left ventricular myocardium following intravenous administration of sonicated albumin microspheres. Am. Heart J., 122, 1660.

Spencer, M. P. (1990). Detection of cerebral arterial emboli with transcranial Doppler. *4th International Symposium on Intracranial Hemodynamics: Transcranial Doppler and Cerebral Blood Flow.* February 11 - 14, Orlando, FL

Spencer, M. P. and Y. Oyama (1971). Pulmonary capacity for dissipation of venous gas emboli. Aerospace Med.,42, 822.

Teague, S. M.; and M. K. Sharma (1991). Detection of paradoxical cerebral echocontrast embolization by transcranial Doppler ultrasound. Stroke, 22, 740.

Vaernes, R. J; H. Klove, and B. Ellertsen (1989). Neuropsychologic effects of saturation diving. Undersea Biomed. Res., 16 (3), 233.

Vik, A.; Jennsen, B. M. ;Ekker, M.; Sjørdahl, and Brubakk, A. O. (1989). Transit time of air bubbles through the lung circulation. Undersea Biomed. Res., 16 (suppl.), 90

Waite, C. L.; W. F. Mazzone; M. E. Greenwood, and R. T. Larsen (1967). Dysbaric cerebral air embolism. In: *Proceedings, 3rd Symposium on Underwater Physiology.* (ed.) C. J. Lambertsen. Williams and Willkins, Baltimore. p. 205.

Wilmshurst, P. T.; J. C. Byrne; and M. M. Webb-Peploe (1990). Relation between interatrial shunts and decompression sickness in divers. Undersea Biomed. Res., 17, (suppl.), 69.

Wittmer, J. F. (1962). Pathogenic mechanisms in gas and fat embolism. Review #4-62, USAF School of Aviation Medicine.

SUBJECT #	MAXIMUM DOPPLER GRADE		TCD BUBBLES	SALINE CONTRAST	
	AMBULATORY	BEDRESTED	AMB.	BEDREST	ECHOCARDIOGRAPHY
1.	0 (1)	0 (7)	.	.	NO ARTERIALIZATION
2.	III (6)	0 (2)	.	.	Lost to follow-up
3.	III (2)	0 (4)	0	.	NO ARTERIALIZATION
4.	IV (15)	IV (3)	0	0	NO ARTERIALIZATION
5.	0 (3)	0 (10)	0	.	Not tested
6.	III (4)	II (5)	0	0	NO ARTERIALIZATION
7.	0 (5)	0 (6)	.	.	not tested
8.	IV (7)	Withdrawn from study	+	.	**Resting** ARTERIALIZATION
9.	IV (11)	0 (8)	0	.	NO ARTERIALIZATION
10.	0 (8)	Lost to follow-up	.	.	Not tested
11.	0 (10)	0 (9)	.	.	NO ARTERIALIZATION
12.	0 (9)	Lost to follow-up	0	.	Not tested
13.	III (13)	II (12)	.	0	NO ARTERIALIZATION
14.	IV (12)	0 (13)	0	.	NO ARTERIALIZATION
15.	Lost	0 (14)	.	.	Not tested
16.	0 (14)	0 (11)	.	.	Not tested
17.	0 (19)	0 (15)	.	.	Not tested
18.	0 (19)	0 (16)	.	.	Not tested
19.	0 (16)	Lost to follow-up	.	.	Not tested
20.	III (21)	III (17)	.	0	NO ARTERIALIZATION
21.	Withdrawn	0 (18)	.	.	**Resting** ARTERIALIZATION
22.	0 (18)	0 (23)	.	.	NO ARTERIALIZATION
23.	IV (20)	0 (22)	.	.	Not tested
24.	IV (22)	0 (20)	0	.	**Resting** ARTERIALIZATION
25.	IV (24)	II (21)	0	0	NO ARTERIALIZATION
26.	0 (23)	0 (24)	.	.	Not tested
27.	Withdrawn from the study				**Resting** ARTERIALIZATION

SUMMARY:

Precordial Grades		TCD Bubbles/Subjects:	With Resting PFO
0 = 12	0 = 17	0/2	
I = 0	I = 0	---	
II = 0	II = 3	0/3	
III = 5	III = 1	0/3	
IV = 7	IV = 1	1/6	1/2
12/24 individ.	5/22 individ.		

Resting R-L Shunts = 4/15 = 26%

N94-11545

A MECHANISM FOR THE REDUCTION IN RISK OF DECOMPRESSION SICKNESS IN MICROGRAVITY ENVIRONMENT

Michael R. Powell, Ph.D.
NASA/Johnson Space Center
Space Biomedical Research Institute,
Environmental Physiology/Biophysics Section
2101 Nasa Road 1
Houston, TX 77058

There is an apparent reduction in incidence of decompression sickness reported by astronauts (from both the USA and the USSR) during extravehicular activity (EVA). The expected incidence, based on studies conducted under unit gravity conditions in Earth-based laboratories, is greater than that encountered during EVA. A biophysical explanation has been proposed for this difference based upon the mechanism of stress-assisted nucleation. Since the partial pressure ratio at which this gas phase forms is considerably smaller in living systems than in quiescent *in vitro* models, it was proposed (cf., E. N. Harvey, mid-1940s) that mechanical forces are involved. In that the lower extremities of astronautics are not gravitationally loaded in microgravity, it is possible that tissue gas micronuclei are but minimally regenerated. Most likely, gas micronuclei formed on Earth (by ambulation under one-g conditions) would be eventually depleted. In a crossover study, 20 individuals were decompressed—from 1 ATA to 0.43 ATA for 3 hours—following either being fully ambulatory at unit gravity or following being hypokinetic and a dynamic (simulated microgravity of 3-day bed rest). The subjects were monitored for gas phase formation by means of precordial Doppler monitoring. The results indicate a reduction in whole body gas phase formation in individuals who were bed rested as compared with themselves when fully ambulatory ($p = 0.02$). In hypokinetic individuals, the protection conferred was equivalent to an extra 175 minutes of oxygen prebreathe. These results are compatible with a hypothesis relating stress-assisted nucleation to the continual formation of tissue gas micronuclei and their gradual depletion with hypokinesia.

N94-11546

Risk of Decompression Sickness in the Presence of Circulating Microbubbles

*K. Vasantha Kumar, M.D.**
KRUG Life Sciences
Houston, TX 77058
Michael R. Powell, Ph.D.
NASA Johnson Space Center
Houston, TX 77058

Abstract:

In this study, we examined the association between microbubbles formed in the circulation from a free gas phase and symptoms of altitude decompression sickness (DCS). In a subgroup of 59 males of mean (S.D) age 31.2 (5.8) years who developed microbubbles during exposure to 26.59 kPa (4.3 psi) under simulated extra-vehicular activities (EVA), symptoms of DCS occurred in 24 (41%) individuals. Spencer grade I microbubbles occurred in 4 (7%), grade II in 9 (15%), grade III in 15 (25%), and grade IV in 31 (53%) of subjects. Survival analysis using Cox proportional hazards regression showed that individuals with >grade III CMB showed 2.46 times (95% confidence interval=1.26 to 5.34) higher risk of symptoms. This information is crucial for defining the risk of DCS for inflight Doppler monitoring under space EVA.

Altitude decompression sickness (DCS) occurs when there is acute reduction in ambient pressure. The symptoms of DCS are due to the formation of a free gas phase (in the form of gas microbubbles) in tissues during decompression. Musculo-skeletal pain of bends is the commonest form of DCS in altitude exposures. In the space flight environment, there is a risk of DCS when astronauts decompress from the normobaric shuttle pressure into the hypobaric space suit pressure (currently about 29.65 kPa [4.3 psi]) for extra-vehicular activities (EVA). This risk is counterbalanced by a judicious combination of prior denitrogenation and staged decompression (1).

Studies on DCS are limited by the duration of the test at reduced pressure. Since only a proportion of subjects tested develop symptoms, the information on DCS is generally incomplete or "censored". Many studies employ Doppler ultrasound monitoring of the precordial area for detecting circulating microbubbles (CMB). Although the association between

CMB and bends pain is not causal, CMB are frequently monitored during decompression.

In this paper, we examine the association between CMB and symptoms of DCS under simulated EVA profiles.

Methods:

The information on a subgroup of 59 males who developed CMB (out of 126 individuals) during various decompression profiles to 29.65 kPa in the hypobaric chamber were examined. The studies involved direct ascent, as well as staged decompression procedures. All the subjects breathed 100% oxygen at the final pressure while performing exercises simulating EVA for a period of three to six hours (1). They were monitored for CMB using the precordial Doppler technique, and graded on the Spencer scale of 0 to IV for severity (2). A 360-minute half-time tissue ratio (TR_{360}) was calculated to account for differences in prebreathe period and staged decompression events.

The distribution of individuals with and without symptoms was examined by using Kolmogorov-Smirnov test or likelihood ratio chi-square test, as appropriate. Univariate survival curves were described using product-limit method. Differences in survival curves were examined by using the Mantel-Cox test statistic (3). Multivariate analyses were carried out using Cox proportional hazards regression model (3,4) with variables such as age, body mass index (BMI), TR_{360}, time to detection of CMB and maximum grade of CMB as covariates. All results with P-values of 0.05 and below were considered as significant.

Results:

The mean (S.D.) age was 31.2 (5.8) years, BMI 23.7 (1.9), TR_{360} 1.72 (0.09), time to detection of CMB 81.4 (61.8) minutes, maximum CMB grade 3.24 (0.95), and time to symptoms 197.9 (104.6) minutes. Twenty-four individuals (41%) presented with symptoms of DCS. All symptoms were mild, joint pain ("bends") and no neurological or circulatory complications were reported. The distribution of individual characteristics by symptom status (present or absent) is given in Table 1.

The symptom-free survival rates for the group with various grades of CMB are given in Table 2.

The Mantel-Cox test for trend showed a significant difference (P=0.004) among the groups with various maximum CMB grades. It may also be seen from the Table that the cumulative survival rates reduced as the maximum grade of CMB was higher. Individuals with higher grades of CMB showed higher risk of symptoms.

Table 1. Individual Distribution By Symptom Status

	Present n=24	Absent n=35
Age (years)	33.3 (6.4)	29.8 (4.8)
BMI	23.5 (1.9)	23.8 (1.9)
TR_{360}	1.7 (0.1)	1.7 (0.1)
Time to CMB (min)	68.4 (57.5)	90.3 (63.9)
Maximum CMB grade*		
≤III	4 (17%)	24 (69%)
>III	20 (83%)	11 (31%)

Values are Mean (S.D.); BMI=Body Mass Index; CMB=Circulating Microbubbles; *P<0.05

Table2. Symptom-free Cumulative Survival Rates

CMB grades	n	DCS	Survival (S.D.)
I	4	2	0.33 (0.27)
II	9	0	1.00
III	15	2	0.87 (0.09)
IV	31	11	0.15 (0.12)

In order to examine this trend, we classified the individuals into two groups- those with maximum CMB grades ≤III and >III. Distribution by maximum CMB grade is given in Table 3.

Table 3. Individual Characters by Maximum Grade of CMB

	>III n=31	≤III n=28
Age (years)	32.2 (6.3)	30.1 (5.0)
BMI	23.7 (1.9)	23.7 (1.9)
TR_{360}	1.73 (0.07)	1.69 (0.11)
Time to CMB (min)	59.3 (51.9)	105.8 * (63.5)

Values are Mean (S.D.); *P<0.05

The risk of DCS in the presence of higher grades of microbubbles was examined by calculating the relative risk values (5). Cox proportional hazards regression was used to adjust for various other factors such as age, BMI, TR_{360} and time to detection of CMB. The results of this analysis are given in Table 4.

Table 4. Relative Risk of Symptoms of DCS

CMB	DCS Yes	DCS No	Crude RR	Adjusted RR+
Grade ≤III	4	24	1.00	1.00
>III	11	20	4.52* (1.76-11.61)	2.46* (1.26-5.34)

RR=Relative Risk; 95% confidence intervals in parentheses
*P<0.01
+Adjusted for age, BMI, TR360, and time to detection of CMB in the Cox proportional hazards regression model.

These results showed that individuals with greater than grade III CMB were at increased risk of symptoms.

Discussion:

Before examining the association between CMB and symptoms of altitude DCS, two important issues must be considered. They are:

* *cause and effect*
* *censoring of information*

Although microbubbles occur during decompression, their relationship to symptoms may not be causal. This is especially a problem in case of bends pain. The pain of bends is thought to be due to the formation of free gas microbubbles in extravascular tissues (2), as opposed to the intravascular circulating microbubbles detected by the precordial Doppler. However, this data could be used in a predictive manner to monitor the development of symptoms of DCS (6). This information is usually censored, so not amenable to traditional methods of analysis.

Survival analysis is useful under these circumstances. The distribution of survival times is divided into a certain number of intervals. For each interval, the proportion with symptoms (or any "event"), and the proportion that were lost or censored are obtained. Then the cumulative proportion of cases surviving through each interval is calculated. In the product-limit method, the cumulative proportion thus obtained is a maximum likelihood estimate (3,4).

Utilizing survival analysis we found that individuals with Spencer grade IV CMB showed 2.46 times higher risk of symptoms, compared to individuals with lower grades. This risk was unchanged, even after adjusting for the influence of other variables in the regression model.

There are several implications from these results. Neurological symptoms and other severe complications of DCS are main concerns under space EVAs. While ground-based studies indicate a 10% to 20% risk of minor DCS symptoms, no cases have been reported from space EVAs.

Several steps have been taken to examine this *"decompression anomaly"* in space. Our analysis showed increased risk of DCS with higher CMB grades during simulated EVA profiles. This finding would provide a strong case for inflight precordial Doppler monitoring of astronauts in the space suit during space EVA. Further, this finding would permit definition of a high risk group for DCS, based on the obtained information on CMB. A program for meeting these objectives is currently being developed at this Laboratory.

References:

1. Waligora JM, Horrigan DJ, Conkin J, Hadley AT. Verification of an altitude decompression sickness prevention protocol for shuttle operations utilizing a 10.2 psi pressure stage. Springfield, VA: NTIS, 1988. NASA Tech Memo 58259.
2. Bennett PB, Elliott DH, eds. The physiology and medicine of diving. Third Edition. London: Bailliere-Tindall, 1982.
3. Harris EK, Albert A. Survivorship analysis for clinical studies. New York: Marcel & Dekker, 1991.
4. Cox DR. Regression models and life tables. J. Roy. Stat. Soc. 1972;34B:187-202.
5. Kahn HA, Sempos CT. Statistical methods in epidemiology. New York: Oxford University Press, 1989.
6. Kumar KV, Calkins DS, Waligora JM, Horrigan DJ. Estimation of survival functions in decompression sickness. Aviat. Space Environ. Med. 1990;61:450.

N94-11547

STRATEGIES AND METHODOLOGIES TO DEVELOP TECHNIQUES FOR COMPUTER-ASSISTED ANALYSIS OF GAS PHASE FORMATION DURING ALTITUDE DECOMPRESSION

Michael R. Powell[1] and W. A. Hall[2]
[1]NASA/Johnson Space Center
Space Biomedical Research Institute,
Environmental Physiology/Biophysics Section
2101 Nasa Road 1
Houston, TX 77058
[2]KRUG Life Sciences, Inc.
1290 Hercules Dr., Ste. 120
Houston, TX 77058

It would be of operational significance if one possessed a device that would indicate the presence of gas phase formation in the body during hypobaric decompression. Automated analysis of Doppler gas bubble signals has been attempted for 2 decades but with generally unfavorable results, except with surgically implanted transducers. Recently, efforts have intensified with the introduction of low-cost computer programs (cf., B. A. Butler, et al., 1991). Current NASA work is directed towards the development of a computer-assisted method specifically targeted to EVA, and we are most interested in Spencer Grade IV. We node that Spencer Doppler Grades I to III have increased in the FFT sonogram and spectrogram in the amplitude domain, and the frequency domain is sometimes increased over that created by the normal blood flow envelope. The amplitude perturbations are of very short duration, in both systole and diastole and at random temporal positions. Grade IV is characteristic in the amplitude domain but with modest increases in the FFT sonogram and spectral frequency power from 2K to 4K over all of the cardiac cycle. Heart valve motion appears to characteristic display signals: (i) demodulated Doppler signal amplitude considerably above the Doppler-shifted blow flow signal (even Grade IV), and (ii) demodulated Doppler frequency shifts are considerably greater (often several kHz) than the upper edge of the blood flow envelope. Knowledge of these facts will aid in the construction of a real-time, computer-assisted discriminator to eliminate cardiac motion artifacts. There could also exist perturbations in (a) modifications of the pattern of blood flow in accordance with Poiseuille's Law, (b) flow changes with a change in the Reynolds number, (c) an increase in the pulsatility index, and/or (d) diminished diastolic flow or "runoff." Doppler ultrasound devices have been constructed with a three-transducer array and a pulsed frequency generator.

Session L3: MEDICAL OPERATIONS

Session Chair: R. Bisson
Session Cochair: R. T. Jennings, M.D.

N94-11548

EVALUATION OF MEDICAL TREATMENTS TO INCREASE SURVIVAL OF EBULLISM IN GUINEA PIGS

B. J. Stegmann[1], A. A. Pilmanis[2], E. G. Wolf[2], T. Derion[2], J. W. Fanton[2], H. Davis[2], G. B. Kemper[2], and T. Scoggins[2]

[1]Hyperbaric Medicine
Wound Care Hyperbaric Medicine
4499 Medical Dr. Sub Level 2
San Antonio, TX 78229

[2]Armstrong Laboratory
AL/CFTS
Brooks AFB, TX 78235-5000

INTRODUCTION: Spaceflight carriers run a constant risk of exposure to vacuum. Above 63,000 ft (47 mmHg), the ambient pressure falls below the vapor pressure of water at 37°C, and tissue vaporization (ebullism) begins. Little is known about appropriate resuscitative protocols after such an ebullism exposure. This study identified injury patterns and mortality rates associated with ebullism while verifying effectiveness of traditional pulmonary resuscitative techniques.

METHODS: Male Hartley guinea pigs were exposed to 87,000 ft for periods of 40 to 115 sec. After descent, those animals that did not breathe spontaneously were given artificial ventilation by bag and mask for up to 15 minutes. Those animals surviving were randomly assigned to one of three treatment groups—hyperbaric oxygen (HBO), ground-level oxygen (GLO_2), and ground-level air (GLAIR). The HBO group was treated on a standard treatment table 6A while the GLO_2 animals received O_2 for an equivalent length of time. Those animals in the GLAIR group were observed only. All surviving animals were humanely sacrificed at 48 hours.

RESULTS: Inflation of the animals' lungs after the exposure was found to be difficult and, at times, impossible. This may be due to surfactant disruption at the alveolar lining. Electron microscopy identified a disruption of the surfactant layer in animals that did not survive initial exposure. Mortality was found to increase with exposure time: 40 sec–0%, 60sec–6¢, 70 sec–40%, 80 sec –13%, 100 sec–38%, 110 sec–40%, 115 sec–100%. There was no difference in the delayed mortality among the treatment groups (HBO–15%, GLO_2–11%, GLAIR–11%). However, since resuscitation was ineffective, the effectiveness of any post-exposure treatment was severely limited.

CONCLUSIONS: Preliminary results indicate that resuscitation of guinea pigs following ebullism exposure is difficult, and that current techniques (such as traditional CPR) may not be appropriate.

N94-11549

A Prototype Urine Collection Device for Female Aircrew. Roger U. Bisson* and Karlyna L. Deiger. Armstrong Laboratory, Sustained Operations Branch, Brooks AFB, TX 78235.

ABSTRACT

INTRODUCTION: Women are gaining increased access to small military cockpits. This shift has stimulated the search for practical urine containment and disposal methods for female aircrew. There are no external urine collection devices (UCD) for women that are comfortable, convenient and leak free. We describe a prototype UCD that begins to meet this need. **METHODS:** Materials used to make custom aviator masks were adapted to mold a perineal mask. First, a perineal cast (negative) was used to make a mold (positive). Next, a perineal mask made of wax was formed to fit the positive mold. Finally, a soft, pliable perineal mask was fabricated using the wax model as a guide. The prototype was tested for comfort, fit and leakage. **RESULTS:** In the sitting position, less than 5 cc of urine leakage occurred with each 600 cc of urine collected. Comfort was mostly satisfactory, but ambulation was limited and the outlet design could lead to kinking and obstruction. **CONCLUSIONS:** A perineal mask may serve as a comfortable and functional external UCD acceptable for use by females in confined environments. Changes are needed to improve comfort, fit, and urine drainage. Integration into cockpits, pressure suits, chemical defense gear, and environments where access to relief facilities is restricted is planned

INTRODUCTION

Changes in the perceived military threat in Europe, military downsizing, budget cuts and other political realities increase the emphasis on long duration and rapid deployment. Global Reach - Global Power espouses a new vision for power projection over global distances. Something as simple and banal as urine containment and disposal contribute to the human factors that can make human endurance limiting in plans for supporting long duration missions.

Congressional action to remove combat restrictions has increased the number of women gaining access to military cockpits. The size of high performance cockpits and personal protective gear can severely restrict opportunities for relief from the physiological need to pass urine. Condom catheters or "piddle packs" have been an acceptable solution for males, but even these solutions encourage some crew members to adopt fluid restriction and other unsatisfactory strategies to avoid urinating inflight. The problem is magnified for the female crew member. There are no external urine collection devices (UCD) for women that are comfortable, convenient and leak free. This shift of women into combat roles that can restrict access to convenient urine relief facilities has stimulated the search for a practical external urine containment and disposal method for female aircrew of high performance aircraft. Solving urine disposal problems for women aviators would be of great benefit to the military and has clinical and non-clinical commercial applications. We describe a prototype UCD that begins to met this need for the female aviator.

METHODS

A female subject volunteered to have a mold made of her perineal area in order to obtain a form for modeling and molding a prototype mask. The subject was placed in the lithotomy position with the thighs only slightly abducted. Hydrophilic vinyl polysiloxan with a hardened acrylic backing was used to make a negative cast of the perineum. This process was similar to the methods used to obtain facial impressions for custom fitting aviator masks. Using the negative cast, a synthetic stone positive impression was poured. The positive impression was used to mold several wax prototype perineal mask forms. After several design trials, we selected a wax prototype from which to model a custom perineal mask. The materials were sent to the Life Support function at Wright-Patterson AFB where a custom latex perineal mask was molded and returned for testing. The prototype mask was worn by the subject for seven continuous hours during each of five days. The mask was held in place by cotton briefs modified to accommodate the outlet tube and an adult diaper. Routine daily activities were carried out limited to ambulation around a small apartment. When urgency occurred a collection bag was attached to the outflow tubing and the subject urinated in sitting or standing positions. Urine flow was gravity dependent for this trial. The diaper and briefs were weighed to quantify the small amount of leakage. The subject commented on comfort and functionality.

RESULTS

Placement of the device was well maintained in the sitting position and with light ambulation. In the sitting position less than 5 cc of leakage occurred with each 600 cc of urine collected. Comfort was satisfactory while sitting, but the prototype was too deep and wide for comfortable ambulation. Central placement of the outlet tube allowed some pooling of urine inferiorly when used in the sitting position. The latex material at the outlet was too pliable. This could lead to kinking of the outlet tube and flow restriction under more severe test conditions. Comfort could be improved during ambulation without sacrificing function if the device could be molded slightly more narrow and with less depth.

DISCUSSION

We have designed a perineal mask that fits against the perineum as a customized UCD for females. It is very similar in principle to a male athletic supporter and cup used to prevent athletic injuries and should have equal comfort and utility. It should be possible to fit 95 percent of all women using 6-10 sizes. Like the present male UCD used in the U-2/TR-1, the device should be reusable and relatively inexpensive. Other external UCDs designed for female use include the Disposable Absorption Containment Trunk (DACT), the Maximal Absorptive Garment (MAG), the Hollister device and similar custom made vaginal seals, and devices modified from ostomy appliances used in clinical medicine.

The DACT is a highly absorbable diaper used in pressure suits by the Air Force. This device is worn throughout the mission until the pressure suit is removed. The DACT is designed to hold up to 900 cc of urine and be used once for a period of seven hours. Problems with the DACT include leakage, dermal irritation, cost and discomfort due to its impermeable construction and the large surface area covered(1). NASA uses a similar device called the Maximal Absorptive Garment (MAG) designed to hold up to 1500 cc of urine. NASA originated a patent for a custom fitted urethral outlet held in place by a soft pliable vaginal seal and an undergarment(2). A similar urethral funnel and vaginal seal is marketed commercially by Hollister Incorporated. The Hollister device is particularly well designed for integration into the pressure suit or cockpit environments. However, its comfort is likened to riding a bicycle seat. Preliminary discussion with female U-2 pilots suggests that it may not be suitable. Some women may find it intolerable for flight of very long durations or flights encountering high G loads(3). Other investigations into the area of female urinary collection devices has been in the field of clinical medicine. Urine collection devices for incontinent women and nursing home patients have utilized adhesives developed for ostomy appliances(4, 5). Use of such devices is not common. To our surprise, we have been unable to find references to a device similar to our perineal mask.

Additional features of our design for female aviator use include adding superabsorbent chemicals to the urine storage bags to simplify disposal and minimize risk of inadvertent contamination of the cockpit from leakage. Specifications for a reusable undergarment to hold the device in place will incorporate a super absorbent pad to retain the small amount of leakage that is probably inevitable in many applications. Future trials for possible use in the U-2/TR-1 pressure suit will incorporate airflow similar to the flow achieved through cabin/suit pressure differentials in the male UCD system. Airflow may assist with flow and improve hygiene. If these tests go well, we will need to locate a manufacturer who is able to incorporate design recommendations related to the depth of the device and increased stiffness at the outlet port.

The development of a comfortable, external UCD for females would be of great benefit. Military applications include cockpit relief during long duration flights, pressure suit environments, and incorporation into chemical warfare defense clothing. Commercial applications include use in any environment where access to a relief facility is limited. Clinical uses in both ambulatory and non-ambulatory incontinent patients could be an attractive benefit of this design. Initial findings have been rewarding. We are looking forward to testing a second generation device which corrects some of the design deficiencies noted in the preliminary test reported here.

ACKNOWLEDGEMENTS

Capt Hanigan, USAF Dental Clinic, Brooks AFB, TX and SRA Walters, Life Support Division, Wright-Patterson AFB, OH contributed substantially to this work.

REFERENCES

1. Barlow, J.F., and S.E. Richardson. "Evaluation of the disposable absorption containment trunk for female U-2 and TR-1 pilots." Aviation, Space and Environmental Medicine. 1991, 62(6):577-9.

2. Michaud R.B. and R.A. Frosch. Urine Collection Apparatus. United States Patent 4,270,539 (filed Apr 27, 1979). United States Patent Office, June 2, 1981.

3. Crook B. and R.E. Sherman. "Proposal for flight test of Hollister female urinary incontinence system." Personal Communication. Nov 1991.

4. Johnson, D.E., H.L. Muncie, J.L. O'Reilly and J.W. Warren. "An External urine collection device for incontinent women. Evaluation of long term use." Journal of the American Geriatric Society. 1990. 38(9):1016-22.

5. Johnson, D.E., J.L. O'Reilly and J.W. Warren. "Clinical evaluation of an external urine collection device for nonambulatory incontinent women." Journal of Urology. 1989. 141(3):535-7.

N94-11550

PROMETHAZINE AND ITS USE AS A TREATMENT FOR SPACE MOTION SICKNESS

James P. Bagian[1] and Bradley G. Beck[2]
NASA/Johnson Space Center
[1]Mail Code: CB
[2]Mail Code: SD23
2101 Nasa Road 1
Houston, TX 77058

Until March 1989, no effective treatment—either prophylactic or symptomatic—for space motion sickness (SMS) had been discovered. Since March 1989, intramuscular (IM) promethazine (PMZ) has been used in the treatment of SMS with extremely favorable results reported by the crew. A retrospective study was undertaken to quantify the efficacy of IM PMZ since its institution and the incidence of its major anticipated side-effect drowsiness and sedation. The results from a standardized crew medical debriefing conducted immediately after landing and follow-up interviews with the crews were used in establishing the efficacy and incidence of side effects from treatment. Only crews from the first 44 Shuttle flights on their first mission were considered. For a total of 132 crewmembers, 96 exhibited symptoms of SMS; and, of these, 20 were treated with IM PMZ. Ninety percent of those receiving IM PMZ 25-50mg received nearly immediate (< 2 hours) relief of symptoms and 75% required no further treatment through the first 2 days of spaceflight. Those not receiving this treatment did not have any near-term resolution of their symptoms, and 50% were still ill through the second day of flight. This represents a significant difference at the $p = .046$ level. In stark contrast to the 60% to 73% incidence of sedation or drowsiness reported in individuals treated with PMZ in terrestrial environment at the doses used here, less than 5% reported these symptoms during spaceflight. IM PMZ is an effective therapy for SMS and is associated with minimal incidence of sedation or drowsiness. This combination of efficacy that is absent of significant side effects represents a substantial improvement in the operational situation of crewmembers afflicted with SMS. Studies to understand the mechanisms underlying these observations will be undertaken in the future.

N94-11551

UPDATE ON THE INCIDENCE AND TREATMENT OF SPACE MOTION SICKNESS

Bradley G. Beck
NASA/Johnson Space Center
Medical Officer
Mail Code: SD26
2101 Nasa Road 1
Houston, TX 77058

Flight surgeons routinely monitor crew symptoms and treatment of space motion sickness (SMS) not only during flight, but also to obtain information postflight from each crewmember. Recent statistics indicate that the incidence of SMS has not changed since STS-26 in September 1988. The percentages of mild, moderate, and severe cases has only changed slightly. The treatment of SMS has significantly changed since STS-26, however. Scopolamine/dexedrine is no longer used as a prophylaxis for SMS symptoms because of evidence of delay in symptoms. Intramuscular promethazine has been used in more than 30 individuals with a reported decrease in symptoms greater than 90%. A delay in symptoms has not been reported, and the duration of certain SMS symptoms has decreased due to use of intramuscular promethazine. Case studies will be discussed and several therapeutic options and doses will be demonstrated. Further treatment possibilities will be examined.

NASA'S CIRCADIAN SHIFTING PROGRAM

R. T. Jennings
NASA/Johnson Space Center
2101 Nasa Road 1
Houston, TX 77058

Abstract unavailable at time of publication.

N94-11552

BASELINE CHARACTERISTICS OF DIFFERENT STRATA OF ASTRONAUT CORPS

Peggy B. Hamm, Ph.D.[1] and L. J. Pepper, D.O.[2]
[1]KRUG Life Sciences, Inc.
Longitudinal Studies
1290 Hercules, Ste. 120
Houston, TX 77058
[2]NASA/Johnson Space Center
Longitudinal Studies
2101 Nasa Road 1
Houston, TX 77058

The Longitudinal Study of Astronaut Health (LSAH) is an epidemiological study designed to study the effects of the occupational exposures incurred by astronauts in health outcomes and changes in physiological variables. Between 1959 and 1991, 195 individuals were selected for the program. The medical standards for selection have remained essentially unchanged since the Mercury Program, but the range and stringency of these criteria have been modified. Demographic and physiological variables identified during the selection year are examined for various strata of the Astronaut Corps. Specifically, age, sex, race, education, usual occupation, military affiliation, medical history, family medical history, visual and hearing measurements, physical exam variables, and specific laboratory values are investigated. Differences are examined for astronauts who (1) were selected prior to 1970 ($n=73$) versus those selected after 1970 ($n=122$); (2) have flown multiple missions versus those who have flown less than two missions; (3) have walked in space versus all others; (4) have more than 500 hours of mission time versus all others; and (5) have gone to the Moon versus all others. Length of time served in the Astronaut Corps is examined for each of these strata.

Session L4: TOXICOLOGY

Session Chair: J. James

N94-11553

COMPREHENSIVE ANALYSIS OF AIRBORNE CONTAMINANTS FROM RECENT SPACELAB MISSIONS

M.L. Matney,* J.F. Boyd,* P.A. Covington,* H.J. Leano,*
D.L. Pierson, T.F. Limero,* and J.T. James

Biomedical Operations and Research Branch
NASA/Johnson Space Center, Houston, TX 77058

* KRUG Life Sciences Inc.
1290 Hercules Drive, Houston, TX 77058

ABSTRACT

The Shuttle experiences unique air contamination problems because of microgravity and the closed environment. Contaminant build-up in the closed atmosphere and the lack of a gravitational settling mechanism have produced some concern in previous missions about the amount of solid and volatile airborne contaminants in the Orbiter and Spacelab. Degradation of air quality in the Orbiter/Spacelab environment, through processes such as chemical contamination, high solid-particulate levels, and high microbial levels, may affect crew performance and health. A comprehensive assessment of the Shuttle air quality was undertaken during STS-40 and STS-42 missions, in which a variety of air sampling and monitoring techniques were employed to determine the contaminant load by characterizing and quantitating airborne contaminants. Data were collected on the airborne concentrations of volatile organic compounds, microorganisms, and particulate matter collected on Orbiter/Spacelab air filters.

The results showed that the STS-40/42 Orbiter/Spacelab air was toxicologically safe to breathe, except during STS-40 when the Orbiter Refrigerator/Freezer unit was releasing noxious gases in the middeck. On STS-40, the levels of airborne bacteria appeared to increase as the mission progressed; however, this trend was not observed for the STS-42 mission. Particulate matter in the Orbiter/Spacelab air filters was chemically analyzed in order to determine the source of particles. Only small amounts of rat hair and food bar (STS-40) and traces of soiless medium (STS-42) were detected in the Spacelab air filters, indicating that containment for Spacelab experiments was effective.

1.0 INTRODUCTION

Shuttle air quality may be degraded by an accumulation or an abrupt release of contaminants in the cabin atmosphere. Since most nonmetallic materials continuously release (or offgas) trace amounts of volatile contaminants, build-up of offgas contaminants from flight hardware materials could reach harmful levels inside the closed environment of the Shuttle. It has been observed in "tight" or "sick" buildings that inhalation of low concentrations of volatile organic compound mixtures may have adverse effects on memory.[1] Events, such as overheating of insulation materials, release of utility chemicals (i.e., refrigerant, fire extinguishant), or chemical spills from payload experiments, have the potential to quickly release high concentrations of volatile contaminants into the cabin atmosphere. These abrupt releases may expose crewmembers to high levels of toxic contaminants, resulting in eye, skin, or respiratory tract irritation and/or systemic toxicity. Accumulation of airborne microorganisms in the closed environment increases the risk of contracting in-flight infections, as observed in

early Apollo missions.[2] Because of the microgravity environment, particles of food, paint chips, lint, dust, skin flakes, and hair are suspended in the Shuttle air before they are trapped onto the air filters. These free-floating particulates are a potential source of eye, skin, or respiratory tract irritation.

Preflight measures to control airborne contaminant levels include evaluation of flight hardware materials and containment of payload experiments and determination of microbial levels inside the Shuttle. Preflight offgas testing is required for all hardware in the flight certification process. Articles or materials that might release toxic amounts of chemicals into the Shuttle atmosphere are identified in preflight offgas testing. Hazards from payload and utility chemicals and materials are evaluated, and appropriate containment is recommended according to the toxicity and amount at risk for release into the cabin atmosphere. Two to three weeks before the launch, Orbiter air and preselected surfaces are sampled for microbial contaminants. Microbial levels greater than 1000 colony forming units per m^3 of air indicate that further cleaning of Orbiter surfaces or air ducts is required, depending on the location of the contamination. Volatile contaminants are evaluated in terms of their spacecraft maximum allowable concentrations (SMACs). SMACs are evaluated and set for each volatile contaminant, thus providing safe crew exposure limits. Limits have also been set for airborne solid particulates; for flights greater than one week, the NASA Panel on Airborne Particulate Matter in Spacecraft has recommended concentrations of 200 $\mu g/m^3$ for particles less than 10 μm in aerodynamic diameter (AD) plus 200 $\mu g/m^3$ for particles 10 to 100 μm in AD.[3]

During the flight, air quality is monitored via archival methods for volatile, microbial, and particulate contaminants. Volatile contaminants are collected from the air using "grab" air and solid sorbent sampling methods for ground-based gas chromatography (GC) and gas chromatography/mass spectrometry (GC/MS) analyses. Microbial contaminants sampled from the cabin air using a centrifugal air sampler are deposited on agar-media and subsequently incubated for ground-based analyses. Particulate levels have been monitored on STS-32/40 missions using the Shuttle Particle Samplers and Shuttle Particle Monitor. Results from these missions have shown that the total particulate concentrations (size range < 2.5 to > 100 μm in AD) of 33 $\mu g/m^3$ (STS-40)[4] and 56 $\mu g/m^3$ (STS-32)[5] in Shuttle air were well below the 200 $\mu g/m^3$ limit.

Special particulate studies were initiated following the STS-40 and STS-42 missions to determine the effectiveness of containment of particulate matter generated in Spacelab experiments. On Spacelab missions, there was a concern that experiment-generated particles might add to the normal particulate load. Since released particulates from the experiments would also be trapped on the Orbiter/Spacelab air filters, it would be possible to collect and analyze such particles from the filter debris. If released into the cabin atmosphere, biological-type particles produced in Spacelab experiments may be a potential inhalation hazard and/or spread infection. Positive identification of particles by visual means is not always possible, therefore, pyrolysis-gas chromatography/mass spectrometry (PY-GS/MS) was adapted for the analysis of organic particles. By heating the particle to a pyrolysis temperature of 600 °C, the particle is converted into a mixture of chemical components of lower mass. The pyrolysis spectrum obtained by PY-GC/MS contains "marker" compounds, which are specific to the type of particle under analysis and can be used to identify an unknown particle. Therefore, the main purpose of this particulate study was to determine, through microscopic and analytical chemistry methods, if particles produced in Spacelab experiments were escaping into the Shuttle atmosphere.

2.0 MATERIALS AND METHODS

2.1 VOLATILE CONTAMINANT SAMPLING

2.1.1 Sampling Cylinders

Stainless steel sampling cylinders were used to collect 300 ml "grab" samples of air inside the Shuttle. By collection of an instantaneous sample, the cylinders provide information on the air quality at the time and location of sampling. Orbiter air was sampled before and during each flight using separate cylinders. The in-flight air sample was collected on the final flight day in order to provide information on the types of chemical species that had been present in the Orbiter. During STS-40, a situation arose in the Orbiter middeck in which it was necessary to collect an extra air sample using the contingency bottle. Spacelab air was collected three times during both missions. Preflight, Orbiter in-flight, and Spacelab in-flight air sampling cylinders were returned to the JSC Toxicology Laboratory and analyzed quantitatively for trace amounts of hydrogen, methane, and carbon monoxide by GC. A more extensive analysis for the detection and quantitation of volatile organic compounds was then performed using a GC/MS.

2.1.2 Solid Sorbent Air Sampler (SSAS)

The SSAS contains eight sorbent tubes that trap and concentrate volatile organic contaminants from the Shuttle atmosphere. As 3 L of air is pumped through the sorbent tube, air contaminants are selectively adsorbed onto Tenax-GC over a known sampling period (typically 24 hours). The SSAS gives an average concentration of contaminants present in the Shuttle as opposed to the instantaneous measurement that the sampling cylinders provide. During the missions, the SSAS unit collected air samples over 7 24-hour periods. Compounds trapped on the Tenax sorbent resin were thermally desorbed and introduced into a GC/MS for detection and quantitation. For the more volatile contaminants, retention volume correction factors obtained from the literature were applied to their measured concentrations in order to estimate the actual concentration.[6]

2.1.3 Data Analysis Methods

The quality of the Shuttle breathing atmosphere may be assessed in terms of a collective toxicity potential (T-value) for all volatile air contaminants present in the Shuttle. The T-value for total air contaminants is estimated by adding ratios of each component concentration (C) to its 7-day spacecraft maximum allowable concentration (SMAC) as illustrated below:

$$T = C_1/SMAC_1 + C_2/SMAC_2 + \ldots C_n/SMAC_n$$

Air containing contaminant mixtures summed to give a T-value below 1.0 is toxicologically acceptable to breathe at the time and location of sampling. For air mixtures having a T-value > 1.0, the contaminant concentration exceeds that of the 7-day SMAC and air quality may be unacceptable for breathing.

2.2 PARTICULATE MATERIAL

2.2.1 Reference Standard Analyses

To prepare for the Orbiter/Spacelab debris analyses, reference standards, such as soiless media (STS-42; Gravitational Plant Physiology Facility), rat hair, food bar, and feces (STS-40; Animal Enclosure Module {AEM} and Rodent Animal Holding Facility {RAHF} animal housing facilities) were received for chemical analysis and were representative of materials contained in the Spacelab experiments. Reference pyrolysis spectra for each standard were obtained by PY-GC/MS for later comparison with the unknown debris particulates.

2.2.2 Shuttle Filter Debris

Orbiter and Spacelab debris were received for

microscopic and chemical analysis. The Orbiter debris was collected twice during the mission by vacuums of the 24 filters located in the flightdeck, middeck, and middeck overhead; all debris collected from these vacuums was placed in one bag. Spacelab debris was collected during postflight vacuuming of the filters.

Orbiter debris, which was received in vacuum bags, was separated into lint/hair and particle fractions; Spacelab debris was received pre-separated. The loose particles were observed under a dissecting microscope. Particles visually resembling the reference standards were collected from the debris, photographed, and placed in individual vials. To prepare for analysis, particles from each vial were placed in a sample crucible and weighed on a microbalance. Sample weights varied, depending on the type and number of particles (food-like particles, 200-250 μg; plant material, 40-80 μg). The particles, which were typically in the 300-500 μm diameter range, were then analyzed by PY-GC/MS. The unknown pyrolysis spectrum obtained by PY-GC/MS was then compared with the reference sample spectrum for identification.

2.3 MICROBIOLOGY

2.3.1 Microbial Air Sampler (MAS)

Microbiological air samples are typically collected early in the mission, midmission, and late in the mission from the Orbiter flightdeck and middeck, and the Spacelab. Using the principle of air centrifugation, the MAS draws in air containing bacteria and fungi, and the air is then exposed to agar-medium strips. Two strips were exposed at each sampling location; one strip is specific for bacteria (trypticase soy agar), and the second strip is specific for fungi (rose bengal agar). After exposure, the agar-medium strips were returned to the JSC Microbiology Laboratory for analysis. Following incubation of the strips, the microbial colonies that formed were counted and reported as colony-forming units (CFU) per cubic meter of air.

3.0 RESULTS

3.1 VOLATILE CONTAMINANT CONCENTRATIONS

3.1.1 Sampling Cylinders

Highlights of the STS-40/42 Spacelab cylinder air analysis are reported in Table 1. Only volatile contaminants having the highest concentrations are shown in Table 1; however, all contaminants detected and quantified in the cylinder samples were used in the T-value calculation. Probable sources for the volatile contaminants are shown in parentheses. Although numerous contaminants were identified, the air was toxicologically safe to breathe with T-values of 0.20, 0.13, 0.21, 0.09, and 0.10.

Orbiter air was sampled on the final flight-day of both missions. However, these samples were not representative of Orbiter air because of low or nonexistent methane and hydrogen concentrations (these metabolic by-products are known to build-up during the mission); the results are therefore not reported.

An additional STS-40 Orbiter cylinder was used to sample air from the Orbiter Refrigerator/Freezer (OR/F) interior as it was producing noxious odors. However, apparently safe contaminant levels (T-value = 0.05) were indicated for the contaminants found. An analysis of contaminants released by the OR/F into middeck air was conducted after the mission to explain the urine-like and aldehydic odors reported by crewmembers. Careful postflight disassembly of the OR/F revealed that an evaporator-fan motor had overheated and was still releasing formaldehyde, ammonia, and possibly hydrogen chloride from polymers that had been heated to at least 180 °C during the mission. Infrared spectroscopy and detector-tube analysis of the vapors produced by the failed motor several days after the mission

Table 1
Analytical Results of STS-40/42 Spacelab Cylinder Air Samples

CHEMICAL CONTAMINANT (concentrations in mg/m^3)	STS-40 0/23:49	STS-40 5/00:57	STS-42 0/03:45	STS-42 4/03:15	STS-42 7/05:45
Halogenated Aliphatics & Aromatics					
trifluorobromomethane (fire extinguishant)	0.01	0.17	14	1.6	6.5
trichlorofluoromethane (offgas)	0.02	0.20	0.18	0.09	0.07
dichloromethane (offgas)	0.18	0.39	0.19	0.39	0.25
Hydrocarbons					
methane (metabolic)	7	46	ND	4	15
toluene (offgas)	0.76	0.03	0.12	0.04	0.11
Ketones					
acetone (offgas,metabolic)	0.54	0.35	0.53	0.73	0.39
Alcohols					
isopropyl alcohol (utility)	7.5	3.8	6.3	1.0	4.3
ethyl alcohol (utility)	0.85	1.64	ND	1.2	1.5
Inorganic Gases					
hydrogen (metabolic)	ND	5.0	ND	1.8	2.3
Miscellaneous					
hexamethylcyclotrisiloxane (offgas)	0.08	0.40	0.78	0.08	0.70
TOTAL T-VALUE	0.20	0.13	0.21	0.09	0.10

confirmed the presence of these contaminants.[7]

3.1.2 Solid Sorbent Air Sampler (SSAS)

Because of the greater volume of air sampled by the SSAS, detection limits are decreased, and consequently additional trace contaminants were collected on the sorbent tubes. Although 52 STS-42 and 108 STS-40 volatile contaminants were detected, only contaminants having the highest concentration and common to both missions are shown in Table 2. Seven out of eight STS-42 SSAS tubes were analyzed, each giving combined toxicity potentials (T-values) varying from 0.16 to 0.26 for Spacelab air. For STS-40, the six SSAS tubes analyzed yielded T-values of 0.06 to 0.15 for contaminants detected in the Orbiter middeck. These low toxicity values indicate that the contaminants retained by the SSAS were well below toxic concentrations.

3.2 PARTICULATE MATERIAL

3.2.1 Shuttle Filter Debris

In order to determine if collected particles from the filter debris originated from the Spacelab experiments, the unknown and reference pyrolysis spectra were compared. Reference spectra "marker" compounds were checked against the unknown spectrum to determine if a match existed. The utility of the technique is illustrated in Figure 1, in which a rat food bar pyrolysis spectrum appears to match that of a filter debris particle. Most unknown particulates required chemical analysis for identification; however, rat

Figure 1
Comparison of Pyrolysis Spectra of Spacelab Particle (A) and Rat Food Bar Reference (B)

a

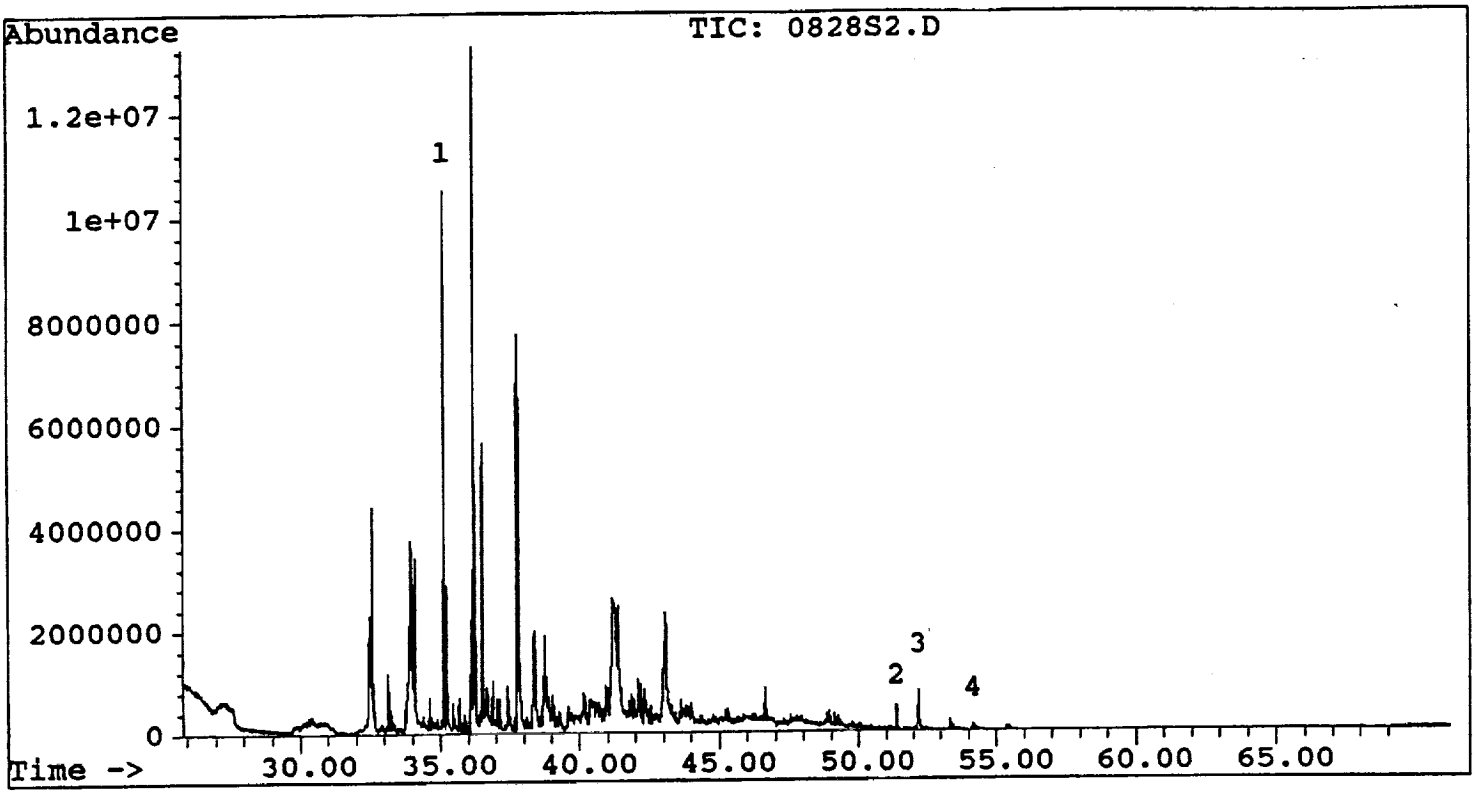

b

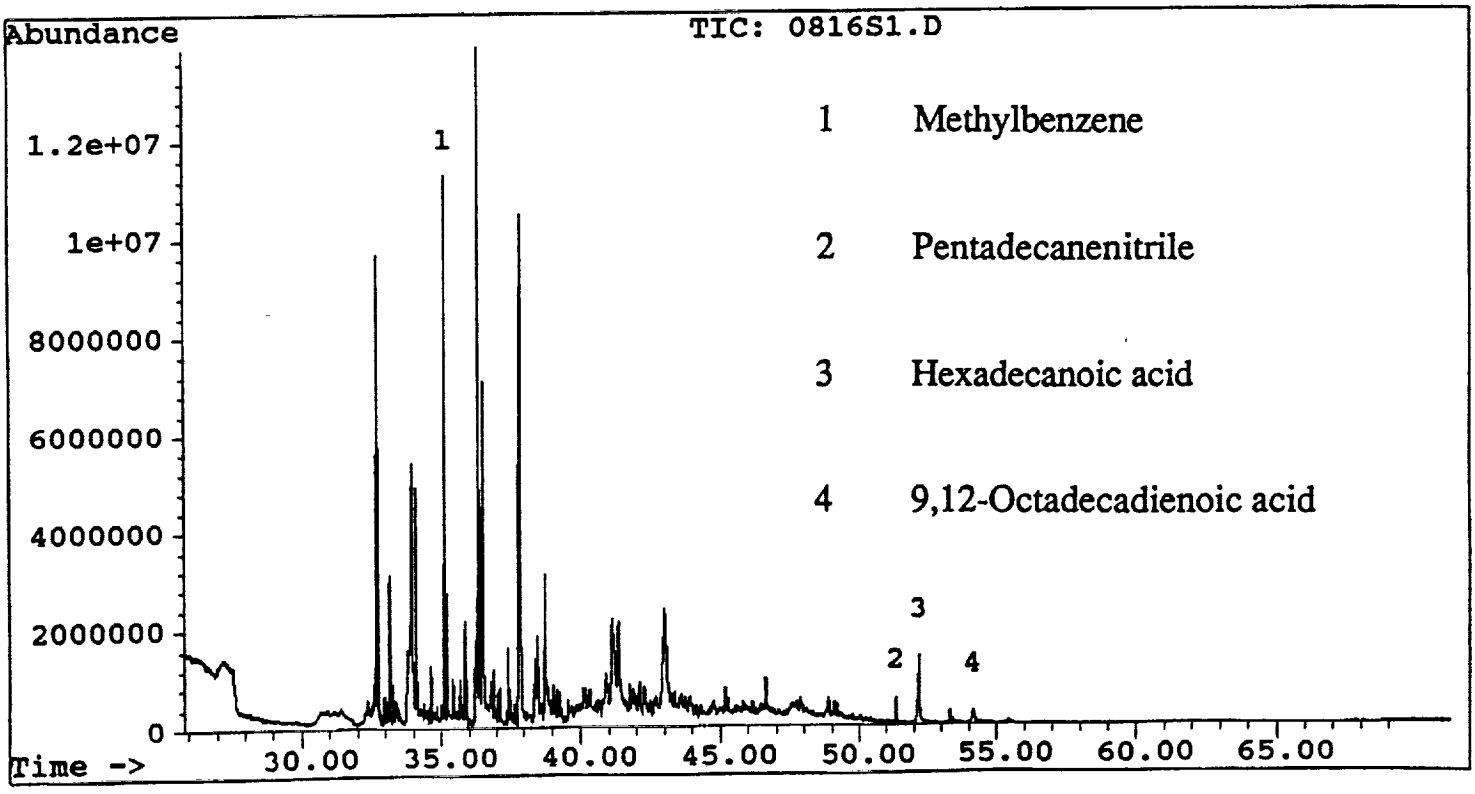

Table 2
Analytical Results of In-Flight STS-40/42
Solid Sorbent Air Samples

CHEMICAL COMPOUNDS (concentrations in mg/m^3)	STS-40	STS-42
Halogenated Compounds		
trifluorobromomethane +	0.1-3.5	16-22
1,1,2-trichloro-1,2,2-trifluoro-ethane +	0.6-2.5	0.1-0.6
trichlorofluoromethane +	1.2-8.7	0.2-1.2
dichloromethane ++	0.2-0.8	0.3-0.6
Hydrocarbons		
2-methyl-1,3-butadiene +	0.1	0.1
Ketones		
acetone	0.2	1.0-1.4
Alcohols		
isopropyl alcohol +	0.5-1.2	3.4-5.9
ethyl alcohol +	1.6-4.3	0.8-5.1
2-methyl-2-propanol ++	0.1	0.1-0.4
Miscellaneous		
hexamethylcyclotrisiloxane	0.1	0.1-0.2
TOTAL T-VALUE	0.1-0.2	0.2-0.3

+ Retention volume corrected values reported
++ STS-40 retention volume corrected values only

hairs in the Spacelab debris were positively identified by microscopic analysis using a compound microscope with 200x magnification and phase contrast.

Particle analysis results, both microscopic and chemical, are summarized for STS-40 and 42 in Table 3. A smaller subset was selected from the original debris to serve as an estimate for overall component levels in the total sample. Percentages of each filter debris component relative to the total number of particles in a group were estimated for the Orbiter and Spacelab filters. The percentage by weight of each component was not taken into account in these estimates, but particle diameters typically ranged from 100-500 μm. Of the animal-related particulates, rat food bar and rat hair were detected in the Spacelab filter debris in trace amounts. A trace amount of soiless media was detected in the Spacelab debris.

3.3 MICROBIOLOGY

3.3.1 Microbial Air Sampler

The results obtained from the STS-40/42 MAS samples are given in Figure 2. For each sample day during STS-40, results from the three sampling locations (Orbiter flightdeck and middeck, Spacelab) were averaged to give the mean concentrations of bacteria and fungi. As the mission progressed, airborne levels of bacteria seemingly appeared to increase. The bacterial mean increased from 120 CFU/m^3 on day 1 to 375 CFU/m^3 on day 7. For STS-42, samples were collected on the middeck and flight deck on days 1, 3, and 6, but Spacelab samples were collected only on day 6. This data did not show the typical increase in bacteria as a function of mission duration. For both missions, bacteria were more prevalent than fungi, which is typically observed.

Table 3
Estimate of Debris Particle Levels

	Orbiter Filter Debris		Spacelab Filter Debris	
	STS-40	STS-42	STS-40	STS-42
Rat hair	-	N/A	+/-	N/A
Rat feces	-	N/A	-	N/A
Rat food bar	-	N/A	+/-	N/A
Soiless media	N/A	-	N/A	+/-

+/- = < 1% - = Nondetectable

Figure 2

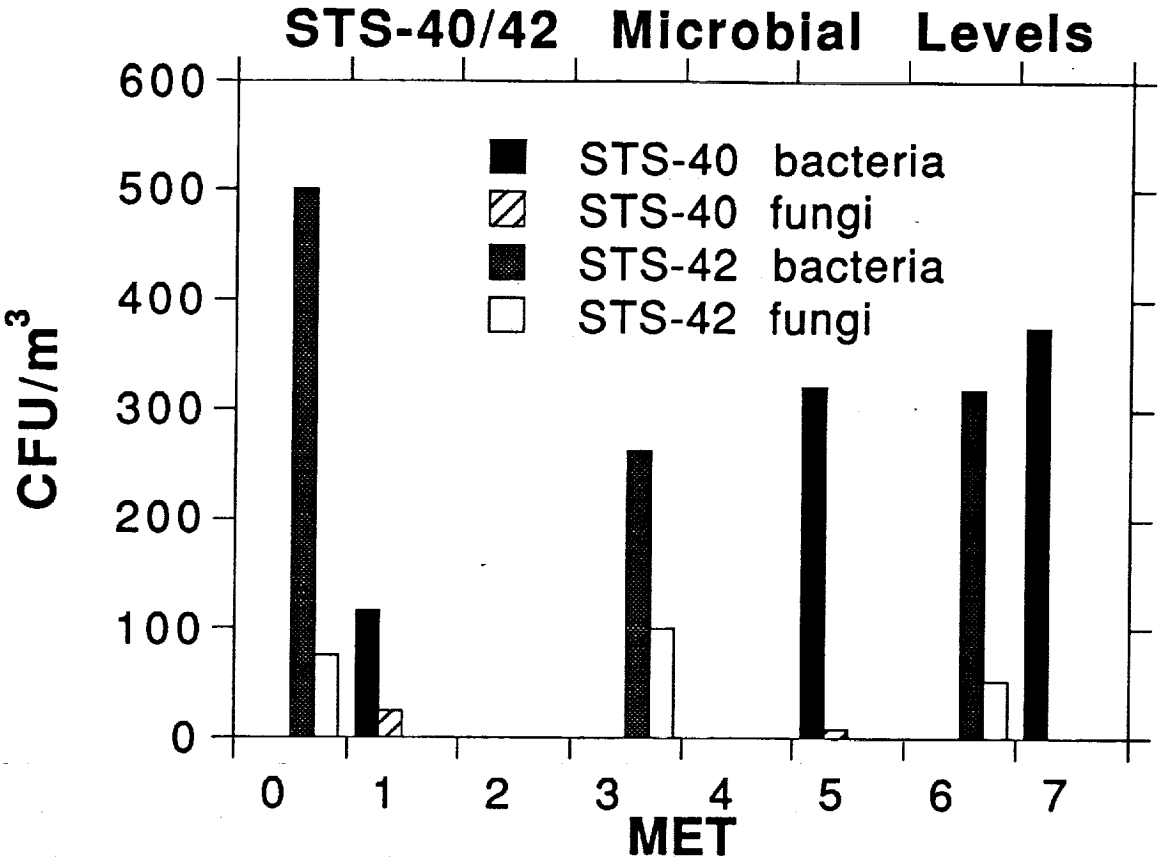

4.0 DISCUSSION

4.1 VOLATILE CONTAMINANTS

Fifty-two volatile contaminants were collected on the SSAS sorbent tubes from the STS-42 Spacelab atmosphere; 108 contaminants were detected in the STS-40 Orbiter middeck. Although fewer compounds were detected during STS-42, the SSAS T-values for this mission were generally higher than those obtained for STS-40 contaminants. STS-40 T-values for individual tubes were 0.15, 0.09, 0.13, 0.06, 0.09, and 0.12, whereas STS-42 values were 0.17, 0.16, 0.22, 0.21, 0.23, 0.20, and 0.26. Therefore, on the average, higher concentrations of contaminants were released into the STS-42 Spacelab atmosphere. However, the T-values for both missions are well below the toxicity potential limit of 1.0, thus indicating toxicologically safe breathing atmospheres.

Although toxicity levels were generally acceptable throughout the STS-40/42 missions, a problem midflight with the OR/F temporarily produced some noxious odors during STS-40. Since these odors caused irritation and nausea in some crewmembers, the source of the odors and the chemicals eliciting the symptoms were investigated by postflight analysis of OR/F components. It was determined that the source of the noxious odors was thermodegradation of polymers in and adjacent to an overheated evaporator-fan motor. Thermodegradation of polymers

may release toxic gases by production of the monomeric unit or elimination of small molecules, such as hydrogen chloride.[8,9] In the case of the OR/F components, the major thermodegradation contaminants causing the symptoms were ammonia, formaldehyde, and possibly hydrogen chloride. Since these contaminants are reactive and are not amenable to GC/MS detection, they were not detected in the bottle sample.

4.2 PARTICULATE MATERIAL

PY-GC/MS chemical analysis was successful in identifying the source of most food-related and plant-like debris particles. Definite matches of unknown debris particles with reference rat food bar and soiless media particles were observed, illustrating the utility of chemical analysis in determining the identification and source of debris particles. Moreover, the combination of microscopic and chemical techniques demonstrated that trace amounts of contaminants from Spacelab experiments were present in the cabin atmosphere. The animal containment facilities (AEM and RAHF) appeared to be effective in containing animal-related particulates, since no rat fecal material was positively identified and only small amounts of rat hair and food bar were detected in the Spacelab air filters. In addition, the GPPF experiment successfully contained soiless media particles; only a trace amount of soiless media was detected in the Spacelab cabin filter.

4.3 MICROBIOLOGY

A general increase in the number of airborne bacteria was observed as a function of mission duration on STS-40. This trend has been observed on some previous flights, but was not observed on STS-42. For both missions, the types and levels of bacteria were similar to those values found in a typical office space. Overall, the crew was not exposed to any unusual microbial risk via the airborne route.

5.0 CONCLUSION

A comprehensive air analysis study of the STS-40/42 Orbiter/Spacelab atmosphere was performed, providing information on the types and degree of contamination present in the Shuttle environment. Based on the analysis of Orbiter and Spacelab atmospheric "grab" samples collected during these missions, the air was toxicologically safe to breathe except during STS-40 when the OR/F was releasing noxious gases into the middeck. During STS-40, it appears that with an increase in mission duration, there was a possible bacterial build-up. This trend was not observed for STS-42. However, the low levels of microbial contaminants in samples collected during the missions indicate that the crew was not exposed to any unusual microbial risk. Chemical analysis of particles collected on Shuttle filters enabled the identification of particles and their source. The STS-40 Orbiter/Spacelab air was free of rat fecal particulates, but small amounts of rat hairs and food bar particles were found in the Spacelab air filters. A trace amount of soiless media was detected in the STS-42 Spacelab cabin filter. The low levels of animal-related and plant-like particles found in the Spacelab filters indicates that the containment for these Spacelab experiments is effective.

ACKNOWLEDGMENTS

Support from the Office of Space Science and Applications is gratefully acknowledged. The authors would like to thank Ms. Patricia Inners for her help with the paper.

[1] L. Molhave, B. Bach, O. F. Pedersen, "Human Reactions to Low Concentrations of Volatile Organic Compounds", *Environment International*, 12, 1986, p. 167-175.

[2] G. R. Taylor, "Recovery of Medically Important Microorganisms from Apollo Astronauts", *Aero. Med.*, 5, 1974, p. 824-828.

[3] National Aeronautics and Space Administration, "Airborne Particulate Matter in Spacecraft", NASA Conference Publication No. 2499, 1988.

[4] B. Y. H. Liu, K. L. Rubow, P. H. McMurry, T. J. Kotz, "Airborne Particulate Matter and Spacecraft Internal Environments: 90-Day Postflight Report", Particle Technology Laboratory Publication No. 802, 1991.

[5] B. Y. H. Liu, K. L. Rubow, P. H. McMurry, T. J. Kotz, D. Russo, "Airborne Particulate Matter and Spacecraft Internal Environments", 21st International Conference on Environmental Systems, San Francisco, CA, July 15-18, 1991, SAE Int'l: Warrendale, PA, 1991.

[6] J. F. Pankow, "Gas Phase Retention Volume Behavior of Organic Compounds on the Sorbent Poly(oxy-*m*-terphenyl-2',5'-ylene)", *Anal. Chem.*, 60(9), 1988, p. 950-958.

[7] J. T. James, "Toxicological Assessment of the Noxious Odors Produced by the OR/F during the STS-40 Mission," (Memorandum SD4/91-308).

[8] W. J. Irwin, Analytical Pyrolysis: A Comprehensive Guide, Marcel Dekker: New York, 1982, p. 293-299.

[9] Kirk-Othmer Concise Encyclopedia of Chemical Technology, John Wiley & Sons, Inc.: New York, 1985, p. 8.

N94-11554

TOXICITY STUDY OF DIMETHYLETHOXYSILANE (DMSES), THE WATERPROOFING AGENT FOR THE ORBITER HEAT PROTECTIVE SYSTEM

Chiu-Wing Lam, Ph.D.[1], John T. James, Ph.D.[2], Darol Dodd, Ph.D.[3], Bruce Stuart, Ph.D.[3], Simon Rothenberg, Ph.D.[3], Mary Ann Kershaw[4], and A. Thilagar, Ph.D.[5]

[1]KRUG Life Sciences, Inc.
Toxicologist
Johnson Space Center, SD4
Houston, TX 77058

[2]NASA/Johnson Space Center
Toxicology
Mail Code: SD4
Houston, TX 77058

[3]ManTech Environmental Technology Inc.
Upton, NY

[4]Brookhaven National Lab
Upton, NY

[5]Sitek Research Labs
Rockville, MD

DMES, a volatile liquid, is used by NASA to waterproof the Orbiter thermal protective system. During waterproofing operations at the Orbiter Processing Facility at the Kennedy Space Center, workers could be exposed to DMES vapor. To assess the toxicity of DMES, acute and subchronic (2-week and 13-week) inhalation studies were conducted with rats. Studies were also conducted to assess the potential of DMES.

Inhalation exposure concentrations ranged from 40 ppm to 4000 ppm. No mortality was observed during the studies. Exposures to 2100 ppm produced narcosis and ataxia. Post-exposure recovery from these CNS effects was rapid (< 1 hr). These effects were concentration-dependent and relatively independent of exposure length. Exposure to 3000 ppm for 2 weeks (5 h/d, 5 d/wk) produced testicular toxicity. The 13-week study yielded similar results. Results from the genotoxicity assays (in viv/in vitro unscheduled DNA synthesis in rat primary heptaocytes, chromosomal aberrations in rat bone marrow cells; reverse gene mutation in Salmonella typhimurium; and forward mutation in Chinese hamster culture cells) were negative. These studies indicated that DMES is mildly to moderately toxic but not a mutagen.

A Combustion Products Analyzer for Contingency Use During Thermodegradation Events on Spacecraft

Steve Wilson, Thomas F. Limero, Steve W. Beck
KRUG Life Sciences Inc., 1290 Hercules Dr., Suite 120, Houston, TX 77058

John T. James
Lyndon B. Johnson Space Center, NASA, SD4, Houston, TX 77058

ABSTRACT

The Toxicology Laboratory at Johnson Space Center (JSC) and Exidyne Instrumentation Technologies (EIT) have developed a prototype Combustion Products Analyzer (CPA) to monitor, in real time, combustion products from a thermodegradation event on board spacecraft. The CPA monitors four gases that are the most hazardous compounds (based on the toxicity potential and quantity produced) likely to be released during thermodegradation of synthetic materials: hydrogen fluoride (HF), hydrogen chloride (HCl), hydrogen cyanide (HCN), and carbon monoxide (CO). The levels of these compounds serve as markers to assist toxicologists in determining when the cabin atmosphere is safe for the crew to breathe following the contingency event.

The CPA is a hand-held, battery-operated instrument containing four electrochemical sensors, one for each target gas, and a pump for drawing air across the sensors. The sensors are unique in their small size and zero-g compatibility. The immobilized electrolytes in each sensor permit the instrument to function in space and eliminate the possibility of electrolyte leaks. The sample inlet system is equipped with a particulate filter that prevents clogging from airborne particulate matter. The CPA has a large digital display for gas concentrations and warning signals for low flow and low battery conditions.

The CPA has flown on 13 missions beginning with STS 41 in October, 1990. Current efforts include the development of a microprocessor, an improved carbon monoxide sensor, and a ground-based test program to evaluate the CPA during actual thermodegradation of selected materials.

INTRODUCTION

The Toxicology Laboratory at NASA Johnson Space Center (JSC) has been directly involved in developing a Combustion Products Analyzer (CPA) to monitor combustion products from a thermodegradation of nonmetallic materials on board spacecraft. The term "thermodegradation," as used in this paper, refers to the full range of events from an overheated electrical component or wire to a major fire. The likelihood of significant thermodegradation events occuring on orbit, as evident by recent incidents on the Space Shuttle, have driven this development effort (1).

The release of potentially toxic gases into the spacecraft atmosphere during a major thermodegradation incident would require the crew to breathe directly from the spacecraft oxygen supply to obtain clean air. Since this oxygen supply is limited, the mission would likely be terminated if the quality of the cabin air could not be varified as safe within a reasonable time. Input from the crew and spacecraft systems as to the magnitude of the event will be very important in the decision-making process. However, thermodegradation of very small quantities of some synthetic materials can produce hazardous levels of decomposition products. Levels of toxic products in the atmosphere would be difficult to assess by observation or symptoms; thus, without real-time monitoring capability, restriction to a conservative decision will lend to an aborted mission. Methods exist for decontaminating the cabin atmosphere of many of the compounds likely to be released from thermodegradation of nonmetallic materials. The CPA has been designed to monitor the effectiveness of these procedures, with the goal of determining when the air is safe for the crew to breathe.

SHUTTLE EXPERIENCE - During Shuttle missions, five thermodegradation incidents are known to have taken place. Although these incidents were relatively minor, each provided valuable information to the NASA Toxicology Laboratory and reinforced the need for the CPA.

The first thermodegradation event occurred on STS-6 in May 1983 (2). During this mission, the crew sensed a persistent odor emanating from the area of a payload experiment (monodisperse latex reactor). Evaluations after the mission revealed that several kapton-teflon insulated wires beneath the dehumidifier were found to be fused together. Postflight testing of the kapton wire did not demonstrate conclusively that the odor came from the fused wires. The crew did not experience any apparent adverse health effects as a result of this incident.

A second thermodegradation incident was reported on STS-28 in August 1989 (3). On the fifth day of flight, a teleprinter cable located on the flight deck shorted for 1.5 seconds. Postflight analysis indicated that 0.1 gram of Teflon had been pyrolyzed during the incident. Although pyrolysis of this amount of teflon did not pose a hazard to the crew, calculations showed that burning of 2 grams of teflon could have caused adverse health effects in the crew (4).

Other events occurred aboard STS-35 in December 1990 (5). During the first day of flight, the crew detected a burning odor from the Digital Display System 1 (DDS), which automatically shut down. During the fifth day of the mission a second unit, DDS2, also failed, emitting a pungent odor. This unit too shut down automatically. Another attempt to power DDS1 that day also produced a burning odor. Postflight analysis led to the conclusion that clogged air filters caused overheating of several electrical components in both DDS units. Crew health did not appear to be affected as a result of this incident.

The most recent incident occurred during STS-40 when a small motor, containing Delrin (polyformaldehyde) and surrounded by foam, seized and overheated. The result was noxious odors which filled the middeck and caused headache and nausea in some crewmembers (6).

Although these relatively limited thermodegradation incidents to date have not affected crew health or performance, they clearly demonstrate the potential for significant problems.

TARGET COMPOUND SELECTION - The first stage in the development of the CPA was to determine which compounds should be monitored. Many variables affect which products are generated in a thermodegration event, e.g. type of material, temperature, oxygen content, microgravity, etc.. Measuring every toxic compound that is generated during a thermodegradation event is impossible. Toxicologists at NASA identified four compounds that will be used as markers for characterizing the air quality during an incident (7). These compounds are carbon monoxide (CO), hydrogen fluoride (HF), hydrogen cyanide (HCN), and hydrogen chloride (HCl). These are not necessarily the most toxic chemicals generated in such an event. However, considering both toxic properties and relative quantities of thermodegradation products likely generated, these 4 chemicals are considered to be the most hazardous (7). In other words, it is unlikely that any thermodegradation event will generate hazardous levels of any other compound without at least one of these targeted chemicals being present at levels affecting crew health and safety. Consequently, the selected compounds would serve as "markers" during decontamination efforts to indicate when the cabin air was safe to breathe. Potential sources of the targeted compounds in the Space Shuttle are listed in Table I. The spacecraft maximum allowable concentrations (SMACs) (8) and threshold limit values (TLVs), set by NASA toxicologists and the American Conference of Governmental Industrial Hygienists (ACGIH) (9), respectively, are listed in Table II.

Table I: Hazardous Thermodegradation Products From Selected Materials

KAPTON	TEFLON	PVC	POLY-URETHANE
CO	CO	CO	CO
HCN	HF	HCl	HCN
	COF_2		

Table II. Exposure Limits (ppm) for Targeted Gases

	CO	HF	HCN	HCl
TLV	50	*3	*10	*5
SMAC (7-day)	25	0.1	1	1

* Ceiling Values

PROTOTYPE DEVELOPMENT - The next step in the CPA development process was to identify the required and desirable features, and specifications for an analyzer capable of measuring the 4 targeted

compounds at meaningful concentrations in the spacecraft atmosphere. This would be followed by an investigation of available technologies to meet the defined criteria.

The required or desirable features included the following: simultaneous measurement of all targeted compounds, highly selective, compact, lightweight, microgravity compatible, impervious to the vibration and shock of launch, simple to use, low maintenance requirements, battery-operated, and no spacecraft resource requirements with the exception of power during extended continuous operating periods (on the order of days). Specifications were developed for response and recovery times, signal-to-noise ratios, weight, volume, battery-operation time, accuracy, detection limits, working ranges, calibration requirements, display requirements, and others.

Four technologies, infrared spectroscopy, catalytic surface sensors, electrochemistry, and length-of-stain indicator tubes, became the focus of the selection effort. Limitations were identified in all the technologies; however, electrochemical sensing met more of the required criteria than any other technology. Companies in the electrochemical sensor industry were identified and contacted. Exidyne Instrumentation Technologies (EIT) of Exton, Pennsylvania, one of only a few companies which manufacture their own electrochemical sensors, was selected to build a prototype combustion products analyzer. The culmination of a 6-month contract with EIT in 1990 resulted in the CPA described below.

The prototype CPA has four electrochemical sensors to monitor CO, HF, HCN, and HCl. The sensors are arranged in a teflon block so that the face of each sensor is exposed to a channel through which ambient air is pumped at a rate of 15 cm/s (10) (Figure 1). A 25-mm particulate filter prevents entry of particles larger than 0.3 μ. The front panel of the CPA is shown in Figure 2 (10). The entire unit weighs 3 lbs., with a volume of only 77 cubic inches. A battery (recharged

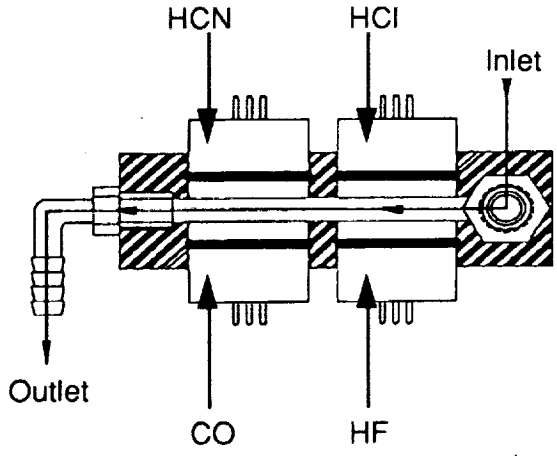

Figure 1: CPA Sensor Block

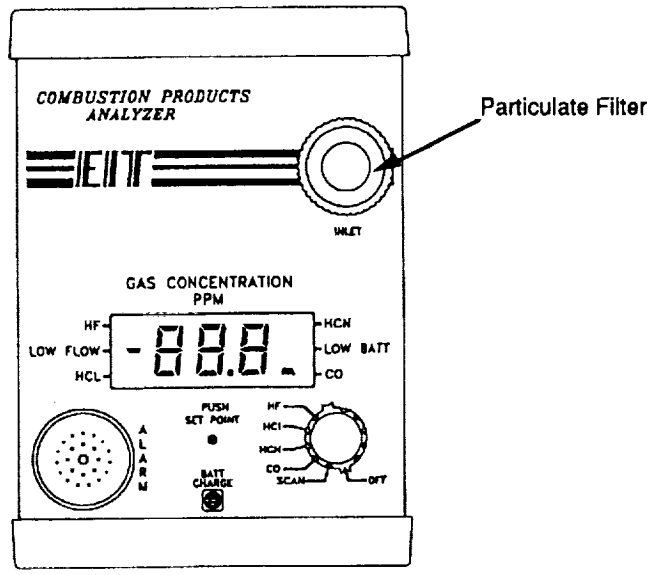

Figure 2: Front Panel of CPA

on 28 VDC power source) provides up to 16 hours of continuous operation. The instrument is capable of operating continuously using 28 VDC spacecraft power. In use, the crew need only switch the instrument from off to the scan mode. In the scan mode, the concentration (ppm) of each compound is displayed sequentially for approximately 5 seconds; however, a single compound can also be selected for continuous monitoring by turning the switch to the appropriate compound position. In order to avoid false readings due to mechanical failures, low-battery and low-flow warnings have been incorporated into this compact instrument. Manual alarm levels can be set to trip an audio alarm when any of the preset values are exceeded. Instrument calibration is easily performed by removing the back panel exposing the zero and span potentiometers for each sensor. The EIT sensors include electronic temperature-compensation capabilities that allow the sensors to operate accurately at temperatures ranging from 5 to 40°C.

SENSOR DESIGN AND THEORY - Many of the electrochemical sensors commercially available today are relatively large and depend on free-flowing liquid electrolyte. EIT's unique sensor design reduced the electrode size and immobilized the liquid electrolyte, thereby decreasing volume and permitting operation in microgravity. A general schematic of the electrochemical amperometric sensors is shown in Figure 3 (10). The gas passes through the first membrane, which is designed to provide a quiescent zone for diffusion. The second gas-diffusion membrane and a sensing electrode are bound to each other. Sandwiched between the counter/reference electrode and the sensing electrode is the electrolyte, immobilized in a microfibrous matrix. Selectivity for each sensor may be gained by choice of electrolyte,

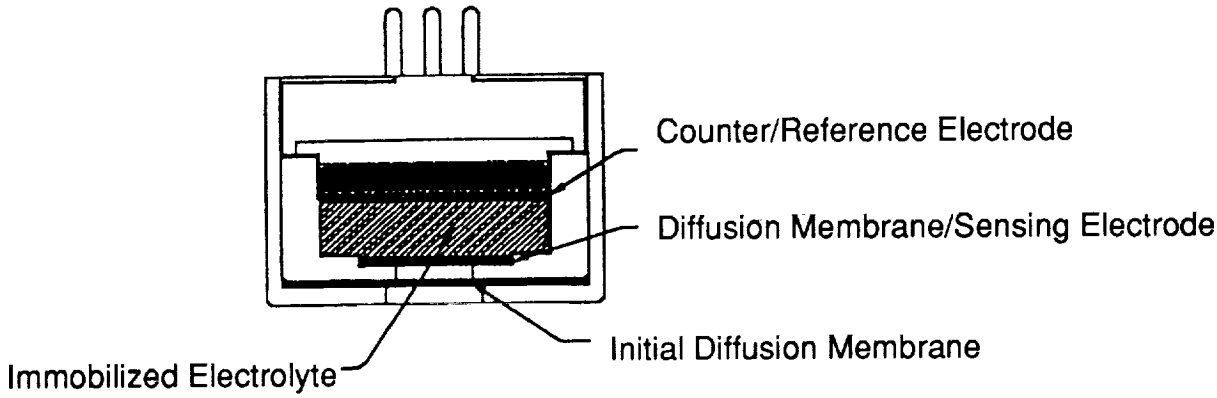

Figure 3: CPA Sensor Schematic

noble metal electrodes, electrode potentials, prefilters, and gas-diffusion membrane materials. Although these sensors can operate by passive air diffusion, a pump was added to ensure adequate response and recovery times.

Each targeted gas diffuses through the membrane and the sensing electrode before reaching the electrode/electrolyte interface, where the electrochemical reactions occur (see Figure 3). The sensing electrode and counter/reference electrode provide the closed circuit necessary for the oxidation-reduction reaction. If sensor conditions are optimized, the reactant of interest will react readily at the electrode/electrolyte interface and the concentration of reactant at the interface will be zero; hence the measured current is proportional to the concentration of the reactant in the bulk gas. Using a modification of Fick's law of diffusion, this can be shown to be a linear relationship (10).

Given the appropriate potential, the CO, HCN, and HCl are direct oxidation reactions, whereas the HF is detected indirectly as an acid gas by a reduction reaction (10).

RESULTS AND DISCUSSION

SENSOR PERFORMANCE - General operating characteristics of the sensors are presented in Table III. The range, resolution, accuracy, repeatability, and reaction times of the sensors are sufficient for the proposed monitoring functions of the CPA during a thermodegradation event. The response and recovery times for the HF sensor, although adequate, are slower than desirable. The slower times can be attributed to the indirect reactions required to detect this compound. Efforts have begun to improve these response times.

One of the most important parameters when evaluating an analytical procedure is the degree of specificity of the technique or reaction. A procedure that is subject to significant false positive or false negative reactions is unreliable and useless. Since the purpose of the CPA is to provide valuable information during a contingency situation, a great deal of effort has been involved in identifying chemicals that either positively or negatively interfere with the sensors producing ambiguous results.

Table III. Results of CPA Sensor Performance Testing

	HCl	HF	HCN	CO
RANGE	0-99.9 PPM	0-99.9 PPM	0-99.9 PPM	0-999 PPM
RESOLUTION	0.1 PPM	0.1 PPM	0.1 PPM	1 PPM
ACCURACY*	± 5%	± 5%	± 5%	± 2%
REPEATABILITY	± 2%	± 2%	± 2%	± 1%
RESPONSE TIME				
RISE TO 80%	2 minutes	5 minutes	1 minute	15 seconds
DECAY TO 90%	2 minutes	8 minutes	1 minute	30 seconds

Table IV. Results of Cross-Sensitivity Testing of CPA Sensors

GAS	CONCENTRATION	HCl	HF	HCN	CO
CO	50 PPM	0	0	0	50
HCl	6 PPM	6	4.0	0	0
HF	5 PPM	0	5.0	0	0
HCN	42 PPM	0.4	-5.7	42	7

Cross-sensitivity reactions within the four gases are shown in Table IV (10). The HCN sensor exhibits no significant cross-sensitivity when exposed to the other targeted gases. The CO sensor shows a cross-sensitivity to HCN gas in a ratio of approximately 6:1– meaning 6 ppm HCN produces a signal in the CO sensor equal to 1 ppm CO. The HF and HCl sensors, however, demonstrate cross-sensitivities that are related to their general response to the acid moiety. These cross-sensitivity reactions are predictable and can be easily corrected using a microprocessor, with fully-compensated data being displayed to the user. Development of a microprocessor has begun and will be discussed further below.

Additionally, the sensors have been exposed to numerous other gases in an effort to identify compounds that can act as interferents. Most of the gases that interfere (ozone, ammonia, sulfur dioxide, fluorine, bromine, chlorine, methyl sulfide, and hydrogen sulfide) either will not be present on spacecraft, exist at extremely low concentrations, or produce an insignificant cross-sensitivity response. The sensors do not respond to other potential interferents (carbon dioxide, ethanol, and methane) that are known to be present in the Shuttle atmosphere in significant quantities.

MISSION RESULTS - Beginning with STS-41 in October 1990, the CPA has flown on all missions, totalling 13 to date. Typical on-orbit use of the CPA involves the collection of baseline readings each day of the mission. Results to date indicate that the sensors have performed nominally on orbit and have remained in calibration during the course of the mission with the exception of a problem with the CO sensor discussed below. The daily readings of the HCl, HCN, and HF sensors have remained very low during these missions, indicating that cross-reacting chemicals that might interfere are not present in significant quantities in the Shuttle atmosphere during nominal operations. Sensor performance is apparently not affected by lift-off or microgravity operation. The average and standard deviation of HCl, HCN, and HF sensor readings for all of the missions is presented in Table V.

A significant problem with the CO sensor was identified very early in the flight test program. Analyses of grab samples collected during the course of the missions found much lower CO levels than those recorded on orbit by the CPA. Although not a routine analysis at the time, hydrogen was found in the grab samples at levels significant for cross-sensitivity considerations. Subsequent testing of the CPA determined that exposing the CO sensor to a hydrogen concentration of 100 ppm produces a response of approximately 50 ppm in the CO sensor (2:1 cross-sensitivity ratio). Furthermore, the CO sensor reading exhibited a slow drift upward the longer the sensor was exposed to the hydrogen.

Table V. Mission Data for HCl, HF, and HCN Sensors

	Avg. Response (ppm)	Std. Dev.
HCl	0.4	0.35
HF	0.4	0.40
HCN	0.1	0.1
n = 128		

EIT and the JSC Toxicology Laboratory embarked on a program to modify the CO sensor to reduce the cross-sensitivity to hydrogen and to stabilize this response. Considerable improvements were made in the cross-sensitivity ratio (approximately 10:1) and response stability to hydrogen by elevating the voltage bias of the sensing electrode with respect to the reference electrode in the electrochemical cell. The polarization of the sensing electrode with respect to the reference electrode resulted in a larger zero offset but was not detrimental to the signal-to-noise ratio. The modifications have resulted in a CPA CO sensor

that has a much improved cross-sensitivity to hydrogen and responds to hydrogen in a predictable manner. The modified sensor has flown on all missions beginning with STS-37 in April 1991. These improvements in the CO sensor greatly increase its value as a trend indicator in the event of a thermodegradation event.

CURRENT AND FUTURE EFFORTS

CURRENT EFFORTS - The focus of current development efforts are in two main areas— 1) further improvements in the cross-sensitivity problems of the CPA and 2) ground-based testing of the CPA in atmospheres containing combustion/pyrolysis products from the thermodegradation of various nonmetallic materials used on the Orbiter.

Current contractual work with EIT is scheduled for completion in the early fall, 1992. The focus of this work is 1) the fabrication and testing of a hydrogen sensor to be used in conjunction with the CO sensor, and 2) the fabrication and testing of a microprocessor capable of compensating outputs for intra-sensor cross-sensitivities. The hydrogen sensor has been built and is currently being tested for long-term stability. The addition of a fifth sensor will require a larger sensor block; however, this will not substantially increase the size of the instrument. An accurate CO concentration will be displayed by having a compensation algorithm in the microprocessor. Using the CO sensor and hydrogen sensor signals and knowing the CO:H_2 cross-sensitivity ratio, corrected data are easily obtained. Alternatively, EIT is exploring ways to reduce the hydrogen interference of the CO sensor to greater than 100:1. The maximum hydrogen level that has been obtained on any mission is in the 300 ppm range. If this approach is successful, the subtraction procedure would be unnecessary. The microprocessor will also be used to correct the HCl and HF for their cross-sensitivities to each other and to HCN. These responses are predictable and compensation is easy and straight forward.

In addition to correcting sensor output data, the microprocessor will provide valuable sensor diagnostic information. When the CPA is turned on, the microprocessor will perform a self-check routine. The microprocessor will electronically pulse each sensor to determine if open circuits exist and monitor the resultant current generated by the sensors for their characteristic output signatures. Sensors that are behaving erratically or severely out of calibration will exhibit an uncharacteristic output signature. If a problem is diagnosed, a display will indicate which sensor is not functioning properly.

The other major ongoing effort is a test program being conducted at the NASA White Sands Test Facility (WSTF) to evaluate the CPA's response to combustion products generated from the thermal decomposition of polymeric materials in air (11). This program is in progress and should be completed by January 1993. The materials to be tested include Kapton (fluorocarbon/polyimide wire insulation), pyrell foam (polyurethane foam), polyvinyl chloride (unplasticized PVC polymer), tefzel (ethylene-tetrafluoroethylene copolymer wire insulation), and an electronic circuit board with components (glass/epoxy laminate with capacitors, resistor, and diode). Although the testing will be conducted under defined conditions in a 1-g environment, the information gathered should be extremely valuable for further definition of sensors needing improvement and limitations of the hardware. Furthermore, successful operation of the CPA in the combustion atmospheres will provide confidence to the crew, toxicologists, etc., that this instrument will provide useful information during an actual combustion event.

FUTURE ENDEAVORS

The next step in the development of operational CPA for Shuttle is the inclusion of the hydrogen sensor and microprocessor into an integrated flight hardware package. If modifications are required, based on findings from the WSTF testing, they would be made during this step.

An important component of the Crew Health Care System (CHeCs) in the Space Station Freedom (SSF) Program is the Compound Specific Analyzer— Combustion Products, known as the CSA-CP. The CSA-CP will be a modified CPA. Major modifications will include the addition of data logging capability, interfacing with the SSF data management and power distribution systems, and on-orbit calibration capability.

Keeping a sensitive instrument calibrated during extended missions is a major concern. In its current configuration, the CPA would require calibration approximately every 60 to 90 days using HCl, HCN, HF, and CO gases and this, clearly, could not be performed on orbit. The Toxicology Laboratory and EIT are working on a unique alternative to the standard calibration method. An entire sensor block, containing all four sensors, and an amplifier and microprocessor for each sensor, will be replaced on a regular basis. The microprocessor will store the calibration curves, which will be developed during ground tests; therefore, replacement of the sensor pack will recalibrate the CSA-CP. Multiple sensor packs, enough to support an extended mission, would be calibrated at the same time, sealed, and stored on the

spacecraft. Sufficient numbers of compact sensor packs could easily be manifested to accommodate extended missions.

The development of a data logger is also being pursued to assist in trend analysis and to provide a record of decontamination effectiveness following a thermodegradation incident. This data logger would also supply information necessary for trend analysis, such as time-weighted averages and coefficients of variance.

CONCLUSIONS

The Toxicology Laboratory at Johnson Space Center identified a need to monitor toxic combustion products during a thermodegradation event on board spacecraft. A development effort with Exidyne Instrumentation Technologies culminated in the fabrication of the Combustion Products Analyzer, capable of measuring 4 targeted gases. Through successful laboratory and flight test programs, some problems were identified, and modifications are ongoing to solve these problems. Ground-based combustion tests with the CPA using selected spacecraft materials have begun. Several other improvements aimed at upgrading the CPA to meet SSF program requirements have also begun.

REFERENCES

1. Limero, Thomas; James, John; Cromer, Raymond; Beck, Steve, "A Combustion Products Analyzer for Contingency Use During Thermodegradation Events on Spacecraft", International Conference on Environmental Systems, San Francisco, California, July, 1991.

2. Huntoon, Carolyn, "STS-6 Toxicology Mission Report", NASA- Johnson Space Center memorandum SD4/82-215, 1982.

3. Huntoon, Carolyn, "STS -28 Toxicology Mission Report", NASA- Johnson Space Center memorandum SD4/89-316, 1989.

4. Communications with Drs. John James, NASA-JSC, King-Lit Wong, Hector Garcia, and Chiu-Wing Lam, KRUG Life Sciences, Inc., August, 1989.

5. Huntoon, Carolyn, "STS-35 Toxicology Mission Report", NASA- Johnson Space Center memorandum SD4/91-027, 1991.

6. Huntoon, Carolyn, "STS-40 Toxicology Mission Report", NASA- Johnson Space Center memorandum SD4/91-362, 1991.

7. Communications with Drs. John James, NASA-JSC, King-Lit Wong, Hector Garcia, and Chiu-Wing Lam, KRUG Life Sciences, Inc., various periods in 1989.

8. "Spacecraft Maximum Allowable Concentrations for Airborne Contaminants", Medical Sciences Division, Biomedical Operations and Research Branch, NASA-Johnson Space Center, May, 1990.

9. "1991-1992 Threshold Limit Values for Chemical Substances and Physical Agents and Biological Exposure Indices", The American Conference of Governmental Industrial Hygienists, Cincinnati, OH, 1991.

10. Cromer, Raymond, "Combustion Products Analyzer (CPA) Development: Final Report", KRUG Life Sciences Contract # 13652 November, 1990.

11. "Test Plan - Evaluation of EIT Combustion Products Analyzer", NASA-White Sands Test Facility, Document No. TP-WSTF-639, December, 1991.

N94-11556

FIVE BIOMEDICAL EXPERIMENTS FLOWN IN AN EARTH ORBITING LABORATORY: LESSONS LEARNED FROM DEVELOPING THESE EXPERIMENTS ON THE FIRST INTERNATIONAL MICROGRAVITY MISSION FROM CONCEPT TO LANDING

C. M. Winget[1], J. J. Lashbrook[1], P. X. Callahan[1], and R. L. Schaefer[2]
[1]NASA/Ames Research Center
Space Life Sciences Payloads Office
Moffett Field, CA 94035-1000
[2]Lockheed Engineering and Science Company
NASA/Ames Research Center
Moffett Field, CA 94035-1000

The problems are numerous for accommodating complex biological systems to microgravity in a relatively large flexible laboratory systems installed in the Orbiter cargo bay. This presentation will focus upon some of the lessons learned along the way from the University Laboratory to IML-1 Microgravity Laboratory. The First International Microgravity Laboratory (IML-1) mission contained a large number of specimens, including: 72 million nematodes, US-1; 3 billion yeast cells, US-2; 32 million mouse limb-bud cells, US-3; 540 oat seeds (96 planted), FOTRAN. All five of the experiments had to undergo significant redevelopment effort in order to allow the investigator's ideas and objectives to be accommodated within the constraints of the IML-1 mission. Each of these experiments were proposed as unique entities rather than part of the mission, and many procedures had to be modified from the laboratory practice to meet IML-1 constraints. After a proposal is accepted by NASA for definition, an interactive process is begun between the Principal Investigator and the developer to ensure a maximum science return. The success of the five SLSPO-managed experiments was the result of successful completion of all preflight biological testing and hardware verification finalized at the Kennedy Space Center (KSC) Life Sciences Support Facility housed in Hangar L. The ESTEC Biorack facility housed three U.S. experiments (US-1, US-2, and US-3). The U.S. Gravitational Plant Phydiology Facility housed GTHRES and FOTRAN. The IML-1 mission (e.g., launched from KSC on January 22, 1992, and landed at Dryden Flight Research Facility on January 30, 1992) was an outstanding success—close to 100% of the prelaunch anticipated science return was achieved and, in some cases, greater than 100% was achieved (because of an extra mission day).

N94-11557

PHYSIOLOGIC MECHANISMS OF CIRCULATORY AND BODY FLUID LOSSES IN WEIGHTLESSNESS IDENTIFIED BY MATHEMATICAL MODELING

K.E. Simanonok, R.S. Srinivasan[1], and J.B. Charles[2]

Universities Space Research Association
[1]KRUG Life Sciences
[2]Space Biomedical Research Institute
Johnson Space Center, Houston, Texas 77058

ABSTRACT

Central volume expansion due to fluid shifts in weightlessness is believed to activate adaptive reflexes which ultimately result in a reduction of the total circulating blood volume. However, flight data suggests that a central volume overdistention does not persist, in which case some other factor or factors must be responsible for body fluid losses. We used computer simulation to test the hypothesis that factors other than central volume overdistention are involved in the loss of blood volume and other body fluid volumes observed in weightlessness and in weightless simulations, and to identify these factors. The results predict that atrial volumes and pressures return to their pre-bedrest baseline values within the first day of exposure to head down tilt (HDT) as the blood volume is reduced by an elevated urine formation. They indicate that the mechanism for large and prolonged body fluid losses in weightlessness is red cell hemoconcentration that elevates blood viscosity and peripheral resistance, thereby lowering capillary pressure. This causes a prolonged alteration of the balance of Starling forces, depressing the extracellular fluid volume until the hematocrit is returned to normal through a reduction of the red cell mass, which also allows some restoration of the plasma volume. We conclude that the red cell mass becomes the physiologic driver for a large "undershoot" of body fluid volumes after the normalization of atrial volumes and pressures.

INTRODUCTION

The circulation and fluid distribution of the human body appear to be immediately and profoundly affected by exposure to weightlessness; blood and interstitial fluid which normally tend to pool in the legs due to gravity become redistributed toward the head (Leach, 1979, Epstein et al., 1980). This causes head congestion, headaches, facial edema, and stimulates a loss of water and electrolytes from all body water compartments through thirst depression and/or renal excretion.

While the measurement of many fluid shift responses in space has proven elusive, and inflight fluid shift data remain somewhat conflicting (Leach, 1987), some valuable measures of responses to weightlessness exist. Blood moves centrally within seconds upon exposure to weightlessness from the standing or sitting position, as measured by changes in the electrical impedance of the thorax during 20 seconds of weightlessness in parabolic flight (Mukai, 1991). In the first few days inflight there is an elevation of hemoglobin concentration (Kimzey, 1977) coincident with a weight loss primarily reflecting a negative water balance. Most of this loss occurs within the first three or four days (Thornton et al., 1987; Nicogossian and Parker, 1982; Thornton and Ord, 1977). Plasma volume decreases rapidly over hours and red cell mass decreases over weeks in space (Thornton et al., 1987; Nicogossian, 1985). These responses to fluid shifts are considered an adaptation to the central circulatory overdistention caused by fluid shifts in weightlessness (Nixon et al., 1979; Charles and Bungo, 1986; Leach, 1987). The final adapted state includes a reduced blood volume, with normal composition eventually regained (Nicogossian, 1985). However, recent results from the SLS-1 mission indicate that some body fluids do not simply decline to new equilibria but that they decrease rapidly to a low point and then begin some recovery (Leach et al., 1992). This "undershoot" of body fluid volumes has also been shown by our previous computer simulations to precede the final cardiovascular adaptation to fluid shifts (Simanonok et al., 1991, 1992).

The fact that fluid shifts probably begin before launch as astronauts wait in the semisupine position (Lathers, 1989) complicates the fluid shift picture, but the net effects on postflight fluid balance are probably not greatly different as a result of the pre-launch posture. Inflight measures of central venous pressure (Kirsch et al., 1984; Gaffney, 1992), suggest that central volume expansion in weightlessness may be very transient, or perhaps masked by physiologic responses to the pre-launch posture and acceleration to orbit. It is likely that several hours in the semisupine position allows time for the physiologic responses to fluid shifts to cause decreases in the astronauts' plasma volumes, actually beginning the long process of cardiovascular adaptation to weightlessness while on the ground.

Logically, if the central hypervolemia produced by a fluid shift could be reduced, then the physiologic responses resulting in fluid losses in weightlessness should also be reduced through a damping of the endocrine, neural, and hemodynamic mechanisms activated by fluid shifts. This concept has been experimentally validated in two water immersion experiments (Simanonok and Bernauer, in review; Simanonok, in review) and theoretically analyzed in computer simulation studies (Simanonok et al., 1991, 1992). Therefore, what may appear at first glance to be a counterintuitive countermeasure--reducing body fluid losses by removing body fluid beforehand--shows promise as a potential method to conserve body fluid volumes and return astronauts to earth in better condition that at present. Simulation results suggest that preadapting the circulation could help to conserve body fluid volumes for weightless exposures of 20 to 30 days duration (Simanonok et al., 1991, 1992).

The purpose of this study was to examine the mechanisms which could explain the loss of body fluids in weightlessness and how the preadaptation countermeasure could act to reduce the magnitude of body fluid losses. We hypothesized that factors other than central volume overdistention could be responsible for the loss of blood volume and other body fluid volumes observed in weightlessness and in weightless simulations. The assumption was made that the physiology of HDT provides a reasonably accurate analog of weightless exposure. This paper describes our progress to date in identifying the primary determinants or "drivers" of the physiologic adaptation of the human body to reduced fluid compartment volumes in weightlessness.

METHODS

A mathematical model derived from the Guyton Model of Fluid, Electrolyte, and Circulatory Regulation (Guyton et al., 1972) was used for this study. The model incorporates known relationships between physical, neural, and hormonal regulators of fluid balance and volume, pressure, and flow in the human circulation and body fluid compartments. It has been modified for weightless simulation by HDT by White (1974), with improvements by Leonard and Grounds (1977). It has been validated by comparison with data from both ground-based and flight experiments (Leonard et al., 1979, 1986).

We modified the model further as described previously (Simanonok et al., 1991) to enable long term simulation with eventual adaptation of the blood and other body fluid compartments to lower volumes during prolonged six-degree HDT. Also, provision was made to enable simulation of blood volume reduction by bleeding. With these modifications, the model was validated for its response to acute hemorrhage by comparing hematocrit changes with experimental hemorrhage data from human subjects (Simanonok, unpublished data).

The difference between the starting supine blood volume before HDT and the equilibrium blood volume after 70 days of HDT was taken as the volume to remove from circulation to preadapt the circulation to fluid shifts. Then another simulation of HDT was run after removal of the preadaptation volume, which was 534 ml, or about 11% of the starting blood volume.

RESULTS AND DISCUSSION

Data in the Figures are plotted on a logarithmic time scale so that all phases of the experiment out to 70 days may be distinguished. Each of the two experiments, head down tilt alone (HDT) or HDT preceded by blood volume reduction (BV REDUCTION + HDT, or PREADAPTED) began with a 30 minute period of baseline supine posture before the assumption of HDT. During the last 18 minutes of the 30 minutes of supine posture during BV REDUCTION + HDT, the

simulated subject was bled at a constant rate of 29.67 ml/min to preadapt the circulation to fluid shifts. This acute change in blood volume due to preadaptation is shown in Fig. 1; the naturally-adapting HDT blood volume falls below the PRE-ADAPTED blood volume after 10 hours and remains slightly less than the PREADAPTED blood volume until the two converge at about 70 days.

The rapid reduction of blood volume in HDT is due to an early decrease in the plasma volume (Fig. 2), which results from an increase in the urine flow (Fig. 3). The initially high urine flow results from increased renal blood flow, glomerular filtration, and appropriate endocrine responses (not shown).

Central vascular engorgement that is believed to occur due to fluid shifts in weightlessness is shown by atrial pressures (Fig. 4) and volumes (Fig. 5) increasing early in HDT, accounting for the increased stroke volume (Fig. 6) and cardiac output (Fig. 7). These expected early responses to fluid shifts show how hydraulic and endocrine factors rapidly act to elevate urine flow and deplete plasma volume. However, atrial volumes and pressures, stroke volume, and cardiac output are all decreased below baseline pre-HDT values within the first day of exposure to fluid shifts. This indicates a lack of a continuing central volume expansion driving the process of circulatory adaptation, and suggests involvement of another mechanism or mechanisms.

Fig. 1. Blood Volume

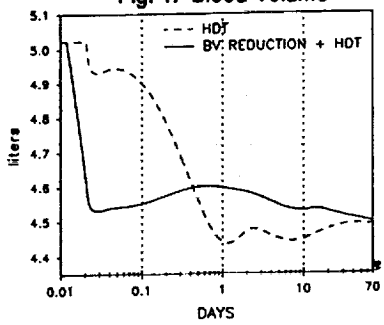

Fig. 2. Plasma Volume

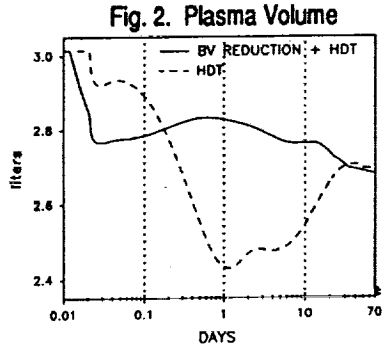

Fig. 3. Urine Flow

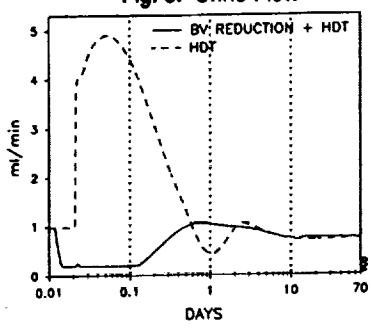

Fig. 4. Atrial Pressures

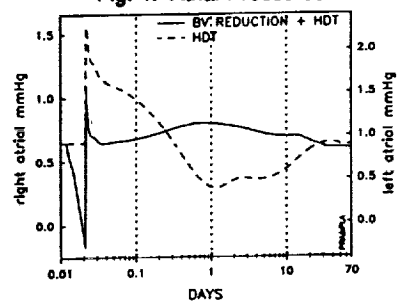

Fig. 5. Atrial Volumes

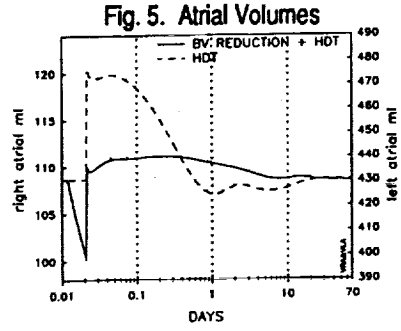

Fig. 6. Stroke Volume

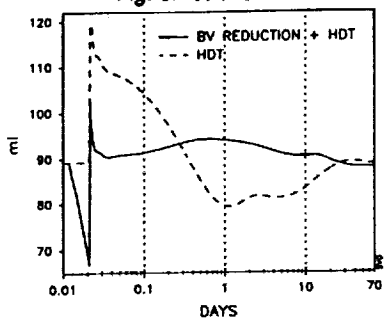

Fig. 7. Cardiac Output

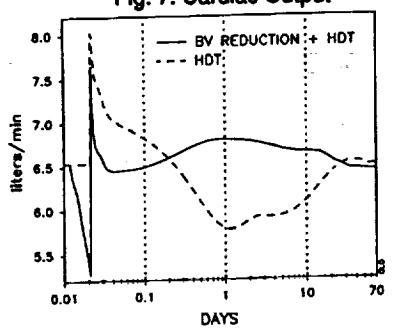

As the plasma volume is decreased by an elevated urine flow, cells and protein concentrate in blood because they are much more slowly eliminated than water and electrolytes. The plasma protein concentration is increased, elevating the plasma colloid osmotic pressure (Fig. 8). This would tend to shift the balance of Starling forces toward net reabsorption, which could explain some initial transfer of fluid from other compartments into circulation. However, the plasma protein concentration is rapidly regulated again at nearly baseline concentrations by Day 2 of HDT, therefore hemoconcentration of protein cannot be a primary driver for more prolonged losses of body fluids. Also, the interstitial colloid osmotic pressure (Fig. 9) rises by almost the same amount in the first two days, which would tend to offset fluid movement caused by an elevated plasma colloid osmotic pressure. In fact, the interstitial colloid osmotic pressure remains elevated for some time after the plasma colloid osmotic pressure returns to near baseline.

Fig. 8. Plasma Protein and Colloid Osmotic Pressure

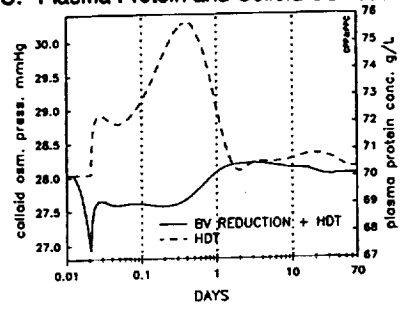

Hemoconcentration of red cells elevates the hematocrit and therefore the viscosity of blood (Fig. 10), which remain high until the red cell mass can be reduced (Fig. 11). An increased viscosity of blood increases the resistance to flow, thereby elevating the total peripheral resistance (Fig. 12). Because this is a precapillary resistance, the capillary pressure is decreased (Fig. 13) until the total peripheral resistance returns to baseline through a reduction of the red cell mass. The interstitial fluid pressure (Fig. 14) is not reduced by the same magnitude, so the net balance of Starling forces is shifted toward a reduced transcapillary pressure and flux (Fig. 15). This causes a depletion of the extracellular fluid volume. It is important to note that there is a large recovery from the "undershoot" of total extracellular fluid when adaptation is complete (Fig. 16).

Fig. 9. Intersitial Fluid Colloid Osmotic Pressure

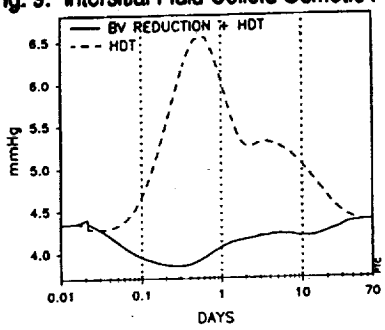

Fig 10. Hematocrit and Viscosity of Blood

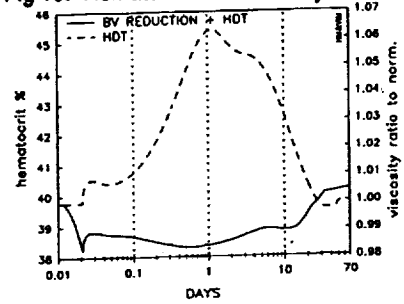

Fig. 11. Red Cell Mass

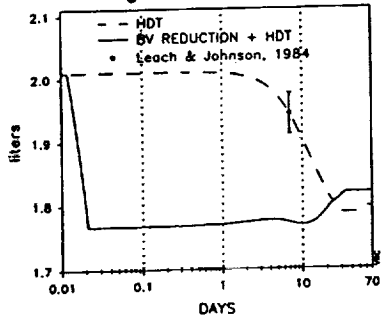

Fig. 12. Total Peripheral Resistance

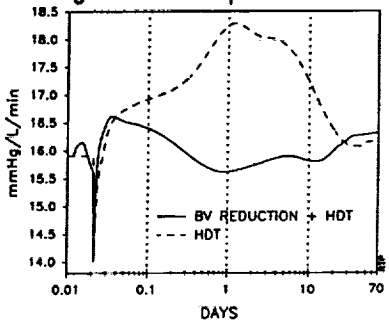

Fig. 13. Capillary Pressure

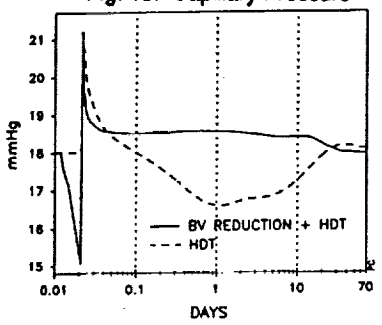

Fig. 14. Interstitial Fluid Pressure and Systemic Lymph Flow

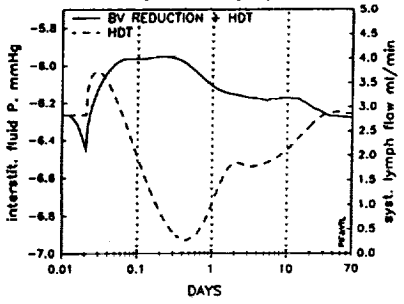

Fig. 15. Transcapillary Pressure and Flux

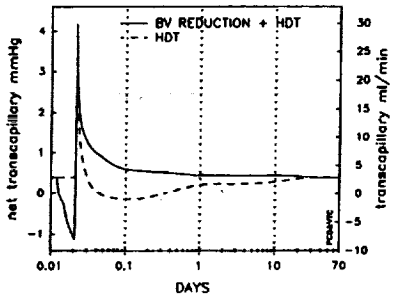

Fig. 16. Extracellular Fluid Volume

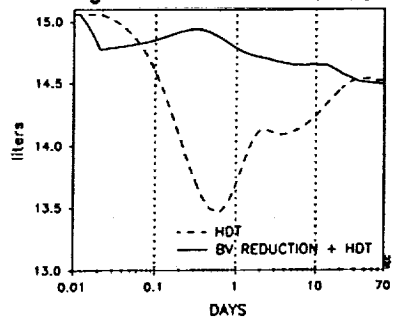

The results indicate how preadaptation of the circulation to a reduced blood volume appropriate for the weightless environment may be an effective countermeasure to much of the fluid losses observed in weightlessness. Simulation showed that pre-HDT reduction of the red cell mass prevents the hemoconcentration and increased blood viscosity that increases total peripheral resistance and shifts the balance of Starling forces toward net microcirculatory reabsorption. This prevents the large "undershoot" of extracellular fluid volume and the smaller "undershoot" of blood volume. However, the final equilibrium volumes are the same whether or not the circulation is preadapted. It therefore appears that the red cell mass drives the intervening "undershoot" of body fluid volumes but does not cause the resetting of the body fluid volumes at lower levels.

Experimental subjects will vary in their physiologic makeup and starting conditions, and consequently they will vary in their responses to fluid shifts. We do not yet have sufficient data to properly validate the entire time courses of the responses we have modeled, although the SLS-1 data do broadly suggest that there is an early drop in body fluid volumes with some later recovery that is also reflected by our Guyton model output. Our simulation began with subjects in a baseline supine position, rather than the upright ambulatory posture, and we did not model the effects of a prelaunch semisupine posture or the tendency of some astronauts to voluntarily dehydrate themselves before launch, as these vary greatly between individuals. Therefore the time course and absolute magnitudes of the changes in variables presented here should be regarded as qualitative rather than quantitative, pending further knowledge of physiologic responses to weightlessness that may be integrated into the model.

In conclusion, we used the modified Guyton model as an analytical tool to determine the primary determinants of the reduction of body fluid volumes in weightlessness. Results show that this process is initiated by a central volume shift that increases atrial volumes and pressures. The central volume expansion provokes a series of physiologic responses that cause a rapid return of central volumes and pressures to baseline through a reduction of the plasma volume. We conclude that the primary determinant or driver for an "undershoot" of body fluid volumes after the normalization of atrial volumes and pressures is the red cell mass.

REFERENCES

Charles JB, Bungo MW. Cardiovascular research in space: considerations for the design of the human research facility of the United States space station. Aviat. Space Environ. Med. 1986;57:1000-1005.

Epstein M, DeNunzio AG, Ramachandran M. Characterization of renal response to prolonged immersion in normal man. J. Appl. Physiol. 1980; 49:184-188.

Gaffney FA. Cardiovascular adaptation to 0-G: results from spacelab life sciences one (abstract) Aviat. Space Environ. Med. 1992;63:439.

Guyton AC, Coleman TG, Granger HJ. Circulation: overall regulation. Ann. Rev. Physiol. 1972; 34:13.

Kimzey SL. Hematology and immunology studies. In: Johnson RS, Dietlein LF (eds). Biomedical Results from Skylab. NASA SP-377, Sup. of Documents, Washington, D.C., 1977;249-282.

Kirsch KA, Röcker L, Gauer OH, Krause R. Venous pressure in man during weightlessness. Science 1984;225:218-219.

Lathers CM, Charles JB, Elton KF, Holt TA, Mukai C, Bennett BS, Bungo MW. Acute hemodynamic responses to weightlessness in humans. J. Clin. Pharmacol. 1989;29:615-627.

Leach CS. A review of the consequences of fluid and electrolyte shifts in weightlessness. Acta Astronaut. 1979;6:1123-1135.

Leach CS. Fluid control mechanisms in weightlessness. Aviat. Space Environ. Med. 1987;58:A74-79.

Leach CS, Alfrey C, Suki WN, Leonard JI, Rambaut PC. Fluid-electrolyte regulation during space flight. In: Nicogossian AE (ed). Spacelab Life Sciences-1 180 Day Preliminary Results. NASA Johnson Space Center, Houston, TX. 1992; pp 3.3.3-1 to 3.3.3-16.

Leach CS, Johnson PC. Influence of spaceflight on erythrokinetics in man. Science 1984; 225:216-218.

Leonard JI, Grounds DJ. Modification of the Long Term Circulatory Model for the Simulation of Bed Rest. NASA Contractor Report (NASA CR-160186), Washington, D.C., 1977.

Leonard JI, Rummel JA, Leach CS. Computer simulations of postural change, water immersion and bed rest: an integrated approach for understanding the spaceflight response. The Physiologist, 1979;22:S31-32.

Leonard JI, White RJ, Rummel JA. Math modelling as a complement to the scientific inquiry of physiological adaptation to space flight: fluid, endocrine and circulatory regulation. In: Hunt J. (ed). Proc. of 2nd Intl. Conf. on Space Physiology, Toulouse, France, 20-22 Nov. 1985, ESA publication no. SP-237, Paris, 1986;233-244.

Mukai CN, Lathers CM, Charles JB, Bennett BS, Igarashi M, Patel S. Acute hemodynamic responses to weightlessness during parabolic flight. J. Clin. Pharmacol. 1991;31:893-903.

Nicogossian AE. Biomedical challenges of spaceflight. In: Deltart RL (ed). Fundamentals of Aerospace Medicine. Lea & Febiger, Philadelphia, 1985;839-861.

Nicogossian AE, Parker JF Jr. Space Physiology and Medicine. NASA SP-447, Sup. of Documents, Washington D.C., 1982;186.

Nixon JV, Murray RG, Bryant C, Johnson RL Jr, Mitchell JH, Holland OB, Gomez-Sanchez C, Vergne-Marini P, Blomqvist CG. Early cardiovascular adaptation to simulated zero gravity. J. Appl. Physiol. 1979;46:541-548.

Simanonok KE. Effects of hypovolemia on the responses to water immersion in men. In review.

Simanonok KE, Bernauer EM. Blood volume reduction as a countermeasure to fluid shifts in water immersion. In press.

Simanonok KE, Srinivasan R, Charles JB. Computer simulation of preflight blood volume reduction as a countermeasure to fluid shifts in spaceflight. Proceedings of the Fifth Annual Space Operations, Applications, and Research Symposium (SOAR 91), Houston, Texas, July 9-11, 1992;605-608.

Simanonok KE, Srinivasan RS, Charles JB. Preadaptation of the circulation by removal of different blood volumes to counteract central fluid shifts. The Physiologist 1992;35:S111-S112.

Thornton WE, Moore TP, Pool SL. Fluid shifts in weightlessness. Aviat. Space Environ. Med. 1987;58:A86-90.

Thornton WE, Ord J. Physiological mass measurements in Skylab. In: Johnson RS, Dietlein LF (eds). Biomedical Results from Skylab. NASA SP-377, Sup. of Documents, Washington, D.C., 1977;175-182.

White RJ. A Long-term Model Of Circulation: Final Report. NASA Contractor Report (NASA CR-147674), Washington, D.C., 1974.

Session L5: RADIATION CONSIDERATIONS

Session Chair: G. D. Badwar

N94-11558

Potential Health Effects of Space Radiation

*Chui-hsu Yang and +Laurie M. Craise
*NASA Johnson Space Center, Houston, TX 77058
+Lawrence Berkeley Laboratory, Berkeley, CA 94720

ABSTRACT

Crewmembers on missions to the Moon or Mars will be exposed to radiation belts, galactic cosmic rays, and possibly solar particle event. The potential health hazards due to these space radiations must be considered carefully to ensure the success of space exploration. Because there is no human radioepidemiological data for acute and late effects of high-LET radiation, the biological risks of energetic charged particles have to be estimated from experimental results on animals and cultured cells. Experimental data obtained todate indicate that charged particle radiation can be much more effective than photons in causing chromosome aberrations, cell killing, mutation, and tumor induction. The relative biological effectiveness (RBE) varies with biological endpoints and depends on linear-energy-transfer (LET) of heavy ions. Most lesions induced by low-LET radiation can be repaired in mammalian cells. Energetic heavy ions, however, can produce large complex DNA damages, which may lead to large deletions and are irreparable. For high-LET radiation, therefore, there is less or no dose rate effects. Physical schielding may not be effective in minimizing the biological effects of energetic heavy ion, since fragments of the primary particles can be effective in causing biological effects. At present the uncertainty of biological effects of heavy particles is still very large. With further understanding of the biological effects of space radiation, the career doses can be kept at acceptable levels so that the space radiation environment need not be a barrier to the exploitation of the promise of space.

INTRODUCTION

With the success of short-duration space flights, the age for long-term exploration is coming. Along with the long-term space exploration come various potential health hazards due to unique physical factors of space environment. These health hazards must be considered carefully to ensure the success of space exploration. Among the physical factors, ionizing radiation in space is an important one. The risk to crew health from radiation exposure is a major issue of human space flight to the Moon and Mars. The crewmembers of a lunar or Mars mission will be unavoidably exposed to ionizing radiation as they travel through the inner trapped proton belt, the outer trapped electron belt, and through the galactic cosmic rays (GCR) of interplanetary space. In addition, outside of the Earth's magnetosphere, there is the possibility for exposure to charged particle radiation from Solar Particle Event (SPE). These space radiations are different from gamma rays and neutrons

in terms of energy absorption and ionization pattern. Although a significant amount of data on biological effects of gamma rays and neutrons have been obtained from atomic bomb survivors , there is no human radioepidemiological data on bioeffects of charged particle radiation. Therefore, very little biological effects of these space radiations in humans are known, and only limited data have been obtained from research studies with animals and cultured cell systems.

EXPERIMENTAL DATA

Extensive studies on biological effects of heavy ions done in the past decade show that charged particle radiation can be much more effective than gamma rays in causing DNA damage, chromosome aberrations, cell killing, mutation, and tumor (1, 2, 3, 4). The relationship between relative biological effectiveness (RBE) and linear energy transfer (LET) is not a simple one. In general, the RBE increases with LET up to about 100-200 keV/um and then decreases steadily to a value less than 1.0 at very high LET. The peak position of the RBE and LET relationship, however, can vary with different biological endpoints. For a given LET value, the RBE can be different for different effects.

Vaious biological, chemical, and physical factors can modify the biological responses to gamma rays (Table I). These factors, however, have much less effect on cells irradiated by heavy ions.

Table I. Radiation Responses and Modifiers

Modifier	X or Gamma Rays	High-LET Charged Particles
Dose Rate	effects reduced at low dose rate	effects enhanced or not changed at low dose rates
Cell Cycle	radiosensitivity highly dependent on cell stage	effects less depend on cell stage
Oxygen	radioresistant increases under hypoxic condition	radiosensitivity about the same under hypoxic condition
Radioprotectants	highly effective in reducing radiosensitivity	not very effective in reducing radiation effects
Repair Inhibitors	significantly increase radiosensitivity	not effective in increasing radiation responses

Oxygen concentration, for example, can change RBE value for survival, and extensive studies on oxygen enhancement (OER) have been reported (5). Under hypoxic condition, the RBE at 10% survival level for heavy ions with LETs greater than 100 keV/um can be as high as 5. This increase of RBE value under hypoxic condition is due to the decrease of OER, i.e., oxygen concentration has less effect on radiosensitivity to high-LET charged particles. The calculated cross section for inactivation under aerobic and hypoxic condition increases with an increase of LET and reaches a plateau value close to measured geometry area of cell nucleus.

For high-LET radiation, normal cells in general show higher RBE value than repair deficient cells, suggesting heavy ions effective in producing irreparable lethal lesions (6). The effect of cell cycle on radiosensitivity of cells was found to be demi-nished with an increase of LET (7), indicating that heavy ions are effective in producing sever DNA damages. Experiments to determine the repair of potential lethal and oncogenic lesions in confluent mouse embryonic cells also showed that the production of irreparable lethal and oncogenic damages was both LET and track structure dependent (8). An analysis of these experimental results indicated that in average more than one heavy particle passing through cell nucleus are needed to inactive a mammalian cell in culture. Chemical radiation protectants, which can reduce the effect of gamma rays in mammalian cells by several folds, were found to be much less useful for high-LET heavy ions.

Although a significant amount of information on biological effects of heavy ions has been obtained, many biological responses to charged particles remain to be determined. The acute effects on high dose protons on central nervous system, intestine, and bone marrow, for example, are not well known. In addition, most mutagenic and caricnogenic studies were done with cultured cell systems, and very few studies have been done with animals. Furthermore, some unique biological effects of heavy ions, such as microlesions, have been reported although not varified. A summary of experimental data available todate is shown in Table II.

INFORMATION NEEDED FOR REDUCING UNCERTAINTY

The uncertainty of biological data for radiation risk assessment is very large at present. The cause of such uncertainty comes in part from incomplete studies of various biological effects and in part from the limitation of radiation facilities. Most radiobiological studies with charged particles were done with single heavy ion beam at high dose rates, because the cost of using accelerators has been very expensive. In space, crewmembers will be exposed to trapped protons and GCR at very low dose rate. For radiation risk assessment, therefore, it is extremly important to determine the biological effects of charged particles at dose rates comparable to that in space and to study possible synergistic effects of mixed particle radiation.

Because there is no human radioepidemiological data for charged particle radiation, experimental results from research studies have to be extrapolated to

Table II. A Summary of Information on Biological Effects of X or Gamma Rays and Charged Particles.

Biological Endpoint	X or gamma rays	Charged particles
Acute Effects:		
1. Central nervous system	+	limited
2. Intestinal system	+	limited
3. Hemapoietic system	+	limited
Late Effects:		
1. Carcinogenesis		
A) In Vivo	+	limited (most from mouse Harderian gland tumor system)
B) In Vitro	+	+
2. Mutagenesis		
A) In Vivo	+	?
B) In Vitro	+	+
3. Embryogenesis	+	very limited
Unique Effects:		
1. Microlesions		
A) Cornea	-	+ (?)
B) Retina	-	+ (?)
2. Eye flash	+ (greying of visual field)	+ (star & streak)

humans for risk analysis. The extrapolation from animal and/or cellular results to humans is a very challenging problem. For example, there are significant difference in radiosensitivity between human fibroblasts and animal cells (10, 11). In addition, human fibroblasts and epithelial cells are much more difficult to be transformed by ionizing radiaiton, as compared to rodent cells. Multi-exposures are required to change the growth properties of normal human cells, and a single dose can be sufficient to cause neoplastic transformation of rodent cells in culture (12).

There is also tissue and organ specificity in carcinogenesis. All these differences will have to be considered when data from animal and/or cells are extrapolated to humans. One of the possible means to solve this difficult problem is to understand the mechanism(s) of radiation effects, through which biophysical models can be built and used to predict biological responses to charged particles.

Charged particles will be fragmented when they traverse through the body. The biological effects of fragmented heavy ion beams have been studied with only a few ions, and results indicated that an iron beam fragmented by 5- and 7-cm polyethylene can be as effective as the primary particles. More information on the effectiveness of fragmented charged particles in inducing various biological effects are needed for a better risk assessment.

Another source of uncertainty of radiobiological data is microgravity. At present, very little is known how does microgravity alter the radiation responses at cellular, tissue, and organ level. The disturbance of body fluids, hormones, and central nervous system by microgravity may have significant effects on radiation responses. Changes of hormone secretion in the body, for instance, may alter the progression of cancer induced by radiation. Research in this area will have to be performed before one can assess radiation risk with confidence.

CONCLUSION

For a long-term mission to the Moon or Mars, crewmembers will be exposed to charged particles in space. Experimental studies showed that high-LET heavy ions can be much more effective than gamma rays in causing various biological effects, including cell killing, mutation, and carcinogenesis. The relative biological effectiveness of heavy ions depends on LET and varies with different biological endpoints. Although a significant amount of information on biological effects of charged particles has been obtained, much more data on acute as well as late effects of heavy ions are needed for radiation protection. Studies on effects of low dose rate, mixed radiation, microgravity, and mechanisms are essential for reducing the uncertainty of radiobiological data. With further understanding of the biological effects of space radiation, the crewmembers can be better protected to ensure the success of space exploration.

ACKNOWLEDGMENTS

This work was supported by NASA (Contract No. T9297R). The technical assistance of the BEVALAC crews in providing heavy ion beams needed for research studies are gratefully acknowledged.

REFERENCES

1. Cox, R., Thacker, J., Goodhead, D. T., and Munson, R. J. "Mutation and inactivation of cultured mammalian cells by various ionizing radiations" Nature (London), 267:425-427 (1977)
2. Blakely, E., Tobias, C. A., Yang, T. C., Smith, K. C., and Lyman, J. T. "Inactivation of human kidney cells by high-energy monoenergetic heavy-ion beams" Radiat. Res., 80:122-160 (1979)
3. Fry, R. J. M., Powers-Risius, P., Alpen, E. L., and Ainsworth, E. J. "High-LET radiation carcinogenesis" Radiat. Res. 104:S-188-195 (1985)
4. Yang, T. C., Craise, L. M., Mei, M., and Tobias, C. A. "Neoplastic cell transforma tion by heavy charged particles" Radiat. Res., 104:S-177-S-187 (1985)
5. Todd, P. W. "Heavy-ion irradiation of cultured human cells" Radiat. Res. Suppl., 7:196-207 (1967)
6. Tobias, C. A., Blakely, E. A., Chang, P. Y., Lomel, L., and Roots, R. "Response of sensitive human ataxia and resistant T-1 cell lines to accelerated heavy ions" Br. J. Cancer, 49(Suppl. VI):175-185 (1984)
7. Blakely, E. A., Ngo, F. Q. H., Curtis, S. B., and Tobias, C. A. "Heavy ion radiobiology: cellular studies" Adv. Radiat. Biology, 11:295-389 (1984)
8. Yang, T. C., Craise, L. M., Mei, M., and Tobias, C. A. "Neoplastic cell transforma-tion by high-LET radiation: molecular mechanisms" Adv. Space Res. 9:131-140 (1989)
9. Yang, T. C., and Tobias, C. A. "Neoplastic cell transformation by energetic heavy ions and its modification with chemical agents" Adv. Space Res. 4:207-218 (1984)
10. Yang, T. C., Stampfer, M. R., and Smith, H. S. "Response of cultured normal human mammary epithelial cells to X-rays" Radiat. Res. 96:476-485 (1983)
11. Yang, T. C., Stampfer, M. R., and Tobias, C. A. "Radiation studies on sensitivity and repair of human mammary epithelial cells" Int. J. Radiat. Biology 56:605-609 (1989)
12. Yang, T. C., Craise, L. M., Prioleau, J. C., Stampfer, M. R., and Rhim, J. S. "Chromosomal changes in cultured human epithelial cells transformed by low- and high-LET radiation" Adv. Space Res. 12:127-136 (1992)

C-3

N94-11559

RADIATION CONSIDERATIONS FOR INTERPLANETARY MISSIONS

Gautam D. Badwar[1], Patrick M. O'Neill[2], and Francis A. Cucinotta[3]
NASA/Johnson Space Center
[1]Mail Code: SN3
[2]Mail Code: VG
2101 Nasa Road 1
Houston, TX 77058
[3]NASA/Langley Research Center
Mail Code - LaRCms 493
Hampton, VA 23665-5225

Galactic cosmic radiation poses a serious radiation hazard for long-duration missions. In designing lunar habitat or Mars transfer vehicle, the worst-case radiation exposure determines shielding thickness and, hence, the weight of spacecraft. Using the spherically symmetric diffusion theory of the solar modulation of GCR, Badwar and O'Neill used data on the differential energy spectra of hydrogen, helium, oxygen, and iron from 1954 to 1989 to show that the flux at 1 A.U. is determined by the diffusion parameter, K, which is a function of the time in the solar cycle. This analysis also showed that the solar minimum of 1976 to 1977 was the deepest minimum in the last 37 years. Using this theory, we have obtained the GCR spectra for all the nuclei and calculated the depth-dose as a function of aluminum shield thickness. Using the ICRP-26 definition of the quality factor, it is shown that the shielding required to stay below the LEO recommended annual limit of 50 cSv is 17.5 $(+8, -3)$ g/cm^2 of aluminum; if the limit is raised to 60 cSv, the required shielding is 9 $(5, -1.5)$ g/cm^2. We also discuss the issues and shielding needs for protection against solar particle events.

MEASUREMENTS OF TRAPPED PROTONS FROM RECENT SHUTTLE FLIGHTS

A. Konradi, G. D. Badwar, L. A. Braby, W. Atwell, and F. Cucinotta
NASA/Johnson Space Center
2101 Nasa Road 1
Houston, TX 77058

Abstract unavailable at time of publication.

N94-11560

LONGITUDINAL STUDY OF ASTRONAUT HEALTH: MORTALITY IN THE YEARS 1959-91

Leif E. Peterson
NASA/Johnson Space Center
Kelsey-Seybold Clinic, P.A.
Mail Code: TSC SD23
2101 Nasa Road 1
Houston, TX 77058

We conducted a historical cohort study of mortality among 195 astronauts who were exposed to space and medical sources of radiation between 1959 and 1991. Cumulative occupational and medical radiation exposures were obtained from the astronaut radiation exposure history data base. Causes of death were obtained from obligatory death certificates and autopsy reports that were on file in the medical records. A total of 18 deaths occurred during the 32-year follow-up period for which the all-cause standardized mortality ratio (SMR) was 142 (95% confidence interval 84 225). There was one cancer death in the buccal cavity and pharyngeal ICD-9 rubric whose occurrence was significantly beyond expectation. Mortality for coronary disease was 59% lower than expected (2 deaths; SMR=41; 95% confidence limit 5 147). The crude death rate for 10 occupationally related accidents was 400 deaths per 100,000 person-years, which is an order of magnitude greater than accidental death rates in mining industries. The SMR of 1027 for fatal accidents was significantly beyond expectation (14 deaths; 95% confidence limit 561 1723) and was similar to SMRs for accidents among aerial pesticide applicators. The 10-year cumulative risk of occupational fatalities based on the exponential, Weibull, Gompertz, and linear-exponential distributions was 10%. Mortality from motor vehicle accidents was slightly higher than expected but was not significant (1 death; SMR=145; 95% confidence limit 2 808). Radiation exposures from medical procedures accounted for a majority of cumulative dose when compared with space radiation exposures. The results of the study do not confirm the impression that astronauts are at increased risk of cancer, but this does not obviate the need for further study. Overall, it was found that astronauts are at a health disadvantage as a result of catastrophic accidents.

N94-11561

OPERATIONAL RADIOLOGICAL SUPPORT FOR THE U.S. MANNED SPACE PROGRAM

Michael J. Golightly[1], Alva C. Hardy[1], William Atwell[2], Mark D. Weyland[2], Dr. John Kern, Ph.D.[2], and Bernard L. Cash[3]
[1]NASA/Johnson Space Center
Mail Code: SN3
2101 Nasa Road 1
Houston, TX 77058
[2]Rockwell International, Space Systems Division
Rockwell International – Houston Operations
555 Gemini Ave.
Houston, TX 77058
[3]Lockheed Engineering and Science Company
P.O. Box 58561
Mail Code: C23C
Houston, TX 77058

Radiological support for the manned space program is provided by the Space Radiation Analysis Group at the NASA/Johnson Space Center. This support ensures crew safety through mission design analysis, real-time space environment monitoring, and crew exposure measurements. Preflight crew exposure calculations using mission design information ensure crew exposures will remain within established limits. During missions, space environment conditions are continuously monitored from within the Mission Control Center. In the event of a radiation environment enhancement, the impact to crew exposure is assessed and recommendations are provided to flight management.

Radiation dosimeters are placed throughout the spacecraft and provided to each crewmember. During a radiation contingency, the crew could be requested to provide dosimeter readings. This information would be used for projecting crew dose enhancement.

New instrumentation and computer technology are being developed to improve the support. Improved instruments include tissue equivalent proportional counter (TEPC)-based dosimeters and charged particle telescopes. Data from these instruments will be telemetered and will provide flight controllers with unprecedented information regarding the radiation environment in and around the spacecraft. New software is being acquired and developed to provide "smart" space environment data displays for use by flight controllers.

SECTION V

SPACE MAINTENANCE AND SERVICING

Session S1: SPACE MAINTENANCE

Session Chair: Scott Smith

SPACE STATION FREEDOM MAINTENANCE

James E. Van Laak
NASA/Johnson Space Center
Mail Code: DE111
2101 Nasa Road 1
Houston, TX 77058

Abstract unavailable at time of publication.

N94-11562

DEVELOPMENT AND EVALUATION OF A PREDICTIVE ALGORITHM FOR TELEROBOTIC TASK COMPLEXITY

M. L. Gernhardt

R. C. Hunter

J. C. Hedgecock

A. G. Stephenson

Oceaneering Space Systems
16920 Texas Ave, Suite C-7
Webster, Texas 77598

ABSTRACT

There is a wide range of complexity in the various telerobotic servicing tasks performed in subsea, space and hazardous material handling environments. Experience with telerobotic servicing has evolved into a knowledge base used to design tasks to be "telerobot friendly." This knowledge base generally resides in a small group of people. Written documentation and requirements are limited in conveying this knowledge base to serviceable equipment designers and is subject to misinterpretation. A mathematical model of task complexity based on measurable task parameters and telerobot performance characteristics would be a valuable tool to designers and operational planners. Oceaneering Space Systems and TRW have performed an independent research and development project to develop such a tool for telerobotic orbital replacement unit (ORU) exchange. This algorithm was developed to predict an ORU exchange degree of difficulty rating (based on the Cooper-Harper rating used to assess piloted operations). It is based on measurable parameters of the ORU, attachment receptacle and quantifiable telerobotic performance characteristics (eg. link length, joint ranges, positional accuracy, tool lengths, number of cameras and locations). The resulting algorithm can be used to predict task complexity as the ORU parameters, receptacle parameters and telerobotic characteristics are varied.

INTRODUCTION

The purpose of the study described here is to identify critical aspects of orbital replacement unit (ORU) changeout operations and to develop an algorithm that can predict the complexity of a teleoperated task based on the physical characteristics of the ORU, its receptacle, and quantifiable parameters of a given robot. The hypothesis was that we could develop an algorithm that predicts a task complexity rating similar to the Cooper-Harper rating used by pilots to characterize aircraft flight operations. We first developed a mathematical model of task complexity based on a combination of ORU and ORU receptacle geometries, robot kinematics, and the number, coordinates and characteristics of video cameras used for the operation. The mathematical model is expressed as the product of second order polynomial equations. The coefficients for the equations were derived by a fit to results of over 1000 different laboratory tests in which the parameters in the mathematical model were systematically varied and the resulting operator determined task complexity ratings (TCRs) recorded. The resulting algorithm is calibrated from laboratory results and can predict TCRs based on measurable parameters of the "worksite" and "work system" which accounts for the design of the ORU, its receptacle and the robot.

The resulting algorithm was tested by bringing in a new group of test subjects and comparing their TCRs to the TCRs predicted by the algorithm. These verification test results showed a significant correlation between the predicted and observed TCRs (> 95% confidence).

Once the algorithm is calibrated for a given robot system it can be used by system planners, without further testing, to:

1) Aid in improving/simplifying ORU design
2) Minimize task complexity/improve task planning
3) Identify design driving and critical verification/validation tasks
4) Optimize camera placement
5) Evaluate impacts of failed cameras, lights and manipulator joints
6) Assess improvements in robot design (link lengths, joint ranges) for a range of ORU exchange tasks
7) Aid in operator training

Alternatively, given a fixed worksite design, this methodology can be used to define the minimal/simplest robot to adequately perform the given operation. An example of this is defining requirements for a special purpose robot such as a materials processing facility robot where the worksite has been defined.

This paper presents the development approach and some evaluations of a predictive algorithm for ORU exchange. This methodology, although developed for ORU's, could be applied to a wide range of telerobotic applications beyond ORU exchange (e.g. robotic worksite set up). It's application, we believe, will significantly reduce design, test and rework time for telerobotic serviced hardware.

SCOPE AND LIMITATIONS

The development of the algorithm was based on a comprehensive set of tests limited by the hardware and laboratory set-up used (Figure 1). Four limitations were:

1. Testing and algorithm development considered only linear insertion of a box type ORU (i.e. no threading operations,]-slots, etc). Thirteen ORU configurations were used for the tests (Figure 2).

2. Testing was performed in a 1-g laboratory environment with controlled temperature, humidity and lighting.

3. Testing was performed with Oceaneering Space System's G.E. robot arm controlled by a spatially correspondent force reflecting master arm.

4. To maximize applicability of the algorithm and verification testing, parameters were normalized where possible.

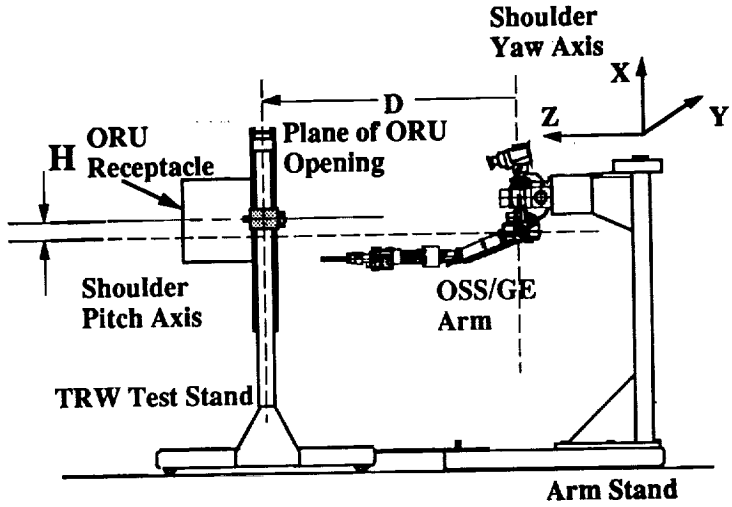

Figure 1. Test Stand and Manipulator Setup

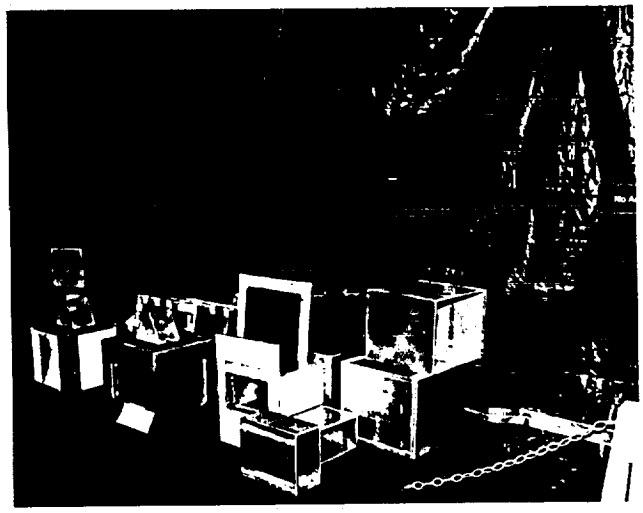

Figure 2. ORU and Receptacle Workpieces

The theoretical framework, depicted in Figure 3, suggests that the motion and information requirements of the needed task, to be successful, must intersect with the work system's (robot/tools) ability to provide motion and information.

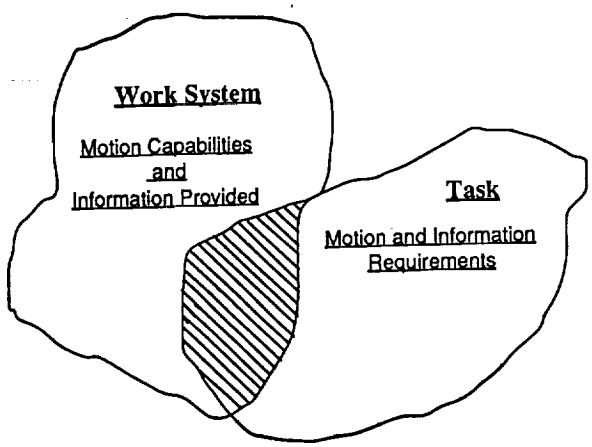

Figure 3. Theoretical Framework

TASK COMPLEXITY RATING SCALE

To describe or evaluate a task's complexity, a rating system is required. Utilizing existing research on task complexity for aircraft characteristics, the Cooper-Harper rating scale was adapted. It is assumed that task complexity of an ORU exchange can be described by the Cooper-Harper aircraft rating scale. The Cooper-Harper scale is a subjective scale used by test pilots and aircraft manufacturers to describe and evaluate the individual characteristics of a test aircraft. It is a 1-10 scale in which a 1 denotes an "excellent, highly desirable" design and a 10 denotes a design that has "major deficiencies" and requires "mandatory improvement". The rating is defined by a series of questions in the form of a decision tree. By answering each question, a pilot is driven to a rating.

To extend the Cooper-Harper rating scale to telerobotic task complexity, modifications were required in the description of the various ratings. Every attempt was made to preserve the integrity of the original decision tree, and it is assumed that the resulting TCR decision tree, (Figure 4), is consistent with the Cooper-Harper scale. The key to the success of this scale in aviation is the understanding of its use by test pilots; this understanding is the result of extensive training both as test pilots and in the use of the scale. The result of this training and familiarity is that each rating means virtually the same thing to every pilot, and that most pilots will assign the same rating to any given aircraft. The same is true for the TCR scale.

Before collecting data for calibrating the predictive algorithm a series of tests were performed to quantify the operator learning curve and develop a consistent interpretation of the TCR scale across test subjects. Test subjects were selected to be representative of SSF telerobotic operators (i.e. engineers with telerobotic operations/test experience but not full time professional

Test subjects were selected to be representative of SSF telerobotic operators (i.e. engineers with telerobotic operations/test experience but not full time professional telerobotic operators). Test subjects performed a representative series of baseline tasks 5 times with completion times recorded (Figure 5). In general, completion times leveled off after the second attempt and we concluded that the operators have an accurate gage of the TCR after the third attempt. Algorithm calibration data was, therefore, recorded after the third attempt.

Initial testing resulted in TCRs with similar trends, but wide numerical variances across the test subjects. Meetings were held to discuss individual interpretations of the TCR scale. Common definitions and interpretations resulted. We then defined a set of reference tasks across the TCR scale. The test subjects used to evaluate the derived algorithm were first "calibrated" by performing the reference tasks prior to performing algorithm calibration test runs.

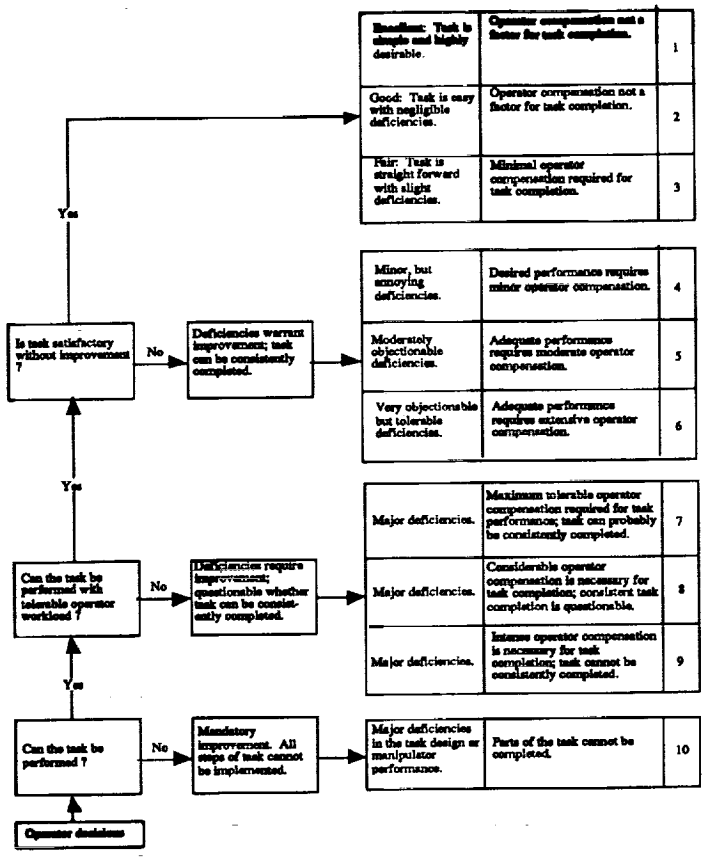

Figure 4. Task Complexity Rating Scale (Modified from the Cooper-Harper Rating Scale)

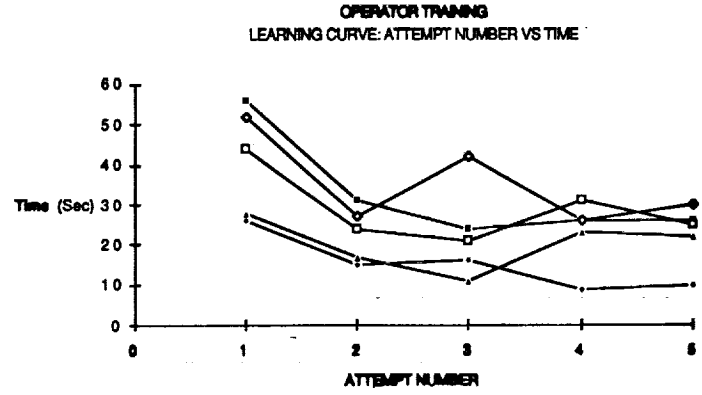

Figure 5. Operator Training Learning Curve

THEORETICAL MODEL OF TASK COMPLEXITY

Oceaneering subsea operations and robot compatible design experience suggest that task complexity is primarily a function of:

- Physical accessibility
- Visual accessibility
- Manipulation requirements
- Human/machine interfaces

These areas were divided into specific variables for individual testing and analysis. The specific variables for each area are described below:

- The physical access aspect of task complexity is influenced and defined by:
  - The gap between the ORU box and the ORU receptacle.
  - The effective interface angle between the box and the receptacle.
  - The ORU box length to gap ratio.
  - The ORU box depth to gap ratio.
  - The access region of the ORU. This is defined as the vertical or horizontal distance from the worksite insertion axis within which the manipulator wrist joint must be to insert the ORU into the receptacle.
- The visual access aspect of task complexity can be quantified by:
  - determining the task requirements in degrees of freedom (DOF) of manipulator motion
  - comparing the task DOF requirements to the manipulator, ORU, receptacle and motion information provided by the available camera views.
- The manipulation requirements can be modeled by comparing task spatial kinematics (6-DOF) to the manipulator kinematics at specific task positions and orientations. This required solving the inverse kinematic equations of motion for the manipulator.
- The man/machine interfaces include monitors and monitor placement, manipulator controls (hand controllers), and camera controls.

The relative importance of each of these areas may vary for different tasks (e.g. inserting and turning a bolt vs linear insertion of an ORU box.) A mathematical model was developed to address the first three items and each of these are discussed below. The human/machine interfaces were qualitatively accessed in an adjunctive series of tests. These interfaces tend to be independent of the ORU/robot interface and thus are not relevant to ORU designers and operational planners (the primary users of the algorithm).

The three areas described above combine to define the overall physical aspect of task complexity. In general, an insertion envelope for the ORU can be defined that must be met by the manipulator and must be visible to the cameras. The cameras must provide information to the operator that relates to the six degrees of freedom of motion available from the manipulator. The operator must control the degrees of freedom such that ORU insertion is possible. To control these degrees of freedom, specific views must be available to the operator that show the critical joint and ORU orientations and motions. The test program was defined to determine these critical views, orientations, and motions. Figure 6 illustrates the relationships described above.

Physical Accessibility - Accessibility Constraint Parameter (ACP)

The box length to gap and depth to gap ratios directly impact the amount of roll, pitch, and yaw misalignment that can be accommodated. For a given box-type ORU and receptacle, four different ratios exist. These ratios are listed below. The dimensions for the gap ratios are labeled in Figure 6. The figure also shows what is meant by the various misalignment tolerances.

Length/Gap Contribution to Roll Tolerance

- H_b/G_x (box height to gap per side in width direction)
- W_b/G_y (box width to gap per side in height direction)

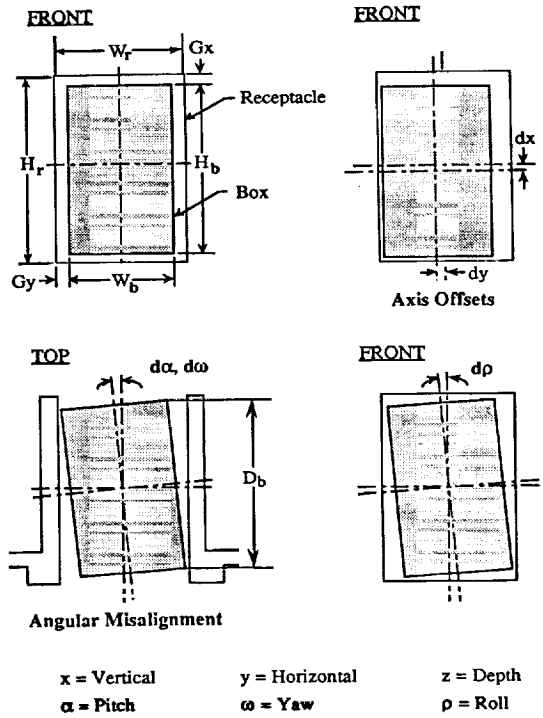

Figure 6. Illustration of Misalignment Tolerances and Gap Ratios

Where:

W_r = Width of Receptacle
W_b = Width of Box (ORU)
H_r = Height of Receptacle
H_b = Height of Box (ORU)
D_b = Depth of Box (ORU)

Depth/Gap Contribution to Pitch and Yaw Tolerance

- L_b/G_x (box depth to gap per side in width direction)
- L_b/G_y (box depth to gap per side in height direction)

For a given depth/gap ratio and given angular misalignments, the larger of the two length/gap ratios determines the amount of roll misalignment (rotational misalignment) that can be accommodated. For given length/gap ratios and a given rotational misalignment, the two depth/gap ratios determine the amount of pitch and yaw misalignment (angular misalignment) that can be accommodated. Figure 7 provides an illustration of the misalignments. The functional relationship for the misalignments are:

Capture*:

$$\theta_{pc} = f\ (H_r, H_b)$$
$$\theta_{yc} = f\ (W_r, W_b)$$

Insertion*:

$$\theta_{pi} = f\ (H_r, H_b, L_b)$$
$$\theta_{yi} = f\ (W_r, W_b, L_b)$$

* actual equations are proprietary

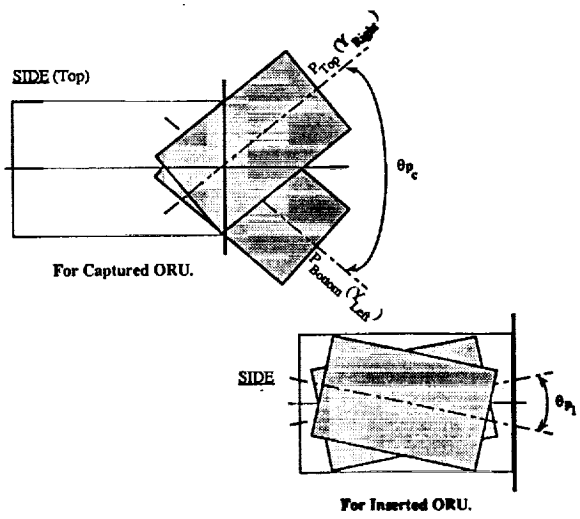

Figure 7. Physical Accessibility Angles

These angular misalignments can be used to establish a boundary into which the wrist of the manipulator must be positioned to ensure the ORU can be inserted. This boundary is referred to as the Wrist Positioned Accuracy (WPA).

Two such accuracies can be defined, which correspond to the horizontal and vertical limitations for a captured ORU. The horizontal limitation is indicated by the yaw wrist positioned accuracy and the vertical limitation is indicated by the pitch wrist positioned accuracy. An illustration of the top wrist positioned accuracy is provided in Figure 8. The functional relationship for the WPA is:

$$WPA_{pc} = f\ (L_b, \text{end-effector length}, \theta_{pc}, H_b)$$

These two wrist positioned accuracies were used to develop a third parameter, the accessibility constraint parameter (ACP). The ACP indicates the task complexity of inserting the ORU assuming that the receptacle is in an optimal position within the manipulator work space and that optimal camera views are provided. The functional relationship for the ACP is provided below:

$$ACP = f\ [(WPA_{pc}, WPA_{yc})^{-1}]$$

Where,

WPA_{pc} = pitch wrist positional accuracy for capture

WPA_{yc} = yaw wrist positional accuracy for capture

As indicated, the ACP is function of the inverses of the wrist positioned accuracies. Therefore, as the accuracies decrease the ACP and consequently, the task complexity increases.

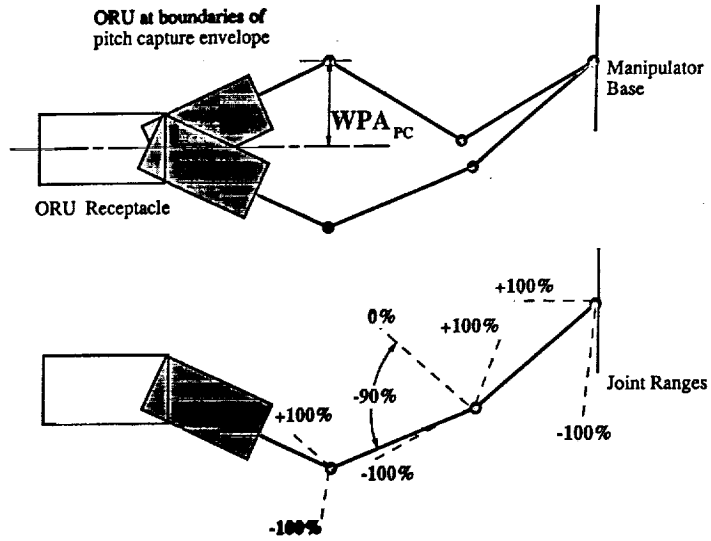

Figure 8. Pitch Wrist Positional Accuracy

Another physical parameter (that will effect the task complexity) is the lead-in geometry the ORU encounters as it enters the ORU receptacle. Given some misalignment of the ORU, the ORU will either;

- Not be captured by the lead-in
- Be captured by the lead-in but cannot be inserted because of geometric non-conformity
- Be captured by the lead-in and inserted through alignment adjustments made by the operator
- Be inserted with negligible effort from the operator because the clearance between the receptacle and ORU is such that the installation process can be completed without use of the lead-in.

The two lead-in parameters that must be considered are the effective contact angle between the ORU and the receptacle and the increase in capture area created by the lead-ins. The operator must work against the effective interface angle during a linear insertion of the ORU. The operator will have a more difficult time inserting the ORU if the interface angle is small. For small interface angles, friction forces between the ORU and the lead-in will be greater. These greater forces make sliding the ORU along the lead-ins more difficult and thus increases task complexity. However, for a given lead-in width (or thickness) a more shallow lead-in angle will also result in a larger capture area and should therefore make the task easier. This suggests that an optimal angle and lead-in width exists. As of this time, the specific impact of the lead-in angle on task complexity has not been included in the algorithm. Tests have indicated that adding a lead-in angle decreases task complexity and that steeper angles are more beneficial than shallow angles.

While the use of a lead-in profile increases the capture area of the ORU, a reduction in the manipulator resolution has the reverse effect. That is, if the manipulator cannot position an ORU within a certain positional accuracy, there will be a reduced chance of capturing the ORU within the ORU receptacle guide. The manipulator resolution is not a single value but an infinite set of values that depend on the position of the manipulator. The manipulator's sensitivity to variations in joint accuracy is a kinematic function of each joint angle, each link length, and the ordering of the joints. Therefore, in some regions of the work envelop slight changes in joint position will produce a greater variance in end-effector position in some directions than in others. The joint resolution is a critical parameter to consider for an unconstrained control mode. For a constrained motion mode, the joint resolution is much less important.

Manipulation Requirements - Kinematic Constraint Parameter (KCP)

The orientation and position of the ORU receptacle within the manipulator's work envelope are major physical constraints to the operator and were examined by studying kinematic limitations. The first kinematic limitation is performed by comparing the manipulator capability to position the wrist joint in the access envelope provided by the ORU and receptacle geometry. If limitations are imposed by the manipulator, then the WPA parameter is adjusted accordingly. The second kinematic limitation is on how much of all the joints are utilizing their joint space. Hence as joint space is used up, the ability to position the manipulator becomes more difficult. For example, an insertion task that involved moving one joint 5 degrees should be easier than a complex manipulation that utilized 100% of the available joint space.

The kinematic constraint parameter is determined by defining the coordinates of the extremes of the capture and insertion envelop relative to a reference data point (i.e. base of robot). An inverse kinematic calculation is performed to calculate the sum of the percent joint space (JS) utilized for each degree of freedom.

$$KCP = f(\%\ JS\ (pitch),\ \%\ JS\ (yaw))$$

Integrating Physical Accessibility and Manipulator Requirements

The combined accessibility/kinematic constrained relationship (AKCR) is expressed simply as a product of the two parameters previously defined when each is expressed as a second order polynomial.

$$AKCR = f\ (ACP, KCP)$$

The coefficients of the ACP and KCP second order polynomials were derived to match the TCRs from the tests to the mathematical model.

Visual Accessibility

The work system's visual equipment determines the amount of information available to the operator. The operator uses this information to determine the ORU position and orientation with respect to the receptacle as well as the orientation of the work system (robot) to the worksite (ORU receptacle). If the visual information is constrained by a lack in either quality or quantity, the task could be very complex and may be impossible to complete.

The system's visual constraints are determined by two parameters; the first parameter is the number and position of cameras, and the second parameter is the lighting condition. The number and position of cameras determines what visual information is presented to the operator. Increasing the amount of visual information was expected, initially, to decrease the task complexity. Visual information is generally increased by increasing the number of cameras focused on the worksite. However, the amount of visual information additional cameras provide may be small if they are placed in improper locations. There is also a point of diminishing returns where the operator cannot effectively process the information provided by each camera because of information overload. In the worst case, additional information can cause operator confusion.

Lighting conditions are also a visual constraint. The lighting conditions influence the value of the information received from each camera view. If the lighting conditions are poor the individual camera views may become useless. Two factors which effect the lighting conditions are the position of the lights and the light intensity. The lighting positions and the worksite configuration determine what areas of the worksite are illuminated and what areas are obscured by shadows. A camera view obscured by shadows may loose some or all of its effectiveness; this could increase the task complexity. On the other hand, shadows may help the operator estimate distances and orientations and could decrease task complexity. Testing indicated that very low light levels (30 lux) are tolerable but the time period required for ocular adjustment is extensive. Figure 9 is a time-lapsed photo taken during the test program. Hence lighting conditions are a time dependent variable and not well suited for inclusion into the algorithm. Lighting in the control room had a big impact on the ease of seeing the monitor display (i.e. no lights were the best for seeing the monitor but made it difficult to locate controls and maneuver within the workstation. Another factor on-orbit will be the relatively rapid movement/changing sun angles with time (90 min./orbit). Because of these complex issues, the lighting effects were not included in the algorithm.

The visual accessibility factors (VAFs) are determined by derived visual coefficients that define the relative importance of visual information in each degree of freedom based on ORU and receptacle geometries. Figure 10 defines coordinates for camera position relative to the worksite (ORU receptacle). Based on this coordinate system the relative importance of camera position as a function of movement of the ORU in a given plane was assessed and verified accordingly. For example, if the task has a low tolerance in pitch then the coefficient (C_ψ) for pitch is large. Consequently, the algorithm then gives considerable weight (importance) for a camera view that provides pitch information. Figure 11 illustrates this point. For pitch information the optimum camera placement is $\psi = 90°$, $\theta = 0°$. Other camera placements do not provide as much information on the pitch orientation of the ORU relative to the receptacle. For example, the $\psi = 0°$, $\theta = 0°$ position provides significantly less information than the optimal position provides.

Figure 9. Time-lapsed Photo of ORU Insertion in Test Fixture

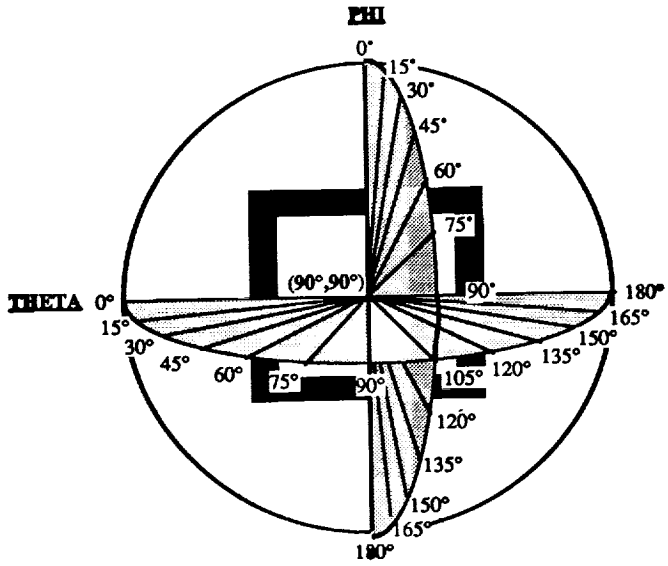

Figure 10. Camera Spherical Coordinate System

Visual diagrams, expressed in radians (e.g. Figure 12) are used to determine the visual information available from each motion direction. Surface representations in each motion direction (degree of freedom) were derived based on fundamental elements for task completion. For example, almost all of the test subjects used either edge or point information of the hardware (ORU and/or receptacle) to insert the ORU. By modeling the quality of edge and point information with respect to the camera positional angles, phi and theta, visual information was quantified. For example, a value of 1 on the surface indicates that the given camera position provides complete information about that DOF and that additional camera

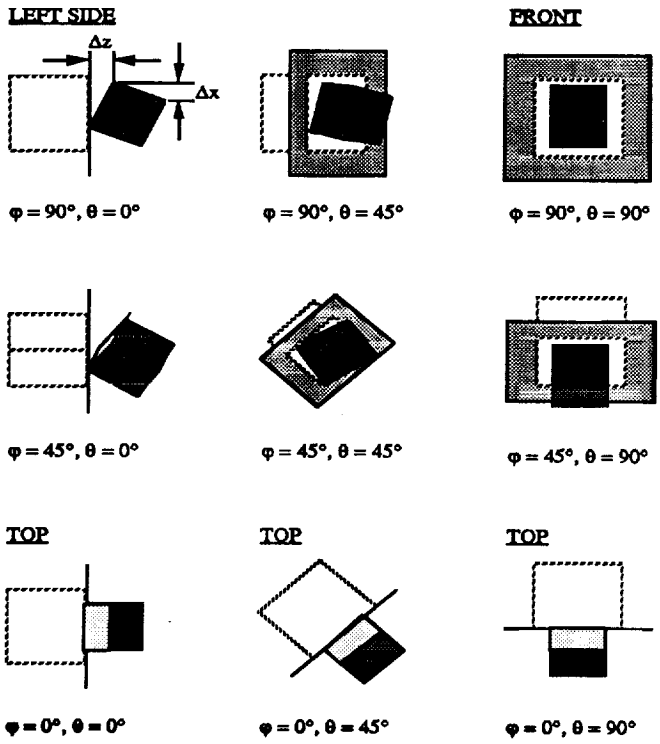

Figure 11. Pitch Visual Information as a Function of Worksite Orientation

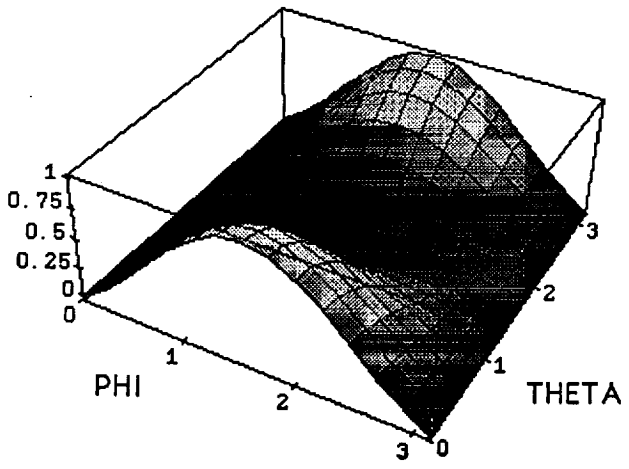

Figure 12. Surface Representation of Pitch Visual Information

views will not help. Other factors, such as the camera field of views and the video image size of vital visual information are also considered in the algorithm and modify the VAF as needed.

Final Task Complexity Algorithm

The final task complexity rating (TCR) algorithm is the product of the accessibility/kinematic constrained relationship (AKCR) and the visual accessibility factor (VAF).

$$TCR = f\,(AKCR * VAF)$$

To solve for the TCR, the algorithm iterates to determine if the task is possible, to calculate the insertion envelope, to determine if the manipulator constrains the insertion envelope and then applies visual impacts in six degrees of freedom.

ALGORITHM CALIBRATION AND VERIFICATION TESTING

Over 1000 tests were performed in the laboratory using a test fixture that allowed the worksite ORU receptacle orientation relative to the robot to be varied and 13 different ORU configurations to be used. The following parameters were varied, first separately and then in controlled groups, to determine individual and coupled effects on task complexity.

- Gaps: from 0.03" to 0.75"
- Width to Gap Ratios: from 7 to 119
- Depth to Gap Ratios: from 24 to 128
- Various Box Aspect Ratios and Sizes:
- Aspect Ratios from .57 to .83 H/W, .26 to 1.36 D/W
- Sizes from 3" to 14.75"
- Lead-In Angles: from 0° to 45°
- Work system to Worksite Variations: over 20 relative positions and orientations
- Number of Cameras: from 1 to 3 cameras
- Placement of Cameras: over 15 camera positions.

The results of these numerous tests were used to curve fit the predictive mathematical models previously developed. An interactive spreadsheet was then developed which calculates the predicted task complexity based upon user supplied worksite and work system parameters. A print out of this spreadsheet is provided in Figure 13. (in the case of Figure 13 the TCR is 6.82).

The integrated task complexity algorithm (mathematical model with coefficients fitted from test data) was evaluated by:

1) Designing a series of tests across the TCR scale on the predictions of the algorithm.

2) Comparing the predicted TCRs to the observed mean values from eight test subjects.

The verification test subjects were new, i.e. did not participate in the algorithm calibration testing. These subjects were trained on the TCR scale and reference tasks prior to performing the verification tests. The verification test results showed a significant correlation between predicted and observed TCR ($P \leq 0.05$) as illustrated in Figure 14.

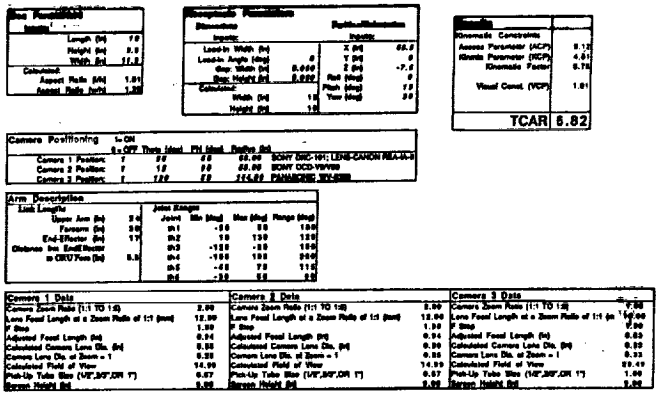

Figure 13. Interactive Input Data

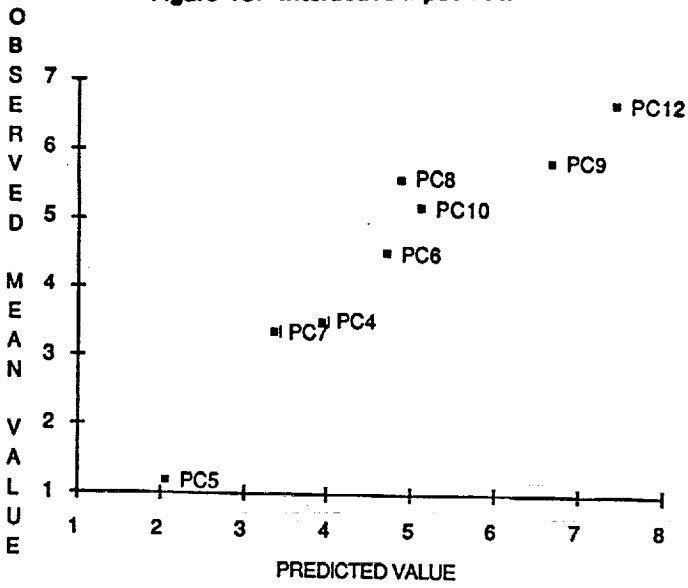

Figure 14. Verification Test Results

APPLICATIONS

We believe the TCR can be used to:

- Improve robot compatible ORU design by reducing weight and hardware complexity
- Minimize task complexity
- Identify design driving and critical verification/validation tasks
- Optimize camara placements and characteristics
- Evaluate impacts of failed cameras, and manipulator joints on complexity of specific tasks
- Optimize robot design (link lengths, joint ranges, camera placements and characteristics) based on a given range of tasks
- Aid in operator training (e.g. set up tasks that vary from low to high TCRs).

Some examples of applications are illustrated in Figure 15 - 17.

Figure 15 illustrates the insensitivity to gap width between an ORU and its receptacle. The gap for the coarse alignment could be reduced to 0.5 inches form 1.2 inches without impacting the TCR.

Figure 16 illustrates that a failed head camera for the same case as shown in Figure 15 does not impact the TCR. The other two camera views in the test were sufficient to perform the task with no more difficulty than when the head camera was operational. This type of knowledge can be very useful to an operational planner in real time when operations are underway.

Figure 17 illustrates the need to keep end effector/tool length under 22 inches to avoid impacting task complexity in this scenario.

On Space Station Freedom, the algorithm, calibrated for the Special Purpose Dexterous Manipulator (SPDM) could be used to minimize the complexity of tasks as they evolve during the operational phase and thus, minimize telerobot operations timelines. In the near-term it could help assess/verify projected task timelines.

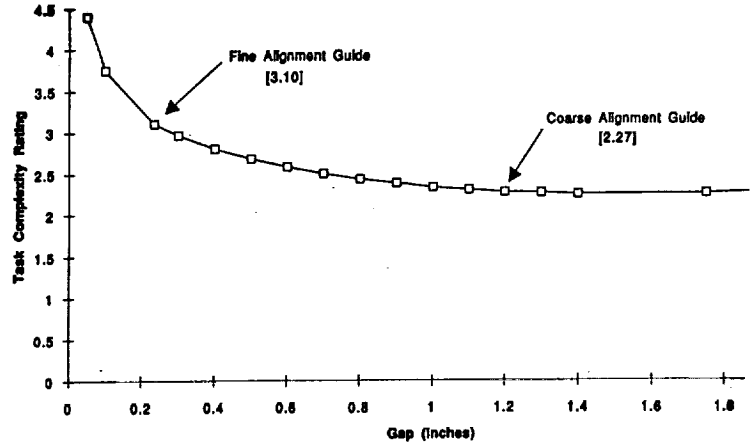

Figure 15. Gap vs Task Complexity (Nominal Camera Views)

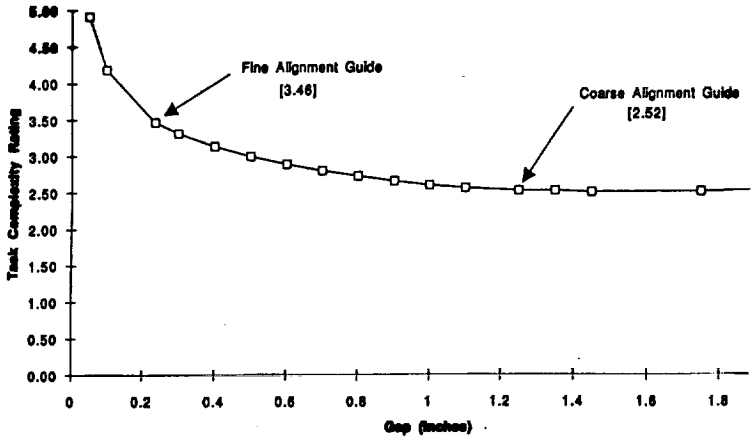

Figure 16. Gap vs. Task Complexity (Failed Head Camera)

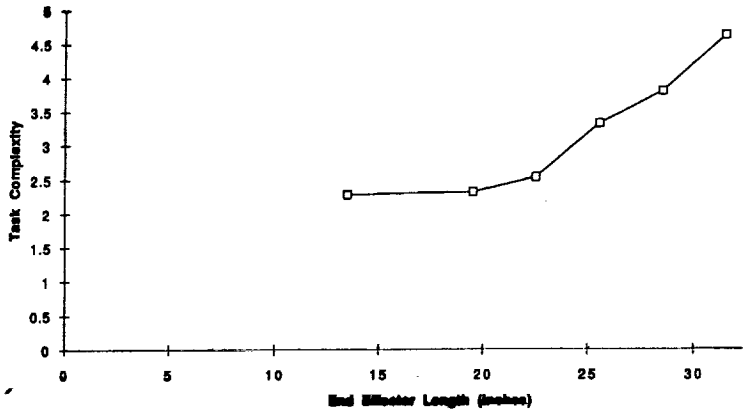

Figure 17. End Effector Length vs. Task Complexity

CONCLUSIONS

A task complexity algorithm has been developed and verified which allows serviceable hardware designers and system operators to predict telerobotic task complexity based on measurable robot and task parameters. Task or robot parameters can be varied to determine their impact on task complexity. The applications of this algorithm are far-reaching including determination of whether or not a task can be reasonably accomplished with failed system components (e.g. cameras, robot joints). As new maintenance tasks evolve on Space Station Freedom, for example, this algorithm, calibrated for the Special Purpose Dexterous Manipulator (SPDM), could be used to predict the Task Complexity and help designers/operators develop ways to minimize complexity and telerobot operations timelines.

ACKNOWLEDGEMENTS

Oceaneering Space Systems (OSS) gratefully acknowledges its partnership with TRW Space and Technology Group. TRW shared with OSS in conceptualizing and funding the development of the task complexity algorithm.

N94-11563

DESIGN FOR TESTABILITY AND DIAGNOSIS AT THE SYSTEM-LEVEL

by

William R. Simpson
John W. Sheppard

ARINC Research Corporation
2551 Riva Road
Annapolis, MD 21401

ABSTRACT

The growing complexity of full-scale systems has surpassed the capabilities of most simulation software to provide detailed models or gate-level failure analyses. The process of system-level diagnosis approaches the fault-isolation problem in a manner that differs significantly from the traditional and exhaustive failure mode search. System-level diagnosis is based on a functional representation of the system. For example, one can exercise one portion of a radar algorithm (the Fast Fourier Transform [FFT] function) by injecting several standard input patterns and comparing the results to standardized output results. An anomalous output would point to one of several items (including the FFT circuit) without specifying the gate or failure mode. For system-level repair, identifying an anomalous chip is sufficient.

We describe here an information theoretic and dependency modeling approach that discards much of the detailed physical knowledge about the system and analyzes its information flow and functional interrelationships. The approach relies on group and flow associations and, as such, is hierarchical. Its hierarchical nature allows the approach to be applicable to any level of complexity and to any repair level. This approach has been incorporated in a product called STAMP® (System Testability and Maintenance Program) which has been developed and refined through more than 10 years of field-level applications to complex system diagnosis. The results have been outstanding, even spectacular in some cases. In this paper we describe system-level testability, system-level diagnoses, and the STAMP analysis approach, as well as a few STAMP applications.

INTRODUCTION

System-level diagnosis has always been an afterthought in system design. Initially (i.e, circa 1930) system-level failures announced themselves. Parts fell off, items quit working, or the failure symptom itself pointed to the subsystem that demanded repair. As systems became more complex a symptom indicated that a failure was restricted to a small list of possible causes. Further testing was undertaken to localize the failure to a level consistent with repair.

As systems have grown in complexity we have been forced to rely on testing that is an outgrowth of product assurance rather than on field-derived maintenance information. The easiest obtainable test information has been that developed from testing by the manufacturer during equipment production. At the same time, the product assurance people placed their resources on intermediate production screening. Realizing that system-level diagnosis was an extremely complex problem, the manufacturer began to screen incoming parts and to test at the detailed subassembly level in an effort to avoid delivering a malfunctioning system. What resulted was a mismatch; that is, the tests that were available to the field technician were not developed for system-level diagnosis, but rather, for system verification purposes. In fact, the tests were designed to avoid any situation where system-level diagnosis was required.

Because of this mismatch, system and test design provided diagnosis that frequently resulted in 40% or higher false "pull" rates, the result of high ambiguity and labor-intensive test procedures, and

false alarms consumed excessive maintenance resources. Studies of the CH-54 and the F-16 showed that troubleshooting actions consumed as much as 50% of the total labor-hours spent for repair.[1] Data for the scheduled airlines revealed similar trends for complex electronics.[2] When systems were sent back to the factory, a bench check was performed and only two outcomes resulted:

- A retest OK indicating improper diagnosis in the field or inadequate bench checking
- An anomalous system to be discarded or dissected for subassembly test

Both of these outcomes are unacceptable.

The situation in system diagnosis continued to deteriorate, and the need for system-level diagnosis was easily recognizable in the late 1970s and early 1980s. Readiness levels for military aircraft were often low, with as few as 50% of the assets available in some maintenance cycle. In the early 1980s, several initiatives such as MATE, IFTE, and CASS were underway, and a number of tools were being developed, such as IDSS, STAMP and I-CAT.[3-8] All of these, to one extent or another, addressed the system-level aspects of testability and diagnosis. The first military specification for testability (MIL-STD-2165) became effective in 1985.[9]

SYSTEM LEVEL TESTABILITY

According to MIL-STD-2165, testability is defined as:

A design characteristic which allows the status (operable, inoperable, or degraded) of an item to be determined and the isolation of faults within the item to be performed in a timely and efficient manner.[9]

The literature generally discusses different types of testability when referring to system-level testability: *inherent* and *achieved* testability. Inherent testability addresses the way the system is designed and encompasses the ability to observe system behavior under a variety of stimuli. Inherent testability is defined by the location, accessibility, and sophistication of tests and test points that may be included in the system. Achieved testability addresses how the system is maintained. It is defined by the results of the maintainability process (such as false alarms, ambiguities, incorrect isolations, no faults found). Note that the *achieved* testability has the *inherent* testability as a goal and no testability as a lower limit.

During the design phase, the testability analysis should provide the following information related to the inherent testability of the system:

- ***Ambiguity Groups***—Components which are and components which are not uniquely identifiable in the current system/test configuration.
- ***False Failures***—When multiple failures occur, any combinations that can provide the same symptoms as an unrelated single failure.
- ***Hidden Failures***—When multiple failures occur, their relationship, if any, and the root cause of the failure hidden.
- ***Information Feedbacks***—Cycles of diagnostic information. Feedbacks typically cause isolation problems and result in larger-than-acceptable ambiguity groups. Mapping feedback is one of the first steps in improving testability by reducing ambiguity groups.
- ***Nondetections***—Components that have failure modes which are not observed by any of the available tests.
- ***Test Disposition***—Necessary additional and unnecessary tests. Eliminating unnecessary tests reduces maintenance complexity and test program set (TPS) test times.
- ***Tolerance to False Alarms***—Any special provisions required by the system to handle potential false alarms.
- ***Operational Isolation***—The probability that one can expect to isolate 1, 2,... or fewer replaceable units. This information is critical for logistic planning.

DIAGNOSIS AT THE SYSTEM LEVEL

As with testability, diagnosis often refers to more than one concept. In this paper, three basic terms are used with the diagnosis descriptions: *detection*,

localization, and *isolation*. Detection refers to the ability of a test, combination of tests, or a diagnostic strategy to identify that a failure in some system element has occurred. This term is often associated with built-in test (BIT) and may actually be the design criterion set upon BIT.

Localization refers to the ability to restrict a fault to some subset of possible causes. This also is associated with a combination of tests or a diagnostic strategy. Clearly, all BIT that can detect must also localize (to at least one of all possible faults). If the localization is sufficient in most cases to undertake repair, we often refer to the BIT as *smart* BIT. BIT, however, is not the only diagnostic technique that localizes. Often automatic test equipment (ATE) and manual isolation techniques use a diagnostic strategy that localizes the fault to a degree sufficient to undertake repairs.

Isolation is often misused to represent that localization has been achieved to a degree consistent with a single repair unit. Actually, it means that, through some test, combination of tests, or diagnostic strategy, the specific cause of a fault has been identified.

A diagnostic strategy should provide a limited set of items:

- A procedure that brings the achieved testability up to the level of the inherent testability.
- A procedure that can fault-isolate (localize) the system while optimizing one or more criteria.

THE STAMP APPROACH

It is assumed that, at any analysis level, when an engineer writes a full-scale physical simulation of the entire system at a specific level of detail, he or she will then be able to answer all of the testability questions by meticulously tracing stimuli through the system to observe responses. This is possible when faults are exhaustively modeled, and the engineer can determine such items as nondetection and ambiguity. Unfortunately, because of the sheer volume of computations required at higher levels of complexity or by a larger system, this is not practical. For example, suppose that we have a very large-scale integrated (VLSI) chip with 10,000 gates, any one of which may be "stuck open" or "stuck at," yielding 20,000 faults to model. If 4 such chips are on board with other components, and 6 such boards make up the digitizer in a color radar display that has 23 such subsystems, we have to model at least 11 million failure modes!

When we began to develop a less computationally intense process, we wanted to build an analysis method that is hierarchical and discards a fair amount of the detail carried along in a physical representation. First, we strip the test of its stimulus-response details and turn it into an information carrier. This is not to say that the details of how the test is conducted are unimportant. In fact, they are essential in actually performing the test. We simply do not carry them along in our analysis (but we do pick them up later). Second, we ignore the details of gates, resistors, and hardware implementations and, rather, consider functions. The latter gives us a hierarchical formulation because functions can be aggregated from combinations of other functions, and we can proceed functionally to any level in the analysis. (A function, of course, carries with it an aggregation of hardware or a piece of hardware.) This in turn provides a way to "repair" functions.

What have we lost? A great deal. We can no longer use our model to provide the stimulus-response details. A computer-aided drawing (CAD) file can no longer be used directly for input, although we may be able to enter some of the details through translation. The solution may be a much grosser localization than a simulation model.

What have we gained? A great deal. We can now perform our testability analysis in a hierarchical manner. We can hypothesize information sources without concerning ourselves with the details of stimulus-response—until and unless we want to actually perform the test. We can play what-if and conduct trade-off analyses at a much simpler modeling level. And we have a full range of information theoretic tools to help us answer the basic testability and fault-isolation questions.

One tool, STAMP, derives measures of testability and synthesizes fault-isolation strategies on the basis of an information flow model of the system under analysis. It is important to understand the fundamentals of information flow modeling and fault-isolation theory. The vehicle for information

flow modeling is a block diagram that represents the functional topology of a given system. Additional data available for the model include hierarchical grouping, special inference, and cost and other weighting criteria. A full range of testability measures and tables is then produced to provide the basic information listed in the "Testability at the System Level" section. The specifics as they apply to the STAMP analysis are detailed in references 10 and 11, which include example computations.

Fault isolation can be described mathematically as a partition process. Let $C = (c_1, c_2,...,c_n)$ represent the set of n components. After the *j*th test, a fault-isolation strategy partitions C into one of two classes:

$$F^j = (c_1^j, c_2^j,..., c_m^j) \qquad (1)$$

where F^j is the set of components that are still failure candidates after the *j*th test (feasible set), and m is the number of components in the set. The complement of this set is given by:

$$G^j = C - F^j \qquad (2)$$

where G^j is the set of components found to be good after the *j*th test (infeasible set). This set will contain m-n components.

By this structure, a strategy will have isolated a fault when F^j consists of a single element or can no longer be subdivided (F^j consists of a component ambiguity group).

It can be proved that for a well-ordered system, a half-interval search technique will provide the minimum number of tests; however, such an ordering rarely exists. The STAMP approach uses an adaptive, information-based strategy, because in seeking to overcome the difficulty of ordering a system for the half-interval technique, it became apparent that if all dependencies in a system were known, the information content of each test could be calculated. If a test is performed, the set of dependencies allows us to draw conclusions about a subset of components.

The process of drawing conclusions about the system from limited information is called inference. For any test sequence, STAMP allows us to compute $(c_1^j, c_2^j,..., c_k^j)$ and the set of remaining failure candidates, namely $F^1, F^2,..., F^j$. An algorithm has been developed to look at the information content of all remaining tests so that the number of remaining tests that must be performed to isolate faults is minimized over the set of potential failure candidates.

STAMP EFFECTIVENESS

It can be shown that for a well-ordered or straightforward serial design, STAMP reduces to the half-interval technique, which is known to be optimal for that case. Unfortunately, the general case is known to be NP-complete,[12] so we are forced to rely on an approximate solution. In a number of applications, the adaptive, information-theoretic approach has provided the mean and the variance of the required number of tests under all failure conditions, either equal to or lower than those resulting from other procedures examined, and often approaching the theoretical minimum values. Table 1 lists a few of the more than 250 systems analyzed by STAMP.

SUMMARY

STAMP emphasizes diagnosis at the system level. This emphasis differs from most other testability analysis tools that operate at the gate or, at most, board level. This system-level emphasis enables STAMP to be hierarchically applied and enables the engineer to approach the testability problem from an information flow standpoint rather than from an electronic simulation. An additional result is that the approach is independent of the underlying technology, thus allowing the analysis of most systems, including hybrids. A shortcoming of this approach is that it cannot be used to directly develop the detailed definitions of the tests. STAMP has been applied to many types of systems, and these applications have been for a large number of system technologies and at varying points in the system life cycle. The results indicate that there is a large potential gain in providing system-level testability and diagnosis analyses.

Table 1. Results of STAMP Applications

System	Customer	Results
ALR-67 Countermeasures Set	NADC/USN	Developed test procedures for TRDs
ALR-62 Warning Receiver	ALC/USAF	Reduced ambiguity groups by over 40%
Air Pressurization System	Int'l Fuel Cells	Unique isolation improved by over 100%
MSQ-103C TEAMPACK	EW/RSTA/USA	Reduced required testing by 87%; portable maintenance aid developed
Mk 84 60/400 Hz Static	NAVSEA/USN	Reduced required testing by 70%; portable frequency converter maintenance aid developed
UH-60A (Black Hawk) Stability Augmentation System	ATL/USA	Reduced mean time to fault-isolate by factor of 10; reduced maintenance complexity by factor of 3
ALQ-131 Podded EW System	ASD/USAF	Reduced mean time to fault-isolate by 75%
ALQ-184 Podded EW System	AFLC/USAF	Reduced false-alarm rate by a factor of 10; developed UUT software procedures
B-2 Bomber DFT Program	USAF/Northrop	Improved specification compliance at the shop replaceable unit (SRU) level by 80%

REFERENCES

1. Cook, Thomas N., et al. "Analysis of Fault Isolation Criteria/Techniques," *Proceedings — Annual Reliability and Maintainability Symposium*, San Francisco, CA, January 1980.

2. Aeronautical Radio, Inc. *Avionics Maintenance Conference Report — San Diego*, 1987. Publication 87-087/MOF-34, Annapolis, MD, August 1987.

3. Cross, G. "Third Generation MATE—Today's Solution." *Proceedings of the 1987 IEEE AUTOTESTCON Conference*, San Francisco, CA, November 1987.

4. Espesito, C. M., et al. "U.S. Army/IFTE Technical and Management Overview." *Proceedings of the 1986 IEEE AUTOTESTCON Conference*, San Antonio, TX, September 1986.

5. Najaran, Captain M. T., "CASS Revisited—A Case for Supportability," *Proceedings of the 1986 IEEE AUTOTESTCON Conference*, San Antonio, TX, September 1986.

6. Franco, J. R. "Experiences Gained Using the Navy's IDSS Weapon System Testability Analyzer," *Proceedings of the 1988 IEEE AUTOTESTCON Conference*, Minneapolis, MN, September 1988.

7. Simpson, W. R., and Sheppard, J. W., "Experiences with a Model-Based Approach to the Fault Detection and Isolation of Complex Systems," *Symposium on Artificial Intelligence Applications in Military Logistics*, Williamsburg, VA, March 1990.

8. Cantone, R. A., and Caserta, P., "Evaluating the Economical Impact of Expert Fault Diagnosis Systems: The I-CAT Experience," *3rd IEEE International Symposium on Intelligent Control*, Arlington, VA, August 1988.

9. *Testability Program for Electronic Systems and Equipment*, MIL-STD-2165, Washington, DC, Naval Electronic Systems Command, January 1985.

10. Sheppard, John W., and Simpson, William R., "A Mathematical Model for Integrated Diagnostics," *IEEE Design and Test of Computers*, Vol. 8, No. 4, December 1991, pp. 25-38.

11. Simpson, William R., and Sheppard, John W., "System Testability Assessment for Integrated Diagnostics," *IEEE Design and Test of Computers*, Vol. 9, No. 1, March 1992, pp. 40-54.

12. Hyafil, Laurent, and Rivest, Ronald L., "Constructing Optimal Binary Decision Trees is NP-Complete," *Information Processing Letters*, Vol. 5, No. 1, May 1976, pp. 15-17.

Biographical Sketches of the Authors

John W. Sheppard holds a B.S. in Computer Science from Southern Methodist University and an M.S. in Computer Science (emphasizing Artificial Intelligence) from The Johns Hopkins University, where he is currently a Ph.D. candidate in Computer Science. His research areas include fault diagnosis, machine learning, neural networks, and knowledge representation. His work has included the development of A.I. techniques and algorithms that are being applied in system diagnosis, knowledge base verification, and software classification. Mr. Sheppard is one of the principal developers of an intelligent, interactive maintenance assistant (Portable Interactive Troubleshooter -- POINTER) which guides a diagnostic process through test choice and evaluation, explains reasoning, and incorporates elements of evidential reasoning and neural networks to process information obtained from uncertain or incomplete testing. Mr. Sheppard is a senior research analyst in the Advanced Research and Development Group at The ARINC Research Corporation. He can be reached by e-mail at sheppard@cs.jhu.edu

William R. Simpson holds a B.S. in Aerospace Engineering from the Va. Polytechnic Institute and State University, an M.S.A. in Engineering Management from the George Washington University, as well as, an M.S. and a Ph.D. in Aerospace Engineering from the Ohio State University. He is also a graduate of the U.S. Naval Test Pilot School in Patuxent River, Maryland. His work in the area of testability and fault diagnosis resulted in the development of the System Testability and Maintenance Program (STAMP) which uses an information flow model to assess system testability and generate efficient fault isolation strategies. He was also a principal developer of the POINTER system which includes reasoning under uncertainty, similarity and explanation based learning, logical inference, and decision optimization. In addition to STAMP and POINTER, Dr. Simpson applied the information modeling approach to non-cooperative target recognition (Non-Cooperative All-Source Target Identification -- NASTI) and to electronic warfare signal sorting (Signal Evaluation for Emitter Recognition -- SEER). He has also participated in the development of neural networks for software classification and reasoning termination. Dr. Simpson is a research fellow in the Advanced Research and Development Group at the ARINC Research Corporation. He can be reached by e-mail at wsimpson@mcimail.com

N94-11564

CREW CHIEF

Jill Easterly
Human Resources Lab
Logistics and Human Factors DIV
Wright Patterson AFB, OH 45433

This software package does ergonomic human modeling for maintenance tasks. Technician capabilities can be directed to represent actual situations of work environment, strengths and capabilities of the individual, and particular limitations (such as constraining characteristics of a particular space suit), tools required and procedures or tasks to be performed.

Session S2: SPACE SERVICING

Session Chair: Maj. Timothy Boles

N94-11565

ON-ORBIT REFUELING

Capt. Pospisil
Human Resources Lab
AFIT
Wright Patterson AFB, OH 45433

Goal is to increase operational availability of space assets by refueling with an expendable launch vehicle (not the Shuttle) in LEO or GEO. Information is drawn from the on-orbit refueling model, COSEMS model, COMA study, and information provided from the San Antonio Air Logistics Center.

N94-11566

ON-ORBIT REFUELING

James S. Moore[1] and Shelby L. Owens[2]
[1]NASA/Johnson Space Center
Manager, Space Servicing
Systems Project Office
2101 Nasa Road 1
Houston, TX 77058
[2]Hernandez Engineering, Inc.
Program Manager, NIO Project
Development Support Contract
17629 El Camino Real
Houston, TX 77058

During the past decade, both NASA and the DOD have conducted numerous space servicing studies. These studies have shown that fluid resupply of on-orbit spacecraft is feasible and would allow for extended spacecraft utilization. In order to prove that the studies have validity, an on-orbit flight demonstration of automatic fluid resupply is required. To embark on this flight demonstration, the systems concepts, operation procedures, and conceptual service and target vehicles must be identified.

Hernandez Engineering, Inc. (HEI), with the direction of the Space Servicing System Project Office of the NASA/JSC New Initiatives Office, has conducted a systems engineering and integration study. The study objective was to develop preliminary concepts for a flight demonstration of automatic rendezvous, proximity operations, capture, and fluid transfer utilizing servicer and target vehicles. HEI awarded subcontracts to Fairchild Space, McDonnell Douglas, Martin Marietta, and TRW to support the conduct of the study.

The results show that a servicer vehicle/target kit can be launched to orbit with an ELV and automatically rendezvous and dock with the explorer platform (EP). The servicer vehicle can then separate from the EP/kit, perform proximity maneuvers, redock with the EP/kit, and perform fluid transfer operations. After the on-orbit flight demonstration is completed, the servicer/kit can be separated from the EP and be deorbited into the Earth's atmosphere.

N94-11567

PRELIMINARY ANALYSIS OF THE BENEFITS DERIVED TO US AIR FORCE SPACECRAFT FROM ON-ORBIT REFUELING

PRESENTED TO

SOAR 92

BY

SCOTT SMITH
SA-ALC/TIEO
KELLY AFB, TX 78241

AUGUST 5, 1992

INTRODUCTION AND DESCRIPTION OF ANALYSES

This analysis was undertaken during FY 91 as a joint effort of SSD/XRP and SA-ALC/TIE as a preliminary step to identify potential benefits from refueling Air Force satellites on orbit. Both economic and operational benefits were included. Operational benefits were related in economic terms to allow evaluation. All economic comparisons were made using FY 91 costs. An additional purpose of the effort was to identify the preferred mission parameters, for an on-orbit refueling system.

A companion study was being concurrently conducted by SSD/XRP and NASA/JPL (JPL Pub D-8240) to develop a hardware concept for an on-orbit refueling system. The mass estimates for refueling missions obtained from the companion study were used in conducting the economic analyses of this benefits study.

For this study, on-orbit refueling was based on the concept developed in the companion JPL study. The concept involves launching an S/C carrying fuel that would be transferred to another "target" S/C which is already in orbit. The two S/C would then rendezvous, dock and transfer fuel. Another fluid, such as a cryogenic, might be included if needed by the target S/C.

The hardware concept for refueling was intended to minimize costs. The re-fueler S/C was designated to be expendable and would contain only the minimal capabilities. It would be launched into the orbit plane and altitude of the target S/C(s). The re-fueler S/C would rendezvous and dock with the target S/C and the fluid transfer would occur. When the refueling mission was completed, the re-fueler S/C would be ejected from the orbit. In order to optimize launch costs, some missions involved launching two re-fueler S/C on one LV. In this case the second re-fueler S/C would be placed in a storage orbit until needed.

The effort covered all Air Force S/C and launch programs that were active during the period of this project. To provide the most realistic results possible, the analyses were based on the generation of S/C in development at the time of this study. The following S/C programs were included in the study:

Defense Meteorological Satellite Program
Defense Satellite Communication System
Defense Support Program
Global Positioning System
Space Based Radar System

The Follow-On Early Warning System and MILSTAR were not included since the requirements for these programs were being significantly revised during the time of this study. For each analysis an On-Orbit Cost was calculated which included non-recurring, recurring and failure costs up to the point of S/C activation. For each S/C program, four analyses were conducted as described below:

Fuel Transfer Analysis

This portion of the study identified the maximum S/C fuel capacity and type, an initial two year fuel supply and an amount to be transferred during a refueling mission. Planned refueling missions would be timed so that the target S/C would not go below a two year fuel quantity.

Operational Analysis

Improving the function and performance of the S/C mission through on-orbit resupply was evaluated in this section. The value of this improvement was quantified and an economic analysis was conducted using the estimated costs of the refueling system. The main areas considered were weight additions to the payload obtained by launching the S/C with less than a full load of fuel and maneuver for either survivability or constellation maintenance. Weight additions to the payload were used to either add performance capacity or increase redundancy and reliability.

Launch Cost Analysis

Possible economic benefits from launching with smaller or larger LV as well as combined launches were identified. The smaller LV alternative included off-loading fuel at launch to allow use of a smaller LV and then refueling on-orbit. Larger LVs were evaluated to determine benefits from including additional fuel and payload on the original S/C launch and not refueling. Combined payloads were evaluated to determine benefits from larger LVs capable of launching two or more S/C.

Lifetime Extension Analysis

Economic benefits were evaluated where refueling could extend the service life of a S/C. In cases where fuel was the first life limiting item, an on-orbit refueling capability was considered as the improvement. In cases where another subsystem was the first life limiting item, the improvement was to off-load fuel at launch and use the weight savings to add redundancy to the life limiting item. This second case also included refueling on-orbit to replace the fuel off-loaded at launch. Economic benefits were determined by estimating the added life gained until the next subsystem failed.

RESULTS

The results of the analyses for each system are summarized in the following sections.

Defense Meteorological Satellite Program

Although DMSP block 6 is expected to be at an altitude that would otherwise make on-orbit refueling attractive, the small 55-75 pound expected fuel capacity does not provide an opportunity for benefits. The expected fuel capacity is approximately the same as the estimated 50 pound weight impact to the target S/C to add on-orbit refueling capability. The historically short time to failure of DMSP subsystems and payloads might offer potential benefits for on-orbit maintenance if a low cost capability could be developed.

Defense Satellite Communications System

DSCS SHF Replenishment, if launched on the Atlas II LV, has potential benefits from both life extension by on-orbit refueling and from operational improvements gained by off-loading fuel to add communications transponders. Potential savings may also be achieved by using a larger LV without on-orbit refueling. The SPO was considering the use of bipropellant for SHF Replenishment S/C. This would negate many of the benefits. Results of the analyses are shown in the following tables.

The lowest cost alternative is to upgrade to the Atlas IIAS LV and include the additional fuel and/or transponders on the SHF Replenishment S/C at launch.

DSCS SHF REPLENISHMENT
MONOPROPELLANT
ALTAS II LV
$302.3 MILLION ON-ORBIT COST

	NO REFUELING	REFUELING ONLY	ONE ADDL TRANSPONDER	TWO ADDL TRANSPONDERS
S/C LIFETIME	10.0 YRS	13.0 YRS	12.5 YRS	13.0 YRS
REFUELING	N/A	7.1 YRS	3.2 YRS	0[1]/6.5 YRS
ANN COST PER TRANS	$5.04 M	$4.88 M	$4.41 M	$4.47 M
NET SAVE PER S/C	N/A	$12.6 M	$42.5 M	$29.2 M

DSCS SHF REPLENISHMENT
BIPROPELLANT
ATLAS II LV
$302.3 MILLION ON-ORBIT COST

	NO REFUELING	REFUELING ONLY	ONE ADDL TRANSPONDER	TWO ADDL TRANSPONDERS
S/C LIFETIME	13.0 YRS	13.0 YRS	13.0 YRS	13.0 YRS
REFUELING	N/A	N/A	4.4 YRS	0[2]/9.1 YRS
ANN COST PER TRANS	$3.88 M	N/A	$4.25 M	$4.48 M
NET SAVE PER S/C	N/A	N/A	$(33.6) M	$(62.6) M

DSCS SHF REPLENISHMENT
NO REFUELING
ATLAS IIAS LV
$319.1 MILLION ON-ORBIT COST

	LIFE EXTEND ONLY	ONE ADDL TRANSPONDER	TWO ADDL TRANSPONDERS
S/C LIFETIME	13.0 YRS	13.0 YRS	13.0 YRS
ANN COST PER TRANS	$4.08 M	$3.57 M	$3.17 M
SAVE PER MONOPROP S/C	$76.0 M	$118.8 M	$164.2 M
SAVE PER BIPROP S/C	N/A	$28.2 M	$73.6 M

DSCS SHF REPLENISHMENT

	ANN COST PER TRANS	SAVE (M) MONO	BIPROP	REFUEL
ATLAS IIAS TWO ADDL TRANSPONDERS	$3.17 M	$164.2	$73.6	N
ATLAS IIAS ONE ADDL TRANSPONDER	$3.57 M	$118.8	$28.2	N
ATLAS II BIPROP NO REFUEL	$3.88 M		$00.0	N
ATLAS IIAS LIFE EXTENSION ONLY	$4.08 M	$73.8	N/A	N
ATLAS II BIPROP ONE ADDL TRANS	$4.25 M		$(33.6)	Y
ATLAS II MONO ONE ADDL TRANS	$4.41 M	$42.5		Y
ATLAS II MONO TWO ADDL TRANS	$4.47 M	$29.2		Y
ATLAS II BIPROP TWO ADDL TRANS	$4.48 M		$(62.6)	Y
ALTAS II MONOPROP REFUEL ONLY	$4.88 M	$12.6		Y
ATLAS II MONOPROP NO REFUEL	$5.04 M	$0.0		N

Additional potential savings may be possible if re-fueler S/C launches can be combined with DSP-1 S/C on the Titan IV SRMU IUS LV. This possibility will only exist if DSP-1 is chosen as the concept for FEWS.

Defense Support Program

Potential benefits were identified from off-loading fuel at launch and adding redundant Reaction Wheel Assembly bearings. Refueling would also offer enhanced maneuver capability. However, the technical difficulties of stopping rotation and then stabilizing the DSP-1 S/C for refueling as well as developing the redundant bearing assemblies appeared to be very large. Estimating the cost of overcoming these technical problems was beyond the scope of this study.

Separately, the concept of "piggy backing" DSP-1/FEWS/DSCS launches with other S/C appeared to offer significant potential cost savings. This potential should be evaluated in depth for all DoD systems using low inclination geostationary/geosynchronous orbits.

As noted above, the future of DSP-1 type S/C will depend on the concept selected for FEWS.

Global Positioning System

A potential savings for GPS IIR was identified from extending fuel lifetime to the 12.2 year MTBF for the S/C. However, results would be highly dependent on actual fuel expenditures for drift orbit maintenance and re-phasing which are much larger than station keeping in the fuel budget. The 0.6325 pounds of extra station keeping fuel would be less than the estimated 50 pound weight penalty for adding refueling equipment to the target S/C. Results of the analyses are shown in the following table.

GPS II R
MONOPROPELLANT

	DELTA 7925 LV		ATLAS IILV
	NO REFUEL	REFUEL	NO REFUEL
S/C LIFETIME	7.5 YRS	12.2 YRS	12.2 YRS
ON-ORBIT COST	$108.5 M	$108.5 M	$125.2 M
ANN COST PER S/C	$14.5 M	$14.0 M	$10.3 M
SAVE PER S/C	N/A	$5.65 M	$51.5 M

Unplanned weight increases could cause the GPS IIR to exceed the capacity of the planned Delta 7925 LV. In this event, utilizing an Atlas II LV would be $51.5 million less costly per S/C than off-loading fuel at launch and refueling on-orbit.

A previous study indicated an "active and spare" constellation maintenance strategy had potential to achieve the same performance with three fewer spare S/C on-orbit than presently planned. The offset would be the weight penalty to equip all GPS IIR S/C with refueling capability and the cost of refueling missions. This would negate the savings from fewer on-orbit spare S/C.

Space Based Radar

Significant potential cost savings were identified for a SBR S/C using either monopropellant or bipropellant. These included life extension by refueling alone and by refueling combined with off-loading fuel at launch to increase the number of battery packs on the SBR S/C. Potential savings were also identified for using a larger LV without on-orbit refueling. These savings were aided by several factors favorable to on-orbit refueling. First, SBR is at an orbit altitude which reduces the launch cost for a re-fueler S/C. Second, the SBR would periodically use fuel to re-boost the S/C due to drag effects of the atmosphere. Finally, the on-orbit cost of SBR is large compared to refueling cost.

The results of the analyses are shown in the following tables.

SPACE BASED RADAR
MONOPROPELLANT
ATLAS IIAS LV
$396.8 MILLION ON-ORBIT COST

	NO REFUEL	REFUEL ONLY	ONE ADDL BATTERY PK	TWO ADDL BATTERY PKS
S/C LIFETIME	7.0 YRS	12.6 YRS	15.2 YRS	18.6 YRS
REFUELING	N/A	5.0 YRS	3.3/8.3 YRS	1.6/6.6/11.6 YRS
ANNL COST PER S/C	$56.7 M	$38.2 M	$33.9 M	$30.8 M
NET SAVE PER S/C	N/A	$222.0 M	$346.1 M	$482.9 M

SPACE BASED RADAR
BIPROPELLANT
ATLAS IIAS LV
$396.8 MILLION ON-ORBIT COST

	NO REFUEL	REFUEL ONLY	ONE ADDL BATTERY PK	TWO ADDL BATTERY PKS
S/C LIFETIME	9.2 YRS	12.6 YRS	14.2 YRS	18.6 YRS
REFUELING	N/A	7.2 YRS	5.0 YRS	2.8/11.0 YRS
ANNL COST PER S/C	$43.3 M	$36.4 M	$32.6 M	$27.8 M
NET SAVE PER S/C	N/A	$86.7 M	$151.7 M	$288.4 M

SPACE BASED RADAR
NO REFUELING
TITAN IV NUS
$475.4 MILLION ON-ORBIT COST

	LIFE EXTEND ONLY	ONE ADDL BATTERY	TWO ADDL BATTERIES
S/C LIFETIME	12.6 YRS	15.2 YRS	18.6 YRS
ANN COST PER S/C	$37.7 M	$31.3 M	$25.6 M
SAVE PER MONOPROP S/C	$238.9 M	$386.3 M	$579.1 M
SAVE PER BIPROP S/C	$70.4 M	$182.7 M	$330.2 M

SPACE BASED RADAR

	ANN COST PER S/C (M)	SAVE MONO (M)	SAVE BI (M)	S/C LIFE (YRS)	RE FUEL
TITAN IV NUS TWO ADDL BATTERIES	$25.6	$579.1	$330.2	18.6	N
ATLAS IIAS BIPROP TWO ADDL BATT	$27.8		$288.4	18.6	Y
ATLAS IIAS MONO TWO ADDL BATT	$30.8	$482.9		18.6	Y
TITAN IV NUS ONE ADDL BATTERY	$31.3	$386.3	$182.7	15.2	N
ATLAS IIAS BIPROP ONE ADDL BATT	$32.6		$151.7	14.2	Y
ATLAS IIAS MONO ONE ADDL BATT	$33.9	$346.1		15.2	Y
ATLAS IIAS BIPROP REFUEL ONLY	$36.4		$86.7	12.6	Y
TITAN IV NUS ADDED FUEL ONLY	$37.7	$238.9	$70.4	12.6	N
ATLAS IIAS MONO REFUEL ONLY	$38.2	$222.0		12.0	Y
ATLAS IIAS BIPROP NO REFUEL	$43.3		N/A	9.2	N
ATLAS IIAS MONO NO REFUEL	$56.7	N/A		7.0	N

RECOMMENDATIONS

The cancellation of the SBR effort in the FY 91 DoD budget, left DSCS SHF Replenishment using monopropellant fuel as the remaining system with meaningful potential benefits from on-orbit refueling. Potential benefits for DSCS SHF Replenishment were also identified from using a larger LV without refueling.

Four sequential follow-on actions were recommended to advance on-orbit refueling to readiness for operational use. The first was to determine if SHF Replenishment would use monopropellant fuel. Second was a more in-depth benefits analysis that would add confidence to the major assumptions made in this preliminary study. This would be followed by an evaluation of whether non Air Force DoD S/C such as Fleet Sat would also benefit from on-orbit refueling. The final recommendation was a decision on committing funds to a technology demonstration of on-orbit refueling capability for DoD S/C.

TERMS AND ACRONYMS

ADDL	Additional
ALC	Air Logistics Center
ANNL	Annual
BATT	Battery Pack
BI	Bipropellant
BIPROP	Bipropellant
DMSP	Defense Meteorological System
DSCS	Defense Satellite Communications System
DSP	Defense Support Program
FEWS	Follow-on Early Warning System
FY	Fiscal Year
GPS	Global Positioning System
IUS	Inertial Upper Stage
JPL	Jet Propulsion Laboratory
LEO	Low Earth Orbit
LBS	Pounds
LV	Launch Vehicle
MILSTAR	Military Strategic and Tactical Relay System
MONO	Monopropellant
MONOPROP	Monopropellant
MTBF	Mean Time Between Failure
NASA	National Aeronautics and Space Administration
NAVSTAR/GPS	Global Positioning System
NUS	No Upper Stage
PK	Battery Pack
PKS	Battery Packs
SA	San Antonio
SBR	Space Based Radar
S/C	Space Craft
SHF	Super High Frequency
SPO	System Program Office
SRMU	Solid Rocket Motor Upgrade
SSD/XRP	Space Systems Division/
SPO	System Program Office
TIE	Technology and Industrial Support Directorate Engineering Division
TRANS	Communications transponder(s)
YRS	Years

SOAR 92

ON-ORBIT REFUELING

AN ANALYSIS OF POTENTIAL BENEFITS

SPACE OPERATIONS, APPLICATIONS
AND RESEARCH SYMPOSIUM

SCOTT SMITH
SA-ALC/TIEO

5 AUGUST 1992

OVERVIEW

- DESCRIPTION OF REFUELER S/C
- DESCRIPTION OF ANALYSES
- RESULTS
  - •• SPACE BASED RADAR
  - •• DSCS
- SUMMARY

DESCRIPTION OF ANALYSES

- FUEL TRANSFER ANALYSIS
- OPERATIONAL ANALYSIS
- LAUNCH COST ANALYSIS
- LIFE TIME EXTENSION ANALYSIS

DESCRIPTION OF ANALYSES

- ALL AF SPACE SYSTEMS EXCEPT FEWS & MILSTAR
- FY 91 COST BASIS
- COSTS INCLUDED

	SPACE		LAUNCH	CONTROL		
	N/R	RECUR	RECUR	N/R	RECUR	OPER
TARGET	●	●	●			
REFUELER	●	●	●	●	●	●

RESULTS
SPACE BASED RADAR

- FUEL TRANSFER ANALYSIS
  - •• MONOPROPELLANT
  - •• BIPROPELLANT

- LAUNCH COST ANALYSIS
  - •• ATLAS IIAS LAUNCH VEH
  - •• TITAN IV NUS LAUNCH VEH

- LIFE TIME EXTENSION ANALYSIS
  - •• ADDED FUEL
  - •• ADDED BATTERY PACKS

RESULTS

SPACE BASED RADAR

LV	ADDL BATTERY	RE FUEL	ANN COST PER S/C MONO	ANN COST PER S/C BIPROP	S/C LIFE TIME
T IV NUS	2	0	$25.6 M	$25.6 M	18.6 YRS
A II AS	2	3/2	$30.7 M	$27.8 M	18.6 YRS
T IV NUS	1	0	$31.3 M	$31.3 M	15.2 YRS
A II AS	1	2/1	$33.9 M	$32.6 M	15.2 YRS
A II AS	0	1		$36.4 M	12.6 YRS
T IV NUS	0	0	$37.7 M	$37.7 M	12.6 YRS
A II AS	0	1	$38.2 M		12.0 YRS
A II AS	**0**	**0**		**$43.3 M**	**9.2 YRS**
A II AS	**0**	**0**	**$56.7 M**		**7.0 YRS**

RESULTS

DSCS REPLENISHMENT

- FUEL TRANSFER ANALYSIS
  - •• MONOPROPELLANT
  - •• BIPROPELLANT
- OPERATIONAL ANALYSIS
  - •• ADDED TRANSPONDERS
  - •• REPOSITIONING
- LAUNCH COST ANALYSIS
  - •• ATLAS II LAUNCH VEH
  - •• ATLAS IIAS LAUNCH VEH
- LIFE TIME EXTENSION ANALYSIS
  - •• ADDED FUEL

RESULTS

DSCS REPLENISHMENT

LV	ADDL TRANS	RE FUEL	ANN COST PER TRANS MONO	ANN COST PER TRANS BIPROP	S/C LIFE TIME
A II AS	2	0	$3.17 M	$3.17 M	13.0 YRS
A II AS	1	0	$3.57 M	$3.57 M	13.0 YRS
A II	**0**	**0**		**$3.88 M**	**13.0 YRS**
A II AS	0	0	$4.08 M		13.0 YRS
A II	1	1		**$4.25 M**	13.0 YRS
A II	1	1	$4.41 M		12.5 YRS
A II	2	2	$4.47 M		13.0 YRS
A II	2	2		**$4.48 M**	13.0 YRS
A II	0	1	$4.88 M		13.0 YRS
A II	**0**	**0**	**$5.04 M**		**10.0 YRS**

DSCS REPOSITIONING

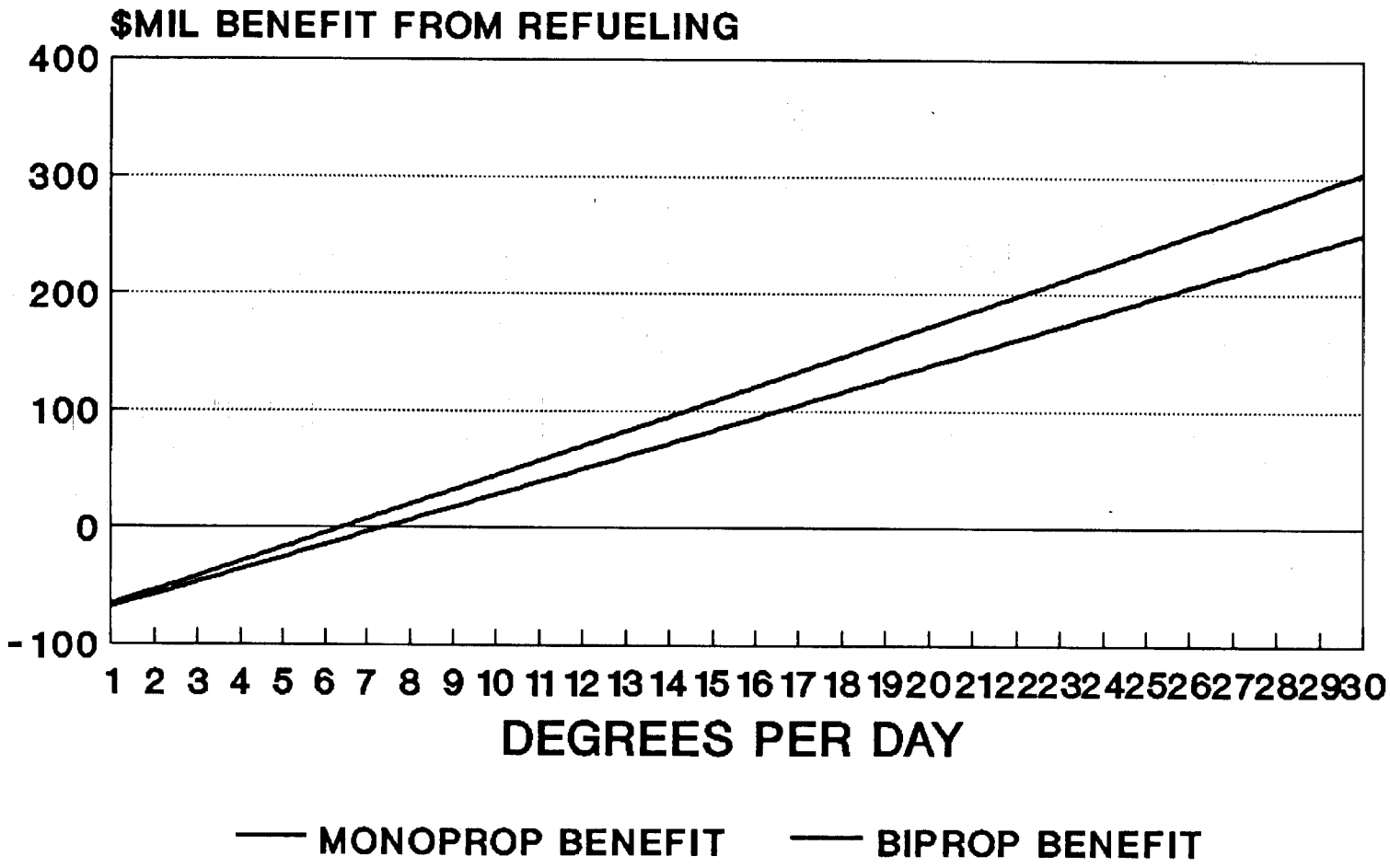

NO ADDED TRANSPONDERS
FUEL IS LIFE LIMITING

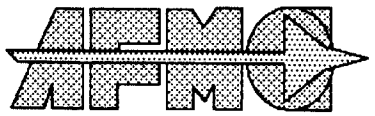

DESCRIPTION OF REFUELER S/C

- NOT A HIGH TECH S/C
- EXPENDABLE
- TAURUS LV FOR LEO
- 2 REFUELERS PER ATLAS II LV FOR GEO
- LOWER COST LV WILL IMPROVE BENEFITS

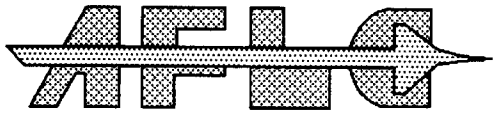

SUMMARY

- RESULTS ARE CASE DEPENDENT
- DSCS - POTENTIAL OPERATIONAL BENEFIT
- DSCS & SBR - POTENTIAL COST BENEFITS
- FUTURE MILSTAR AND FEWS ANALYSES

ON-ORBIT REFUELING: AN ANALYSIS OF POTENTIAL BENEFITS

Scott Smith
SA-ALC/TIEO
Kelly AFB, TX

Abstract unavailable at time of publication.

Session S3: SPACE ASSEMBLY

Session Chair: Charles T. Wooley

IN-SPACE OPERATIONS FOR LUNAR AND MARS SPACE TRANSFER VEHICLES

James L. Raper, Sr.*
Space Exploration Initiative Office
NASA Langley Research Center
Hampton, Virginia

Rick C. Vargo**
McDonnell Douglas Space Systems Company
Kennedy Space Center, Florida

Abstract

The objective of this paper is to discuss the in-space operations required to process the lunar and Mars mission vehicles envisioned in early studies for the Space Exploration Initiative (SEI). Recent studies, which have examined the degree to which on-orbit operations change as a function of the Earth-to-orbit (ETO) launch vehicle size, identified a common set of on-orbit vehicle processing tasks, and generated functional requirements for in-space processing nodes, are summarized in this paper.

Timelines for on-orbit processing of two different lunar transfer vehicles (LTVs) were developed to compare a "current practice", labor-intensive EVA approach to ones utilizing telerobotics and advanced automation. LTV aerobrake concepts ranging from simple deployment to considerable assembly are compared. Similar timelines for the on-orbit processing of a nuclear Mars transfer vehicle (MTV) are also presented. Aerobrakes can be processed in a timely manner, and should not be ruled out for SEI misssions. The "tall pole" time interval for on-orbit vehicle initial processing is the delivery of elements to orbit, not the processing tasks.

A discussion of the low-Earth-orbit (LEO) infrastructure required to support on-orbit vehicle processing is presented. The LEO infrastructure required to support on-orbit space transfer vehicle processing operations is determined by the complexity and amount of on-orbit processing operations, which is dictated by the design of the flight vehicle. Processing support can be an integral part of each vehicle to be assembled, or it can be permanent infrastructure remaining in LEO. Use of deployed rather than assembled aerobrakes minimizes on-orbit operations. Early lunar missions with expendable vehicles will not require on-orbit processing if the ETO launcher is large enough, but later space-based reusable LTVs will. All MTVs proposed for the SEI are inherently large and will require significant on-orbit processing operations.

The paper concludes with a discussion of hardware design recommendations and specific technology needs that will minimize the required on-orbit operations. On-orbit processing time savings of up to 66% could be realized if the recommendations and technologies are incorporated into the space transfer vehicles.

Introduction

This paper discusses those on-orbit processing operations that will probably be required for some of the Space Exploration Initiative space transfer vehicle elements. Also included is discussion of some aspects of the on-orbit infrastructure that may be required to support such operations. The emphasis of this paper is the amount of time these processing operations might require and how this time duration changes as a function of how the operation is executed and how the hardware is designed. On-orbit processing operations include the assembly activity as well as operations related to inspection, protection from orbital debris, storage, checkout, fueling, crew transfer, etc.

On July 20, 1989, President Bush described the Space Exploration Initiative as consisting essentially of " . . . back to the Moon to stay . . . and on to Mars." In the intervening years, he has endorsed the SEI objectives on many occasions by further defining the goal, providing policy guidance on architectures, identifying a possible role for international participation, establishing a timetable, and requesting budgetary support. The most recent evidence of continuing strong administration commitment is his issuance of Space Policy Directive No. 6 outlining participation of the DoD, DoE and DoC and establishing a National Program Office to be led by the NASA Associate Administrator for Exploration.[1]

In addition to the ongoing NASA studies of how such an initiative might be implemented, Gen. Thomas Stafford was designated to lead a National Synthesis Group beginning in late 1990 to further define several possible approaches for mission implementation. The group's report outlined four mission architectures that define mission scope and possible implementation approaches.[2] Each of these mission architectures has been examined in detail (reference 3 documents the NASA analysis of one of the architectures) to further define implementation requirements and hardware system details.

* Deputy Manager, Associate Fellow AIAA
** Technical Specialist, Senior Member AIAA

Emphasis is currently being directed at defining the details of the initial unmanned precursor lunar missions. A first manned landing could occur as early as 1999. The First Lunar Outpost (FLO) Study is a current NASA in-house, intercenter multi-team effort designed to identify approach, details, schedule, cost, technology requirements, and required new system developments. An early conclusion of the studies has been that a single large heavy-lift launch vehicle (HLLV), larger than Saturn V, would be required for each cargo and manned launch. Each mission consists of a cargo and a piloted launch that proceed independently to the Moon. Many of the study results obtained over the last few years, under the MSFC contracts cited in references 4 through 7, have provided the basis for the approaches being refined in the current FLO studies.

The use of a single launch vehicle (if available) for each element of the manned lunar mission eliminates on-orbit processing operations. This approach would seem to be appropriate in the current national economic environment and as a simplifying approach for a first manned mission, if a large HLLV is developed. Reliance on a plan to develop such a large HLLV, shown in Figure 1, for early and later lunar missions has the added value of defining the launch vehicle required for the Mars missions. Such requirements must be defined now if the NLS program is to provide such a vehicle rather than require that two new launch vehicles be developed in parallel. If, however, the required capability (mass and volume) HLLV is not available for the FLO, a smaller launch vehicle could be utilized with the result that some degree of on-orbit processing operations will be required.

The least amount of on-orbit operations occurs with a dual-launch for each mission element and an on-orbit rendezvous/capture scenario (capture being a refinement to the Apollo-style collision docking). Figure 2 shows such a mission profile from a recent MSFC study.[4] Figure 3 shows the launch vehicle manifesting for this type mission.[6] Note that the second piloted launch requires an undock-and-recapture maneuver between the return capsule and lunar lander (similar to that of Apollo) prior to rendezvous/capture with the first launch payload. A significant aspect of the first launch is to minimize propellant boil-off while waiting for about a month until the second launch arrives in LEO. The rendezvous/capture scenario has been adequately demonstrated in the past, but could be automated with advanced technologies for additional development cost.

Utilizing an even smaller ETO vehicle (Shuttle, Titan IV, small NLS, etc.) would stretch the delivery/assembly period over a longer time span and result in more hardware pieces to receive, inspect, assemble, and checkout. [8,9] It is for this scenario that on-orbit processing operations and the supporting infrastructure become significant mission elements and require an unrealistic number of ETO launches.

In later years when there are several missions to the Moon each year, and hardware recovery, refurbishment, and reuse are demonstrated to be economical, such LEO operations and infrastructure will be required. The lunar transfer ve-

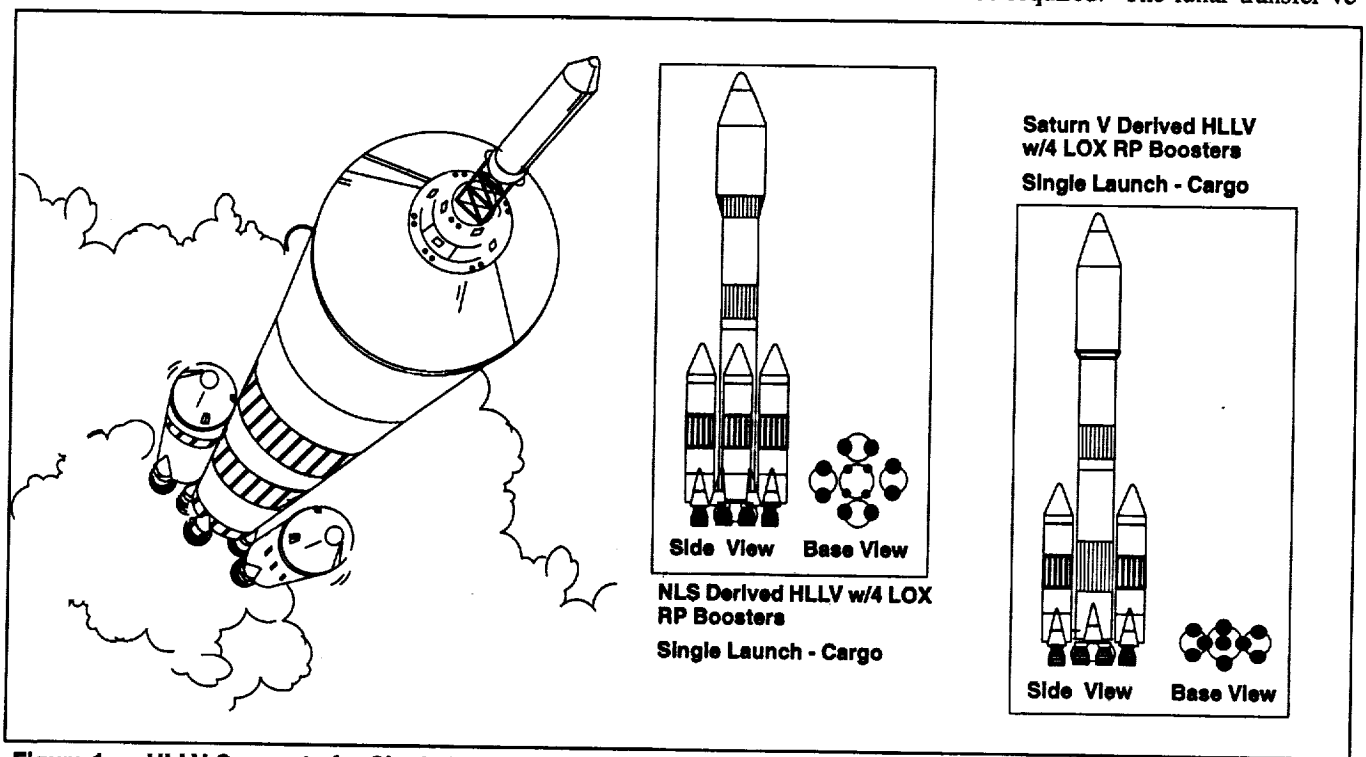

Figure 1 HLLV Concepts for Single Launch to Moon

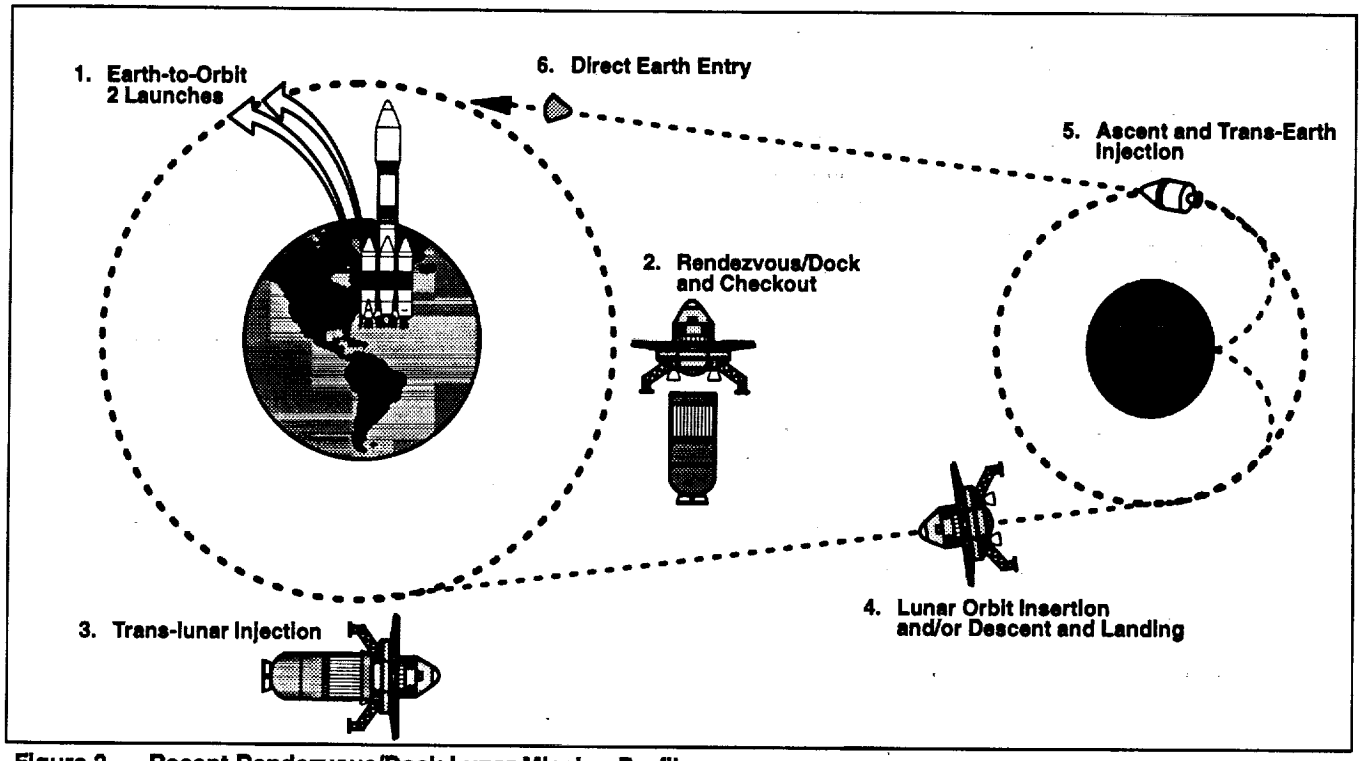

Figure 2 Recent Rendezvous/Dock Lunar Mission Profile

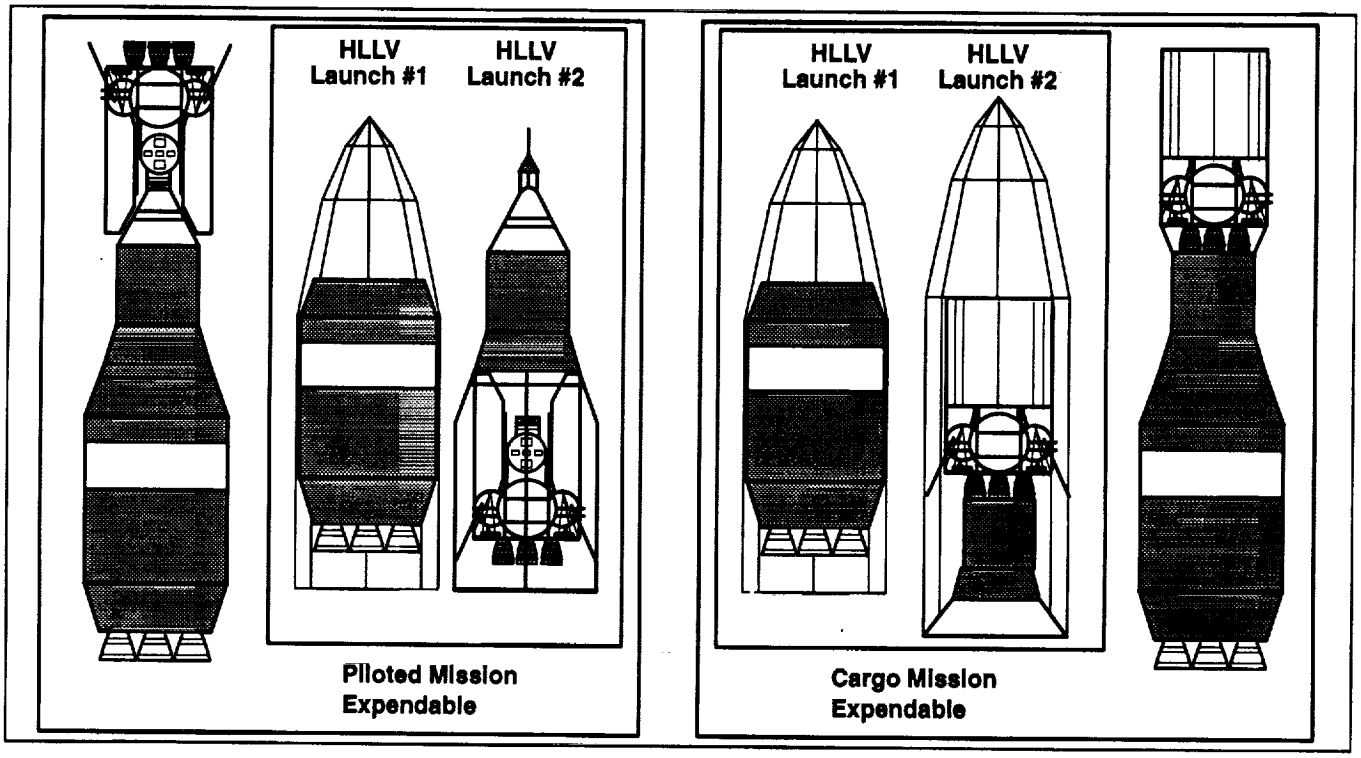

Figure 3 Launch Manifest for Rendezvous/Dock Lunar Mission

hicle would be based and fueled at a LEO node, and a shuttle or its SSTO successor vehicle would be used to ferry fresh crews and cargo between Earth and the LEO node. The need for very large lunar HLLV is then eliminated.

However, the very large HLLV (150 to 250mt) will be required for all Mars missions in order to minimize the number of launches and delivery time for the Mars transfer vehicle elements. Figure 4 indicates that 7 launches to LEO, with a 150mt launch vehicle, is required.[5,10] The reference 11 study indicates a similar number of launches and examines several approaches for implementing on-orbit operations. One approach involves a self-contained robotic assembly, capability in the payload to capture and assemble the hardware pieces into a space transfer vehicle. A second approach involves the same self-contained robotic assembly, but adds a depot node for storing hardware awaiting assembly, and for storing special assembly hardware and elements, such as a orbital debris shields until required for the next mission. Of these two assembly scenarios, the later approach minimizes the mass penalty on the departing Mars vehicle.

A third approach is the Space Station, or other free-flying LEO node, to support the on-orbit processing operations. Of the three approaches, this scenario imposes least mass penalty associated with on-orbit processing on the departing Mars vehicle. However, this scenario requires the most effort to establish the LEO supporting infrastructure.

Reference 12 has examined those tasks that must be performed in orbit to inspect, assemble, store and test a Mars (or lunar) transfer vehicle. Table 1 presents these functions for scenarios where more than two launches per piloted or cargo mission are required. Table 2 presents those on-orbit supporting systems required to enable these functions. A significant finding of this study was that the same in-space operations are required for each expendable space transfer vehicle regardless of launch vehicle size, and are repeated for each ETO launch. A recent MSFC trade study on ETO launch vehicle size, summarized in Figure 5, utilized these findings.[13] Consequently, the capabilities and systems required in a supporting role in orbit do not vary depending upon the size of

Table 1 Functions Involved in On-Orbit Operations

- **Deploy and erect structures**
- **Attach and assemble/disassemble components**
- **Inspect structures and components**
- **Calibrate systems and components**
- **Rendezvous and dock hardware**
- **Receive, berth and store components**
- **Maneuver components into position**
- **Manipulate structures and components**
- **Test and verify assemblies, systems, and components**
- **Make utility connections**
- **Provide effective lighting**
- **Communicate**
- **Generate and store power**
- **Control large space structures**
- **Provide thermal, radiation and debris protection**
- **Manage cyro fuel transfer and storage**
- **Manage mission data**
- **Provide support for contingency operations**

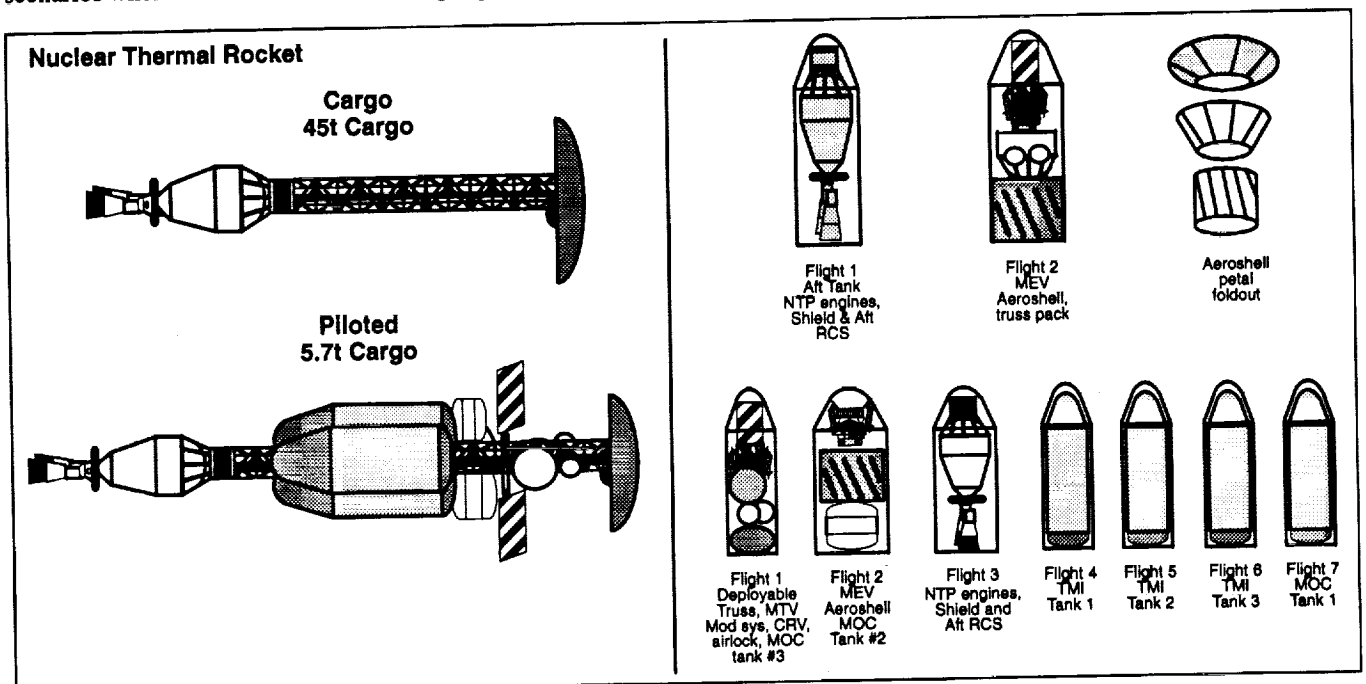

Figure 4 Launch Manifest for Mars Mission with 150mt Vehicle

Table 2 Supporting Systems Required for On-Orbit Operations

- Structural
- Robotic manipulators
- Data management computers and software
- Power generation and storage
- Communications hardware and software
- Remote sensors
- Visual inspection hardware and software
- Cryogenic fuel control
- Docking and berthing mechanisms
- Lighting units (fixed and moveable)
- Guidance, navigation and control
- Storage
- Shielding

the ETO launch vehicle. The design of the system, and the degree of astronaut involvement, is a function of which on-orbit infrastructure scenario is selected. This selection is strongly influenced by the technologies employed, which are discussed in the later section on Design Recommendations and Technologies.

Lunar Mission Hardware Assembly Operations

The on-orbit assembly and refurbishment of two different lunar transfer vehicles (LTVs) has been examined using approaches with varying degrees of automation in order to bracket the best and worst case scenarios. Additionally, two aerobrake concepts were studied, which vary from a self-deploying design to one that requires the assembly of 19 large panels. Previously developed methodologies and databases were used for these analyses.[14] Timelines refer to work shifts that are 8 hours in duration, and are for a dedicated on-orbit vehicle processing crew of four.

Lunar Transfer Vehicle Assembly and Turnaround

Quantifiable Space Shuttle ground processing tasks at Kennedy Space Center (KSC), as well as actual Shuttle EVA and remote manipulator experience in space, were used as analogies for LTV on-orbit assembly, refurbishment, and checkout tasks.[14] An Assembly/Servicing Facility located at Space Station Freedom (SSF) was used for LTV processing, and is further described in a following section on LEO Assembly Node Infrastructure.

The Option 5 LTV shown in Figure 6 was defined by the 90-Day Study on the Human Exploration of the Moon and Mars.[15] It has a core stage consisting of a crew module, core propellant tanks, and four RL-10 main engines. Liquid hydrogen and oxygen propellants are carried in four drop-tanks which are mated on orbit. An aerobrake requiring assembly

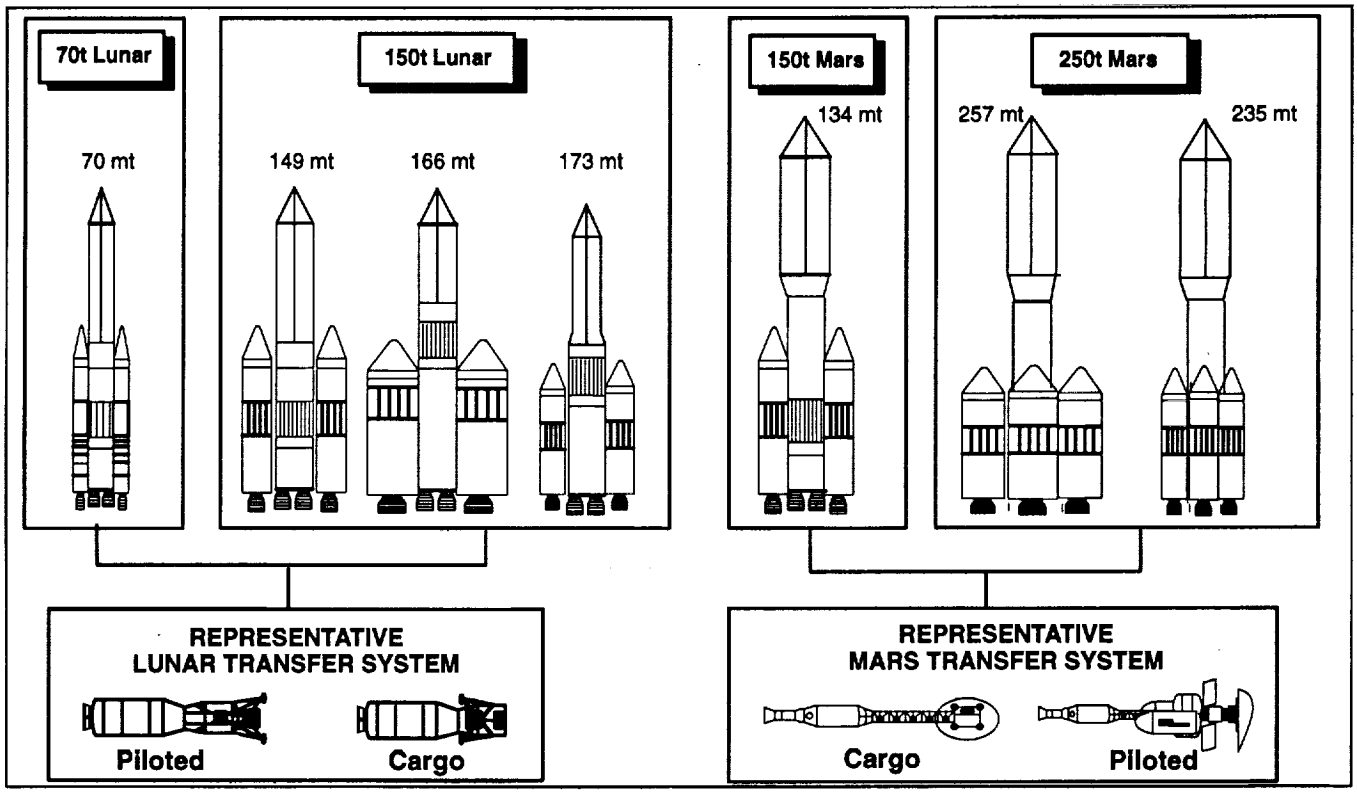

Figure 5 Summary of Trade Study to Assess Impact of Launch Vehicle Size on Complexity of On-Orbit Operations

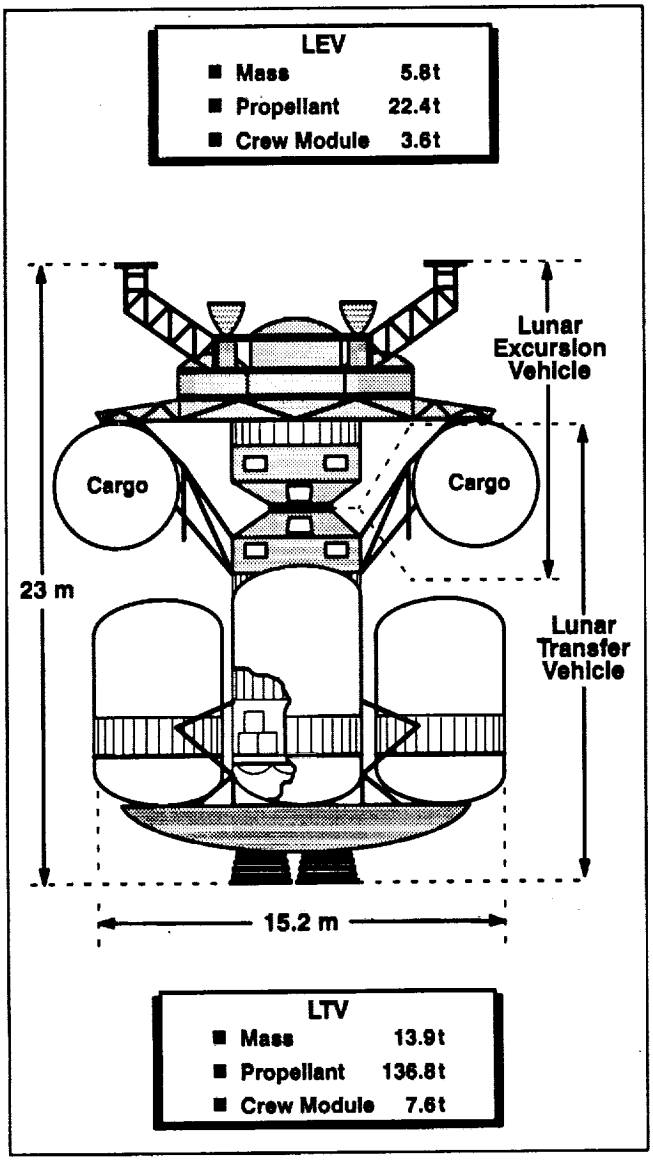

Figure 6 Option 5 Lunar Transfer Vehicle Configuration

of eight petals attached to a circular core is used for Earth-orbit capture at the end of the mission. Two cargo pods are carried by the LTV for transfer to a separate lunar excursion vehicle (LEV), which is based in lunar orbit. Three 71-ton Shuttle-C HLLVs and one Shuttle flight are required to deliver the LTV components to LEO. The processing scenario used for this Option 5 LTV is heavily dependent on use of EVA astronauts to accomplish manual tasks. Initial assembly of this LTV was estimated to take 69.5 work shifts (including 27 shifts of EVA), and is shown in Figure 7. Refurbishment and turnaround between missions will take 182.5 work shifts (including 53 EVA shifts), and is shown in Figure 8. Use of advanced telerobotics reduced the required EVA hours by 79%. If operation of the telerobots is performed from the ground, a 49% savings of IVA astronaut time can also be achieved. However, in order to achieve these savings in EVA and IVA astronaut hours, the total elapsed processing time may increase by 50% for initial assembly and 62% for turnaround.[14]

The second LTV selected for analysis, shown in Figure 9, was the Lunar 1-B Piloted Case LTV defined for the Marshall Space Flight Center's (MSFC) ETO Size Trade Study.[13] This LTV is based on Martin Marietta Corporation's (MMC) 4E-5B configuration[6], modified by substituting a Boeing crew module[7], and consists of a single propulsion/avionics/crew module core vehicle with five RL-10 main engines and six propellant drop-tanks. An improved deployable aerobrake (discussed further in the next section on Aerobrakes for Earth Return) is left in lunar orbit while the rest of the vehicle descends to the lunar surface. Following launch of the LTV from the lunar surface, the LTV rendezvous with and captures the aerobrake, and returns to SSF in Earth orbit via an aerocapture maneuver. Five 70-ton HLLVs are required to loft these LTV components to LEO,

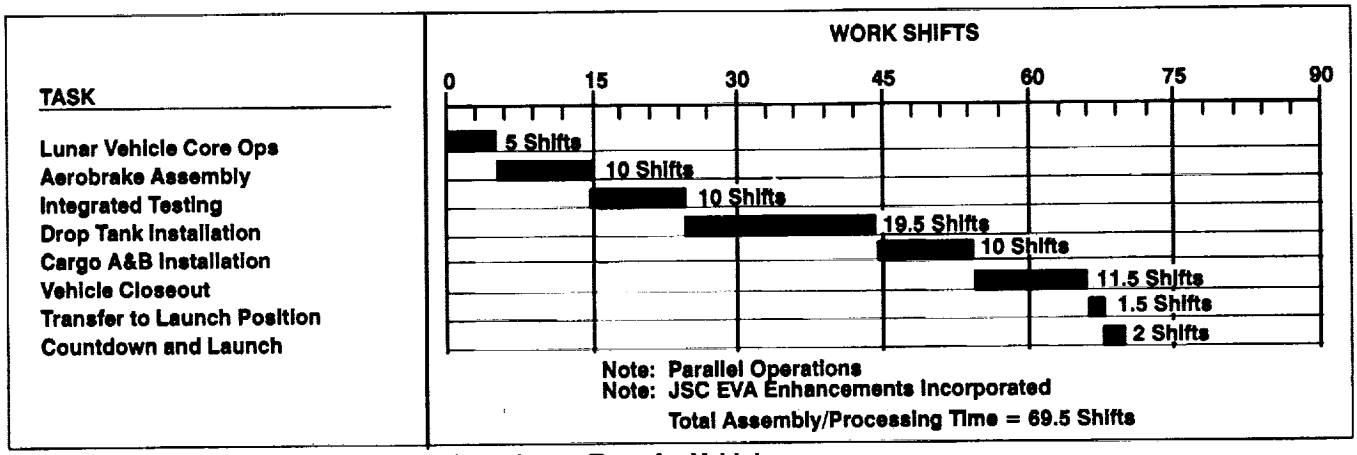

Figure 7 Assembly Timeline for Option 5 Lunar Transfer Vehicle

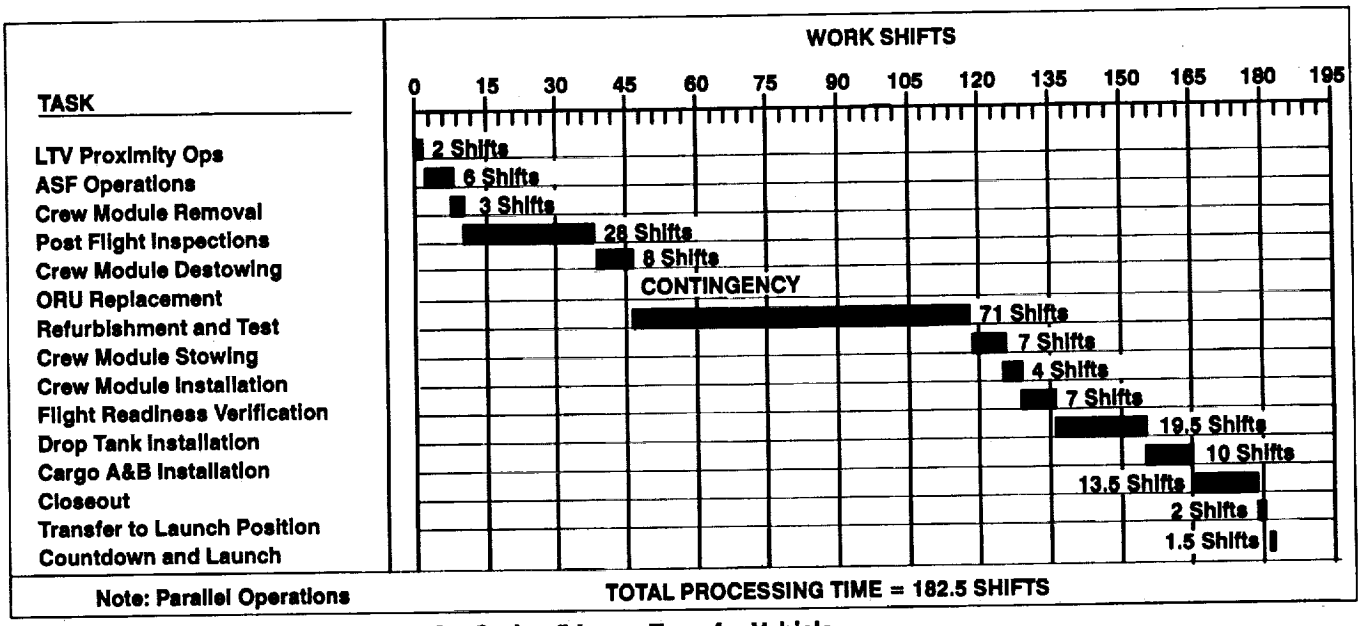

Figure 8 Refurbishment Timeline for Option 5 Lunar Transfer Vehicle

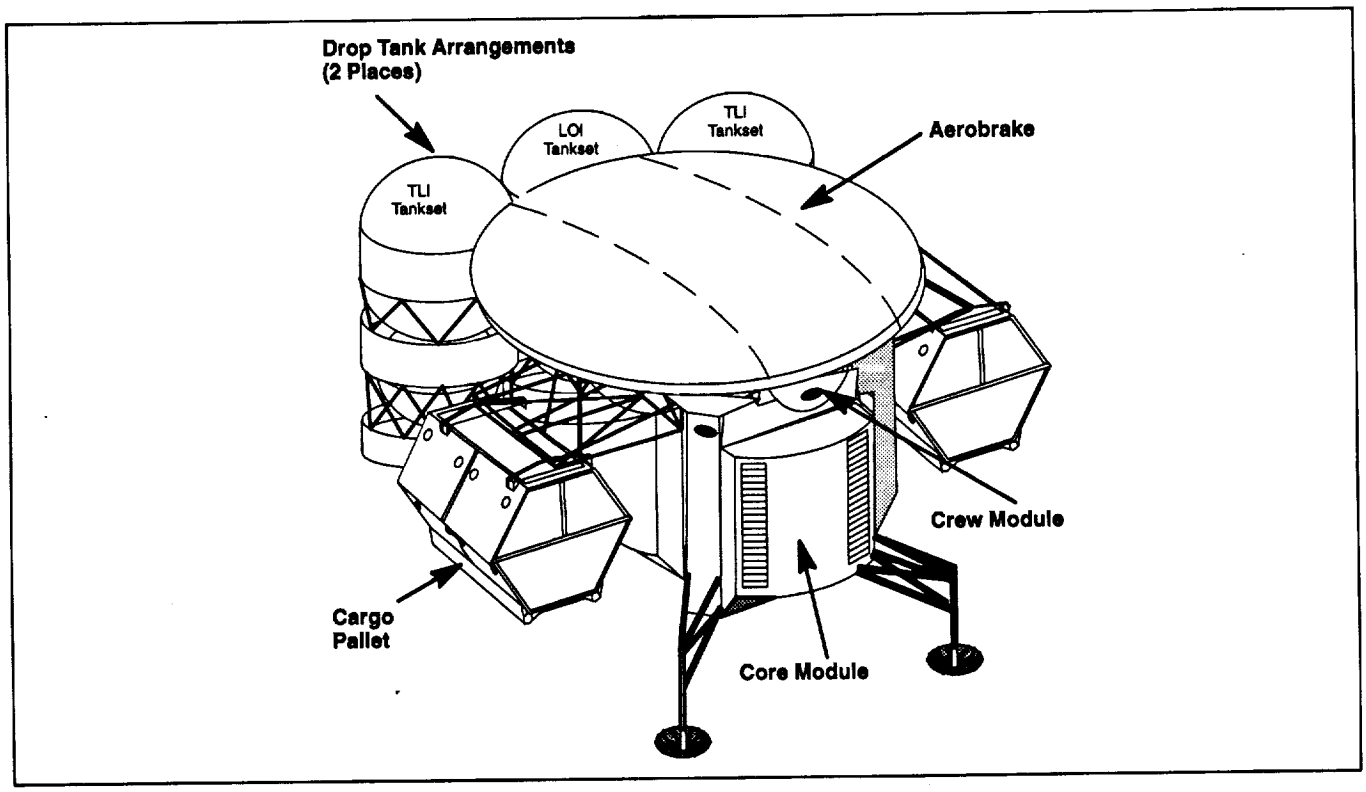

Figure 9 MMC Lunar Transfer Vehicle Configuration

as shown in Figure 10. A processing philosophy that minimizes on-orbit operations by forcing the LTV to be as robust and autonomous as possible was implemented at the direction of NASA Headquarters' Office of Exploration. Using this philosophy, initial assembly of the modified MMC LTV was estimated to take only 33 shifts (Figure 11), while turnaround between missions would take only 61.5 shifts (Figure 12). This represents a savings of 52% for assembly and 66% for turnaround as compared to the Option 5 LTV, while completely eliminating required EVA. These savings are made

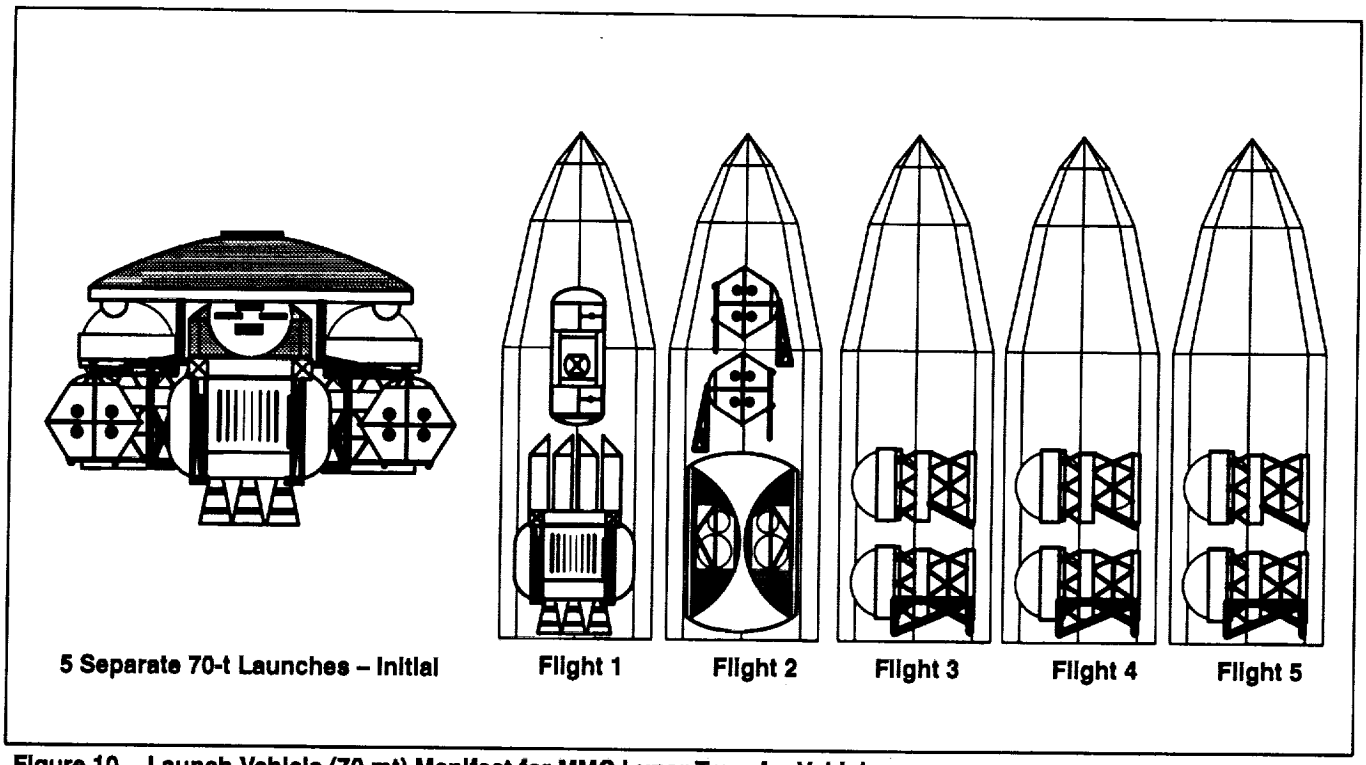

Figure 10 Launch Vehicle (70 mt) Manifest for MMC Lunar Transfer Vehicle

possible by incorporating the design recommendations and advanced technologies which were identified to reduce the labor intensive tasks based on vehicle processing analogies at KSC. These are discussed in detail in a following section on Design Recommendatons and Technologies.

For either the EVA-intensive Option 5 LTV assembly or the modified MMC LTV telerobotic assembly, the time interval between the HLLV ETO launches is longer than the time required to assemble and test the components. Therefore, ETO launch frequency is the limiting factor that determines the on-orbit processing time for initial LTV assembly.

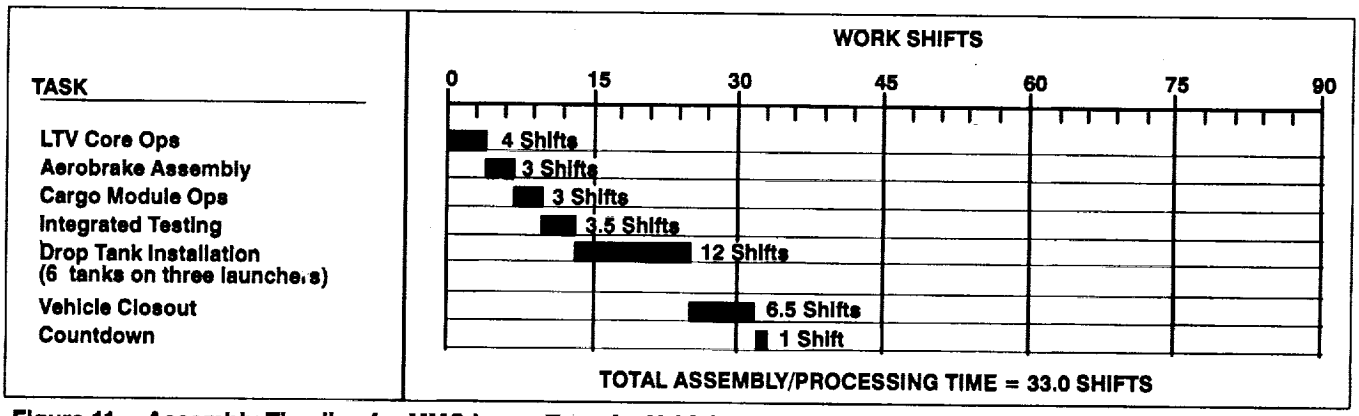

Figure 11 Assembly Timeline for MMC Lunar Transfer Vehicle

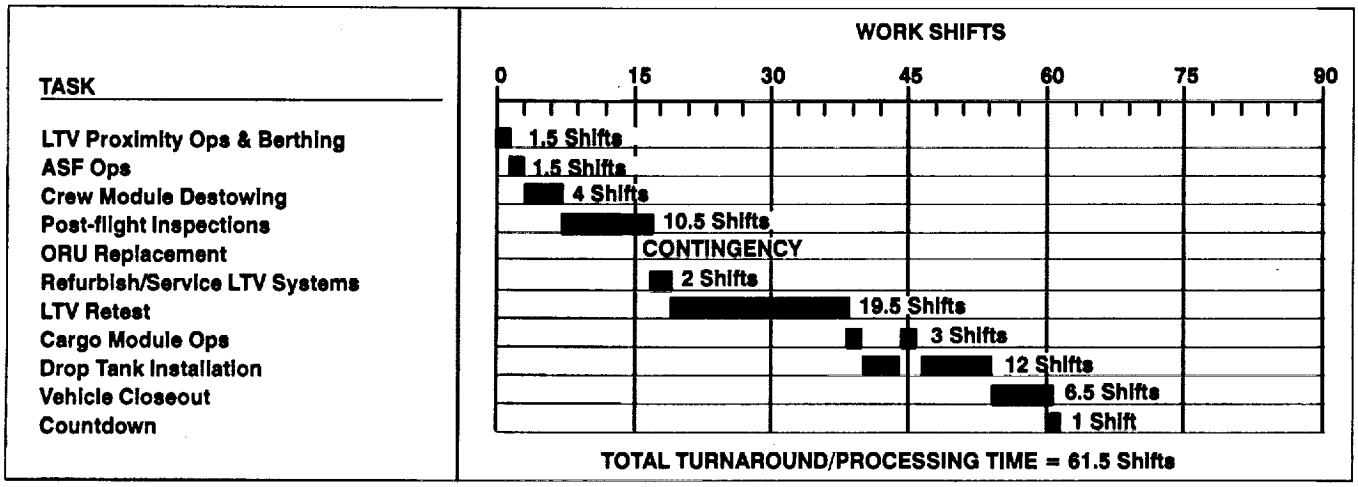

Figure 12 Refurbishment Timeline for MMC Lunar Transfer Vehicle

Aerobrakes for Earth Return

The aerobrake concept generated by Langley Research Center's Space Exploration Initiative Office is shown in Figure 13. It is 50 feet in diameter, has a lift-to-drag (L/D) ratio of 0.15, and consists of 19 hexagonal panels with pre-atttached thermal protection tiles.[16] This concept purposely included

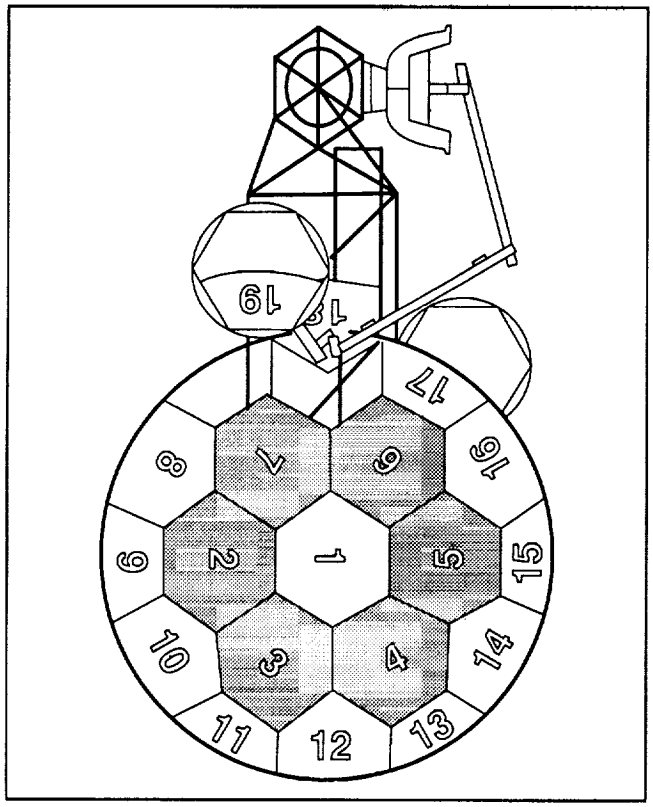

Figure 13 Robotic Assembly of Hex-Panel Aerobrake Configuration

assembly and was selcted to evaluate packaging a large aerobrake in a small volume. Such a concept could also be valuable where a higher packaging density is required in a large volume HLLV to minimize the number of ETO launches. Joint design is such that a total of 305 captive bolts (spaced at one foot intervals along the joints) require torquing. However, no thermal protection closeout is required along the panel joints. Upon completion of aerobrake structural assembly, the docking ring, attitude control thruster assemblies, hydrogen boil-off storage tank, and avionics package must be installed and verified. In accordance with the NASA Headquarters' Office of Exploration philosophy to make on-orbit operations as autonomous as possible, a scenario using telerobotic assembly was developed. Assumptions included the addition of a turntable to Space Station Freedom, and use of the station's telerobots for this assembly scenario. The resulting 80.7 hour (10 shift) processing flow is shown in Figure 14.

To bracket the opposite end of the on-orbit operations spectrum (i.e., no assembly and no supporting infrastructure required), the Martin Marietta rigid deployable aerobrake shown in Figure 15 was analyzed. It is 45 feet in diameter, and has an L/D of 0.14. This aerobrake is the one used for the assembly analysis of the previously described modified MMC LTV.[17] All docking mechanisms, attitude control thrusters, propellant tanks, and avionics are pre-integrated into the aerobrake prior to launch. Following electro-mechanical self-deployment of its side wings, a pressure decay leak check between joint seals is performed to verify joint integrity. The deployment and checkout flow of 23 hours (3 shifts) for this aerobrake is shown in Figure 16.

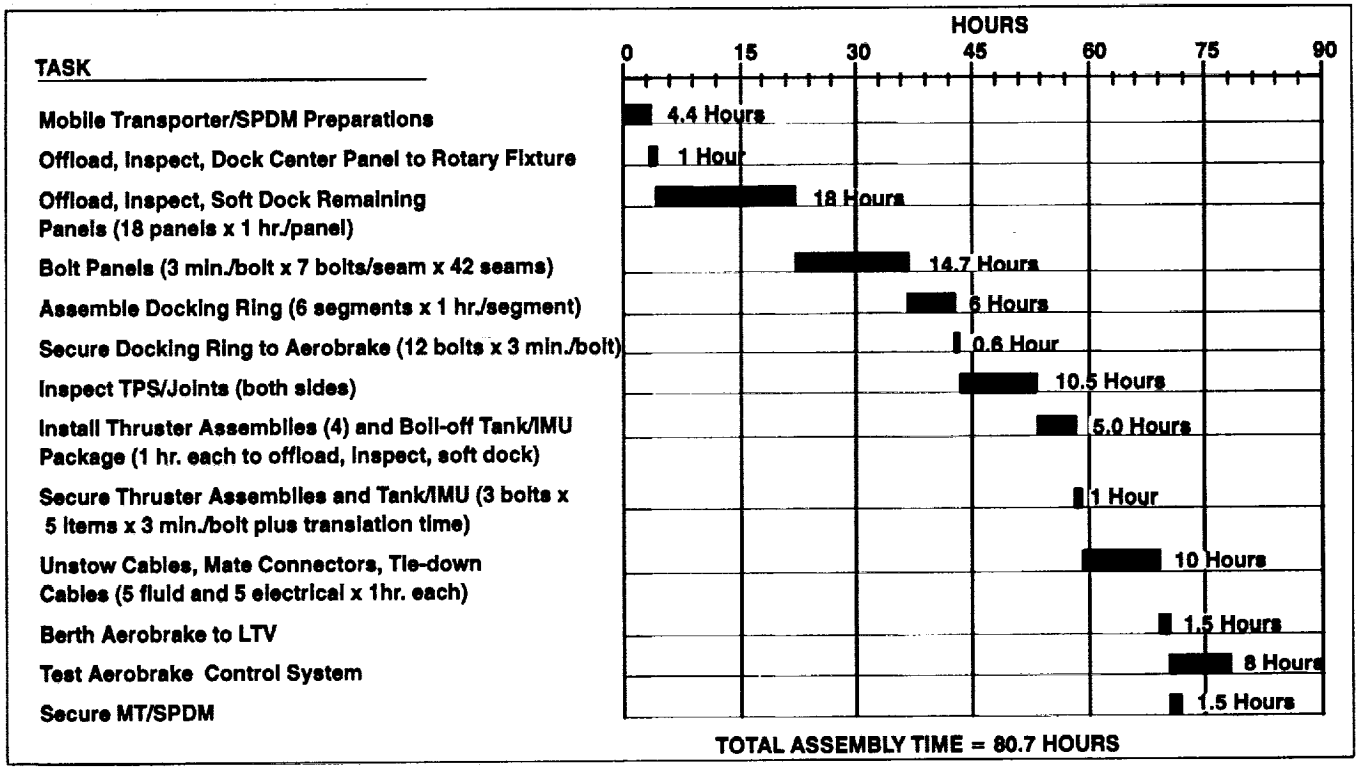

Figure 14 Assembly Timeline for Hex-Panel Aerobrake

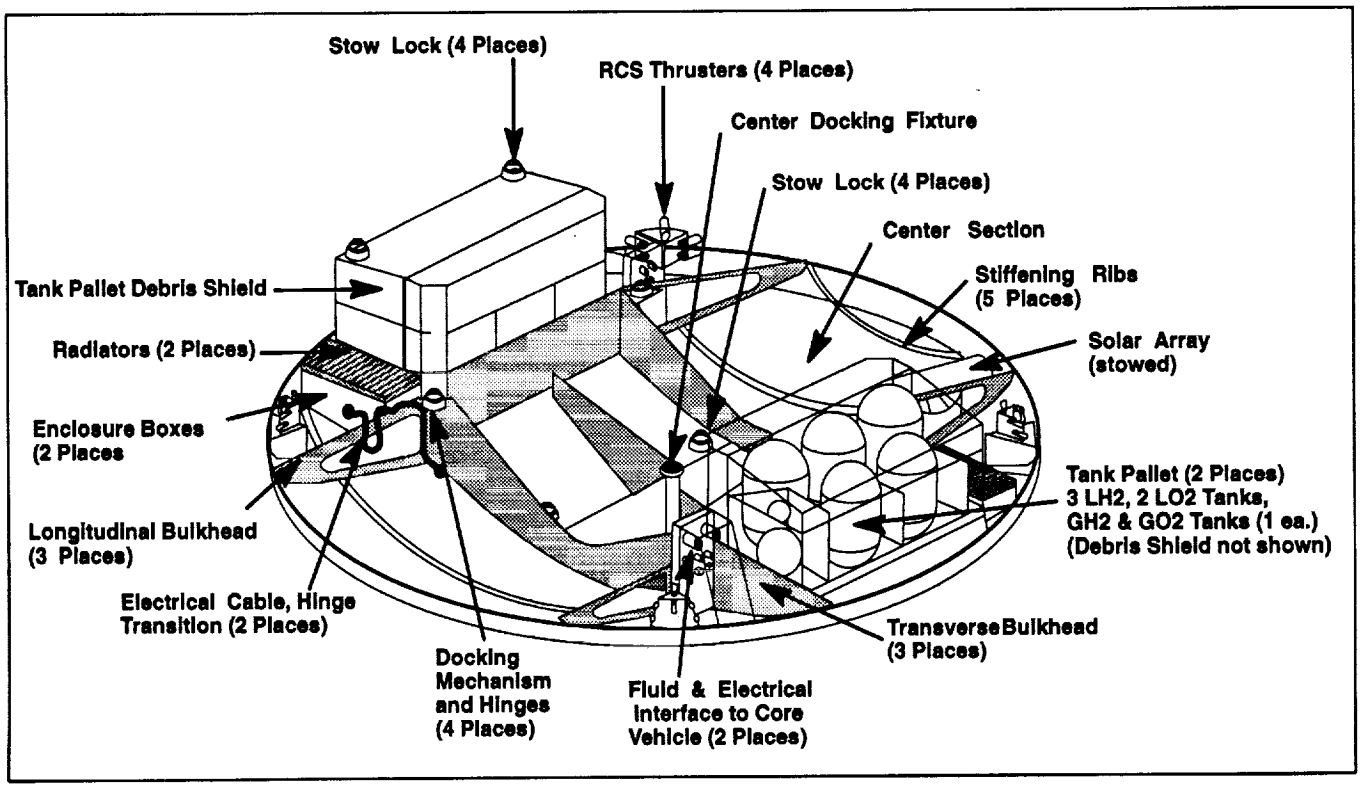

Figure 15 MMC 3-peice Aerobrake Configuration

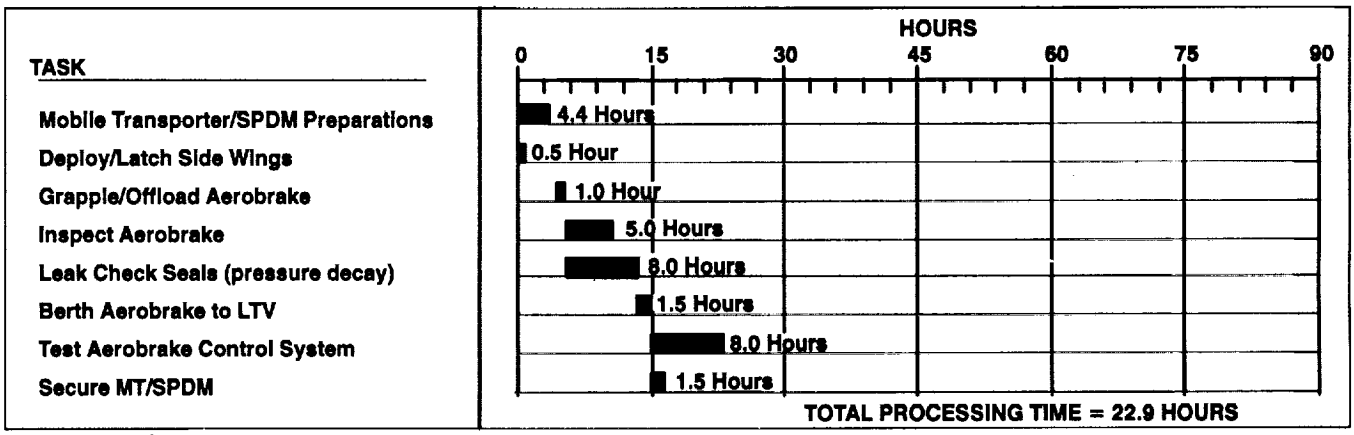

Figure 16 Processing Timeline for 3-piece Aerobrake

These two examples of aerobrake LEO processing, along with the EVA/telerobotic co-operative assembly of the Option 5 LTV eight petal aerobrake demonstrated with a neutral bouyancy simulation,[18] indicate that on-orbit assembly of aerobrakes can be accomplished in a timely manner, and should be considered as an option for the Space Exploration Initiative. Large diameter ETO launch vehicle shrouds currently being considered for SEI will permit lunar aerobrakes in the 50 foot diameter class to be launched fully ready for flight.

Mars Mission Hardware Assembly Operations

On-orbit assembly analyses were performed for nuclear thermal propulsion (NTP) Mars transfer vehicles (MTVs) manifested on both 200-ton and 150-ton HLLVs. The application of aerobraking at Mars orbit aerocapture, Mars entry, and Earth return are also addressed.

Mars Transfer Vehicle Assembly

The MSFC/Boeing NTP Mars transfer vehicle, shown in Figure 17, was analyzed for on-orbit assembly.[19] The forward core vehicle consists of the crew habitat module, along with attitude control, power (solar arrays), thermal control, communications, and avionics systems. Attached to the habitat module is the crew return vehicle (CRV) used for direct entry upon Earth return. Connecting the forward core vehicle to the aft core propellant tank and twin nuclear engines is a strongback structure consisting of three conical trusses, which are nested together for ETO launch, and then separated, flipped, and mated together on orbit. Three additional drop-tanks filled with liquid hydrogen are mated to the truss structure and twin 12-inch propellant feedlines are connected between the drop tank manifold and the aft nuclear propulsion system. Remotely mated umbilicals on carrier plates were substituted for the Boeing baselined Marmon clamps (which would be difficult for a robot to install). A high L/D Mars excursion vehicle (HMEV) is docked directly to the crew habitat module, and contains the pre-integrated Mars surface habitat and science payloads. These MTV components are manifested on five 200-ton HLLVs. The HMEV is manifested to be launched on the side of an HLLV as shown in Figure 18. The MTV is 101 meters in length and total mass prior to Earth departure is 817 tons.

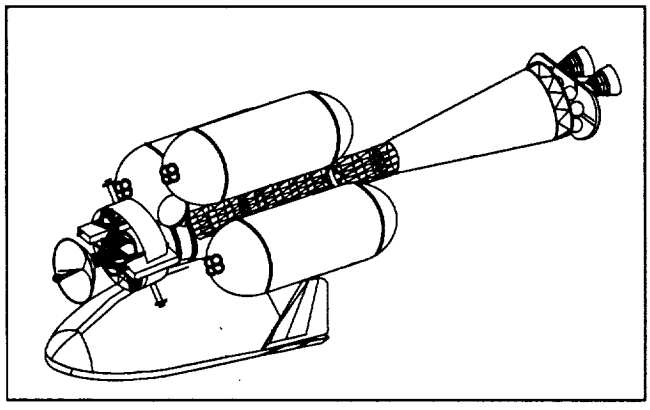

Figure 17 Boeing Mars Transfer Vehicle Configuration

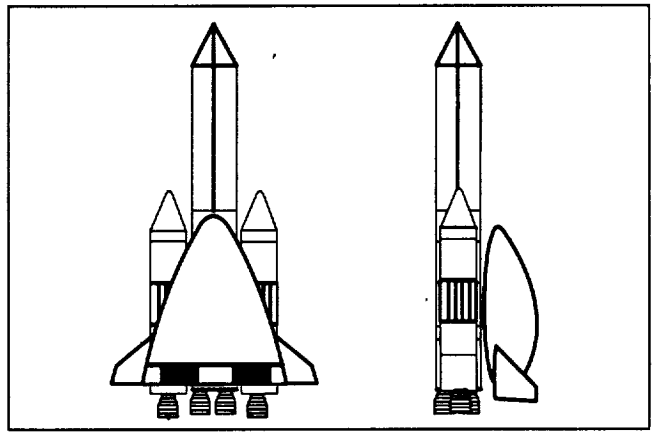

Figure 18 Boeing Concept for Launching Assembled Mars Entry Vehicle

The telerobotic on-orbit processing flow of 43 shifts for assembly of this MTV is shown in Figure 19. As with the LTV assembly flows previously discussed, the interval between ETO launches is longer than the time required to assemble the MTV components being brought up by each HLLV. A minimum assembly node, which can provide attitude control and electrical power, and serve as a platform for a manipulator arm (with a dextrous end effector) and debris shield storage, is baselined for this analysis. Possible node concepts that could accommodate MTV assembly are discussed in a following section on LEO Node Infrastructure. If the "self-build" or "free-flyer" concept is selected, additional tasks and time must be added to the processing flow for top-off of expended MTV consumables. Mandating that the propulsion system nuclear reactors be launched cold (no prior run

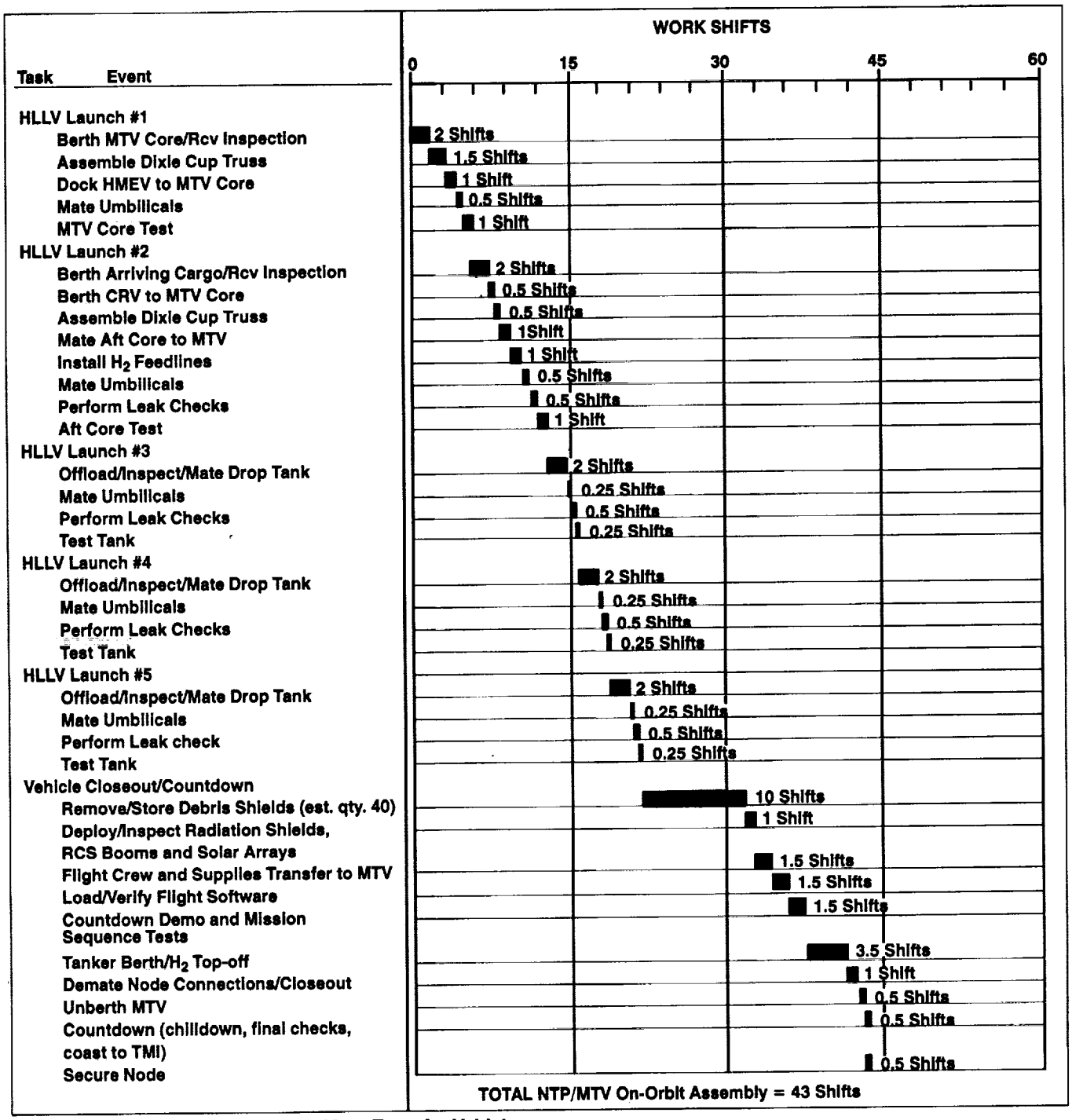

Figure 19 Assembly Timeline for Mars Transfer Vehicle

time) eliminates build-up of fission products and associated radiation hazards.

Manifesting a similar piloted MTV, shown earlier in Figure 4, on a smaller 150 ton HLLV would require seven ETO launches.[13] Additional propellant tanks, debris shields, and aerobrake deployment and checkout operations would add 18 shifts to the on-orbit processing flow for the 200-ton HLLV-manifested MTV.

Mars Mission Aerobrake Applications

The utilization of aerobrakes (any vehicle element which uses aerodynamic forces for velocity reduction) for several phases of the Mars mission can result in significant vehicle LEO mass reductions. These phases are capture into Mars orbit after transit from Earth, entry to the Mars surface from Mars orbit, and capture into Earth orbit or direct Earth entry after transit from Mars. Preliminary studies indicate that aerobrake diameters of about 100 feet will be required for Mars orbit aerocapture and about 50 feet for Mars entry and Earth aerocapture return. Delivery of such large, fully assembled aerobrakes to Earth orbit could require an approach such as that illustrated in Figure 18 or a very large HLLV shroud. Alternatively, an assembly approach as illustrated in Figure 13, or a deployable approach, as illustrated in Figures 15 and 20, would be required. Figure 21 is a recent MSFC folding concept for the Mars entry aerobrake where heating rates and loads are relatively lower than for Mars/Earth aerocapture or Earth entry. The assembly approach of Figure 13 would obviously require the most on-orbit supporting infrastructure. The deployable approach for Figure 20 essentially eliminates assembly, but would require many of the typical on-orbit functions i.e., inspection etc. Likewise, the umbrella approach of Figure 21 also essentially eliminates assembly but would require other on-orbit functions.

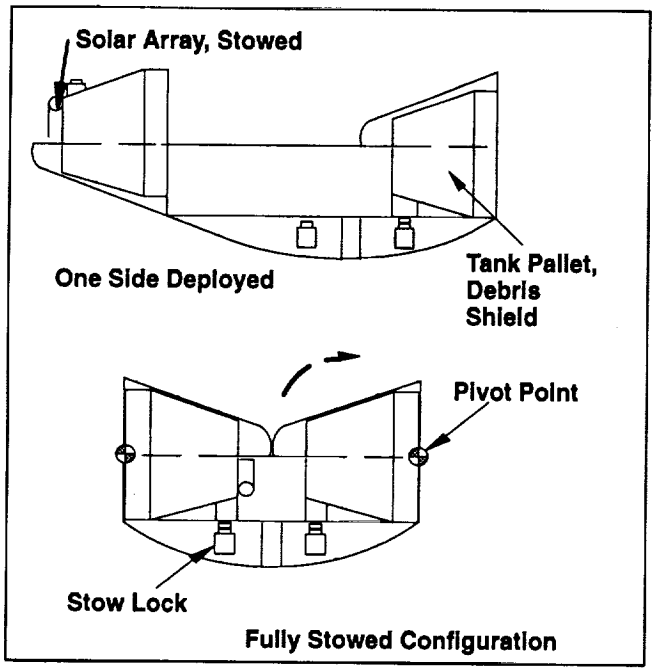

Figure 20 Three-piece Aerobrake Folding Geometry

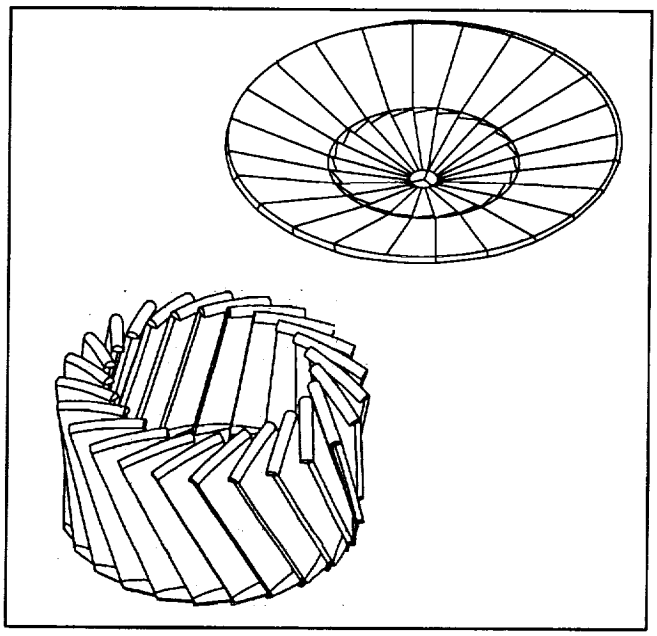

Figure 21 Boeing Umbrella Aerobrake Configuration

No one aerobrake size or structural concept will suffice for all potential lunar and Mars mission applications. Viable aerobrake concepts have been developed for each potential application. A significant consideration for each concept is to optimize, within practical limits, the combination of aerobrake packaging for delivery to Earth orbit and the required on-orbit operations.

LEO Assembly Node Infrastructure

Recent studies have begun to indicate those mission scenarios which will likely need an orbital supporting infrastructure. Whether any supporting infrastructure for any mission is required depends heavily on the size and design of the space transfer vehicle and the number of launches from the Earth required to deliver the vehicle elements to low earth orbit. Based on current SEI architecture concepts and today's launch vehicles, either a lunar or a Mars transfer vehicle would require multiple launches to LEO and would require some degree of on-orbit support to assemble and checkout the vehicles. While HLLVs possessing the required lifting and volume capabilities may become available to permit single launch lunar missions, HLLVs with similar capabilities for a Mars mission are extremely unlikely. Thus, it can be stated with assurance that Mars vehicle assembly will require a degree of on-orbit support. This eventual need for a Mars mission LEO infrastructure should be considered when selecting lunar mission approaches.

Studies such as this have been undertaken and require further effort before an appropriate approach for a particular mission or a class of missions is identified. The high costs associated with on-orbit supporting infrastructure will force careful justification of such a mission element. The on-orbit supporting elements will likely be selected only if they are an enabling element that has no practical substitute in space transfer vehicle design or launch vehicle capability.

References 12 and 20 are two of the recent studies about the on-orbit support functions to be provided by the on-orbit infrastructure. Reference 21 is a preliminary look at the technologies requiring advancement if these functions are to be provided. Not all these functions or technologies would be required in a first mission, but are thought to be needed by the time repetitive Mars missions and a permanent lunar base are being implemented. Early lunar missions may be single-launch, or at least dual-launch rendezvous/capture missions, and will probably each be self-sufficient and independent of any on-orbit support.

The break point for requiring on-orbit support and infrastructure appears to occur when the space transfer vehicle requires more than two launches, requires fueling operations, requires robotic or EVA assembly, or involves refurbishment operations prior to a next mission. Several on-orbit supporting infrastructure concepts have been studied, ranging from an evolved Space Station Freedom to a smaller free-flying assembly node to self-contained robotic arms on the vehicle being assembled.

Figure 22 is an early concept of how Space Station Freedom might evolve to accommodate assembly, checkout, and refurbishment of lunar and Mars vehicles. Recent studies seem to indicate that the large size of the current Mars vehicle concepts are not compatible with the current Space Station Freedom resources available. Figure 23 is a concept for an assembly/servicing facility for processing lunar transfer vehicles, and would be located on a lower keel truss of the evolved station.[22] Reference 23 indicates that many Space Station Freedom elements may be usable as SEI vehicle elements.

Figure 24 shows a man-tended orbital node for Mars vehicle assembly. Depending upon launch vehicle size, as many as five (250mt) to seven (150mt) HLLV launches could be required to deliver all vehicle elements to Earth orbit. Besides assembling and checking out the vehicle, its elements must be protected from orbital debris for the assembly duration. A minimum of 30 days between launches is expected. Man-tended implies that the crew is sheltered elsewhere, perhaps at Space Station Freedom, during the assembly and check-

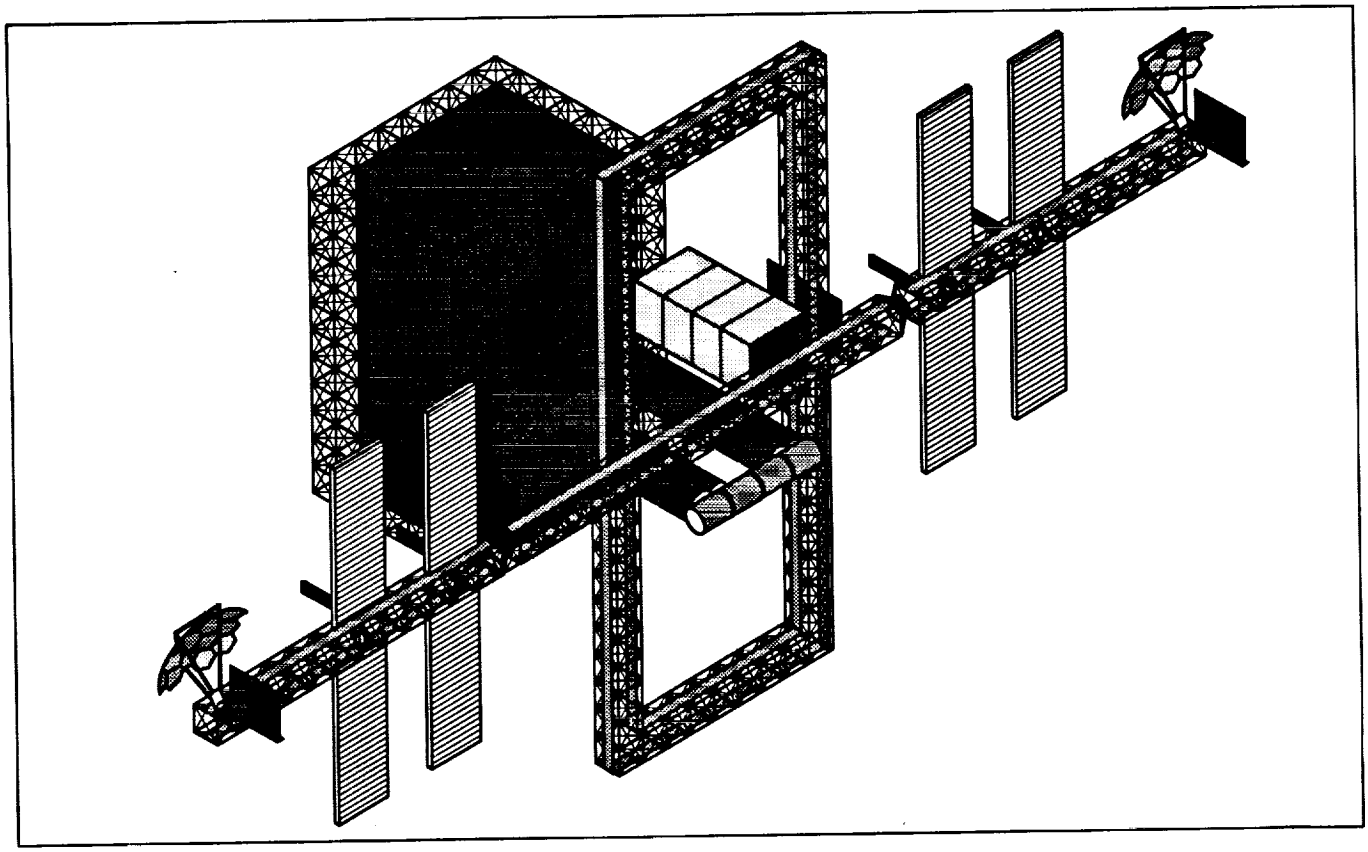

Figure 22 Space Station Evolution Concept for Mars Mission Accommodation

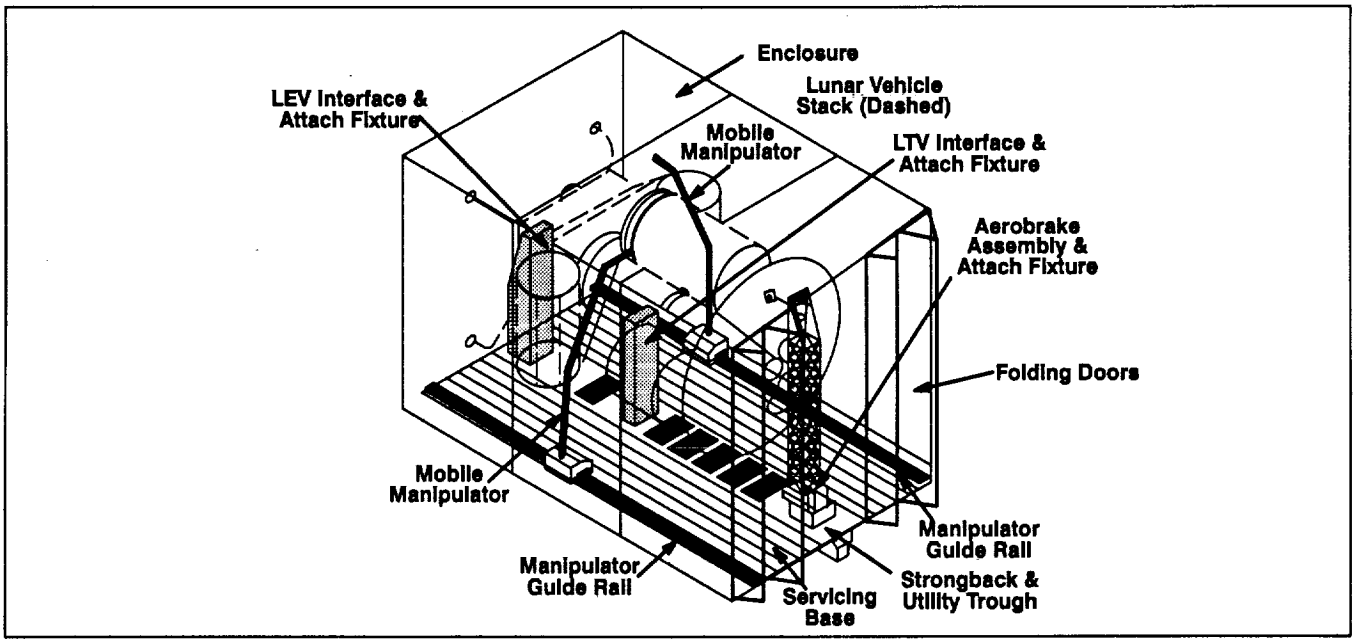

Figure 23 Space Station Hangar Concept for Lunar Vehicle Processing

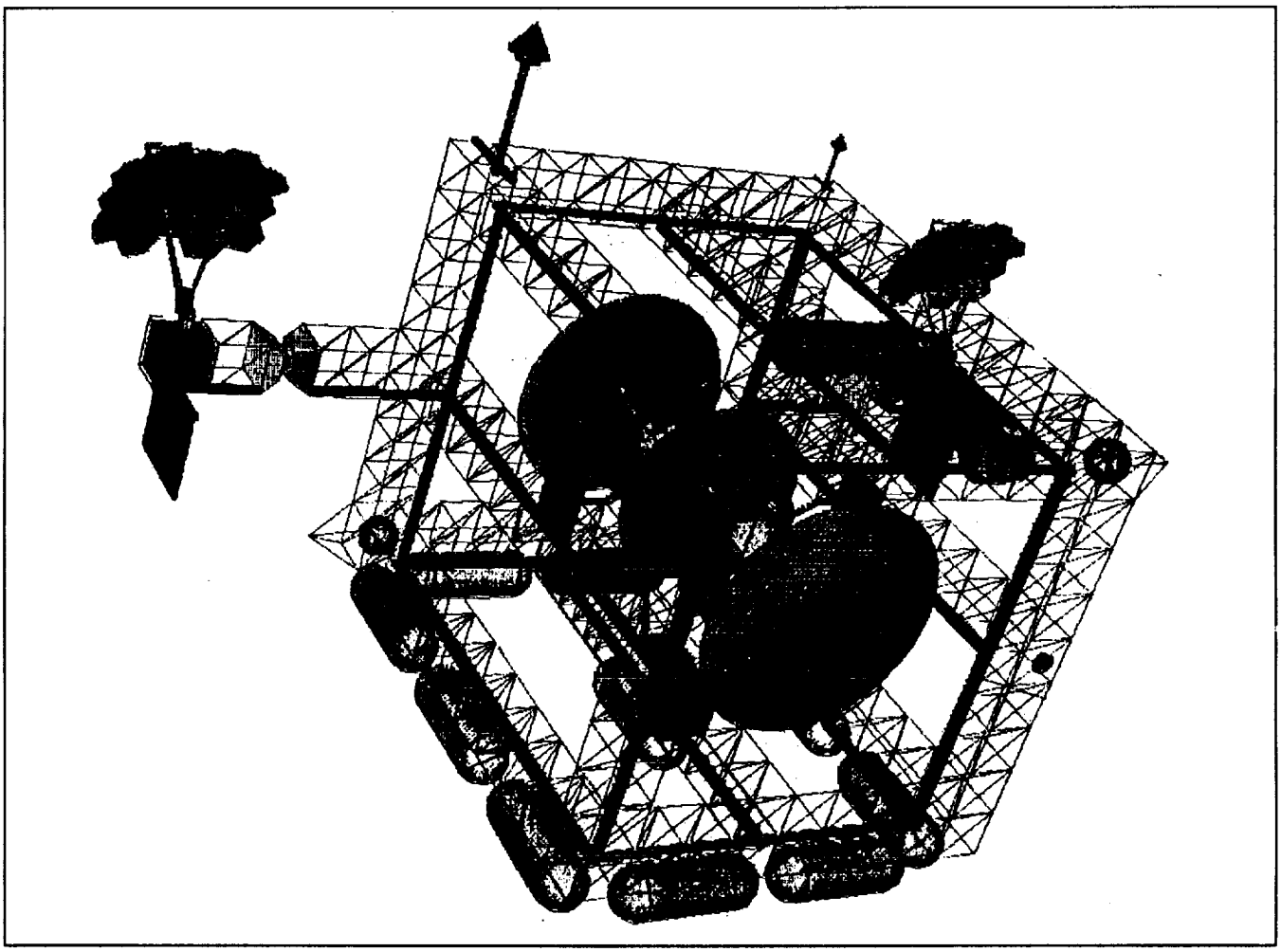

Figure 24 Concept of LEO Node for Vehicle Assembly

out period. While the man-tended approach may be intended to reduce cost, it will require a crew transportation vehicle to move between nodes. Such a man-tended node may or may not contain fueling tanks, depending upon safety demands. Figure 25 is an early concept for a fueling depot node. Safety considerations and vehicle design will determine if such an independent node is appropriate. If so, crew transport is again required. Figure 26 is a more recent Boeing concept for Mars vehicle assembly. It would be man-tended and specific to the processing scenario for a Mars transfer vehicle.

A final recent concept for supporting on-orbit operations has been developed by Boeing and involves a robotic crawler with arms able to effect self-assembly through berthing and other robotic operations. While astronaut involvement on-orbit is minimized, there would be mass inefficiencies in the vehicle required to support the robotic hardware. Additional time, logistics, and cost to replenish vehicle consumables will be required if the vehicle must serve as its own assembly node. Also, provision for orbital debris shielding offers another complexity and inefficiency, unless the shields are left in Earth orbit. If such hardware is left in LEO and not used for subsequent missions, disposal in a safe manner is required.

Requirements for the LEO supporting infrastructure can only be generalized at present, and is not required for some mission concepts. More mature launch and space transfer vehicle concepts will permit further definition of these requirements. Mars vehicle assembly and the reusable-hardware mission scenarios will require a supporting on-orbit infrastructure.

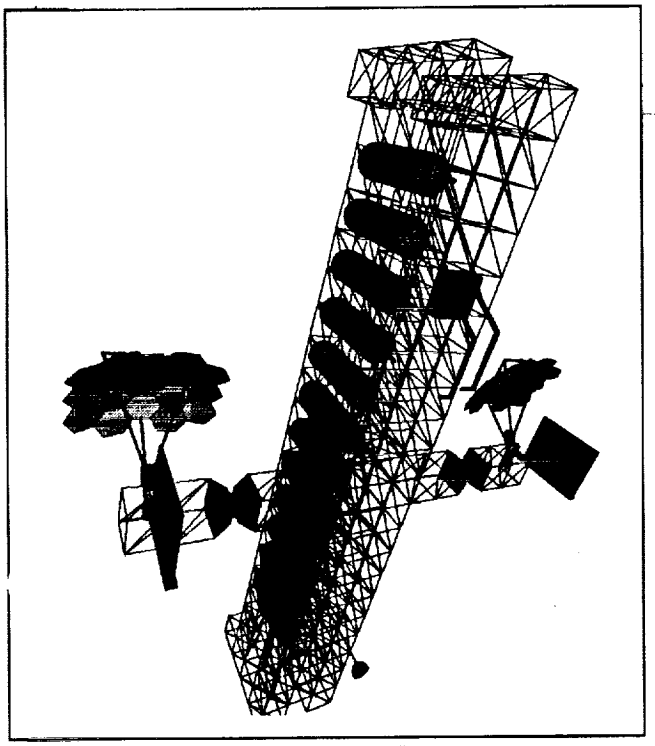

Figure 25 Concept of LEO Fuel Depot

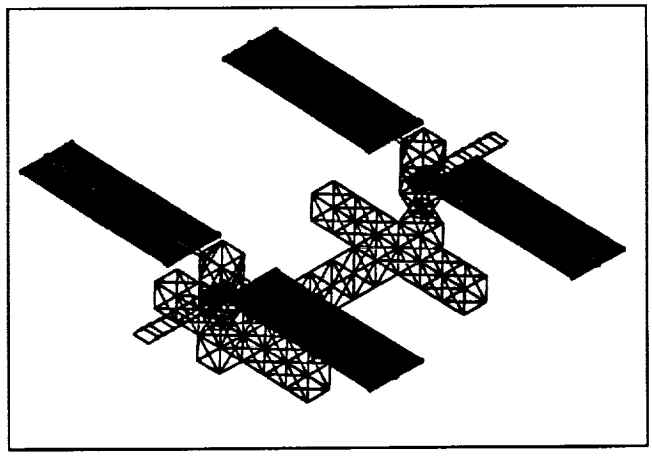

Figure 26 Concept of Minimal LEO Node for Mars Vehicle Assembly

Design Recommendations and Technologies

The design recommendations and technology needs listed in Tables 3 and 4 are applicable to any manned or unmanned space vehicle which utilizes on-orbit processing operations. They have been selected for the high leverage they will provide in reducing the the most labor intensive tasks identified from vehicle processing analogies at KSC.

A prime example of these savings is the elimination of 16 shifts of EVA required to intrusively inspect LTV main engine turbopumps with borescopes, by incorporating built-in engine plume analysis sensors for detection of turbopump blade and bearing-wear long before failure. Other propulsion recommendations include using electromechanical actuators for engine gimbaling, thus eliminating the need for complex, service-intensive hydraulic systems. To minimize the risk of on-orbit propellant leaks, which may be difficult to isolate and repair, propellant systems should be integrated on the ground as complete stages whenever possible. Use of expendable propellant drop tanks for reusable vehicles presents a significant risk to mission reliability due to the repeated disturbances of critical cryogenic connections. Propellant resupply using fluid transfer from tankers or a propellant depot will reduce opportunities for leaks, thus increasing mission reliability.[24] The need for redundant seals on all fluid system components is evidenced by the hydrogen leaks that grounded the Space Shuttle fleet in 1990 due to single seals on valve shafts.

Attachment recommendations include autonomous electrical and fluid umbilical connections (using a structually mated carrier plate), which would eliminate many EVA hours for this recurring task. Orbital replacement units (ORUs) need to be of a "snap-in" modular design with self-

Table 3 Vehicle Design Recommendations

GENERIC	PROPULSION
■ Design serviceable hardware for ease of EVA/ telerobotic access, including sufficient spacing between parts ■ Design for automation with self-aligning mating components, partial-turn connectors, and pre-defined visual cues ■ Include integrated grapple fixtures on all manipulated elements ■ Design to allow on-orbit disassembly to facilitate repair or recovery for assembly problems ■ Provide EVA backup capability for all telerobotic tasks ■ Minimize number of parts to be handled/assembled	■ Integrate propellant tanks, engines, and manifolds on ground whenever possible ■ Develop engines not requiring intrusive inspection and servicing ■ Utilize electromechanical actuators for engine gimbaling ■ Utilize propellant transfer from tanker/depot for reusable vehicles ■ Utilize redundant seals on all fluid joints
ATTACHMENT	**CREW MODULE**
■ Provide automated umbilical mate/demate with auto-verification of interface ■ Provide "snap-in" mounting of ORUs ■ Avoid threaded fasteners	■ Skylab type waste management unit ■ Berth transfer vehicle directly to pressurized node for servicing

mating connections. Threaded fasteners for on-orbit use should be avoided since galled threads on fasteners have been a very common problem on flight hardware at KSC. Captive, partial-turn fasteners will facilitate both EVA and telerobotic connection tasks.

Crew module refurbishment recommendations begin with a "Skylab" type of commode (utilizing fecal bags) to eliminate the lengthy refurbishment required for a "Shuttle" type waste management facility. The labor intensive refurbishment of the crew module between missions requires IVA access from pressurized modules in order to eliminate what would otherwise be excessive EVA transfers. Coupled to this is the desire to leave the crew module attached to the LTV core vehicle to eliminate the reconnection and verification tasks. It is therefore recommended that a returning transfer vehicle be berthed directly to a pressurized node. Use of a pressurized transfer tunnel (similar to an airport jetway) is an alternative if the vehicle must be berthed in a remote facility (such as a hanger on the SSF lower keel).

Table 4 Needed Technologies for On-Orbit Vehicle Processing

- Robotics
  - Dexterous end effectors
  - Automated umbilicals
- Artifical Intelligence/Expert Systems
  - Inspection
  - Diagnostic checkout
- Vehicle Health Management
  - BIT capable of fault detection/isolation to ORU level
- Zero-Gravity Cryogenic Fluid Management
  - Transfer
  - Long term storage
  - Leak detection/isolation
- Advanced Power Components
  - Fuel cells
  - Batteries

Generic design guidelines will enable and enhance both EVA and telerobotic accomplishment of tasks and ensure that recovery from problems is possible. Access to hardware requiring servicing or change-out, without having to first remove other hardware, has been a major design problem on current flight vehicles. Whenever telerobotics and automation are used to replace EVA for accomplishment of manual tasks, EVA back-up capability must be maintined for contingencies.

The advanced technologies needed to implement these vehicle design recommendations are listed in Table 4. Robotic technologies, such as dexterous end effectors and automated umbilicals, will eliminate much of the needed EVA. Expert systems using artificial intelligence for inspection and diagnostic testing will permit significant reduction in astronaut IVA hours for vehicle processing. Inspection is a repetitive task which can be automated with "before and after" image comparison techniques to detect anomalous conditions. Vehicle health management (VHM) with "built-in test" (BIT)

equipment (sensors and software) could provide fault isolation capability to the ORU level and greatly reduce the amount of orbital support equipment needed. VHM should also provide automated verification of continuity across all pins when umbilicals are mated. Finally, VHM could perform system and component trend analysis, thus eliminating unnecessary retest of healthy components.

Zero-gravity transfer and long term storage of cryogenic fluids is required, along with leak detection and isolation techniques. Advanced fuel cells and batteries could greatly reduce the extensive conditioning and monitoring that current components require.

Current programs such as Space Shuttle and Space Station Freedom started out down the path of reduced operations and life cycle costs. As budget realities set in, development and application of advanced technologies were cut, with the resulting impact of increased operations and costs downstream. If advanced technologies are not mandated for SEI flight vehicles, on-orbit processing can still be accomplished using EVA and SSF-era telerobotics. However, the magnitude and complexity of labor-intensive tasks will greatly increase, with resulting negative impacts to on-orbit infrastructure requirements and costs. It should also be noted that incorporation of these advanced technologies into vehicle designs not only facilitates on-orbit processing operations, but should also reduce the complexity and time required for ground checkout at the launch site. Additional rationale, along with readiness levels for these and other technologies applicable to on-orbit vehicle processing operations, are discussed in Reference 21.

Concluding Remarks

All studies to date indicate that Mars transfer vehicle assembly will require some degree of on-orbit support. On-orbit support for lunar vehicles may be needed, depending on the mission scenario and ETO launcher selected. Any scenario involving more than two ETO launches per transfer vehicle, fueling operations, robotic or EVA assembly, or refurbishment operations prior to a next mission, will likely require a LEO supporting infrastructure.

Any on-orbit supporting infrastructure required for LEO vehicle processing operations is determined by the complexity and amount of on-orbit assembly and servicing operations, which in turn is dictated by the design of the flight vehicle hardware elements.

On-orbit supporting infrastructure elements will be used only if they are enabling elements that have no practical substitutes in space transfer vehicle design or launch vehicle capability.

The on-orbit processing operations required to prepare any large space transfer vehicle for its initial mission are the same regardless of ETO launcher size. However, the number of repetitions of those tasks is a function of the ETO launch vehicle size. Refurbishment of reusable manned vehicles increases the quantity and complexity of tasks.

The time interval between HLLV ETO launches is longer than the time required to initially process (either manually or telerobotically) the vehicle components being brought up by each HLLV.

On-orbit assembly of aerobrakes can be accomplished in a timely manner and should be considered as an option for the Space Exploration Initiative. Deployable aerobrakes eliminate assembly, therefore reducing on-orbit operations and supporting LEO infrastructure requirements.

Space transfer vehicles must allow simple and adequate access to all serviceable hardware without having to remove and replace (and retest) other hardware in the way.

On-orbit vehicle processing can be accomplished with current technologies and practices, but incorporation of advanced technologies into space transfer vehicle designs will greatly reduce the complexity and magnitude of labor-intensive tasks.

Acknowledgements

Results of work performed by McDonnell Douglas Space Systems Company, Kennedy Space Center Division, under NASA contract NAS10-11400, are included in this paper.

The authors are pleased to thank the following individuals for their assistance in developing material for this paper:

Mr. Mike Tucker, NASA Marshall Space Flight Center, for space transfer vehicle concepts and manifests used by the ETO-Size Trade Study.

Mr. John Hodge, Martin Marietta Astronautics Group, Denver, and his associates for additional details on their 3-piece deployable aerobrake.

Dr. Steven Katzberg, NASA Langley Research Center, for results of his study of aerobrake assembly utilizing minimum Space Station Freedom accommodation.

Mr. Charles Cockrell, NASA Langley Research Center, for his study results, figures, and tables, which define the required on-orbit operations and supporting functions.

Mr. Brent Sherwood and Ms. Patricia Buddington, Boeing Aerospace and Electronics, Huntsville, for additional details on their Mars nuclear vehicle assembly and orbital support concepts.

Mr. Henry Woo, Rockwell International, Downey, for sharing early results of his study of Mars nuclear vehicle assembly.

Finally, the authors wish to thank Mr. Gary Hayes of McDonnell Douglas and Ms. Cindy Wyatt of NASA Langley for their preparation of the text and figures for this paper.

References

1. National Space Policy Directive 6, March 9, 1992.

2. America at the Threshold - Report of the Synthesis Group on America's Space Exploration Initiative, May 3, 1991.

3. Analysis of the Synthesis Group's Space Resource Utilization Architecture, EXPO Document XE-92-002, February 7, 1992.

4. Space Transportation Infrastructure Study, NAS8-37588, General Dynamics Space Systems Division, San Diego, CA.

5. Space Transfer Concepts and Analysis for Exploration Missions, NAS8-37857, Boeing Aerospace and Electronics, Advanced Civil Space, Huntsville, AL.

6. Space Transfer Vehicle Concepts and Requirements Study, NAS8-37856, Martin Marietta Astronautics Group, Denver, CO.

7. Space Transfer Vehicle Concepts and Requirements Study, NAS8-37855, Boeing Aerospace and Electronics, Space Transportation, Seattle, WA.

8. Engineering Analysis for Assembly and Checkout of Space Transportation Vehicles in Orbit, D 615-11900, NAS2-12108, Boeing Aerospace and Electronics, Huntsville, AL, February 20, 1989.

9. NASA Office of Exploration, FY1989 Annual Report, Vol. IV: Nodes and Space Station Freedom Accommodation, NASA TM 4170.

10. Space Transfer Concepts and Analyses for Exploration Missions, NAS8-37857, Program Cost Estimates and Schedules, Phase 1, D615-10028, Boeing Aerospace and Electronics, Advanced Civil Space, Huntsville, AL.

11. Woo, H. H., et al.: In-Space Operations Driven Mars Transfer Vehicle System, Rockwell International, Downey, presented at AIAA 29th Space Congress, Cocoa Beach, April 21-24, 1992.

12. Cockrell, C. E.: On-Orbit Assembly Operations and In-Space Infrastructure, NASA-Langley, AIAA 92-1646, presented at AIAA Space Programs and Technologies Conference, Huntsville, March 24-27, 1992.

13. Duffey, J.: Infrastructure Study (NAS8-37588) for Marshall Space Flight Center, General Dynamics Space Systems Division, San Diego, CA, December 1991.

14. Vargo, R., et al.: Lunar Transfer Vehicle On-Orbit Processing, McDonnell Douglas Space Systems Company, Kennedy Space Center, FL, December 1990.

15. Report of the 90-Day Study on Human Exploration of the Moon and Mars, National Aeronautics and Space Administration, November 1989.

16. Katzberg, S., et. al.: Minimum Accommodation for Aerobrake Assembly, Phase II Study Final Report, National Aeronautics and Space Administration, Langley Research Center, Hampton, VA, January 1992.

17. Hodge, J., et. al.: On-Orbit Assembly Aerobrakes, Table-Top Discussions, Martin Marietta Astronautics Group, Denver, CO, March 1992.

18. Anderson, D., et. al.: Aerobrake Assembly Using EVA/ Telerobotic Cooperation - Results of Neutral Buoyancy Testing, McDonnell Douglas Space Systems Company, Huntington Beach, CA, AIAA-91-0791, presented at AIAA 29th Aerospace Science Meeting, January 1991.

19. Woodcock, G., et. al.: Space Transfer Concepts and Analysis for Exploration Missions, Phase 2 Final Report, Boeing Advanced Civil Space Systems, Huntsville, AL, December 1991.

20. Simon, M. C.: The Role of Orbital Transportation Nodes in Human Space Exploration, General Dynamics Space Systems Division, San Diego, AIAA 92-1717, Presented at AIAA Space Programs and Technologies Conference, Huntsville, AL, March 24-27, 1992.

21. Johnson, J. II, et. al.: In-Space Processing (ISP) Technology Plan-Preliminary, IHM-0-91-02, General Dynamics Space Systems Division, San Diego, CA, NAS1-19242, November 1991.

22. Troutman, J. P. and Ganoe, G.: Lunar Vehicle Assembly and Processing on Space Station Freedom, NASA Langley, presented at 27th Space Congress, April 1990.

23. Boyer, D.: Space Station Freedom Technology for Manned Interplanetary Spaceflight, McDonnell Douglas Space Systems Company, Huntington Beach, AIAA 92-1421, presented at AIAA Space Programs and Technologies Conference, Huntsville, AL, March 24-27, 1992.

24. Vargo, R., et. al.: On-Orbit Assembly/Servicing Task Definition Study and Advanced Automation for In-Space Vehicle Processing Study – Combined GFY 1991 Annual Reports, McDonnell Douglas Space Systems Company, Kennedy Space Center, FL, December 1991.

N94-11569

In-Space Assembly -Servicing Requirements

Charles E. Cockrell
Chief Engineer - System Safety, Quality & Reliability Division
Study Performed for Space Exploration Initiative Office
NASA - Langley Research Center
Hampton, Virginia 23665

Abstract

A method for developing the requirements for in-space assembly, servicing, and checkout of proposed Mars space transfer vehicles is discussed. Required in-space operations and functions are identified in relation to various Earth to Orbit (ETO) vehicles by looking at the manifesting options of baseline Mars Space Transfer Vehicles (STV). Each operation is then reduced to a minimum complexity state resulting in a set of operational primitive functions. These primitive functions are used to assess the tradeoffs between robotic, telerobotic, and EVA operations. The study demonstrates that the complexity of the in-space operations remains stable with ETO vehicle size, and therefore the functions, and ultimately the infrastructure required to support proposed missions, are relatively unaffected by varying the ETO vehicle size within the range considered for this study.

Background

In undertaking a study of this or any other issue the first question which needs to be asked is, why do the study at all? In the area of in-space assembly/servicing requirements, several compelling reasons exist. The first is that the ability to live and work in space is essential to the future of NASA. In-space operations are an inherent part of all spacecraft mission scenarios. In generic form in-space operations consists of all activity that takes place between launch from the earth and landing back on earth or on another planet. Assembling and servicing operations are only subcategories of the overall in-space operations picture. The ability to assemble proposed spacecraft, and provide essential servicing during a mission is a critical aspect of mission success. The current baseline Mars STV is a case in point. Current estimates indicate that seven launches will be required to place all of the propellent and hardware in orbit, with over of fifteen months elapsing between the first and last launch. During this period of time the hardware components must be assembled, stored, maintained, and inspected. Systems must be available to provide power, communicate status, provide thermal control, inspect, assemble, manipulate, maneuver, and calibrate the vehicle. Failure to understand the technologies and the systems required to carryout these operations will have a direct impact on the safety of the crew, their ability to carry out a successful mission, and the total life cycle mission cost.

The second reason to undertake such a study is the need to understand operations early in the mission design process. In an era of tight budgets, and high expectations from the administration, the congress,

This paper was previously presented at the AIAA/SAE/ASME/ASEE 28th Joint Propulsion Conference and Exhibit on July 6-8, 1992 in Nashville, TN. It is reprinted here with permission.

and the public, NASA cannot afford to wait until the later stages of mission planning to consider the impact of operations at the detail level. A look at our current space transportation system underscores this point. The orbiter was designed to achieve a given performance level, with support operations being developed later in the program to fit the vehicle design. As a result of this approach extensive rework, refurbishment, and/or replacement is required between each launch. The development of a detailed support operations scenario as an integral part of the vehicle design process would have identified some of the labor intensive limitations imposed by the design, and resulted in simpler, more efficient methods for achieving the original design intent which was assured access to space. Some of the current operations and servicing requirements for mating the orbiter to the external tank could not be carried out in space with the present design. However, the functions which are carried out by these operations must necessarily be performed in space to mate vehicle components to propellent tanks. If we fail to consider the requirements that each necessary function or operation places on the design of the vehicle, we will quickly drive total mission cost to unacceptable levels, and jeopardize NASA's commitment to total quality throughout mission life.

The third reason for considering operations at this point is that we in NASA, in the early days after Apollo, made a promise to the public in return for their enthusiasm, excitement and support. That promise was that we, as a nation, would learn to live and work in space. Based on current talk within the agency in general, and within the Space Exploration Initiative (SEI) office in particular, doubts are raised as to whether we still believe we can achieve the promise. We owe the public a clear answer, not only to decide for ourselves if we can still keep the promise, but to also inform the public of the level of activity which will be necessary to achieve the promise if we believe we can do so.

Introduction

The primary objective of the study was to approach the issue of requirements from a systematic viewpoint. We did not start with a list of what we thought might be nice, nor did we start from a platform or waystation concept and work backwards to decide what we could do with the systems that were available. We started by determining what needed to be accomplished. The expected output was a list of top level requirements generated from the operations which were dictated by vehicle design, ETO limitations, and ground based integration capability. In addition we attempted to determine the minimum manpower which would be required to carry out the operations using robotics, telerobotics, or EVA. We attempted to hold to the legacy expressed in the Synthesis Report[1] of "ensuring optimum use of man-in-the-loop". As the report stated "Don't burden man if a machine can do it as well or better, and vice versa". Going into the study we neither required or eliminated any method of carrying out the operations.

The approach taken for the study was to first understand current thinking on the Space Exploration Initiative (SEI) strategy and options. We then selected a baseline Mars STV and launch vehicle. Because of the options which were being developed with respect to Heavy Lift Launch Vehicles (HLLV) we decided to carry both a 150 metric tonne and a 250 metric tonne vehicle through the study. There was a clear understanding that both the ETO vehicle and the Mars STV would change as the program evolves. However, sufficient thought had been given to current concepts that all of the necessary ingredients are in-

cluded, and any changes would have little impact on the top level operations which would be required.

Use was then made of information developed under an Infrastructure Study[2] led by the Marshall Space Flight Center (MSFC), with participation by the Langley Research Center (LaRC), the Stennis Space Center (SSC), the Kennedy Space Center (KSC), and the Lewis Research Center (LeRC). This study manifested the baseline Mars STV on both 150 tonne and 250 tonne vehicles. In addition, the study looked at the trade-offs which would be required, because of the manifest, on both ground based and in-space operations. By making use of these trade-offs we were able to develop a top level operational scenario detailing the steps which must take place in space. Basic functions, and ultimately functional primitives, were generated from this operational scenario for in-space assembly of the Mars STV. These basic functions allowed generation of hardware systems and subsystems necessary to perform the functions. We then looked at both the functional primitives and the hardware systems and subsystems to make a determination of whether EVA or robotic techniques were best suited to the activity. These systems and subsystems became the requirements for any in-space infrastructure which will be used to carry out the goal of learning to live and work in space.

SEI Mission Options

Three potential mission options have been suggested for vehicle integration for the SEI program as follows:

- Direct launch of fully integrated vehicles
- Rendezvous and docking in LEO with preintegrated components
- Assemble in space

Direct launch of fully integrated vehicles imposes severe limitations on the design of the STV, and the mission duration, due to the volume constraints of the ETO launch vehicle shroud, and the initial mass in low earth orbit (IMLEO) capability.

For purposed of this study we have defined rendezvous and docking as involving no more than two launches to low earth orbit with most hardware integration being performed on the ground. Two major components would be placed in LEO by separate launches and would be joined in orbit by automated latching techniques.

In-space assembly has been defined as involving multiple launches. Preintegration of large complex components would still be accomplished on the ground. However, major system and subsystem integration would be performed in space.

Current SEI mission strategy calls for both piloted and cargo lunar missions to be completed using the direct launch of fully integrated vehicles if possible. Rendezvous and docking would be used if sufficient HLLV capability has not been developed by the mission need date. Mars STV's present a different problem. Although the cargo vehicle could be broken into two major components which allows utilization of

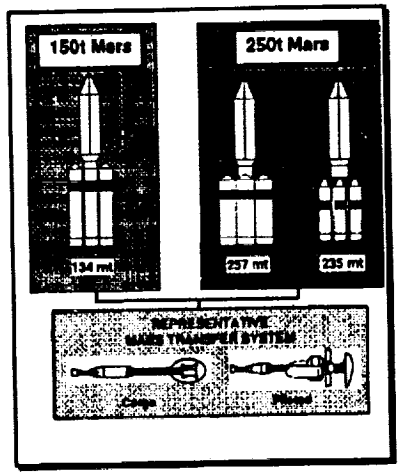

Figure 1: ETO Vehicle Classes

rendezvous and docking techniques, the mass and volume requirements of the piloted vehicle dictates that in-space assembly be performed. Figure 1 shows both the 150 tonne and 250 tonne classes of ETO vehicles which were considered in the reference 2 Infrastructure Study.

Assumptions

The following assumptions were made prior to the start of the study:

- The components that were determined to be required for an in-space infrastructure would be available as required.
- Enabling technologies would be developed to a sufficient level and in sufficient time to be incorporated into required systems as needed.
- Current technology and the advances which we expect to achieve over the next decade make telerobotic operation more practical than autonomous operation. Therefore, telerobotics would be considered as the first alternative to EVA operations.
- All hardware components would be inspected upon arrival on orbit.
- All components would be secured to the launch structure with remotely activated latches.
- The launch vehicle/structure would be capable of rendezvous with the infrastructure.
- Space Station Freedom (SSF) would be operational during the advance development phase of any program for infrastructure development.
- Launch centers would be determined by KSC based on ground processing requirements, and resource availability.
- The baseline Mars STV would be the 2016 reference NERVA derivative Nuclear Thermal Rocket (NTR) propulsion concept, defined by Boeing Defense and Space Group in their Phase I Space Transfer Concepts final report[3] to MSFC in March 1991.

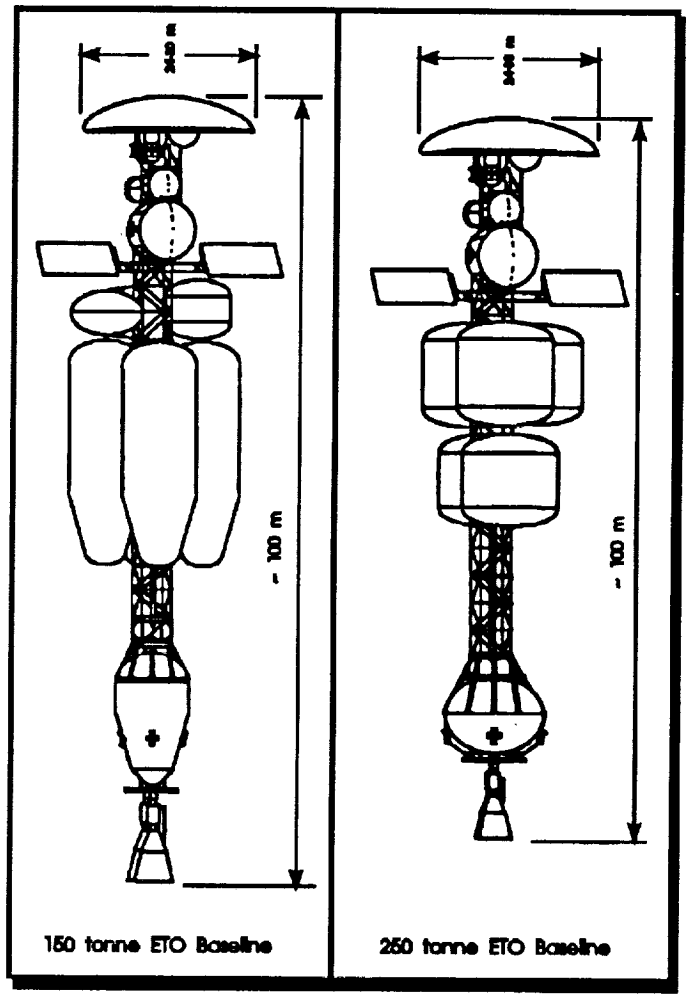

Figure 2: Mars STV Baseline Concepts

Discussion

During the reference 2 Infrastructure Study the baseline Mars STV was modified with different size propellent tanks for a 250 tonne ETO vehicle so that it would more effectively utilize the volume and IMLEO capability of the larger launch vehicle. Figure 2 shows the Mars STV concepts for each class of ETO vehicle considered.

The baseline Mars STV has a mass of 735,190 Kg which includes 525 tonnes of propellant and 92 tonnes of inert mass for the propulsion system. Figure 3 shows the baseline vehicle manifesting on a 150 tonne ETO vehicle as developed in the reference 2 infrastructure study. Figure 4 provides the same

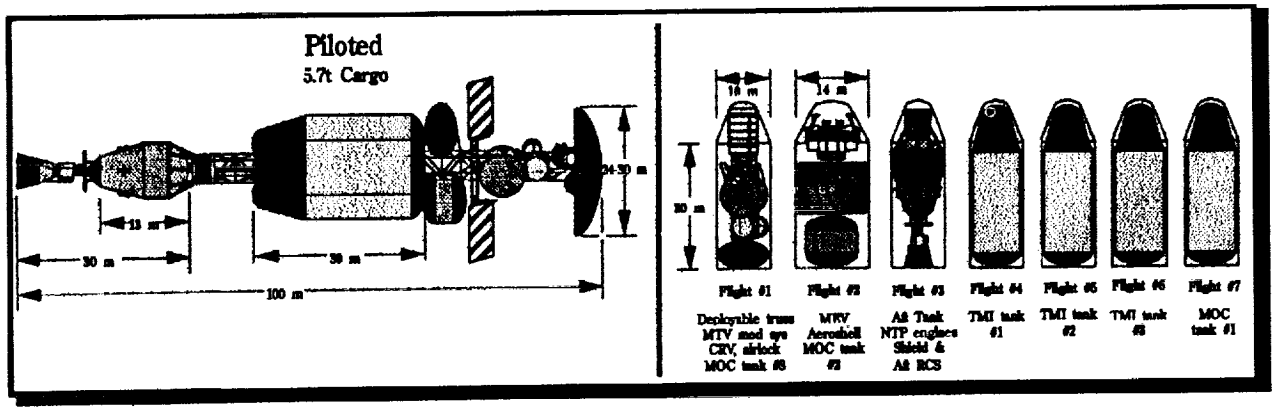

Figure 3: 150t ETO Vehicle Manifesting

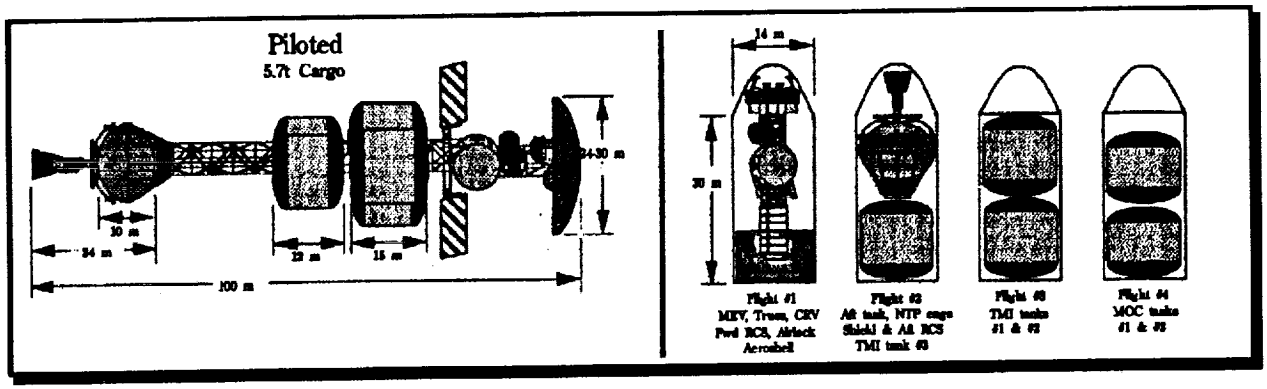

Figure 4: 250t ETO Vehicle Manifesting

information for the Mars STV as it was modified for a 250 tonne ETO vehicle.

Impact of Ground Based Operations

Recent in-house studies performed at KSC[4] reviewed the launch facilities and ground based operational requirements which would be imposed by a National Launch System (NLS). These studies identified a 150 tonne HLLV which could be used to launch the Mars STV. The HLLV ground processing time was determined to be 79 days between launches. Because of the constraints of other operations at KSC it was assumed that serial processing of the Mars STV launch vehicles would be required. This serial processing, along with the 79 day ground processing time, results in a total of 474 days between the time that the components included in the first launch arrive on orbit, and the time that the components from the seventh launch are available for assembly. Since MOC tank #3 is manifested on the first launch, cryogenic hydrogen boil-off must be considered as a part of the fuel management functions which are identified in the study.

Results

Once the manifesting of the baseline Mars STV's had been completed, a top level operational scenario was developed. This scenario looked at the major operations which would be necessary to accept, on orbit, the components from each launch and then assemble, mate, store, and maintain these components until the vehicle integration was completed. The completed state was defined to be, when all of the components, propellent, and expendable had been assembled and/or loaded on board the Mars STV, and the vehicle had been fully checked out and prepared for engine firing for trans Mars injection (TMI). This included transfer of the crew

for final checkout and verification functions.

The operational scenarios for the first two launches, for both a 150 tonne ETO vehicle and a 250 tonne ETO vehicle are as follows:

Operational Scenario for 150 tonne ETO Vehicle:

Launch # 1
- Activate Communications / Power Systems
- Checkout / Calibrate On-Board Inspection Systems
- Inspect Components / Verify Health after Launch
- Demate MOC tank #3 from Launch Structure
- Maneuver MOC tank #3 to Storage / Berth Location
- Demate Remaining Components from Launch Structure
- Deploy Truss Structure
- Verify Truss is Locked in Deployed Configuration
- Activate Monitoring System
- Manage STV Attitude for Thermal Control
- Provide Debris Protection

Launch # 2
- Receive, Rendezvous, Dock Components from Second Launch
- Checkout On-Board Health Monitoring Systems
- Inspect Components / Verify Health
- Demate MEV from Launch Structure
- Maneuver and Attach MEV to Truss Structure
- Demate Aeroshell from Launch Structure
- Deploy Aeroshell
- Inspect Aeroshell Joints and Seals
- Repair, Reseal TPS Joints as Required
- Provide Inspection / Verification Data to Mission Control
- Demate MOC tank #2 from Launch Structure
- Manipulate MOC tank #2 into Position
- Attach MOC tank #2 to Truss Structure
- Unberth and Manipulate MOC tank #3 into Position
- Attach MOC tank #3 to STV Truss Structure
- Verify All Joint Connections
- Make All Utility (Communication/Power/Health) Connections
- Make Fuel Connections between MOC tank #2 & Manifold
- Perform Fuel Connection Leak Check

Operational Scenario for 250 tonne ETO Vehicle:

Launch # 1
- Activate Communication / Power Systems
- Checkout / Calibrate On-Board Inspection Systems
- Inspect Components / Verify Health After Launch
- Demate Components from Launch Structure
- Maneuver and Berth Aeroshell / Launch Structure
- Deploy Truss Structure
- Verify Truss is Locked in Deployed Configuration
- Demate Aeroshell from Berth / Launch Structure
- Deploy Aeroshell
- Attach Aeroshell to Truss and Inspect Joints / Seals
- Repair/Reseal Joints as Required
- Provide Lighting for Remote Inspection
- Provide Inspection / Verification Data to Mission Control
- Activate Large Space Structure Control System
- Manage STV Attitude for Thermal Control
- Provide Debris Protection

Launch # 2
- Receive, Rendezvous, Dock Components from Second Launch
- Checkout On-Board Health Monitoring Systems
- Demate Components from Launch Structure
- Inspect Components / Verify Health
- Maneuver and Berth TMI tank #3
- Demate Aft Components from Launch Structure
- Maneuver Aft Components into Position
- Attach Aft Components to Truss Structure

- Verify Joint Connections
- Make Utility (Communication, Power, Health) Connections
- Unberth and Manipulate TMI tank #3 into Position
- Attach TMI tank #3 to STV Assembly
- Make Fuel Connections between TMI tank #3 and Manifold
- Perform Fuel Connection Leak Check

During the study it was determined that all of the operations which are necessary to bring the Mars STV to a fully integrated condition occurred during the first two ETO launches. After the operations listed for the second launch have taken place for both ETO vehicle options, we began to repeat the operations of maneuvering, attaching, receiving, manipulating, testing, etc.. For the remaining launches no new operations were identified. This led to the development of a list of basic operational functions which are repeated during the assembly and servicing phase of Mars STV deployment. These basic functions are as follows.

Basic Operational Functions

- Deploy & Erect Structure
- Attach & (dis) Assemble Components
- Inspect Structure & Components
- (re) Calibrate Systems & Components
- Receive, Rendezvous & Dock Components
- Checkout Systems & Subsystems
- Berth & Store Components
- Maneuver Components into Position
- Manipulate Structures & Components
- Test & Verify Assemblies & Components
- Make Utility Connections
- Provide Effective Lighting
- Communicate
- Generate & Store Power
- Control Large Space Structures
- Provide Thermal & Radiation Protection
- Provide Debris Protection
- Manage Cryo Fuel Transfer & Storage
- Manage Mission Data
- Provide Support for Contingency Operations

During the study it also became clear that we could address the operational functions in two different ways. First, we could break the operational functions into several categories such as contingency support operations, operational support, and mission functional primitives. Second, we could use the operational functions to define the systems which make up the top level requirements for an in-space infrastructure which would be required for on-orbit integration of the Mars STV's.

Operational Categories

This first method of addressing the functions demonstrates the interdependencies and interrelationships of the various operational functions in each of the categories, with the primitives being used to determine the optimum method of carrying out each of the functions.

The contingency support operations make use of most of the infrastructure systems, but come into play only when normal operational functions are out of tolerance, or when the crew is arriving. As an example component change out would occur only when an individual system failed to function during in-space verification, or if a system had been damaged during operation. The self correcting capability would be utilized if a component did not fit as planned, or if alignment problems were encountered because of tolerance buildup or thermal changes to the structure. These examples also point out the need for early consideration of the in-space operations. Any problem which might call on the contingency support functions needs to be considered during the design process.

The operational support functions are those which primarily involve control of the infrastructure and its activities, or provide support

to the functional primitives in carrying out the primary mission of the infrastructure.

The third category includes those functions which are necessary to complete the primary mission of an infrastructure, which is to assemble and service a Mars STV. These are the activities which require direct intervention by EVA, robotic, or telerobotic techniques. Functions in this category have been reduced to a set of functional primitives. The reduction in this manner is not intended to indicate ease of carrying out the function. In fact, just the opposite can be true. Some of the assembly and servicing activities can involve many of the functional primitives which, when combined, can become very difficult operations. The primitive functions can themselves be further reduced to a set of very difficult operations on a detail level. Also some of the operations which require reasonable simple application of the primitive functions can become very difficult due to the nature of the component being acted on. For example the act of moving the TMI tanks into position for attachment to the truss structure involves simple actions. However, when the tanks are nearly full of hydrogen propellent, in a zero gravity environment, any movement of the tank can cause a shifting of the hydrogen propellent setting up a dynamic oscillation which must be damped out. In this case an operation which involves simple functions becomes very difficult to carry out.

The basic operational functions in each of the three categories are listed below:

Contingency Support Operations:

Component Changeout
Tool Storage
Capture & Retrieval
Self Correcting Capability
Assist with Crew Transfer

Operational Support:

Lighting
Communication
Power Generation
Power Storage
Facility Control & Monitoring

Data Management
Component Storage / Berthing

Mission Functional Primitives:

Acquire	Rotate
Attach	Transport
Maneuver	Verify
Manipulate	Withdraw
Berth	Test
Inspect	Operate
Install	Insert

These mission functional primitives are activities which are ideally suited to advance telerobotic operation. Independent studies[6] have looked at the timelines which would result from using EVA, IVA and telerobotic operations. These studies indicate that total elapsed processing time would increase by 62% if the operations were performed telerobotically from the ground instead of using EVA. However, the operations can easily be performed telerobotically from the ground within the 79 day launch center for the HLLV. Total life cycle cost would decrease dramatically by using telerobotic operations. The only activity occurring on-board an infrastructure between launches is assembly and servicing functions, or station keeping. There would be no impact if assembly time were doubled or tripled over what would be required by EVA activity so long as the activity could be carried out prior to the next launch. The studies indicate that even with the increased time for telerobotic operations the majority of the time between launches would still be spent in a station keeping mode.

Functions/System Matrix

The second method of addressing the basic operational functions results in an extensive matrix which relates each of the functions to the systems and subsystems which are necessary to perform the functions. This matrix is shown in tables 1a through 1d. Each of the systems or subsystems listed directly serves at least one of the functions, or there is some connectivity between the system/subsystem and the function. An iterative process was employed in developing the matrix. First, the systems which were directly requiredle for performing a function were listed. Each system was then reevaluated against every other function to determine if there was any connectivity to the other functions. In other words, although a function did not require a specific system to perform the activity, could that activity be enhanced by using systems that are necessary to carry out some other function?

The resulting systems/subsystems become the top level requirements for an in-space infrastructure to support the assembly and servicing of a Mars STV. The requirements are independent of any current infrastructure concept. They provide a basis for evaluating concepts as to their ability to carryout required operations. These top level infrastructure system requirements are listed below:

Required Systems

- Structural for supporting the other systems
- Robotic Manipulators for assembly
- Computers & Software for Data Management
- Power Generation & Storage
- Communication Hardware & Software
- Remote Health Monitoring Sensors
- Visual Inspection Hardware & Software
- Cryogenic Fuel Control
- Docking, Berthing Mechanisms
- Lighting Units (Fixed & Moveable)
- Guidance, Navigation & Control
- Storage Mechanisms
- Shielding (Thermal, Debris, Radiation)

Conclusions

In-space assembly and servicing of Mars Space Transfer Vehicles will be required.

The infrastructure required to carry out the assembly and servicing activity is determined by the operational functions.

Within a given range of ETO vehicle sizes the infrastructure requirements are independent of the launch vehicle sizes.

The systems and subsystems defined by this study are the top level requirements for an infrastructure.

The complexity of the operations which must take place in space for assembly and servicing of the Mars STV are independent of launch vehicle size.

The frequency with which the assembly and servicing operations must be carried out is entirely dependent on launch vehicle size.

The functional primitives which have been defined in this study are ideally suited for telerobotic operation.

The 79 day launch centers required for ground based processing of the ETO vehicle is considerably longer than the time required for telerobotic assembly of the STV components.

Recommendations

There are four major recommendations resulting from this study. The first recommendation should carry the highest priority with the other three carrying about the same weight.

1. We must include in-space operational analysis as an integral part of current planning for all future missions. If we fail to consider detail in-space operational analysis from the conceptual mission stage forward we will quickly drive mission costs to unacceptable levels, and jeopardize NASA's commitment to total life cycle quality.

2. We must conduct a more detailed analysis of the interdependencies between in-space operations and ground based processing.

3. We need to carry the operational scenario's presented in this study to a more detailed level, and develop the operational timelines for specific mission scenario's.

4. We should conduct system analysis studies of each proposed Mars STV assembly option (Free Flyer, Saddle, Mini Depot, Platform) with respect to the requirements developed under this study, so that we can better understand their applicability for future use.

In addition numerous lower level recommendations could be generated with respect to developing and refining concepts for In-Space Assembly and Servicing (ISAS) Facility Infrastructures. These recommendations would cover the field from in-depth system/subsystem analysis, through facility concept development, to performing detail life cycle cost analysis of various options. Each of these are essential to developing our ability to live and work in space, and for our journey to other planets.

References

1. America at the Threshold - Report of the Synthesis Group on America's Space Exploration Initiative; May 3, 1991

2. Duffey, J.: Infrastructure Study (NAS8-37588) for Marshall Space Flight Center, General Dynamics Space Systems Division, San Diego, CA; December 3, 1991

3. Wookcock, G., et al.: Space Transfer Concepts and Analysis for Exploration Missions, Phase 1 Final Report, Boeing Defense & Space Group, Advance Civil Space Systems, Huntsville, AL; March 1991

4. Page, Don: National Launch System (NLS) KSC Facilities, Kennedy Space Center in-house study; March 4, 1992

5. Cockrell, C. E.: On-Orbit Assembly Operations and In-Space Infrastructure, NASA-Langley Research Center, AIAA 92-1646, presented at AIAA Space Programs and Technologies Conference, Huntsville, AL; March 24-27, 1992

6. Vargo, R., et al.: Lunar Transfer Vehicle On-Orbit Processing, McDonnell Douglas Space Systems Company, Kennedy Space Center, FL; December 1990

In-Space Assembly-Servicing Requirements

Question: Is the Function served by the System/SubSystem, or, is there Any Connectivity between the Function and the System/SubSystem?

Systems/Sub Systems \ Functions	Deploy/Erect Structure	Test/Verify Ass'y/Components	Attach/(dis)Assemble Components	Communicate	Generate/Store Power	Provide Effective Lighting	Inspect Structure/Components	(re)Calibrate Systems/Components	Control Vehicle Attitude	Make Utility Connections	Provide Thermal/Radiation Protection	Manage Cryo Transfer / Connections	Manage Mission Data	Provide Debris Protection	Control Large Space Structures	Receive/Rendezvous/Dock	Checkout Systems/SubSystems	Maneuver Components to Store/Ass'y	Berth/Store Components	Manipulate Structure/Component	Provide for Supportability (#)	# Provide Self Correcting Capability	# Conduct Training	# Store/Transfer Support Systems	# Support Nuclear Systems	# Changeout Components	# Provide/Store Tools/Components	# Capture/Retrieve Loose Objects	# Assist Crew Transfer	-	-	-	-
Structures																					X												
Trusswork(Preintegrated, Space Assembled)	X		X				X				X				X	X			X	X					X		X						
Smart Structures	X	X	X	X			X	X			X		X		X	X	X								X								
Joint Connections	X		X				X			X					X	X			X						X	X	X						
Rails			X													X		X	X						X								
Robotic Systems																					X												
Manipulators (Fixed, Moveable)	X	X	X	X			X	X		X		X				X		X	X	X			X	X	X	X	X	X					
Alignment Sensors	X	X	X	X			X	X		X		X			X	X	X	X	X	X		X			X	X							
Mobile Transporters			X	X				X								X		X		X		X	X		X	X	X	X					
Rail Crawlers			X	X				X					X			X		X		X		X	X		X	X		X					
End Effectors/Tools	X	X	X					X		X		X	X			X		X		X				X	X	X	X	X					
Joining Mechanisms (Bolts, Pins, Latches)	X		X							X		X			X	X			X	X	X				X	X	X						
Data Management Systems (Computers)																																	
Artificial Intelligence			X				X	X	X				X		X			X		X		X	X		X								
Large Storage Devices (Gbytes)		X	X	X			X	X	X				X		X		X	X		X		X			X								
Real Time Distributed Processing Devices	X	X	X	X			X	X	X			X	X		X	X		X		X		X			X			X					
Fault Tolerant Systems			X				X	X	X	X		X	X		X		X	X		X		X			X								

Table 1a:

Chief Engineer

In-Space Assembly-Servicing Requirements

Systems/Sub Systems \ Functions	Deploy/Erect Structure	Test/Verify Ass'y/Components	Attach/(dis)Assemble Components	Communicate	Generate/Store Power	Provide Effective Lighting	Inspect Structure/Components	(re)Calibrate Systems/Components	Control Vehicle Attitude	Make Utility Connections	Provide Thermal/Radiation Protection	Manage Cryo Transfer / Connections	Manage Mission Data	Provide Debris Protection	Control Large Space Structures	Receive/Rendezvous/Dock	Checkout Systems/SubSystems	Maneuver Components to Store/Ass'y	Berth/Store Components	Manipulate Structure/Component	Provide for Supportability (#)	# Provide Self Correcting Capability	# Conduct Training	# Store/Transfer Support Systems	# Support Nuclear Systems	# Changeout Components	# Provide/Store Tools/Components	# Capture/Retrieve Loose Objects	# Assist Crew Transfer	-	-	-	-	-
Data Management Software		X	X	X			X	X	X			X	X		X	X	X	X	X	X		X		X	X	X	X	X					
Diagnostics Tools	X	X	X				X	X	X	X	X	X	X		X	X	X			X		X			X								
Automated Checkout Tools	X	X	X				X	X			X	X	X		X	X	X	X				X			X	X							
Teleoperations Interfaces	X	X	X	X			X	X		X		X	X			X		X		X			X	X	X	X	X	X					
Error Recovery Systems								X					X				X			X		X			X								
Task Sequence Systems	X	X	X							X		X	X		X	X	X	X		X		X			X	X	X						
Part Collision/Avoidance Systems	X		X	X									X			X		X		X					X								
Redundancy/Conflict Resolution Systems			X				X		X			X	X		X		X			X		X			X								
Communications Systems (Data, Voice, Video)																					X												
Image Processing Systems	X	X	X	X		X	X	X		X		X	X		X	X	X	X	X	X				X	X	X		X	X					
Cameras	X	X	X	X		X	X			X		X			X	X	X	X	X	X				X	X	X		X	X					
Antenna(s)	X	X	X	X		X	X	X	X	X		X			X	X	X	X	X	X		X			X	X		X	X					
Data Collection/Processing Systems	X	X	X	X		X	X	X	X	X		X	X		X	X	X	X	X	X		X			X	X								
Power Systems																					X													
Radiators					X						X				X							X			X									
Solar Arrays	X	X	X	X	X	X	X	X	X	X		X			X	X	X	X		X		X		X	X	X								
Solar Dynamics	X	X	X	X	X	X	X	X	X	X		X	X			X	X	X		X		X		X	X	X								

687

Table 1b:

Chief Engineer

In-Space Assembly-Servicing Requirements

Systems/Sub Systems \ Functions	Deploy/Erect Structure	Test/Verify Ass'y/Components	Attach/(dis)Assemble Components	Communicate	Generate/Store Power	Provide Effective Lighting	Inspect Structure/Components	(re)Calibrate Systems/Components	Control Vehicle Attitude	Make Utility Connections	Provide Thermal/Radiation Protection	Manage Cryo Transfer / Connections	Manage Mission Data	Provide Debris Protection	Control Large Space Structures	Receive/Rendezvous/Dock	Checkout Systems/SubSystems	Maneuver Components to Store/Ass'y	Berth/Store Components	Manipulate Structure/Component	Provide for Supportability (#)	# Provide Self Correcting Capability	# Conduct Training	# Store/Transfer Support Systems	# Support Nuclear Systems	# Changeout Components	# Provide/Store Tools/Components	# Capture/Retrieve Loose Objects	# Assist Crew Transfer	-	-	-	-	-
Batteries	X	X	X	X	X	X	X	X	X	X		X	X		X	X	X	X		X		X			X	X							
Power Distribution Networks	X		X	X	X	X	X	X	X	X		X			X	X	X					X		X	X	X		X					
Utility Connections	X		X	X	X	X	X	X	X	X		X				X	X					X		X	X	X							
Cables	X		X	X	X	X	X	X	X	X		X				X	X					X		X	X	X							
Test/Inspection/Validation Systems																					X												
Machine Vision Sensors		X	X				X	X		X			X		X	X	X	X	X	X		X			X	X							
NDE Tools	X	X	X				X	X					X		X		X					X	X		X	X							
Leak/Contamination Sensors		X					X	X		X		X	X				X					X			X	X							
Specialized Inspection Sensors	X	X	X				X	X		X	X	X	X		X		X					X			X	X							
Built In Test Sensors/Equipment	X	X	X				X	X		X	X	X	X		X		X					X			X	X							
Data Collection/Procession Systems	X	X	X				X	X		X	X	X	X		X		X	X	X			X			X	X							
Fuel Management Systems																					X												
Fuel Storage Tanks (GO2, GH2)			X						X			X			X	X									X								
Fuel Transfer Lines			X						X			X			X										X								
Fuel Control Systems (Values,Pumps,etc)			X					X	X	X		X			X							X	X		X								
Fuel Line Connections/Mechanisms			X					X	X	X		X													X								

Table 1c:

Chief Engineer

In-Space Assembly-Servicing Requirements

Systems/Sub Systems \ Functions	Deploy/Erect Structure	Test/Verify Ass'y/Components	Attach/(dis)Assemble Components	Communicate	Generate/Store Power	Provide Effective Lighting	Inspect Structure/Components	(re)Calibrate Systems/Components	Control Station Attitude	Make Utility Connections	Provide Thermal/Radiation Protection	Manage Cryo Transfer / Connections	Manage Mission Data	Provide Debris Protection	Control Large Space Structures	Receive/Rendezvous/Dock	Checkout Systems/SubSystems	Maneuver Components to Store/Ass'y	Berth/Store Components	Manipulate Structure/Component	Provide for Supportability (#)	# Provide Self Correcting Capability	# Conduct Training	# Store/Transfer Support Systems	# Support Nuclear Systems	# Changeout Components	# Provide/Store Tools/Components	# Capture/Retrieve Loose Objects	# Assist Crew Transfer	-	-	-	-	-
Life Support Systems																					X												
Habitats						X		X			X		X	X		X													X				
Closed Loop ECLSS								X					X									X							X				
Manned Systems								X					X		X		X					X	X						X				
EVA/IVA Systems (Suits, Airlocks)		X				X		X					X		X	X	X			X		X	X	X					X				
Lighting Systems	X	X	X		X	X	X										X				X			X		X			X				
Docking Adapters			X												X	X			X		X			X	X	X		X	X				
Latching Mechanisms	X		X					X		X		X			X	X			X		X			X	X	X	X	X	X				
Thruster Pods								X	X						X	X		X			X	X							X				
Attitude Control Systems							X	X	X				X		X	X		X			X	X							X				
Control Moment Gyros							X	X	X				X		X	X		X			X	X							X				
Storage Enclosures											X			X	X				X		X			X		X	X	X					
Shielding											X			X	X						X		X		X								
Safety Contingency Systems		X		X	X	X	X	X	X	X	X	X	X	X	X	X	X			X	X	X	X	X	X	X			X				

Table 1d

Chief Engineer

Session S4: SPACE MAINTENANCE AND SERVICING LOGISTICS

Session Chair: Lt. Col. Gary Johnson

N94-11570

FORECASTING THE IMPACT OF VIRTUAL ENVIRONMENT TECHNOLOGY ON MAINTENANCE TRAINING

Mark S. Schlager, Duane Boman, & Tom Piantanida
SRI International
333 Ravenswood Avenue
Menlo Park, CA 94025
(415) 859-2881

Robert Stephenson
Plans and Programs Dir. (AL/XPX)
Bldg. 125 Armstrong Laboratory
Brooks AFB, TX 78235
(512) 536-3213

ABSTRACT

To assist NASA and the Air Force in determining how and when to invest in virtual environment (VE) technology for maintenance training, we identified possible roles for VE technology in such training, assessed its cost-effectiveness relative to existing technologies, and formulated recommendations for a research agenda that would address instructional and system development issues involved in fielding a VE training system. In the first phase of the study, we surveyed VE developers to forecast capabilities, maturity, and estimated costs for VE component technologies. We then identified maintenance tasks and their training costs through interviews with maintenance technicians, instructors, and training developers. Ten candidate tasks were selected from two classes of maintenance tasks (seven aircraft maintenance and three space maintenance) using five criteria developed to identify types of tasks most likely to benefit from VE training. Three tasks were used as specific cases for cost-benefit analysis. In formulating research recommendations, we considered three aspects of feasibility: technological considerations, cost-effectiveness, and anticipated R&D efforts. In this paper, we describe the major findings in each of these areas and suggest research efforts that we believe will help achieve the goal of a cost-effective VE maintenance training system by the next decade.

1 INTRODUCTION

Virtual environment (VE) technology holds great promise for maintenance and other technical training applications. VE capabilities (e.g., stereoscopic 360 degree field of regard, natural interactivity, tactile feedback, 3-D sound) can create a feeling of presence [1] that many believe will enhance the learning experience in ways that other technologies cannot [2, 3, 4]. The ability to faithfully simulate task environment characteristics makes VE attractive for training tasks that are performed under unusual conditions (e.g., zero gravity) or that involve the risk of injury or damage to equipment. As a computer-based technology, it can be used in locations where space is limited (e.g., shipboard, in space) and can be configured to deliver training on large numbers of tasks that would otherwise require a suite of hardware trainers. A VE simulation can also accommodate more than one person at a time, and, through networking, participants need not all be in the same physical location. As part of a study to help NASA and the Air Force determine how and when to invest in VE technology for maintenance training, we were asked to (1) establish the need for VE technology in maintenance training by identifying categories of tasks for which VE would offer effective training, (2) assess VE's cost-effectiveness relative to existing technologies, and (3) formulate recommendations for a research agenda that would address instructional and system development issues involved in fielding a VE training system.

2 VE TECHNOLOGY SURVEY

In the first phase of the study, we surveyed VE technology researchers and manufacturers to identify current and emerging capabilities, forecast maturity, and estimate costs for VE component technologies. The survey covered more than 50 organizations from government, industry, and academia. The survey findings are described in detail in a companion paper [5].

Here we cover two major aspects of the survey: key characteristics that define a VE simulation and critical VE technology research areas.

2.1 Characteristics of VE Simulation

Most VE systems share a cluster of essential elements that globally define the virtual environment. We briefly describe these characteristics to minimize confusion as to what constituted a VE system for the purposes of the study.

Immersion in the virtual environment. VE systems can provide the user with a sense of immersion, that is, of being within the display rather than viewing it from outside. Immersion makes VE simulations much more realistic than through-the-screen simulations. Making the sense of immersion compelling requires coordination of sensory inputs to the user, so that the sensory attributes of virtual objects seem to be attached to those objects. It also requires the use of wide-field-of-view images so that the user's peripheral vision, not just central vision, is stimulated.

Interactivity with elements of the virtual environment. The user should not only be a witness to events transpiring within the virtual environment, but a participant as well. Users must be able to navigate the virtual space and manipulate virtual objects within that space. Manipulations should have specifiable consequences that may vary with the simulation. For example, an astronaut standing on the surface of a simulated planet who fires a vertical thruster must accelerate at a rate consistent with the gravitational attraction of that planet. Interactivity also extends to other participants of the VE. An instructor must be able to change the viewpoint and orientation of a trainee as the task requires and examine the simulation from the viewpoint of the trainee.

Sensory displays. The term *display* is used in its broadest sense, referring to making an impression on the senses. Specific examples of sensory displays include video screens, arrays of tactors in the fingertips of gloves, and speaker arrays that produce localized sound sources in the VE. Early examples of VE training simulators will probably include only auditory and visual displays; the more sophisticated systems to follow will incorporate haptic displays, as well. VE simulations that lack haptic displays may be able to convey inertial and tactile information through other sensory channels (e.g., auditory or visual feedback).

Remotely sensed and synthesized sensory images. Information presented on the sensory displays of VE training systems is likely to include audio, video, and possibly haptic images. These images will be primarily synthesized from a computer database, but remotely sensed images may be incorporated into the simulation in some instances. Synthesized images may be generated from a variety of databases, including CAD diagrams, electrical and hydraulic schematics, and other electronic blueprints used in the design of the objects represented in the VE simulation.

2.2 VE Technology Recommendations

VE technologies were divided into nine major components:

- Visual display systems (head-mounted and CRT-based)
- Position/orientation trackers
- 3-D audio interfaces
- 3-D/6-D input devices
- Gesture-recognition input devices
- Haptic interfaces
- Automatic speech recognition systems
- Computer hardware
- Software.

Most VE technologies are in early phases of development, and current VE system components have restricted capabilities that limit the fidelity of the simulation. These limitations create sensory distortions that make many tasks difficult to perform in a VE. They can disorient the participant and even lead to simulator sickness. These and related problems limit the use of current VE technologies as training devices. Industry R&D will quickly improve many aspects of VE technology; however, much of the work will be aimed at producing low-cost components that will sell in high volume. In many cases, these components will not fulfill Air Force or NASA requirements for effective training devices. Further R&D funding will be needed to produce the high-quality devices needed for Air Force and NASA maintenance training systems. Here we describe those areas for which additional R&D efforts will be most critical.

2.2.1 Visual Display Systems

The low spatial resolution of present VE visual displays is a major limitation in application development. Only a few of the simplest maintenance training applications can be realized with present VE visual display resolution. Additional funding may be required to produce the small-diagonal, high-resolution head-mounted displays (HMDs) needed for maintenance training applications. Specifications of importance for VE visual display devices include field-of-view, spatial resolution, refresh rate, and color performance. Several technologies and visual display designs have promise for developing high-resolution VE visual displays. In our judgment, it is premature to choose a single VE visual display technology or design at this time. Consequently, our recommendations include research in:

- High-resolution, small-diagonal HMD screens
- Multiple-screen HMD configurations
- Optical fibers for high-resolution, projection HMDs
- Eye-tracking systems to be used in variable-resolution HMDs
- Adjustable optics to provide wide-angle or high-resolution viewing.

2.2.2 Position/Orientation Trackers

Tracking the position and orientation of the VE-system participant is essential for developing highly interactive simulations. In most cases, six degrees of freedom must be tracked: three spatial-position coordinates and three orientation angles. Several technologies are currently being used for 6-D tracking in VE systems, including magnetic, ultrasound, mechanical, optical, and analog tracking devices. At present, each of these tracking technologies is under intense development. Major specifications to consider with tracking technologies are system range, resolution, repeatability, update rate, lag, and environmental robustness. The improvements needed in position/orientation-tracking systems include increases in tracking range, reductions in time delays, and minimization of encumbrances such as cabling. Efforts should be directed toward developing low-cost optical tracking systems and hybrid tracking systems using low-delay analog devices in conjunction with a remote-sensing system for periodic recalibration.

2.2.3 Haptic Interfaces

VE interfaces that involve the sense of touch are referred to as haptic interfaces. These interfaces fall into two main categories: force-feedback interfaces, which provide information about the mass and inertia of objects and forces applied to them, and tactile interfaces, which provide information about the shape and surface roughness of objects. Development of tactile-feedback interfaces is proceeding rapidly, with devices being fitted into gloves and other garments. The main problem facing the inclusion of these devices in VE simulations is to determine their proper use. Force-feedback interfaces are at a more fundamental stage of development, with applications being limited to providing force information to the hand and arm. Considerable

technological development will be required for them to become useful in VE systems. Task-specific force-feedback devices may be useful in many maintenance training applications.

2.2.4 Computer Software

The development of efficient and effective VE software will have the greatest impact on creating cost-effective VE maintenance training systems. Although VE software is being developed by many organizations, these packages do not fulfill the special needs of maintenance training applications. At present, multiple software packages are required to produce a VE application. First, virtual objects are created using graphics modeling software. Then, the simulation dynamics are programmed using another software package. The latter package usually controls the simulation as well, although additional software may be needed to provide image rendering. Ideally, VE software should provide each of these functions, as well as others, including:

- Importation of CAD models and databases
- Anthropometric modeling
- Authoring environment
- Networking capabilities.

Although software is being developed for providing each of these capabilities, no fully integrated package has been implemented. Many enhancements will need to be made in VE software before cost-effective maintenance training simulations can be developed.

3 MAINTENANCE TRAINING INTERVIEWS

In a series of interviews, we collected information from experienced maintenance technicians, instructors, and instructional developers from the Air Force, NASA, and DoD contractors. The respondents nominated 19 aircraft maintenance task categories and 3 space maintenance task categories as possible candidates for VE training. Each task category was ranked on five selection criteria designed to identify those tasks that would benefit most from VE training. Table 1 shows the 10 highest-rated task categories. The interviews also yielded a wealth of information on maintenance task characteristics, current maintenance training practices and costs, training system descriptions, and trends that could affect future training.

Table I. Candidate Task Categories

Space Maintenance:
- EVA
- Teleoperations
- Telerobotics

Aircraft Maintenance:
- Engine Maintenance.
- Engine Run Test
- Fireguard
- Fuel System Maintenance
- Inspections
- Safety Procedures
- Marshaling

To the extent possible, we also sought to identify particular capabilities and system performance levels that would be required to field a successful VE maintenance training system. The information gained from the interviews, together with our own knowledge of current VE

applications and maintenance training principles and systems, formed the basis of a cost-effectiveness analysis using three of the task categories identified. Rather than attempt a comprehensive discussion of our findings, we will report only our general conclusions. The interested reader is encouraged to read the full report (in preparation) for more detail.

3.1 Maintenance Training Issues

Three major conclusions were drawn from the interview data:

A need exists for the kind of training VE offers. Safety and training impact are major factors in VE's appeal. It could, for example, simulate the consequences of following improper procedures (e.g., shortcuts), give instructors more flexibility in monitoring and testing students' performance, and provide students more meaningful feedback.

VE could fill a gap between the two predominant current training technologies. VE combines many of the benefits of hardware-based simulation with those of computer-based delivery, providing higher-fidelity simulation than interactive videodisc (IVD) lessons and more flexibility and instructional features than hardware-based simulators.

VE-based training could be cost-effective for many applications. Using the cost data collected in the interviews, we conducted a cost-effectiveness analysis comparing VE with current training technologies. In each of three sample applications, the results suggest that VE-based training could be a cost-effective addition to, or replacement for, existing training systems. [The reader is encouraged to refer to the project final report (in preparation) for details and cost assumptions.]

3.1.1 Aircraft Maintenance

Technical schools and field training detachments (FTDs) are hampered by an inadequate supply of up-to-date equipment. OJT suffers from a lack of standardization and instructional feedback. Training development and upgrading are costly processes that often lag behind training needs. Training systems and courseware have difficulty keeping pace with weapons system modifications. High-fidelity hardware/software simulators, although ideal for small numbers of students, are extremely costly and not available in large enough quantities to accommodate the large numbers of maintenance students. Low-end systems do not provide the fidelity to train to mastery on many tasks. Our look at future trends in aircraft maintenance identified several potential challenges, including discontinuation of the use of actual aircraft for training, reduction of equipment time available for OJT, and further consolidation of maintenance specialties. These problems are sufficiently acute to warrant looking into new technologies such as VE to ease the training burden.

VE systems will not be inexpensive; currently, a system containing the appropriate capabilities (if available) would be far too costly to compete with other technologies. Our data suggest, however, that cost should not be a deterrent to exploring VE as a future alternative. Our estimates--using costs projections for VE technologies at maturity--show that VE could be used cost-effectively throughout much of training. VE system development, maintenance, and upgrade costs are expected to be well within the range of costs currently expended for IVD courseware and hardware/software trainers. We also expect VE to enjoy life-cycle cost savings and benefits comparable to those attributed to other computer-based training technologies [6] [7].

Whether VE simulation will make a cost-effective training delivery tool depends on several factors, including the required capabilities of the system, the nature of the tasks to be trained, and the alternative means of delivering the instruction. The "ideal" solution might employ several levels of systems. The concept of using multiple levels of simulation is being employed in aircrew training to eliminate training bottlenecks on full-fidelity flight simulators. The idea is to

use lower-fidelity "part-task" simulators to teach cockpit familiarization and basic procedures before moving on to the high-fidelity simulator. In maintenance training, the role of part-task trainer could be filled by VE systems.

3.1.2 Space Maintenance

NASA has a continuing interest in the development of VE simulations for use in both its ground operations and space missions. Much of NASA's interest stems from the fact that it is difficult and expensive to practice on earth procedures meant to be performed in a zero-g environment. Extravehicular activity (EVA) tasks, for example, were forecast to be prime candidates for VE training. Currently, training is conducted for specific missions on full-scale replicas and in neutral-buoyancy simulators. As discovered on a recent satellite rescue mission, the practice provided on these systems may not be sufficient to perform tasks such as satellite coupling in space. It is hoped that VE simulations will provide an appropriate representation of the physics of a zero-gravity environment, thereby supporting mission planning and rehearsal, as well as general training. Another task (planned for the space station) is the use of extravehicular robots controlled by technicians inside the space station. Although no training for this task category is currently conducted, NASA is experimenting with VE and dome projection systems to determine which provides a more accurate representation of the task environment.

The small student population and the limited number, special purpose, and short duration of space missions have enabled space maintenance training to get along with a small number of very expensive trainers. This situation is likely to change with the construction and habitation of the space station. New classes of maintenance tasks will have to be taught to larger numbers of students. It is unclear whether current training practices (e.g., zero-g profile flights) or simulators (e.g., neutral-buoyancy or dome simulators) can handle the increased training needs. Such systems are expensive, and they have inherent limitations in simulating space maintenance tasks. VE simulations (albeit with their own limitations) may prove to be a relatively inexpensive alternative to hardware-based training systems. Because the physical laws that govern interactions among objects in a virtual environment are part of the program that controls the simulation, VE can simulate interactions in zero-g (or other gravitational) environments. With improvements in force-feedback systems, VE systems will also be able to simulate inertial characteristics of objects, something that is difficult to achieve with conventional simulations.

Another factor that will become increasingly important as space missions get longer is the ability to maintain skills acquired before the mission. On long missions, skill levels developed during the ground-based rehearsal phase can diminish unless some means is provided to maintain the skill. Mass and space constraints eliminate hardware-intensive simulations for skill maintenance during space flight. An alternative would be a general-purpose VE simulator. By deploying the appropriate task simulation in the onboard VE system, an astronaut would be able to maintain the skill level achieved on earth. Moreover, in an anomalous situation, a ground station could transmit data for generating a new scenario, which could then be used to guide the astronaut through practice runs on emergency procedures that had not been rehearsed on earth.

3.2 Training Research Recommendations

To provide effective VE maintenance training systems, research will be needed in several areas, including user interaction methods, learning benefits of VE, instructional strategies, and testing. Recommendations were made in each of these areas.

3.2.1 User Interaction Methods

Effective use of VE devices (e.g., 3-D/6-D input devices) and techniques (e.g., virtual menu screens, voice commands, and hand gestures) will require an understanding of how simulator

interactions can best be performed. Most interactions can be performed by a variety of methods. Present VE system interactions are generally restricted by the available user interface devices and styles. A number of conventions have been created for these interactions, but it is generally accepted that these conventions do not produce optimal interaction. Information from assessment of VE system interactions can be used to greatly enhance usability by both experienced and naive participants. Studies should be conducted to develop and evaluate:

- Methods for navigating within a simulated environment
- Methods for manipulating virtual objects
- Command modes for steering simulations
- Methods for interaction within multi-participant applications

3.2.2 Effects of VE Systems on Learning

VE systems have the potential to enhance many aspects of learning (e.g., complex knowledge structures, procedural and spatial skills [8], pattern recognition) as compared with other modes of instruction. Unfortunately, the effects of VE simulation on the acquisition of knowledge and perceptual, cognitive, and motor skills are not well understood. Studies should be conducted to understand the role(s) that VE systems can play in achieving various training objectives, and the advantages of VEs over other technologies for the development and retention of knowledge and skills and their transfer to the actual environment. Factors that may affect learning include:

- Immersion (HMD) versus window-on-the-world (CRT)
- 2-D versus 3-D display
- Dynamic versus static objects
- Interactive versus passive participation
- Effects of scale and perspective
- Effects of varying fidelity.

The advantage of VE technology over other training media will depend on the kind of task being learned and the stage of skill acquisition. For example, both electronics troubleshooters and jet engine mechanics must have a sophisticated functional representation, or mental model, of the target system. A logical case could be made that students in either or both disciplines would develop a more complete or useful mental model of the target system from a VE simulation than from the same information presented via another medium (e.g., 2-D model on a CRT). Empirical data on this issue are lacking, however. It is quite possible that the mechanical task environment requires a spatial component in the mechanic's mental model that is not present (or necessary) in the troubleshooter's model. It remains to be demonstrated that VE training in a 3-D world would facilitate the acquisition and use of that representation on the job. The availability of a third dimension can serve to simplify the presented mental model in cases where it is able to reveal patterns or relationships that are hard to discern in two-dimensional representations (e.g., molecular structures). If, however, representation of a third dimension leads training developers to implement more complex mental models, this virtue could be lost. Research investigating whether, and under what conditions, a VE simulation is more effective than CRT-based simulations in conveying a mental model would determine an important role for VE training systems.

Another issue concerns possible advantages of acquiring additional mental representations of the content to be learned. A mechanic's expertise is tied closely to perceptual skills (e.g., hearing a "faulty" sound, feeling a warp, seeing a crack, or estimating distance). If the sense of presence and kinesthetic experience with the virtual system facilitate learning of these skills, then a VE simulation would have advantages over a conventional CRT display of the same 3-D graphics. On the other hand, if the value of VE technology for promoting learning about systems lies in the

provision of interactive three-dimensional graphics, the use of VE technologies (e.g., head-mounted display, 3-D audio) that are more costly is unnecessary.

3.2.3 Instructional Strategies

In our report, we assume that a typical VE training system will incorporate several advanced technologies (e.g., intelligent authoring and delivery, speech recognition, software simulation, and modeling technologies). Although some of these components have already been synthesized into prototype training systems, fielding a VE system will not be simply a technical matter. VE will add a level of complexity to training delivery that is not well understood. An important implementation issue will be understanding how best to employ VE technology to achieve a given training objective. Experience with some nontraining VE applications suggests that users should be free to explore the virtual world without encumbrance. Training studies using other technologies, however, indicate that guided exploration and structured tutorial are more effective for some objectives. VE development efforts have not yet dealt with the problems associated with such issues. Questions regarding how, and how much, the system should intrude into the environment will be important in determining both the effectiveness and acceptability of VE as a training tool. Studies should be conducted to develop effective training methods in a VE.

A related issue involves the stage(s) of training (or skill development) in which VE is most effective. Our interview respondents suggested that for some tasks, VE can be used early in training to familiarize the student with the job environment. For other tasks, VE would be most effective in hands-on training to develop procedural, perceptual, and cognitive skills. Research is needed to identify task characteristics that determine the appropriate timing and quantity of VE training. Studies should be conducted to develop guidelines specifying how VE and other technologies can be used in concert to optimize the benefits of each.

3.2.4 Testing Studies

Testing is an area in which VE shows much promise. Current commonly used methods tend to suffer from either a lack of content validity (e.g., use of written tests when task skills are at issue) or a lack of standardization (e.g., lack of reliable scoring for performance tests). VE could be used to test the qualifications of a student for promotion to the next stage of training, and to assess the continuing competency of journeyman technicians. VE might also offer a more effective alternative to current methods in the administration of aptitude and job-screening tests. Although not the focus of this study, the trend toward performance-based aptitude and screening tests clearly suggests a role for the kind of simulation offered by VE systems.

4 CONCLUSIONS AND NEXT STEPS

Although its role is clear in training that otherwise would not be feasible, the utility and cost-effectiveness of VE as a general-purpose maintenance training tool remains untested. Several obstacles must be overcome before VE can offer the benefits envisioned by its promoters. To be useful as a maintenance training delivery system, VE systems must achieve a higher level of technical sophistication than is currently available (e.g., higher visual resolution), and they must be cost-effective in comparison with alternative training delivery systems. Moreover, VE systems will have to prove their effectiveness for learning. This will mean developing a research base from which we can draw inferences about which VE and companion technologies are appropriate for a given application, and developing guidelines for effective feedback and user interaction protocols (e.g., how should a user move around: gestures, voice commands, physical movement?). It will also require an understanding of how this new form of simulation affects knowledge (e.g., mental model) and skill (e.g., spatial reasoning) acquisition.

Virtual environment systems are expected to become commonplace within the next decade, so it is essential that government and industry prepare to exploit this technology as it matures. One major question that must be answered concerns whether VE systems will provide more efficient and effective means of accomplishing specific training goals than comparable traditional systems. Like most questions of this complexity, this one has no simple answer; VE systems will be cost-effective in some applications, but not in others. We are currently formulating a plan for the suggested VE research, focusing on the development of demonstration systems for selected maintenance training applications. The plan will include recommendations for research priorities and sequencing, as well as the coordination of efforts among DoD and NASA organizations. The plan addresses hardware and software procurement and facilities requirements, including the relative advantages of centralized versus decentralized facilities. It also considers the impact of ongoing VE R&D as well as training R&D in closely related areas.

ACKNOWLEDGMENTS

The work reported in this paper was conducted under NASA contract # ECU90-117 to SRI International as part of a cooperative agreement between NASA and the Air Force. The authors gratefully acknowledge the guidance of the VE interest group made up of Air Force, Navy, and NASA research personnel and the enthusiastic participation of personnel at ATC HQ, Randolph AFB; ALC Technology and Industrial Support Directorate, Hill AFB; ATC 3760 Technical Training Wing, Sheppard AFB; SAC 436 Strategic Training Wing, Carswell AFB; ATC 3306 Training Development Squadron, Edwards AFB; several offices within ASD, Armstrong and Wright Labs, Wright-Patterson AFB; Remote Operator Interaction Lab and the Space Station Training Office, NASA/Johnson Space Center; Army Crew Station R&D Facility, NASA/Ames Research Center; and a large number of commercial R&D organizations.

REFERENCES

1. Zeltzer, D., "Autonomy, Interaction, and Presence," PRESENCE, Vol. 1, No. 1, 1992, pp. 127-132.

2. Helsel, S.K., "Virtual Reality as a Learning Medium," INSTRUCTIONAL DELIVERY SYSTEMS, Vol. 6, No. 4, July/August, 1992, pp. 4-5.

3. Muller, D.G., & Leonetti, R., "A Major Technological Advancement in Training," INSTRUCTIONAL DELIVERY SYSTEMS, Vol. 6, No. 4, July/August, 1992, pp. 15-17.

4. Bricken, M., "Virtual Reality Learning Environments: Potentials and Challenges," Human Interface Technology Laboratory white paper, University of Washington, Seattle, 1991.

5. Boman, D, Schlager, M.S., Gille, J., & Piantanida,T., "The Readiness of Virtual Environment Technology for Use in Maintenance Training," in PROCEEDINGS OF THE INTER-SERVICE/INDUSTRY TRAINING SYSTEMS CONFERENCE, San Antonio, TX, November 2-5, 1992.

6. Rushby, N., "Near Enough to the Real Thing," PERSONNEL MANAGEMENT, Vol. 20, October, 1989.

7. Baughman, M.L., Hudspeth, D., Kendrick, D., & Thore, S., "Workstations in Education and Training," ARPA Order No. 6675/4, DARPA, Austin TX, July, 1991.

8. Regian, J.W., Shebilske, W.L., & Monk, J.M., "A Preliminary Empirical Evaluation of Virtual Reality as an Instructional Medium for Visual-Spatial Tasks," JOURNAL OF COMMUNICATION, in press.

N94-11571

ON-ORBIT SERVICING FOR USAF SPACE MISSIONS– A PHASED DEVELOPMENT APPROACH

Bill Shanney
The Aerospace Corporation
P.O. Box 3430
Sunnyvale, CA 94088-3430

On-orbit servicing has been studied for years by the U.S. Air Force Space Systems Division, which recently cosponsored the Space Assembly, Maintenance, and Servicing Study with NASA and SDIO; but an Air Force servicing program has yet to emerge. The Air Force has a limited set of servicing requirements, and the practices of "pipelining" (incremental improvements to a space vehicle series) and orbital sparing provide many similar benefits. It is postulated that an Air Force program will be initiated in response to a new critical mission requirement that calls for a spacecraft with the operational character of a Servicer, which will evolve into a servicing program. Such a requirement may be emerging. The Air Force organizations charged with on-orbit test safety for the Department of Defense are concerned with the hazard from uncontrolled reentry of low Earth orbit test spacecraft, which are increasing in number. Analysis and observation of actual reentries show that debris reaches the Earth's surface. A phased development of a system to remove these spacecraft from orbit can evolve into a servicing program.

N94-11572

MORE SENSE FOR LESS CENTS: COST EFFECTIVE SERVICING OF REMOTE SENSING SATELLITES

Jeannie Lee, Tom Misencik, Bill Robertson, and Jack Sliney
Dynamics Research Corporation
1755 Jefferson Davis Highway, Ste. 802
Arlington, VA 22202

This paper addresses the design considerations for Earth observation spacecraft bus and payload subsystems such that cost-effective spacecraft maintainability is enhanced through optimized reliability and the application of robotic on-orbit support. In the past, for most satellites maintainability has been associated with the clever application of telemetry reconfiguration and the use of redundant systems as necessary over the life cycle of the spacecraft. This presentation addresses the opportunities and challenges of leveraging the extensive work already accomplished in the development of on-orbit servicing technologies.

The example that is illustrated in the paper is a constellation of Earth observation satellites located in Sun-synchronous orbits. These highly inclined, retrograde orbits nodally regress in such a way as to keep pace with the Earth's movement around the Sun. As such, Earth-sensing systems in SS orbit always view the Earth with the same Sun shadow angle. Both the industrially advanced and developing nations have great interest in placing Earth observation and other sensing systems in orbit with these parameters. It is estimated that by the year 2000, there will be upwards of 30 Earth observation platforms in the region between 600 and 900 km altitude and 97 to 99 deg inclination. Lower altitude orbits would, of course, be possible with the existence of a service vehicle to either reboost or replenish propellants. Some of the platforms, such as the EOS, will house multiple experiment payloads. With appropriate design of such a platform, it is feasible that experiments could be upgraded and new instruments added by the service vehicle years after the platform was initially orbited. International standardization of orbital replacement units (ORUs), fluid couplings, and docking interfaces would allow the servicing of participating nation satellites by a common support infrastructure. Conceptually, the infrastructure consists of transfer/service vehicles, either free flying or stationed at space-based support platforms (SBSPs) at discrete altitudes and inclinations. These SBSPs serve as the focal point for receipt and storage of ground-launched ORUs, consumables, and satellites as well as serving as staging areas for OMVs, OTVs, and robotic Servicer elements. In addition, the SBSPs serve as holding areas for failed or degraded ORUs until such time as they can be returned to Earth.

Cost effectiveness, however, depends on amortizing the investment in such a support infrastructure over a sufficient number of eligible spacecraft and in reaping other cost benefits. Some of these benefits are preplanned product improvement (P31), fluid replenishment, system reboost, and relaxation of redundancy requirements. The paper describes, first, an area for potential international cooperation and, second, an analysis of how design consideration based on quantifying the cost of reliability can offer significant enhancement to spacecraft maintainability.

N94-11573

ASSURED MISSION SUPPORT SPACE ARCHITECTURE (AMSSA) STUDY

Commander Rob Hamon
US Space Command
Mail Code: 35
Peterson AFB, CO 80914

The assured mission support space architecture (AMSSA) study was conducted with the overall goal of developing a long-term, requirements-driven integrated space architecture to provide responsive and sustained space support to the combatant commands. Although derivation of an architecture was the focus of the study, there are three significant products from the effort. The first is a philosophy that defines the necessary attributes for the development and operation of space systems to ensure an integrated, interoperable architecture that, by design, provides a high degree of combat utility. The second is the architecture itself; based on an interoperable system-of-systems strategy, it reflects a long-range goal for space that will evolve as user requirements adapt to a changing world environment. The third product is the framework of a process that, when fully developed, will provide essential information to key decision makers for space systems acquisition in order to achieve the AMSSA goal.

It is a categorical imperative that military space planners develop space systems that will act as true force multipliers. AMSSA provides the philosophy, process, and architecture that, when integrated with the DOD requirements and acquisition procedures, can yield an assured mission support capability from space to the combatant commanders. An important feature of the AMSSA initiative is the participation by every organization that has a role or interest in space systems development and operation. With continued community involvement, the concept of the AMSSA will become a reality. In summary, AMSSA offers a better way to think about space (philosophy) that can lead to the effective utilization of limited resources (process) with an infrastructure designed to meet the future space needs (architecture) of our combat forces.

Session S5: SPACE SYSTEMS DESIGN CONSIDERATIONS

Session Chair: Jeffrey Hein

N94-11574

DEFINITION OF SPACECRAFT STANDARD INTERFACES BY THE NASA SPACE ASSEMBLY AND SERVICING WORKING GROUP (SASWG)

Robert Radtke
Tracor Applied Sciences, Inc., Kingwood, Texas

Charles Woolley
NASA JSC, Houston, Texas

Lana Arnold
Lockheed / ESC, Houston, Texas

Abstract

The purpose of the NASA Space Assembly and Servicing Working Group is to study enabling technologies for on-orbit spacecraft maintenance and servicing. One key technology required for effective space logistics activity is the development of standard spacecraft interfaces, including the "Basic Set' defined by NASA, U.S. Space Command, and industry panelists to be (1) navigation aids, (2) grasping, berthing, and docking, and (3) utility connections for power, data, and fluids. Draft standards have been prepared and referred to professional standards organizations, including the AIAA, EIA, and SAE space standards committees. The objective of the SASWG is to support these committees with the technical expertise required to prepare standards, guideline, and recommended practices which will be accepted by the ANSI and international standards organizations, including the ISO, IEC, and PASC.

1. INTRODUCTION

The Space Assembly and Servicing Working Group (SASWG) is a NASA organization with over 700 individual members from government, industry, and academia dedicated to the study of enabling technologies for spacecraft maintenance and servicing. Currently, an Interface Standards Committee (ISC) is composed of 60 voluntary members who are preparing and reviewing draft documents which have been referred to professional standards organizations to become standards, guidelines, or recommended practices. After thorough review by the professional standards organization, with the assistance of SASWG ISC members, the document is adopted by the standards organization, and referred to the American National Standards Institute (ANSI) for referral to international standards organizations.

Three organizations have accepted SASWG interface standard projects. They are (1) the American Institute of Astronautics and Astrophysics (AIAA), (2) the Electrical Industry Association (EIA), and (3) the Society of Automotive Engineers (SAE). Each organization is accredited by ANSI to develop the American National Standards. Only ANSI serves as the U.S. member of international standards organizations such as the International Organization for Standardization (ISO), the International Electrotechnical Commission (IEC), and the Pacific Standards Congress (PASC).

The SASWG ISC is composed of NASA, U.S. Space Command, U.S. Air Force, U.S. Navy, and industry personnel organized into five functional areas (mechanical, electrical, fluid, thermal, and optical). Functional chairmen, elected for their areas of expertize, lead 10 draft standards projects.

While the SASWG has set an objective to create international spacecraft standards to support space maintenance and servicing, it should be noted that there are other compelling reasons to support international spacecraft standards. Joint U.S. Government and industry activity is needed to support both private sector interests in government-to-government standards negotiations. Firstly, it is unlikely that industry alone will provide the necessary financial support for U.S. representation. Secondly, industry cannot perform a adequate role of negotiator to assure a means for U.S. manufacturers to meet international standards and continue to have access to international markets.

Recently SASWG spacecraft standards panel discussions have described the need for a "Basic Set" of interface hardware standards for satellites and platforms. The set is to include (1) Navigation Aids, (2) Grasping, Berthing, and Docking Interfaces, and (3) Utility Connectors (electrical power, data, and fluid connectors, as required by spacecraft for on-orbit maintenance). It is the objective of the SASWG to develop international standards for these critical interfaces.

2. DISCUSSION

2.1 Current SASWG Interface Standards Projects

Documents have been referred to professional standards organizations for review and approval.

American Institute of Aeronautics and Astronautics

(1) Grasping / Berthing / Docking - AIAA Guideline, Serviceable Spacecraft Committee on Standards (SS COS)
(2) Flight Releasable Grapple Fixture (FRGF) - AIAA Standard, Committee SS COS
(3) Magnetic End Effector - AIAA Guideline, Committee SS COS
(4) Utility Connector - AIAA Guideline, Committee SS COS

Electrical Industry Association

(5) Electrical Connector - Sub-Miniature - EIA Standard, Committee CE 2.0
(6) Electrical Connector - Large - EIA Standard, Committee CE 2.0
(7) Fiber Optic Connector - EIA Guideline, Committee F-06

Society of Automotive Engineers

(8) Fluid Connector - SAE Recommended Practice, Committee G-3
(9) Hex Head Bolt and Socket - SAE Standard, Committee E-25
(10) Replaceable Thermal Insulation - SAE Technical Project, Committee EAAATA–3 (planned for 1992)

2.2 SASWG INTERFACE STANDARDS PREPARATION METHODOLOGY

The SASWG ISC standardization process is performed in six steps:

1) Identify and discuss key standards issues during face-to-face meetings and report in SASWG ISC Minutes.
2) Prioritize candidate hardware interfaces projects by consensus vote.
3) Identify committee members from industry and government and elect a project leader.
4) Prepare draft standards, guidelines, and recommended practices (mostly performed with communication by facsimile and telecon).
5) Refer draft documents to professional standards organizations for review and approval.
6) Attend professional standards organizations committee meetings and provide consultation, especially for technical requirements unique to spacecraft design and operations.

3.0 AMERICAN INSTITUTE OF ASTRONAUTICS AND ASTROPHYSICS INTERFACE STANDARDS PROJECTS

3.1 AIAA GUIDELINE FOR THE SERVICEABLE SPACECRAFT GRASPING / BERTHING / DOCKING INTERFACES

This guideline provides technical information for the design of three mechanical interfaces required for spacecraft servicing -- grasping by telerobotic or visual manipulation, berthing of payloads or spacecraft, and docking of spacecraft. Achieving a degree of commonality individually and collectively for this general class of interface will simplify the servicing of a variety of orbital replaceable units (ORU's), Attached payloads, platforms, Space Station Freedom, satellites, and other passive and mobile spacecraft. The invaluable experience of past missions from Gemini to the Shuttle Orbiter provides the basis for the information contained in this document.

3.2 FLIGHT RELEASABLE GRAPPLE FIXTURE (FRGF) STANDARD

This standard establishes the interface design requirements for three standard grapple fixtures - Flight Releasable Grapple Fixture (FRGF), Rigidized Sensing Grapple Fixture (RSGF), and Electrical Flight Grapple Fixture (EFGF). Design requirements are provided for the Grapple Fixture interface and Extravehicular Activity (EVA) release interface. It should be noted that there are three new non-standard grapple fixtures models - Flight Releasable Light Weight Grapple Fixture (LWGF), Auxiliary Grapple Fixture (AGF), and Electrical Light Weight Grapple Fixture (ELWGF). The light weight grapple fixtures are a solution to the weight / budget problems of payloads.

3.3 MAGNETIC END EFFECTOR STANDARD

The Magnetic End Effector has been developed to provide a dextrous end effector for the Shuttle Remote Manipulator System (RMS). Work is progressing to perform a flight demonstration. This standard establishes the interface design requirements for the end effector to payload interface.

3.4 UTILITY CONNECTOR GUIDELINE

This guideline reviews the development of a utility connectors for spacecraft servicing systems. Utility connectors are designed for fully automated remote operation, separate from and independent of any docking mechanism, operation after a docking mechanism is rigidized, and are compatible with both single point and three point docking mechanisms. Designs are reconfigurable for monopropellant, bipropellant, and cryogenic resupply.

4.0 ELECTRONIC INDUSTRY ASSOCIATION INTERFACE STANDARDS PROJECTS

4.1 STANDARD FOR CONNECTORS, ELECTRICAL, RECTANGULAR, BLIND-MATE, SCOOP-PROOF

This standard provides terminology, description and requirements of a blind-mate, scoop-proof, rectangular shell series of electrical connectors for serviceable spacecraft for use during space and ground support activities. Aspects such as size, alignment, mating force, material requirements, reliability, durability, weight, electrical and physical characteristics, and temperature range are covered. The intent is to insure compatibility to both unmanned and robotic based servicing modes.

4.2 STANDARD FOR CONNECTORS, ELECTRICAL, RECTANGULAR, BLIND-MATE, SCOOP-PROOF, LOW-FORCE, SUBMINIATURE

This guideline is for a rectangular electrical connector similar to the connector above, except for the size and locking mechanism. This connector is smaller, and may utilize release levers designed to be compatible for Extravehicular Activity (EVA) or robotic engagement and release.

4.3 GUIDELINE FOR CONNECTORS, FIBEROPTIC

This guideline provides design requirements for fiberoptic connectors for spacecraft use. NASA Long Duration Exposure Facility (LDEF) experience has shown that conventional fiberoptic connectors survived the space environment without any degradation or loss in performance.

5.0 SOCIETY OF AUTOMOTIVE ENGINEERS INTERFACE STANDARDS PROJECTS

5.1 FLUID COUPLINGS FOR SPACECRAFT SERVICING

The objective of this recommended practice is to provide high level design, development, verification, storage, and delivery guidelines for fluid couplings and its ancillary hardware for spacecraft servicing. The couplings shall be capable of resupplying storable propellants in a variety of space environments.

5.2 HEX HEAD BOLT AND SOCKET INTERFACE

This standard provides and design and materials requirements for a 8 and 12 millimeter hex head bolt to spacecraft fastening. Dimensions and clearances were determined to assure bolt and socket compatibility over the temperature extremes of space as part of a Special Project prior to the preparation of a draft standard for spacecraft fasteners.

5.3 REPLACEABLE THERMAL INSULATION

This recommended practice provides design concepts for candidate mechanisms to attach thermal insulation to orbital replacement units (ORUs) and other spacecraft services where thermal insulation degradation is likely to occur requiring the replacement of the thermal insulation blanket.

6. CONCLUSION

The purpose of the NASA Space Assembly and Servicing Working Group Interface Standards Committee is to prioritize spacecraft mechanical, electrical, fluid, thermal, and optical interface projects selected by member consensus, prepare draft standards, guideline, and recommended practices, refer to professional standards organizations, and assist with document review, approval, and referral to international standards organizations.

7. ACKNOWLEDGMENTS

The authors acknowledge the contributions of project leaders, Allen Thompson, Consultant, David Ball, USAF, Ed Carter, Lockheed / ESC, Tom Nelson, USAF, Al Haddad, Lockheed / MSC, Bob Davis, Retired NASA GSFC, Herb Patterson, SAIC, Mark Falls, NASA JSC, Mike Withey, ILC Space Systems, and SASWG ISC Members. This work could not be performed without the continued support of Dick Weinstein, NASA Code QE and George Levin, NASA Code M.

8. REFERENCE

Arnold, Lana, Woolley, Chuck, and Radtke, Robert, "SASWG Interface Standards Committee, Draft Standards, Guidelines, and Special Projects," Lockheed / ESC, Houston, Texas, March , 1992.

N94-11575

THE GUIDE TO DESIGN FOR ON-ORBIT SPACECRAFT SERVICING (DFOSS) MANUAL: PRODUCING A CONSENSUS DOCUMENT

Janice Nyman
Environmental Research Institute of Michigan (ERIM)
P.O. Box 134001, Ann Arbor, MI 48113-4001

ABSTRACT

Increasing interaction and changing economies at the national and international levels have accelerated the call for standardization in space systems design. The benefits of standardization--compatibility, interchangeability, and lower costs--are maximized when achieved through consensus. Reaching consensus in standardization means giving everyone who will be affected by a standard an opportunity to have input into creating that standard.

The DFOSS manual was initiated with the goal of developing standards through consensus. The present Proposed Guide derives from work begun by the Space Automation and Robotics Center (SpARC), a NASA Center for the Commercial Development of Space, and has continued as a standards project through the American Institute of Aeronautics and Astronautics (AIAA). The Proposed Guide was released by AIAA in January 1992 for sale during a one-year, trial-use period.

DFOSS is a response to the need for one document that contains all the guidelines required by on-orbit spacecraft servicing designers for astronaut extravehicular activity and/or telerobotic servicing. The manual's content is driven by spacecraft design considerations, and its composition has been achieved by interaction and cooperation among Government, industry, and research organizations. While much work lies ahead to maximize the potential of DFOSS, the Proposed Guide represents evidence of the benefits of industry-wide consensus, points the way for broader application, and provides an example for similar projects.

INTRODUCTION

The Design for On-Orbit Spacecraft Servicing (DFOSS) project commenced in 1988 at the Space Automation and Robotics Center (SpARC), located at the Environmental Research Institute of Michigan (ERIM) in Ann Arbor, Michigan. SpARC is one of 17 NASA-sponsored Centers for the Commercial Development of Space (CCDS).

CCDS centers are consortiums of academic, research, and private-sector institutions, which are committed to strengthening the bonds between Government, scientific, and industrial organizations. The underlying CCDS objective is to pursue research that results in products that are economically viable for commercialization. SpARC's mission in meeting

the CCDS objective is to facilitate the commercialization of space and space technologies through the application of automation.

While formulating its mission goals, SpARC organizers looked at the requirements for the successful commercialization of space. They had discussions and meetings with representatives of space-community organizations where the importance of reducing costs and promoting compatibility and interchangeability were stressed. SpARC recognized that one way to meet that need would be through a single document that contained all the guidelines needed by on-orbit spacecraft servicing designers for astronaut extravehicular activity and/or telerobotic servicing.

SpARC envisioned DFOSS as a comprehensive overview document that, as a living document, would provide up-to-date guidelines for designers of serviceable spacecraft. The guidelines would provide a starting point for a designer and would be based on the most current material available.

CONSENSUS AS A GOAL

From the beginning of the DFOSS project, SpARC shared its vision of producing a consensus document, promoted the benefits of standardization through consensus, and solicited wide participation. One of SpARC's consortium members, the Industrial Technology Institute, and one of its industrial participants, Fairchild, provided initial material and support at the project's inception in 1988. SpARC provided project management and document production. When SpARC had taken DFOSS as far as it could with the relatively narrow participation taking place within the Center, it more actively sought a wider participation that would bring it closer to the goal of producing an industry-wide consensus document.

In November 1990, the American Institute for Aeronautics and Astronautics (AIAA Serviceable Spacecraft Committee on Standards (SS/COS) adopted DFOSS as a guidelines project. In the context of the AIAA Standards Program, consensus means that every affected person has an opportunity to comment on the draft standard and that those comments are treated in a fair and considerate manner (French 1991). Through the SS/COS DFOSS Working Group, experts from several space-community organizations came together and assumed responsibility for updating and completing the various chapters; SpARC continued its role of project management and document production.

GUIDELINES CONSIDERATIONS

As the SS/COS DFOSS Working Group proceeded, we continued the approach used by SpARC, which was based on the premise that serviceable space-based systems require unique design considerations. These considerations (Figure 1) dictate the options available to a designer

who must develop a viable and cost-effective system. Restrictions and requirements imposed on the design of serviceable space-based systems must be successfully integrated with the requirements and objectives of a particular space mission. If such issues are not considered, the resulting system design will be either too costly or too difficult to maintain.

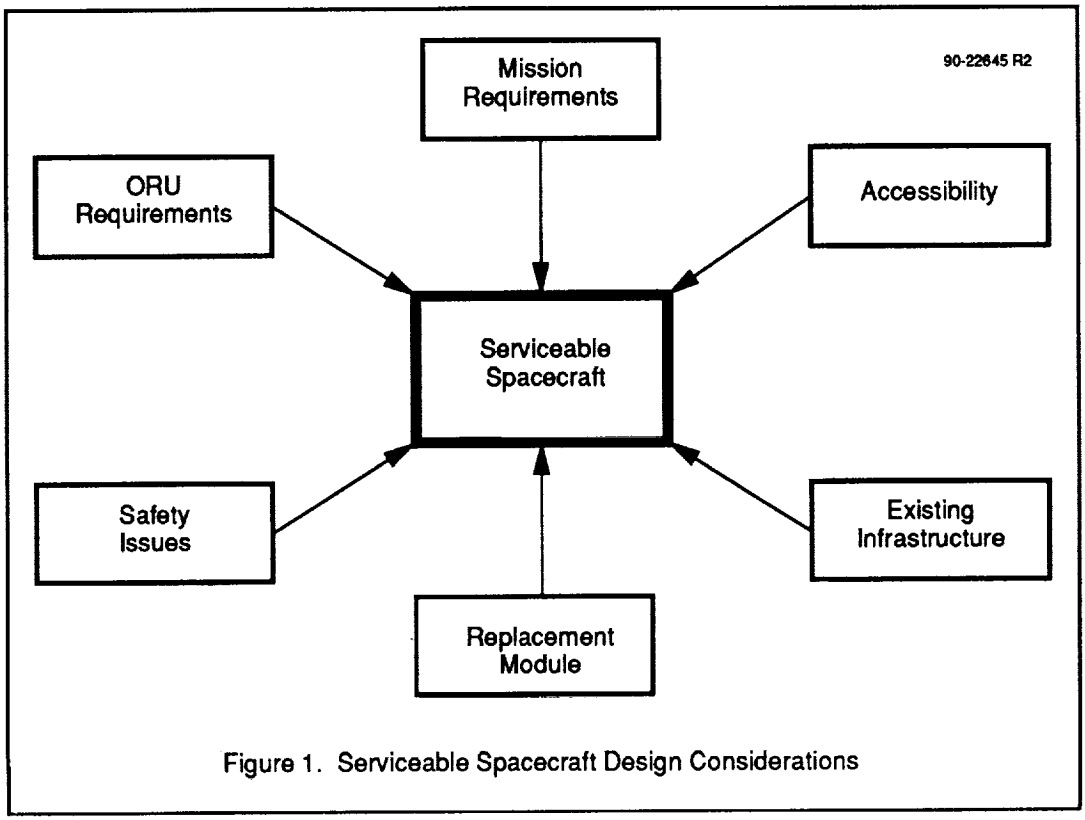

Figure 1. Serviceable Spacecraft Design Considerations

In addition to the spacecraft design considerations, we targeted two goals for the DFOSS guidelines. We felt it essential that the guidelines:

1. Serve as an architecture for: (a) mission-specific guidelines for the design of serviceable spacecraft, (b) specific guidelines for a class of serviceable vehicles, and (c) guidelines for a type of device.

2. Provide an easily referenced format for the information required for a designer to: (a) specify the design requirements and (b) specify the design of serviceable spacecraft.

MANUAL CONTENTS

Through an intensive and dedicated effort by many experts throughout the space community (see Acknowledgments), the Review Copy of the Proposed Guide was completed in the fall of 1991. These guidelines provide a starting point for a designer. Although some of the material has not previously appeared in print, the majority of it is a restatement, reorganization, and compilation of data from valued sources as articulated and selected by the document's many contributors.

The contents of the Proposed Guide flow out of the DFOSS design methodology, with each topic forming a chapter as shown in Figure 2.

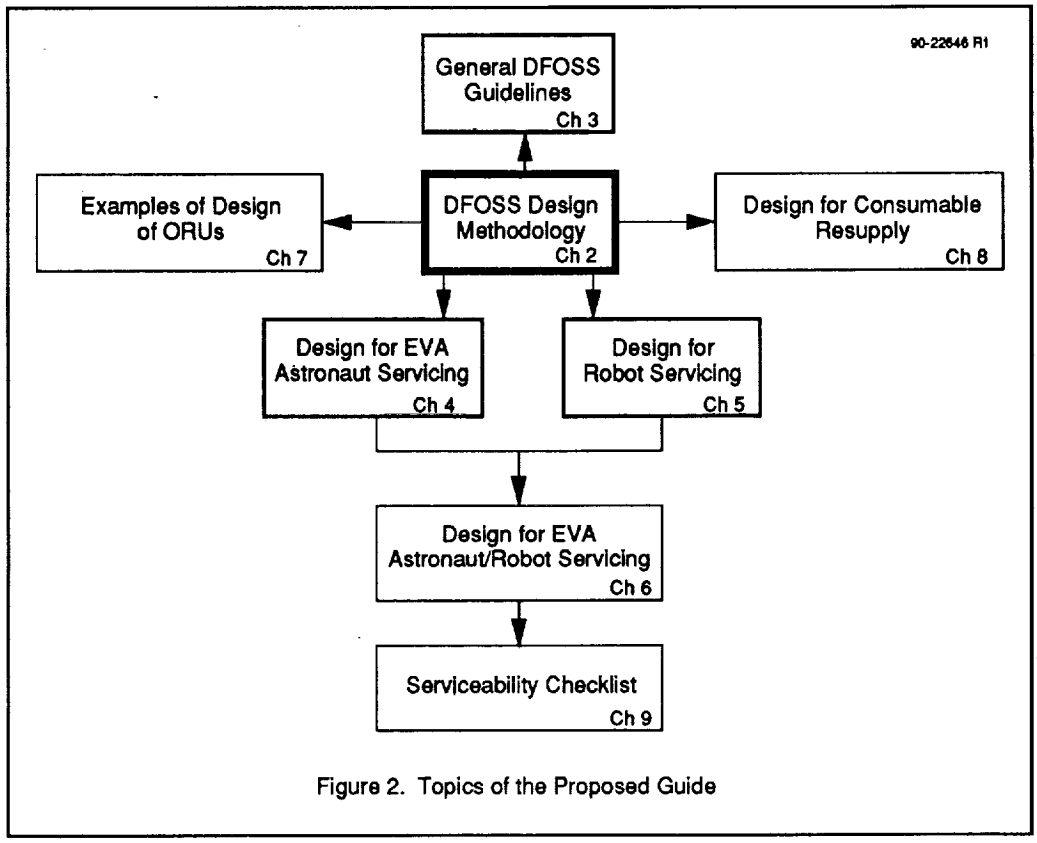

Figure 2. Topics of the Proposed Guide

The manual is approximately 350 pages long and contains approximately 300 figures. It was written, illustrated, and formatted in an easy-to-read and easy-to-use style, as illustrated by the sample pages in the appendix.

CONCLUSION AND FUTURE PLANS

It is generally understood that guides and standards are only as current, valid, and acceptable as the input that created them. The way to test input is to produce a consensus document that draws on a given discipline as widely as possible. Our first step was to produce the Proposed Guide through the collaboration and input of the Working Group. Our second step was to include critique sections in the Proposed Guide to solicit comments from all users. Third, the availability of the Proposed Guide continues to be announced through AIAA publications, presentations, on-line cataloging, mailings, handouts, and so forth. Based on the feedback from the critiques, the SS/COS DFOSS Working Group will decide how to proceed, using the consensus mechanism, to complete a revised Guide.

ACKNOWLEDGMENTS

Rodney Bennett (USAF Space Systems Division/ALII), Joseph Cardin (Moog Inc.), Steve Chucker (McDonnell Douglas Space Systems Company), Robert E. Davis (Goddard Space Flight Center), James D. Duffy (PRC Inc.), Paul W. Elwell, Jr. (Moog Inc.), James E. French (AIAA Headquarters), Frank G. Gallo (NUS), Barney Gorin (AIAA SS/COS), Paul Grippo (Consultant), William O. Keksz (Fairchild), Otto Ledford (PRC Inc.), Mark Lueker (ARINC Research Corp.), Wayne Markison (USAF Space Systems Division/ALII), James S. Moore (AIAA SS/COS), Charles Perrygo (IDEA), Robert Radtke (Tracor Applied Sciences), George J. Sawaya (AIAA SS/COS), Dick Spencer (Martin Marietta), Robert Trevino (Johnson Space Center), and Charles Woolley (Johnson Space Center).

REFERENCE

French, James E., "Draft Standards Introduction for AIAA Publications Catalog," AIAA, Washington, DC, November 1991.

CHAPTER

4

DESIGN FOR EVA ASTRONAUT SERVICING

4.1 INTRODUCTION

This chapter presents guidelines and information for designing equipment and payloads that are intended for servicing by an extravehicular activity (EVA) crew member. EVA can provide an effective means for service, maintenance, repair, or replacement of spacecraft equipment without the need to return the equipment to a pressurized environment, return it to Earth, or abandon it. In a microgravity (zero-g) environment, EVA crew member capabilities, relative to an Earth-based (one-g) environment, are improved for certain functions and degraded for others. The advantages of the space environment allow the crew member unlimited mobility in any direction and relatively effortless translation of equipment and payloads. The main factors that may degrade crew member performance are pressure suit limitations, inadequate crew member restraint, crew scheduling constraints (6 hours), unpredictable crew motion sickness, or improperly designed tools and equipment.

This chapter provides designers with information and data that take into account the capabilities and constraints of an EVA-suited astronaut and provides guidelines for designing equipment and payloads that are compatible with the EVA crew member's physical capabilities and limitations.

The current capabilities and constraints of an EVA-suited crew member and how they influence the design of serviceable equipment and payloads will be addressed in the following sections, which include:

- Alignment Aids (4.2)
- Anthropometry (4.3)
- Clearances (4.4)
- Controls and Displays (4.5)
- Electrical Connectors and Cables (4.6)
- EVA Enhancement Systems (4.7)
- EVA Restraint and Lighting Equipment (4.8)

4.4.3 TOOL CLEARANCE

• *Drive Tool Clearance*—Provide a 2.5 cm (1 in) minimum diameter clearance around fasteners for insertion, actuation, and removal of the drive end of the tool, as shown in Figure 4.4-2.

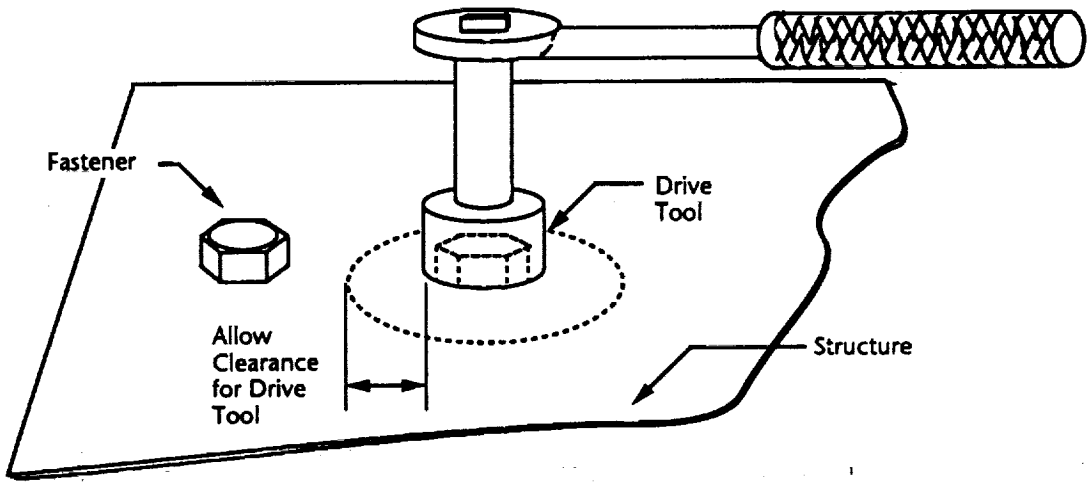

Figure 4.4-2. Drive Tool Clearance

91-21515

• *Tool Handle and Surface Clearance*—Provide a minimum of 7.6 cm (3 in) clearance for tool engagement between the tool handle engaged on a fastener or drive stud and the surrounding hardware and structure (e.g., ORU). In addition, the tool handle should be able to maintain this clearance through a full 90-degree operation-envelope as shown in Figure 4.4-3 and should allow right- or left-handed operation.

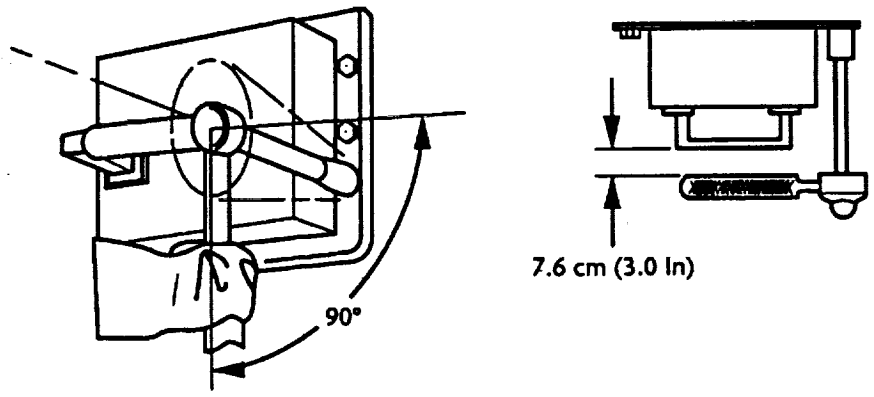

Figure 4.4-3. Minimum Sweep Clearances Between Hand Tools and Hardware/Structures

91-21514

4.4 CLEARANCES

4.4.1 INTRODUCTION

To facilitate EVA tasks, sufficient clearances between an EVA suit and surrounding structures must be provided. Guidelines for defining these clearances are provided in the following sections:

- EVA Glove Clearance (4.4.2)
- Tool Clearance (4.4.3)
- Translation Route Clearance (4.4.4)

4.4.2 EVA GLOVE CLEARANCE

• *Reaching Into Aperture*—For payload servicing operations that require reaching into an aperture, designers should position equipment as close to the exterior surface as possible and allow sufficient volume for access by the EVA glove and for visibility by the crew.

• *Work Envelope*—The minimum work envelope required for an EVA-gloved hand is shown in Figure 4.4-1. A clearance envelope 20 cm (8 in) in diameter by 36 cm (14 in) [nominal] deep will allow an EVA crew member to manipulate most hand-operated latches, switches, buttons, knobs, and other controls. However, the aperture must be increased for operation of valves, connectors, and latches requiring torquing motions or heavy force application.

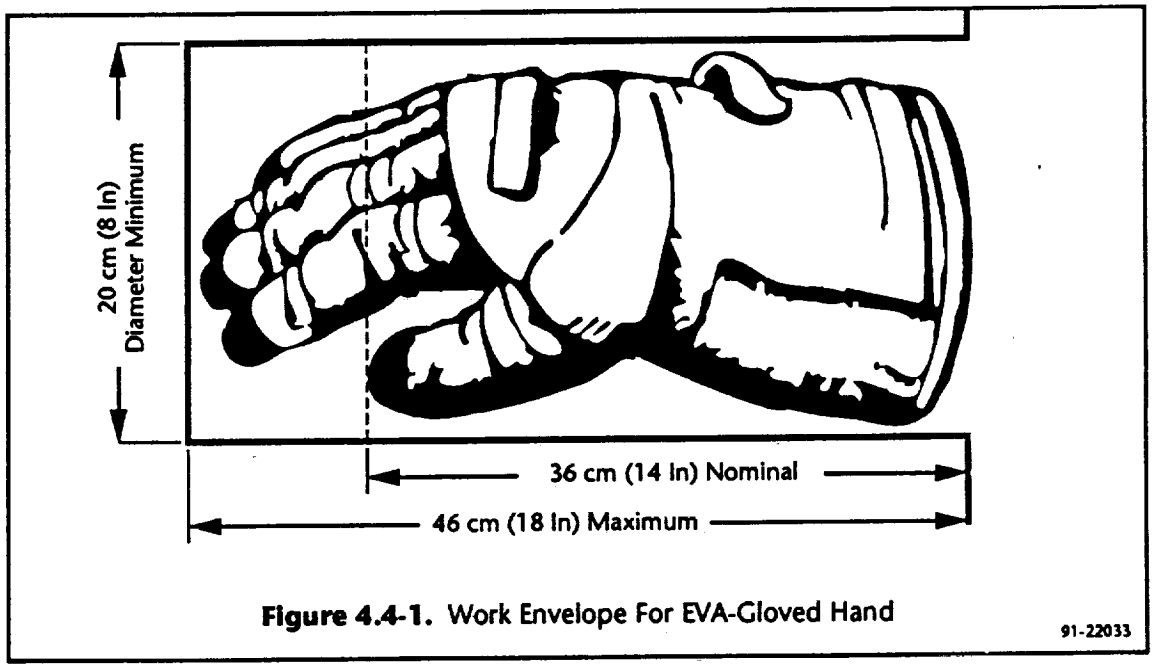

Figure 4.4-1. Work Envelope For EVA-Gloved Hand

91-22033

THE NATIONAL LAUNCH SYSTEM ADVANCED DEVELOPMENT PROGRAM A BRIEF OVERVIEW

J. A. Battenburg
NLS Joint Program Office
SMC/CJED
Norton AFB, CA 92409

Abstract

A broad-based Advanced Development Program is being conducted to modernize the technological base and support the systems design of the National Launch System. While the principal concentration of efforts has been in propulsion, significant work is being accomplished in all of the disciplinary areas associated with space launch. Tasks are selected that offer reduced costs. increased reliability, and enhanced operability with anticipated task completion times which are consistent with NLS development.

Introduction

Reaching the NLS goals for a low cost, highly reliable, highly operational launch system presents a challenge which requires a combination of strategies. These strategies include launch system design for operations, exploitation of vehicle scale and flight rate effects where appropriate, simplified operational and payload interfaces, and use of existing and advanced technologies properly focused and applied to the space launch discipline. Technology activities of the NLS are conducted in an Advanced Development Program (ADP) which is closely coupled to the system design and whose purpose is to validate those cost effective technologies which support NLS requirements, are applicable to the NLS system design and operational concepts, and are available to support the NLS schedule.

The ADP is implemented as a set of technology tasks which are selected to provide the maximum benefit to the NLS. The objective of each task is to demonstrate those benefits so the applicable technology can be incorporated into the NLS with high confidence and low risk. These demonstrations will include design of prototypes at as near full scale as practical. The most important products of these demonstrations are the validation of cost, producibility, operability, and performance characteristics. The ADP is organized in five major areas: (1) Propulsion; (2) Avionics and Software; (3) Structures, Materials and Manufacturing; (4) Aerothermodynamics and (5) Operations. Objectives of each of these areas in support of a low cost, highly reliable NLS are summarized below.

Propulsion

The focus of the propulsion area is to enable the development of a low cost, robust liquid oxygen-liquid hydrogen engine. In order to achieve the objective of low cost, emphasis has been placed on reducing manufacturing and fabrication costs at the piece-parts level. This is best accomplished by reducing the number of parts in each sub-element of the engine assembly, by fabricating in a near net shape form. One technique for accomplishing this is the use of precision castings to replace current expensive machining operations A structural jacket and all manifolds of the main combustion chamber has been successfully cast as a single piece using an advanced precision casting process. Housing components of the hydrogen turbopump have also been cast. Several other techniques are being investigated that show promise to significantly reduce the cost of previously labor-intensive processes. A vacuum plasma spray process has been successfully used in the fabrication of the cooler liner of the combustion chamber. This, along with several other techniques for fabricating the cooler liner, show promise of reducing the time required to build this item. In addition to the development of these processes funding has been allocated to bring on-line a complete set of cryogenic engine test facilities to allow for the full-scale development and testing of the turbomachinery components as well as prototype and and production engines.

Avionics and Software

With the rapid turnover in avionic component technology, the primary focus in the avionics area is to develop open ended avionic architectures to serve the entire family of NLS vehicles. Designing in the ability to easily upgrade avionics as new technology becomes available is critical. This program emphasizes the development of common hardware and software as well as standardized interfaces. This work is expected to allow the eventual design of the avionics system for the initial NLS vehicles to inexpensively accept improvements in the avionics (without redesigning the whole system) when initial components become obsolete. Work in the adaptive guidance area will enhance meeting initial vehicle requirements for engine-out capability and for accommodating changes in weather (primarily winds aloft), payloads and orbital requirements.

Guidance, navigation, and control mission data loads have historically required long lead times and significant manpower to prepare and validate. Only slight variations in mission, payload and/or environmental conditions require a recomputation and validation of the mission data load. The development of modern adaptive and robust AGN&C techniques in this program will eliminate a vast portion of the initial preparation work and will accommodate a wide variation in mission requirements and environmental deviations on the day of the launch. To further improve launch reliability and reduce stand-down time we are developing a Light Detection and Ranging (LIDAR) system to obtain wind profiles and atmospheric density along the booster's predicted flight path, rather than relying on current methods which are unable to provide timely data when the atmospheric conditions are rapidly changing.

Structures, Materials and Manufacturing

Key projects in the structures, materials and manufacturing area include efforts to develop and fully characterize a new family of aluminum alloys using lithium as an alloying element. The resultant materials offer significant improvement in strength, stiffness, and weight reductions over conventional alloys. Developing aluminum-lithium will provide for significant weight and risk reduction in the vehicle structures presently baselined in conventional aluminum for both the launch vehicles and the new upper stage. (Structural weight reduction is particularly critical for the 1.5 stage NLS 2 and for the NLS upper stage since it translates pound-for-pound into payload growth). Alternatively, the incorporation of aluminum-lithium could result in higher structural margins. The overall effect is expected to produce meaningful cost savings for the NLS program. Further, cost reductions will be accrued by demonstrating net shape technology for manufacturing sub-elements of the tank and dry bay structure. Very large extrusions of T-stiffened barrel sections have been fabricated to replace the expensive and time-consuming machining operations that are currently used in tank walls. Superplastically formed stiffeners that may have application for the dry bay structure (intertank, shroud and aft adaptor) have also been successfully fabricated. A welding process has been demonstrated that automatically tracks the seam, provides data for statistical process control, and practically eliminates manual inspection.

Aerothermodynamics and Recovery

While initial NLS vehicles are not required to have recoverable systems, sufficient effort is required to insure that detailed vehicle design activity can proceed and still preserve the ability to implement recovery features in the future. Funding in this area has been used to validate the viability of currently developed recovery methods and understand the significant cost trade-offs for recovery in general. It is vital to obtain this understanding prior to finally establishing vehicle designs since features to accommodate future recovery must be incorporated. A large-scale parafoil has been successfully drop tested with a 14,000 lb payload to demonstrate precision recovery of high cost elements of the vehicle. Another project is designed to show feasibility of recovering a propulsion/avionics module. A wind tunnel program to determine aerodynamic properties of the reentry body has been completed; a sub-scale water drop test demonstrated flotation properties; and a half-scale ocean recovery of the module has been demonstrated. The current effort is concentrating on the design of a deployable spray shield that will inhibit sea water entry into the module when entering and floating in the ocean. Future efforts will concentrate on developing specific full scale recoverable designs consistent with established system configurations.

Operations

A significant percentage of current launch system costs are due to manpower intensive launch processing, checkout and "on-pad" time. The objectives of the operations area are to adapt current technologies for application to the NLS to significantly reduce manpower and the time required for vehicle assembly, checkout, and launch operations. Object oriented data base and expert systems technologies are being developed to enable program-wide administrative, design, functional health and operations information to be readily accessed. Electromechanical actuators and laser initiated pyrotechnics are also being developed to minimize delays caused by hydraulic systems tests and pyrotechnics safe-arming procedures. Future tasks are planned to lay the foundation to establish an efficient and flexible launch complex supported by an effective decision support system.

Summary

The fundamental success of the NLS program depends on modernizing the technology base of our current launch vehicles and enabling technological innovations to be introduced in the future to facilitate continuous improvement. The ADP has concentrated on developing the launch system technologies which are currently (or nearly) available, that offer low risk and high payoff, through the demonstration of readiness for designers to utilize for NLS.

Session S6: ROBOTICS AND AUTOMATION FOR SPACE MAINTENANCE AND SERVICING

Session Chair: Dr. Neville Marzwell

A SYSTEM FOR EVALUATING MAN-MACHINE INTERFACE EFFECTIVENESS

Mike Maher
Westinghouse Electric Corporation
181, P.O. Box 746
Baltimore, MD 21203

Abstract unavailable at time of publication.

N94-11577

SUPERVISED AUTONOMOUS CONTROL, SHARED CONTROL, AND TELEOPERATION FOR SPACE SERVICING

Paul G. Backes
Jet Propulsion Laboratory
California Institute of Technology
Pasadena, California

ABSTRACT

A local-remote telerobot system for single and dual-arm supervised autonomy, shared control, and teleoperation has been demonstrated. The system is composed of two distinct parts: the local site, where the operator resides, and the remote site, where the robots reside. The system could be further separated into dual local sites communicating with a common remote site. This is valuable for potential space missions where a space based robotic system may be controlled either by a space based operator or by a ground based operator. Also, multiple modes of control integrated into a common system is valuable for satisfying different servicing scenarios. The remote site single arm control system is described and its parameterization for different supervised autonomous control, shared control, and teleoperation tasks are given. Experimental results are also given for selected tasks. The tasks include compliant grasping, orbital replacement unit changeout, bolt seating and turning, electronics card removal and insertion, and door opening.

I. INTRODUCTION

Supervised autonomous control, shared control, and teleoperation may be utilized for Space Station Freedom robotics applications. In teleoperation, trajectory points generated by an operator's motion of a hand controller are continuously sampled and communicated to a robot to track. In supervised autonomous control, autonomous commands are generated and then sent for execution on the robot. Trajectories are generated autonomously by specifying segment endpoints and trajectory parameters. The autonomous commands can be saved, simulated, and/or modified before sending them to the remote site for execution. Shared control is the merging of autonomous and teleoperation control. For example, the operator could specify the trajectory with the hand controller and the autonomous system could control the contact forces with the environment.

The planned baseline telerobotics capability for the Space Station is teleoperation with a Space Station based operator. Supervised autonomous control and shared control could provide valuable additional capability. Space Station based control, where the operator resides on the Space Station, could utilize supervised autonomy, shared control, or teleoperation. For ground (Earth) based control, there is expected to be an approximately 8 second round trip time delay for commands to the Space Station. Laboratory experiments indicate that time-delayed ground based control of Space Station robots can be safely achieved using supervised autonomous control. With such a system there would be dual local sites, one on Earth and one on the Space Station, communicating with a common remote site.

The basic architecture of the system provides a remote site capability with simultaneous multiple sensor based control and a local site capability which can generate commands and parameterization to send to the remote site. The Generalized Compliant Motion with Shared Control (GCMSC) [1] task primitive provides the remotes site system multi-sensor based control. The User Macro Interface (UMI) [2, 3] provides the local site task description and command sequencing. The utilization of sensors, both real and virtual, enhances task execution capability both by providing alternative approaches for executing a task and by making task execution more robust. A very simple

robotic system might have purely position control of a robot from a trajectory generator. Adding a hand controller allows the operator to perform position teleoperation. A force-torque sensor makes force/compliance control possible and therefore robust contact tasks. A virtual force field sensor can aid the operator during teleoperation to keep the robot away from joint limits and objects.

A task execution primitive is a function which controls a manipulator to perform the task described by its input parameter set. It generates the desired setpoints and performs the required control. The parameter list is the interface between a higher level task planning system and task execution. The planning system only needs to know how to describe the desired behavior of execution by setting the input parameters of the task primitive.

The paper will focus on the remote site GCMSC control and parameterization for specific tasks as well as give experimental results. The GCMSC primitive [1] and UMI [2, 3] have been described in previous publications. The paper is organized as follows. Section II discusses the input parameter set of the primitive and section III describes the control architecture. Motion control is described in section IV, monitoring and status reporting in section V, and command results in section VI. Section VII describes the implementation environment and section VIII discusses specific task parameterization and gives experimental results. Section IX describes new developments which extend the technology. Section X gives conclusions.

II. INPUT PARAMETER SET

The input parameter set is composed of five parameter types: system, trajectory, fusion, sensor, and monitor. Sensors generally have control and monitoring parameters. The addition of a sensor would normally require the addition of sensor and monitor input parameters for that sensor. The parameters are described throughout the remainder of the paper and are printed in bold letters.

III. CONTROL ARCHITECTURE OF THE PRIMITIVE

The GCMSC primitive provides six sources of robot motion which can be used individually or simultaneously. These sources of motion have two basic types: nominal motion trajectory generator and sensor based motion. The trajectory generator provides a feedforward Cartesian nominal position X_d of the NOM frame. Each of the sensors provides a perturbation to the nominal position of the NOM frame and these are all merged at the current NOM frame and the result is integrated with the past cumulative sensor based motion. The virtual restoration springs motion takes the integrated cumulative sensor based motion and tries to reduce it. The Generalized Compliant Motion control architecture is similar to position based impedance control [4, 5, 6, 7, 8].

The motion is programmed using the following kinematic ring equation.

$$trBase \cdot trTn \cdot trNom \cdot trDel \cdot trDrive = trBase \cdot trTnDest \cdot trNom \quad (1)$$

The WORLD frame is a fixed coordinate frame. **trBase** is the constant transform from the WORLD frame to a frame fixed in the manipulator's fixed first link, BASE. $trTn$ is the variable transform from BASE to a frame fixed in the terminal link of the manipulator, TN. This transform changes each sample interval during control and is computed based on the results of all other inputs. **trNom** is the constant transform from the TN frame to the frame in which Cartesian interpolated motion will occur, NOM. $trDel$ is the variable transform which has the integration of all sensor based motion. $trDrive$ is the variable transform which provides Cartesian interpolated motion [9]. This transform is initially computed to satisfy the initial conditions of the transforms in the ring equation and is interpolated to the identity transform at the end of the nominal motion. **trTnDest** is the constant transform used to specify the nominal destination of the TN frame (is the expected value of the $trTn$ transform at the end of nominal motion). At each sample interval, the trajectory generator calculates $trDrive$, sensor based motion calculates $trDel$, and then $trTn$ is computed by solving equation 1. Inverse kinematics computes

the joint angles equivalent to $trTn$ and the robot controller servos the manipulator to these joint angles.

Most of the sources of input can specify their inputs in a coordinate frame specific to their functionality; nominal motion in NOM, teleoperation in TELEOP, force control in FORCE, etc. This is useful because the inputs may be most effectively specified in separate frames. For example, see the door opening task in Section VIII.

There are two time segments of motion during the execution of GCMSC: the nominal motion segment and the ending motion segment. When the primitive starts, it executes the nominal motion segment with the specified Cartesian interpolated motion and all other sensors. Motion stops if a monitor event is triggered or Cartesian interpolated motion completes. If the nominal motion segment completes normally, then the end motion segment begins. Exactly the same control occurs except there is no Cartesian interpolated motion; only the sensor based motion is active. But, whereas during the nominal motion segment the termination conditions were not being tested, they are tested during the ending motion and the motion can stop on a monitor event, time, or a termination condition. The ending motion is needed after the nominal motion segment to relax forces built up due to the nominal motion. Also, testing for ending conditions may not be desired until the nominal task is complete.

IV. MOTION CONTROL

The general architecture for control in GCMSC has been described above. The control for the individual inputs will be described in this section.

IV.A. Trajectory Generator

Trajectory generation is done utilizing the RCCL [10] trajectory generator. The $trDrive$ transform is initially given by

$$trDrive = (trTnInit \cdot trNom)^{-1} \cdot trTnDest \cdot trNom \quad (2)$$

where $trTnInit$ is the initial value of $trTn$. $trDrive$ is then linearly interpolated from this initial value to the identity transform at the end of the motion. The interpolation is controlled by the input parameters **timeVelSel**, **timeVelVal**, and **accTime**. **timeVelSel** selects whether to finish the motion in a specified time or with a specified velocity. **timeVelVal** is the time or velocity to execute the motion in. **accTime** is the time to ramp up to maximum velocity.

IV.B. Force Control

Force control is implemented independently in each degree of freedom of the Cartesian force control frame FORCE. The control modifies the position setpoint to control the forces [11, 12]. The result of force control each sample interval is the perturbation transform $trDelFc$. The first step of force control during a sample interval is the projection of forces[1] from the force-torque sensor frame to the SENSE frame (**trSense** is the transform from the NOM frame to the SENSE frame). A 6 DOF wrist force-torque sensor supplies forces and torques along and about the axes of the SENSOR frame centered in the force sensor. These are then projected to equivalent forces in the TN frame using rigid body force transformations. The load (the complete composite body beyond the force sensor) forces due to gravity are then computed. The mass and center of mass of the load with respect to the TN frame are given in the **massProp** input parameter. The current TN frame orientation with respect to the gravity vector is used with the load mass properties to determine the gravity load forces in the TN frame. These are then subtracted from the total sensed forces in the TN frame. The resulting forces and torques are those due only to contact and are then projected to the SENSE frame. The forces in the SENSE frame are then passed through a filter which reduces their magnitude by the values in the input vector parameter **deadZone** (if one of the force magnitudes is initially less than the **deadZone** value, then it is set to zero). The deadZone filter is useful to reduce drift due to inaccuracies in the mass properties of the load.

Force control is calculated in the FORCE frame using the forces projected into the SENSE

[1] in this paper the term forces generally implies a 6 vector of both forces and torques

frame. (**trForce** is the transform from the NOM frame to the FORCE frame). The FORCE and SENSE frames will usually coincide but there are cases where they may be different, such as leveling a plate on a surface where the SENSE frame is at the center of the plate and the FORCE frame is at the point of contact. If the SENSE and FORCE frames were both at the point of contact, then no moments would be felt and therefore no rotation due to force control would occur since the force line of action would be through the control frame.

The **selVectFc** selection vector selects which of the 6 DOF of the FORCE frame are to have force control. In these degrees of freedom, the contact forces which were projected from the TN frame to the SENSE frame are subtracted from the six setpoints in the **forceSetpoints** vector input parameter. The resulting force errors are then multiplied by the constants in the **forceGains** vector input parameter to produce a differential motion vector of six perturbations in the FORCE frame, three translations and three rotations given by

$$\vec{d}_f = (d_{fx}, d_{fy}, d_{fz}, \delta_{fx}, \delta_{fy}, \delta_{fz}) \quad (3)$$

The magnitudes of the elements of the $\vec{d}_f$ vector are then limited. The maximum magnitudes of the $\vec{d}_f$ perturbations per sample interval are the velocity limits given in the **maxForceVel** input parameter multiplied by the sample interval.

The ${}^{FORCE}trDelFc$ transform is a differential translation and rotation transform with elements given by $\vec{d}_f$ [9]. The $trDelFc$ transform is then transformed to the NOM frame. $trDelFc$ with respect to the FORCE and NOM frame are related by the following equation.

$${}^{NOM}trDelFc \cdot trForce = trForce \; {}^{FORCE}trDelFc \quad (4)$$

The $trDel$ transform of equation 1 is then updated with the perturbation due to force control with

$$trDel = {}^{NOM}trDelFc \cdot trDel \quad (5)$$

Premultiplication is required rather than postmultiplication because the motion is with respect to the NOM frame.

IV.C. Dither Sensor Control

Dither signals can be used to perturb the motion independently in each degree of freedom of the DITHER frame. Presently only a triangular waveform is available although other waveforms will be implemented such as sinusoidal and square. Dither is useful to overcome stiction, e.g., when pulling a pin out of a hole. The magnitude and period of the dither waveforms for each DOF of the DITHER frame are given in the input parameters **ditherMag** and **ditherPeriod**. As with force control, the inputs in each degree of freedom are elements of a differential translation and rotation transform, $trDelDt$ which is transformed to the NOM frame in the same manner as for $trDelFc$. The $trDel$ transform then updated with the perturbation due to the dither waveforms with

$$trDel = {}^{NOM}trDelDt \cdot trDel \quad (6)$$

IV.D. Teleoperation Sensor Control

The teleoperation sensor is actually a 6 DOF hand controller. Each sample interval the change in joint angles of the hand controller are read and put in a differential vector. This vector is multiplied by the hand controller Jacobian to get the input Cartesian motion perturbations. The appropriate Jacobian is used depending on the **teleMode** parameter to compute the Cartesian motion with respect the the hand controller grip which would be tool mode teleoperation, or with respect to a frame fixed with respect to the hand controller base, which would be used for world or camera mode teleoperation. These perturbations are then transformed to the TELEOP frame which is given with respect to the NOM frame by the input parameter **trTeleop**. Again, the mode determines how the perturbations are transformed to the TELEOP frame. **trCamera** is used for camera mode teleop to specify the present operator viewing orientation. The details of the various modes of teleoperation are explained in [13]. The **selVectTp** selection vector selects which degrees of freedom of teleoperation inputs to include and **teleGains** are weightings for the inputs. The **maxTelVel** limits the rate of teleoperation inputs.

Force reflection is also available in the system. The robot contact forces are sent to the hand controller where they are reflected to forces felt by the operator at the hand grip. Force reflection was not used during the tasks in Section VIII.

IV.E. Joint Sensor Control

The joint sensor control provides joint limiting. This prevents the arm from going into a joint limit or singularity. Joint angle perturbations for all the joints are computed and put into a differential vector. A joint angle perturbation is computed with

$$\Delta\theta = K_\theta(\theta_{actual} - \theta_{limit})^{-1} \quad (7)$$

where K_θ is the gain, θ_{actual} is the actual joint angle, and θ_{limit} is the limit that the joint is approaching, either as a joint limit or singularity. The differential vector is multiplied by the Jacobian to get the required Cartesian motion. This is transformed to the NOM frame and added to *trDel* as is the case with the other previous sensors.

IV.F. Virtual Restoration Springs Control

The virtual restoration springs act on the *trDel* transform to pull it towards the identity transform. This reduces the accumulated motion due to sensory inputs and causes the actual motion to approach the nominal motion. Virtual springs are applied in the DOFs specified by the **selVectSp** input parameter. Four virtual springs are used, one along each translational degree of freedom and one orientational spring. For the translational DOFs, the spring lengths are equal to the displacement vector, $\vec{p}$, elements of the *trDel* transform (*trDel* is a homogeneous transform with column vectors $\hat{n}$, $\hat{o}$, $\hat{a}$, and $\vec{p}$). The translational perturbations due to the virtual springs, $\vec{d}_s$, are then the spring lengths multiplied by the translational spring gains in the **springGains** vector, $\vec{k}_s$, input paramter, i.e., $d_{sx} = -k_{sx}p_x$, $d_{sy} = -k_{sy}p_y$, and $d_{sz} = -k_{sz}p_z$.

Virtual springs for orientation is applied about one axis with respect to the NOM frame. The selection of this axis depends upon the number of orientation degrees of freedom specified in **selVectSp**. The axis is $\hat{u}$ and the angular displacement about this axis is θ. If all orientation DOFs are selected, then $\hat{u}$ is the equivalent axis of rotation of the *trDel* transform and θ is the equivalent angle about the axis. If no orientation DOFs are selected, then no orientation perturbation is applied due to virtual springs. If only one orientation DOF is selected, then the corresponding axis $\hat{x}$, $\hat{y}$, or $\hat{z}$ is aligned by the orientation virtual spring. $\hat{u}$ and θ are selected such that a rotation about $\hat{u}$ by θ will align the selected axis. The virtual springs orientation perturbation is then $\delta_{s\theta} = -k_{s\theta}\theta$. The four virtual springs perturbation magnitudes are then limited to the magnitudes given in the **maxSpringVel** vector input parameter as the force control perturbations were limited by the **maxForceVel** values. The *trDel* transform is then updated with the perturbations due to virtual springs with

$$\begin{aligned} trDel &= trans(\hat{x}, d_{sx}) \cdot trans(\hat{y}, d_{sy}) \cdot \\ &\quad trans(\hat{z}, d_{sz}) \cdot rot(\hat{u}, \delta_{s\theta}) \cdot trDel \end{aligned} \quad (8)$$

where $trans(\hat{v}, d)$ is a translation of d along the $\hat{v}$ axis and $rot(\hat{v}, \delta)$ is a rotation of δ about the $\hat{v}$ axis.

V. MONITORS

Various parameters are continuously monitored during execution. The magnitudes of the translational part of *trDel* and the equivalent rotation of the orientational part of *trDel* are compared against the input parameters **posThreshold** and **orientThreshold**. If the values grow larger than the thresholds, then the motion stops. Also, the vector magnitudes of the contact forces and torques in the FORCE frame are compared against **forceThreshold** and **torqueThreshold** and motion stops if one of them is larger than the threshold. If the distance to a joint limit or singularity is less than the angles in the **jSafetyLimit** input vector, then motion stops.

Anther monitor is the termination condition monitor. It is used during the end motion (see section III). The end motion continues until all of the specified termination conditions are satisfied or until the time limit given by the **endTime** input parameter is passed. The **select** input parameter is a bit mask which selects which termination conditions to test for. Any combination of termination conditions can be tested. All termination conditions relate to forces and torques in the SENSE frame or sensor based motion specified by the *trDel* transform. Each termination condition is calculated as a moving average of data sampled each 200 ms over a window of **testTime** ms. Satisfaction of a termination condition means that its magnitude is less than its associated input parameter limit. The **endTransErr** condition is the mag-

nitude of the *trDel* transform $\vec{p}$ vector including only the position degree of freedom components. The **endAngErr** condition is the magnitude of the virtual restoration springs angular displacement, θ, described above. The **endTransVel** and **endAngVel** parameters are the rate of change of the **endTransErr** and **endAngErr** conditions. The **endForceErr** and **endTorqueErr** parameters are the magnitudes of the force and torque error vectors in the SENSE frame including only the force controlled degrees of freedom. The **endForceVel** and **endTorqueVel** parameters are the rate of change of the **endForceErr** and **endTorqueErr** conditions.

During execution of the primitive, the system executive reports the status of execution to the local site system. The report includes information such as contact forces and joint angles.

VI. COMMAND RESULTS

Various possible causes for the motion to stop have been described above. When the motion stops, the cause is returned to the local site system along with the system status. Each possible cause of motion termination has a unique command result code.

VII. IMPLEMENTATION ENVIRONMENT

The remote site with the GCMSC primitive and the local site with UMI are operational in the JPL Supervisory Telerobotics (STELER) Laboratory running PUMA 560 manipulators with six DOF wrist force-torque sensors and servoed grippers. The GCMSC primitive was written in the C programming language using utilities from the robot control C library (RCCL) [10]. The manipulator control is multiple rate with the Cartesian level control of the GCMSC primitive at a different rate from the joint level servo control. Presently the Cartesian level control (all control associated with the GCMSC primitive including trajectory generator and sensor based motion) runs with a 10 ms sample interval and the joint servo control has a 1 ms sample interval. Details on the hardware configuration of the system can be found in [14].

VIII. RESULTS

Various tasks have been executed in the JPL STELER lab utilizing the User Macro Interface for task description and sequencing and Generalized Compliant Motion with Shared Control for task execution. These tasks include compliant grasp, orbital replacement unit removal and insertion, bolt seating and turning, electronics card removal and insertion, and door opening. The different tasks utilized different combinations of the six sources of motion. For each task below, only the mentioned motion sources were used. All distance units used below are mm, forces are Newtons (N), and torques are N-mm. The **forceGains** input vector translation gains units are mm/N and orientation gains units are deg/N-mm. The **maxForceVel** vector has translation units of mm/sec and orientation units of deg/sec. The **springGains** input vector has three translational gains with units mm/mm and an orientation gain with units deg/deg.

The compliant grasp task utilized force control to both level the grippers on the grapple lug and to adjust the position of the robot as the fingers closed. The **trForce** transform was selected so the FORCE frame was between the robot fingers. The **forceSetpoints** input vector was all zeroes except for a force of -10 N along Z. The **forceGains** input vector was (0.02, 0.02, 0.02, 0.00003, 0.00003, 0.00003). The compliant ungrasp task opened the gripper while using force control to null out contact forces and virtual springs to make sure the gripper would not drift. The **forceSetpoints** input vector was all zeroes. The **forceGains** input vector was the same as for the compliant grasp task. The **springGains** input vector was (0.007, 0.007, 0.007, 0.015).

The orbital replacement unit (ORU) removal task utilized force control to pull the ORU and attached pin out of the passive connector. The arm carrying the ORU is shown in figure 1. The **massProp** inputs were 4.87 kg at position vector (in mm) (-90.3, -4.5, 336.6) relative to the T6 frame. The **trForce** transform was a translation of 400 mm along the T6 Z axis. The **forceSetpoints** input vector was all zeroes except for a force of 15 N along Z. The **forceGains** input vector was (0.02, 0.02, 0.02, 0.00001, 0.00001, 0.00001). The **maxForceVel** input vector was (30, 30, 30, 5,

Figure 1: Manipulator carrying ORU

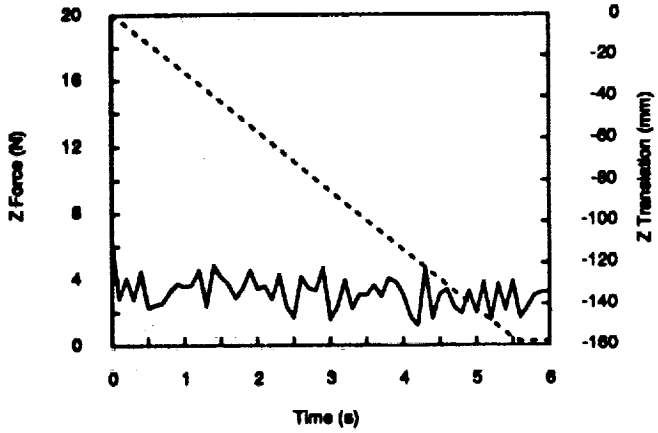

Figure 2: ORU removal task: solid is force along FORCE Z; dashed is translation along FORCE Z

5, 5). Figure 2 shows the force and displacement along the FORCE frame Z axis during the task. The figure shows that the **maxForceVel** of 30 mm/sec limited the velocity due to force control to 30 mm/sec so that the force could not reach its setpoint. The motion stopped on the position monitor with **posThreshold** input parameter of 160 mm.

The ORU insertion task used the same parameters as the oru removal task except that the task completed on the time monitor and the force setpoint along Z was -15 N. Figure 3 shows the force and displacement along the FORCE frame Z axis during the task.

The bolt seating task utilized Camera mode shared control teleopertion. The **teleMode** parameter specified Camera mode teleoperation. The **trTeleop** transform put the TELEOP frame on the socket shaft. The **forceGains** input vector was (0.03, 0.03, 0.03, 0.00003, 0.00003, 0.00003).

The bolt unscrew task used force control to cause the bolt to turn. The **trForce** transform was selected so that the FORCE frame was above the socket. The **forceSetpoints** input vector was (0, 0, -5, 0, 0, 6000). The **forceGains** input vector was (0.01, 0.01, 0.01, 0.00001, 0.00001, 0.00001).

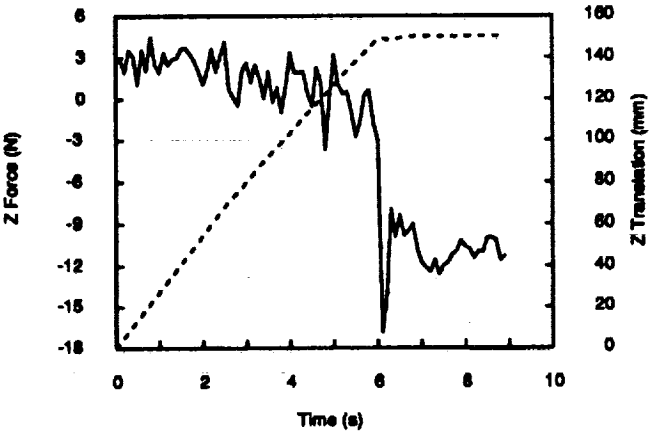

Figure 3: ORU insertion task: solid is force along FORCE Z; dashed is translation along FORCE Z

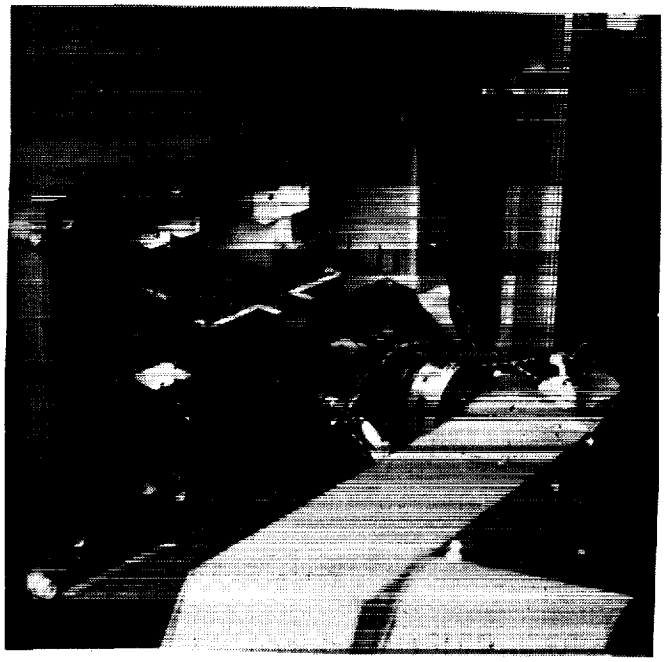

Figure 4: Electronics card insertion and removal

Figure 5: Operator at local site OCS

The -5 N force kept the socket on the bolt. The 6000 N-mm torque caused the bolt rotation. The **orientThreshold** input parameter of 90 degrees caused the task to terminate after the bolt rotated 90 degrees. The bolt screw task was the same except that a torque of -6000N-mm was used to screw the bolt on. The task terminate either on the **orientThreshold** of 90 degrees or on time if the bolt would not turn any more.

Four tasks were used for electronics card insertion and removal, as shown in figure 4. A real electronics card and chassis were used in the experiment. The first task was camera mode shared control teleoperation where the operator used the hand controller to partially insert the card into the card slot. The operator at the local site operator control station is shown in figure 5. Camera mode teleoperation caused the robot to move in the same direction relative to the cameras mounted on the camera arm (see figure 1) as the operator's hand moved relative to the stereo display monitor. Force control with zero setpoints was used to null out the contact forces between the card and the slot. The **teleMode** parameter specified Camera mode teleoperation. The **trTeleop** transform put the TELEOP frame on the electronics card. The **forceGains** input vector was (0.03, 0.03, 0.03, 0.00003, 0.00003, 0.00003).

Once the electronics card was successfully placed in the chassis slot, autonomous commands were used to slide the card to the backplane and seat it in the backplane. Sliding the card to the backplane was done using force control. The **forceSetpoints** input vector was (0, 0, -15, 0, 0, 0) and the **forceGains** input vector was (0.01, 0.01, 0.01, 0.00001, 0.00001, 0.00001). Figure 6 shows the translation and forces along the FORCE frame Z axis. A larger force is needed to seat the card in the backplane than was used to slide the card to the backplane. To seat the card in the backplane, the force along the FORCE Z axis was set to -60N and the same **forceGains** were used. The results are shown in figure 7. Unseating the electronics card from the backplane is achieved by applying a force of 60 N along the FORCE frame Z axis. After the card breaks free of the backplane, a velocity limiting filter limits the velocity using the **maxForceVel** input parameters (2.5, 2.5, 2.5, 3, 3, 3). The results are shown in figure 8.

Shared control was used for the dome cleaning task as shown in figure 9. A **trTeleop** transform of 290 mm along T6 Z was selected so that the TELEOP frame was in the middle of the pad. The operator was given three hand controller degrees of freedom of input - two tangential to the dome surface and one about the surface normal as specified

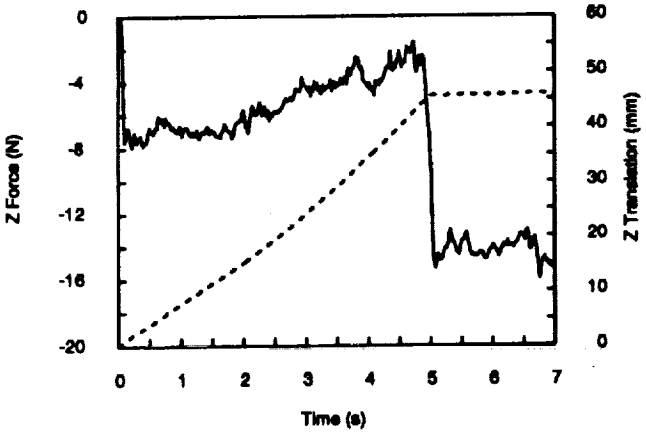

Figure 6: Electronics card sliding to the backplane: solid is force along FORCE Z; dashed is translation along FORCE Z

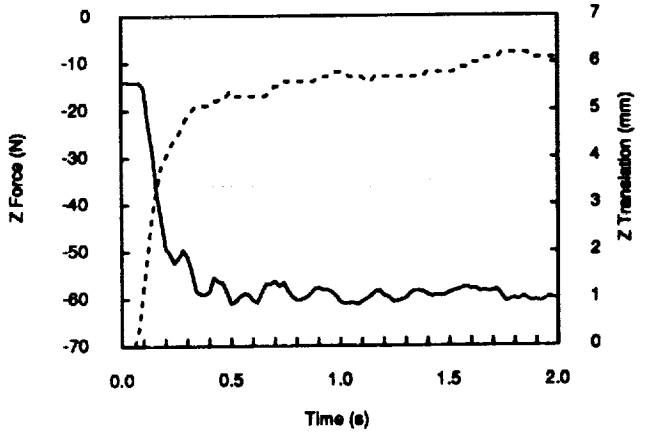

Figure 7: Electronics card seating in backplane: solid is force along FORCE Z; dashed is translation along FORCE Z

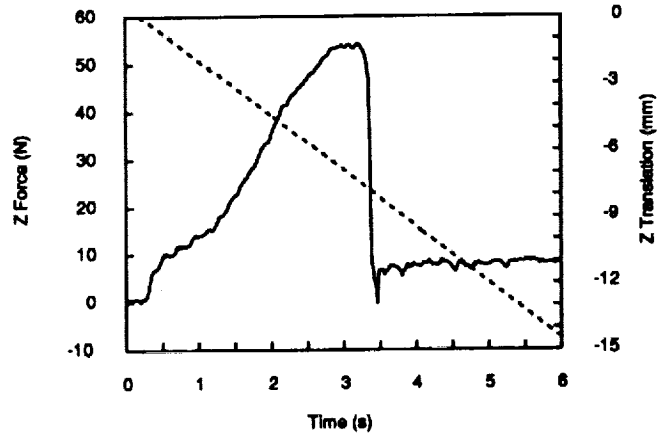

Figure 8: Electronics card unseating from backplane: solid is force along FORCE Z; dashed is translation along FORCE Z

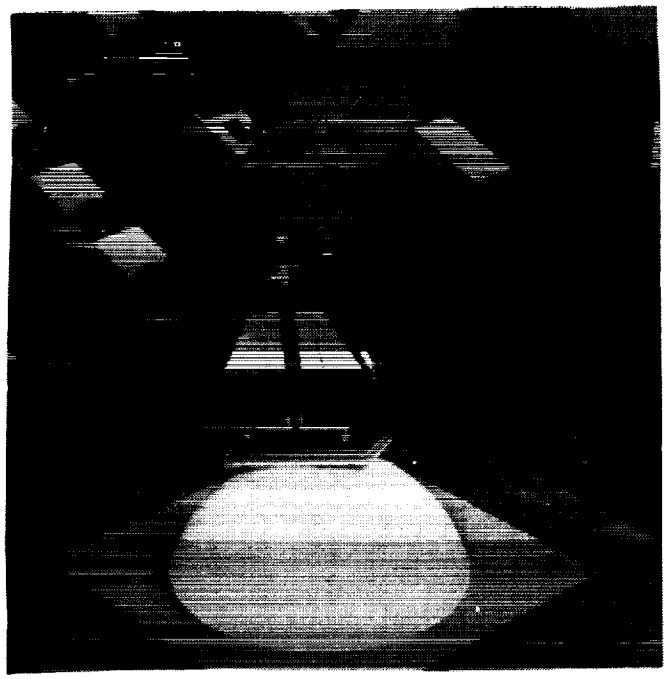

Figure 9: Dome cleaning task

in the **selVectTp** input vector (1, 1, 0, 0, 0, 1). The FORCE frame was the same as the TELEOP frame. The **forceSetpoints** input vector was (0, 0, -20, 0, 0, 0) and the **forceGains** input vector was (0.02, 0.02, 0.02, 0.00012, 0.00012, 0.00002). The 20 N force caused the pad to stay in contact with the curved surface. When the pad was moved so that the FORCE frame was not at the point of contact, then the 20 N would generate a moment and the pad would automatically rotate until the FORCE frame was again at the contact point. In this way, the operator could polish the dome surface but could not cause motion with the hand controller which would cause damage to the surface.

The last task is the door opening task which was done with both shared control teleoperation and autonomous control. The door task is shown in figure 10. For the door opening with teleoperation task, the **trTeleop** input transform was selected so that the TELEOP frame Z axis was along the hinge axis. The trForce input transform placed the FORCE frame at the knob where the robot was grasping the door. The **forceSetpoints** input vector was all zeros and the **forceGains** input vector was (0.015, 0.015, 0.015, 0.00002, 0.00002, 0.00002). The operator opened and closed the door simply by a one DOF rotation of the hand con-

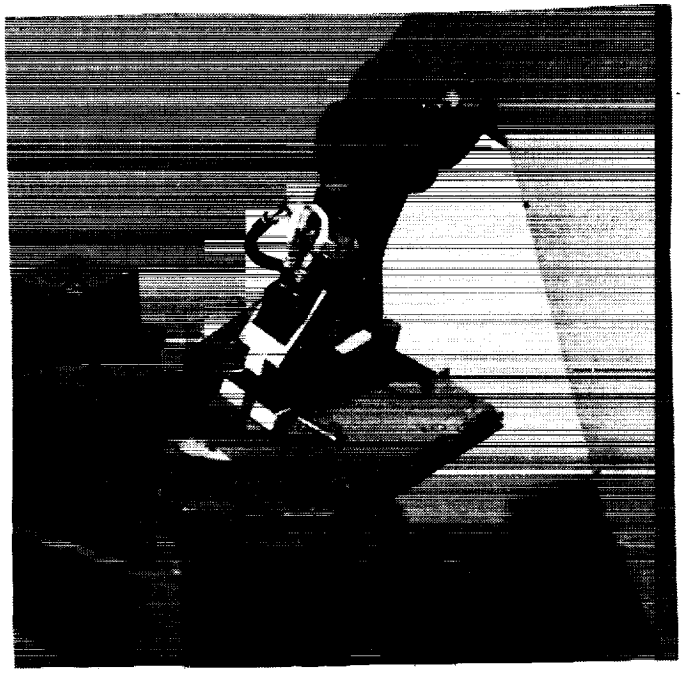

Figure 10: Door opening task

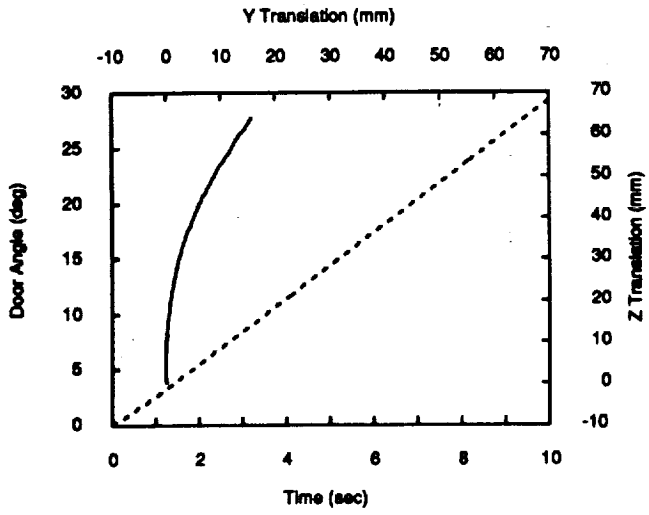

Figure 11: Autonomous door opening results: solid is motion of FORCE frame; dashed is rotation of NOM frame (hinge axis)

troller grip.

For the door opening with autonomous control task, the autonomous trajectory generator was used instead of teleoperation inputs to cause the nominal motion. The **trNom** input transform placed the NOM frame such that its Z axis was along the door hinge axis. The **forceSetpoints** and **forceGains** input vectors were the same as for the compliant teleoperation case above. Virtual springs were necessary so that the motion due to force control would not cause the actual motion to drift far from the reference nominal trajectory. The **springGains** input vector was set to (0.007 0.007 0.007 0.015). The **select** termination condition input was set to select the **endAngErr** as the termination condition to monitor; **endAngErr** was set to 0.1 deg. A relative autonomous motion was specified to rotate the NOM frame by 30 degrees. The results are shown in figures 11 and 12. The figures show that the door was successfully opened 30 degrees.

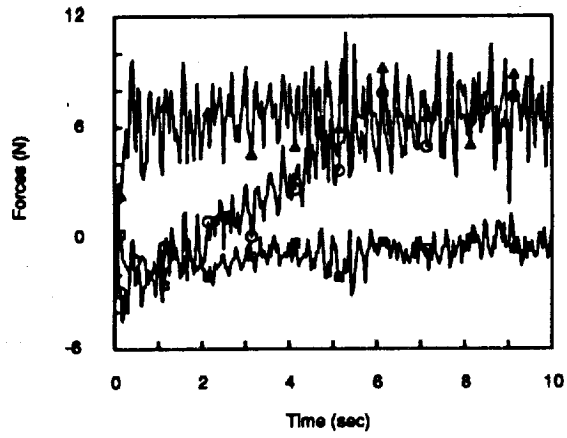

Figure 12: Autonomous door opening results: forces along FORCE frame X (□), Y(○), and Z(△) axes

The value of the virtual springs is shown by executing the same task but with the **springGains** input vector elements set to zero. The results are shown in figure 13. In this case the door opened a maximum of only 21.6 deg. The maximum rotation occurred when the trajectory gener-

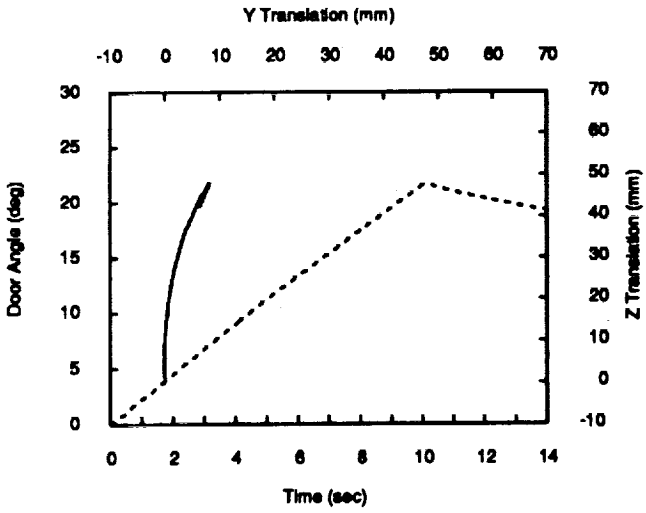

Figure 13: Autonomous door opening results (no virtual springs): solid is motion of FORCE frame; dashed is rotation of NOM frame (hinge axis)

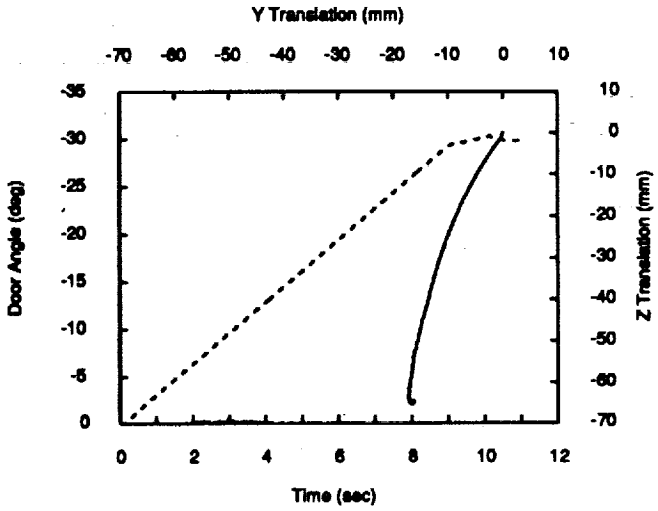

Figure 14: Autonomous door closing: solid is motion of FORCE frame; dashed is rotation of NOM frame (hinge axis)

ator finished. After that, the ending motion time segment began and the door slowly began closing due to its gravity weight. The ending condition of 0.1 deg. from the 30 deg. goal was never satisfied so it stopped on the **endTime** timeout. The reason that the door did not open all of the way is that the forces in the FORCE frame caused compliant motion to resist the nominal trajectory generator motion and there were no virtual springs to offset this motion.

The door opening task was followed by a door closing task. The same parameters as for the door opening task were used, including virtual springs, except that the nominal motion was negative 32 deg. and different termination conditions were used. A 32 deg. motion was used to be sure to have at least the 30 deg. of motion needed. The **select** termination condition input was set to select the **endTransVel** and **endAngVel** as the termination conditions to monitor; **endTransVel** was set to 1 mm/sec and **endAngVel** was set to 0.1 deg/sec. The results are shown in figures 14 and 15. The figures show that the door was successfully closed 30 degrees. The motion is nearly linear until the door makes contact and is closed at 30 deg. Then the rotation stops which triggers the termination condition.

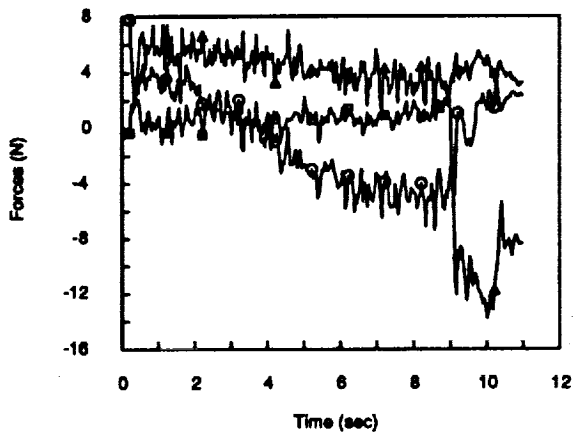

Figure 15: Autonomous door closing results: forces along FORCE frame X (□), Y(○), and Z(△) axes

IX. DUAL-ARM AND IMPEDANCE BASED REDUNDANT ARM CONTROL

The GCMSC primitive has been generalized for dual-arm cooperative control teleoperation, supervised autonomy, and shared control with the Dual-Arm Generalized Compliant Motion primitive [15]. It was then generalized for impedance based control of a six DOF manipulator [13] and then impedance based control of a redundant seven DOF manipulator [16].

X. CONCLUSIONS

A local-remote control system with unified autonomous control, shared control, and teleoperation has been described. The local site generates teleoperation and autonomous commands which are communicated to the remote site. The remote site uses a parameterized task primitive to execute tasks. The execution of various tasks in the laboratory demonstrates the capability of the system.

ACKNOWLEDGEMENTS

The research described in this paper was performed at the Jet Propulsion Laboratory, California Institute of Technology, under contract with the National Aeronautics and Space Administration.

REFERENCES

[1] Paul G. Backes. Generalized compliant motion with sensor fusion. In *Proceedings 1991 ICAR: Fifth International Conference on Advanced Robotics, Robots in Unstructured Environments*, pages 1281–1286, Pisa, Italy, June 19–22 1991.

[2] Paul G. Backes and Kam S. Tso. Umi: An interactive supervisory and shared control system for telerobotics. In *Proceedings IEEE International Conference on Robotics and Automation*, pages 1096–1101, Cincinnati, Ohio, May 1990.

[3] Paul G. Backes. Ground-remote control for space station telerobotics with time delay. In *Proceedings AAS Guidance and Control Conference*, Keystone, CO, February 8-12 1992. AAS paper No. 92-052.

[4] N. Hogan. Impedance control: An approach to manipulation: Part i — theory. *ASME Journal of Dynamic Systems, Measurement, and Control*, 107:1–7, March 1985.

[5] N. Hogan. Impedance control: An approach to manipulation: Part ii — implementation. *ASME Journal of Dynamic Systems, Measurement, and Control*, 107:8–16, March 1985.

[6] N. Hogan. Impedance control: An approach to manipulation: Part iii — applications. *ASME Journal of Dynamic Systems, Measurement, and Control*, 107:17–24, March 1985.

[7] Dale A. Lawrence and R. Michael Stoughton. Position-based impedance control: Achieving stability in practice. In *Proceedings AIAA Conference on Guidance, Navigation, and Control*, pages 221–226, Monterey, Ca, August 1987.

[8] Dale A. Lawrence. Impedance control stability properties in common implementation. In *Proceedings IEEE International Conference on Robotics and Automation*, pages 1185–1190, 1988.

[9] R. P. Paul. *Robot Manipulators: Mathematics, Programming, and Control.* The MIT Press, 1981.

[10] J. Lloyd, M. Parker, and R. McClain. Extending the rccl programming environment to multiple robots and processors. In *Proceedings IEEE International Conference on Robotics and Automation*, pages 465–474, 1988.

[11] Paul G. Backes and Kam S. Tso. Autonomous single arm oru changeout — strategies, control issues, and implementation. Jet Propulsion Laboratory Engineering Memorandum 347-88-258 (internal document). Published as BACK90F, November 22 1988.

[12] J. A. Maples and J. J. Becker. Experiments in force control of robotic manipulators. In *Proceedings IEEE International Conference on Robotics and Automation*, pages 695–702, 1986.

[13] Paul G. Backes. Multi-sensor based impedance control for task execution. In *Proceedings IEEE International Conference on Robotics and Automation*, Nice, France, May 1992.

[14] Samad Hayati, Thomas Lee, Kam Tso, and Paul G. Backes. A testbed for a unified teleoperated-autonomous dual-arm robotic system. In *Proceedings IEEE International Conference on Robotics and Automation*, 1990.

[15] Paul G. Backes. Dual-arm supervisory and shared control space servicing task experiments. In *Proceedings AIAA Space Programs and Technologies Conference*, Huntsville, AL, March 24-27 1992. AIAA paper No. 92-1677.

[16] Paul G. Backes and Mark K. Long. Redundant arm control in a supervisory and shared control system. In *Proceedings AIAA Space Programs and Technologies Conference*, Huntsville, AL, March 24-27 1992. AIAA paper No. 92-1578.

N94-11578

SPACE STATION MAINTENANCE STUDIES USING PLAID GRAPHICS

Mary E. Helm
Lockheed Engineering and Sciences Company
2400 Nasa Road 1
Houston, TX 77058

The Graphics Analysis Facility (GRAF) has been used frequently to study extravehicular activity (EVA) maintenance scenarios on Space Station Freedom. The ability to use 3-dimensional visualization gives one a more accurate estimate of the Space Station environment. Moreover, human EVA and robotic kinematics can be accurately simulated for columetric reach and collision detection analysis. An animation of this kind was developed for J. Van Laack's group (NASA/JSC) to study and discover problem areas involved with doing external Space Station maintenance tasks. On the EVA side, it was discovered that items such as handholds and temporary restraint mechanisms should more effectively facilitate EVA movement about the Space Station structure for the suited personnel. Issues concerning CETA cart configuration, PWP stowage locations, and locations of EVA stowage areas were also identified by use of the animation. In the area of EVA versus robotics, it was found that there is a strong desire to make EVA and robotics interfaces compatible on items such as replacement units and unpressurized logistics carriers. The animation also showed that the use of robotics within an EVA task increases the difficulty and duration of the task setup, leaving less time available for the maintenance task itself. Graphics animation provides a mechanism to simultaneously analyze several mission parameters (i.e., EVA reach, volumetric analysis, and task timelines), and thus has proven to be an effective method for mission evaluation.

N94-11579

ROBOTIC SERVICING ON EARTH ORBITING SATELLITES

Mr. Stanford Ollendorf
NASA/Goddard Space Flight Center
Mechanical Systems Division
Code: 720
Greenbelt, MD 20771

An articulated calibration experiment (ACE) concept study was conducted by the NASA/ Goddard Space Flight Center (GSFC) to prove the feasibility of instrument calibration by a resident robot on the EOS spacecraft. This study provided a basis for determining the most suitable robot design and operations concepts required to perform accurate instrument calibration on the EOS platform. During the study, first-order dynamics of robot walking and docking motions as it moves about were evaluated to determine the accelerations and torques imparted into the spacecraft. The major perturbation to the spacecraft was the effect of robot motion and impact on the EOS platform attitude control system. If not carefully controlled, these levels could exceed the maximum allowable levels. As a result of the EOS/ACE feasibility study, a GSFC robotic ground development effort has been established. This effort, as described on the paper, will identify the technology required to resolve issues associated with robot in-space servicing dynamics and its impact on spacecraft and designs. Of primary concern are those relating to robot contact loads, docking of robotic systems on space platforms, and basic motion and mobility.

AUTHOR INDEX

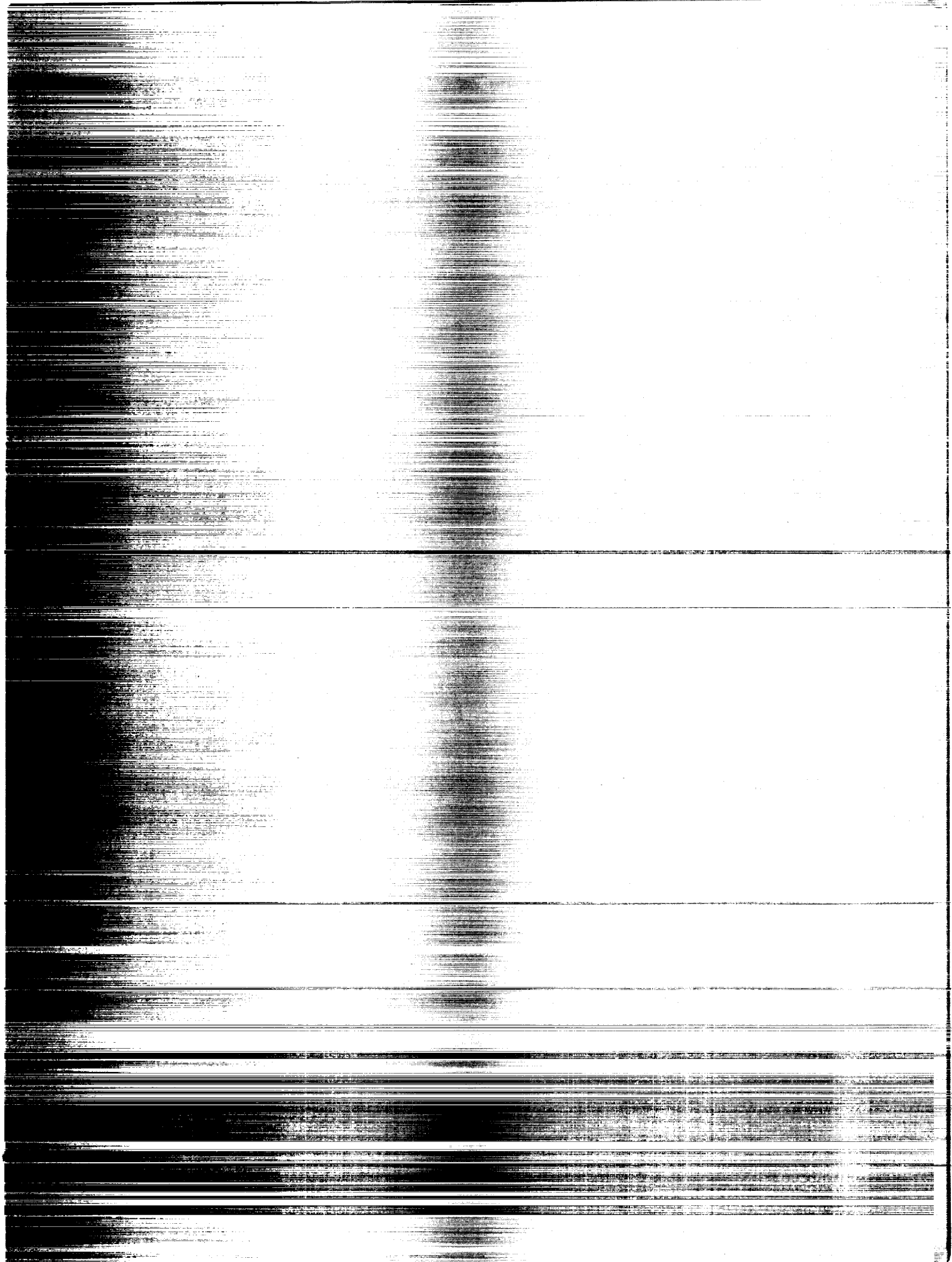

REPORT DOCUMENTATION PAGE

1. AGENCY USE ONLY *(Leave blank)*	2. REPORT DATE	3. REPORT TYPE AND DATES COVERED
	February 1993	Conference Publication

4. TITLE AND SUBTITLE
Sixth Annual Workshop on Space Operations Applications and Research (SOAR '92)

5. FUNDING NUMBERS

6. AUTHOR(S)
Kumar Krishen, Editor

7. PERFORMING ORGANIZATION NAME(S) AND ADDRESS(ES)
Lyndon B. Johnson Space Center
Houston, TX 77058

8. PERFORMING ORGANIZATION REPORT NUMBER
S-710

9. SPONSORING / MONITORING AGENCY NAME(S) AND ADDRESS(ES)
National Aeronautics and Space Administration
Washington, D.C. 20546
U.S. Air Force, Washington, D.C. 23304

10. SPONSORING / MONITORING AGENCY REPORT NUMBER
NASA CP-3167

11. SUPPLEMENTARY NOTES

12a. DISTRIBUTION / AVAILABILITY STATEMENT
Publicly available
National Technical Information Service
5285 Port Royal Road
Springfield, VA 22161

12b. DISTRIBUTION CODE

Subject Category: 99

13. ABSTRACT *(Maximum 200 words)*

This document contains papers presented at the Space Operations, Applications and Research Symposium (SOAR) hosted by the U.S. Air Force (USAF) on August 4-6, 1992, and held at the Johnson Space Center (JSC) Recreation Center. The symposium was cosponsored by the Air Force Materiel Command and by NASA/JSC. Key technical areas covered during the symposium were robotics and telepresence, automation and intelligent systems, human factors, life sciences, and space maintenance and servicing. The SOAR differed from most other conferences in that it was concerned with Government-sponsored research and development relevant to aerospace operations. More than 135 papers, 36 exhibits, 2 panel discussions, and several keynote speeches were included in SOAR '92. The USAF and NASA programmatic overviews were also held for each of the five technical areas. These proceedings, along with the comments and suggestions made by the panelists and keynote speakers, will be used in assessing the progress made in joint USAF/NASA projects and activities and to identify future collaborative/joint programs. The SOAR '92 symposium was the responsibility of the USAF/NASA Space Technology Interdependency Group (STIG) Operations Committee (SOC). Symposium proceedings include papers covering various disciplines presented by experts from NASA, the USAF, universities, and industry.

14. SUBJECT TERMS
Space, ground, operations, automation, robotics, life sciences, medical protocols, knowledge acquisition, expert systems, telepresence, virtual reality, training systems, biomedical, debris, space shuttle, Space Station Freedom, lunar outposts, Mars missions

15. NUMBER OF PAGES
716

16. PRICE CODE

17. SECURITY CLASSIFICATION OF REPORT	18. SECURITY CLASSIFICATION OF THIS PAGE	19. SECURITY CLASSIFICATION OF ABSTRACT	20. LIMITATION OF ABSTRACT
Unclassified	Unclassified	Unclassified	